

The role of the S6K2 splice isoform in mTOR/S6K signalling and cellular functions

Olena Myronova

A thesis submitted to the University College London in fulfilment with the requirements for the degree of Doctor of Philosophy

London, November 2015



Research Department of Structural and Molecular Biology
Division of Biosciences
University College London
Gower Street
London, WC1E 6BT
United Kingdom



Ludwig Institute for Cancer Research
666 Third Avenue, 28th floor
New York, N.Y. 10017 USA

Declaration

I, Olena Myronova, declare that all the work presented in this thesis is the result of my own work. The work presented here does not constitute part of any other thesis. Where information has been derived from other sources, I confirm that this has been indicated in the thesis. The work here in was carried out while I was a graduate research student at University College London, Research Department of Structural and Molecular Biology under the supervision of Professor Ivan Gout.

Olena Myronova

Abstract

Ribosomal S6 kinase (S6K) is a member of the AGC family of serine/threonine protein kinases and plays a key role in diverse cellular processes, including cell growth, survival and metabolism. Activation of S6K by growth factors, amino acids, energy levels and hypoxia is mediated by the mTOR and PI3K signalling pathways. Dysregulation of S6K activity has been implicated in a number of human pathologies, including cancer, diabetes, obesity and ageing. The family of S6Ks consists of two proteins S6K1 and S6K2, which are encoded by different genes. Most of research has been done on S6K1, while little is currently known about specific functions of S6K2. Recently, several novel splicing variants of human S6K2, termed S6K2-S1, S6K2-S2 and S6K2-S3, have been identified in our laboratory. The aim of this thesis was therefore to study the function of S6K2-S1 splicing isoform in normal and cancer cells and its role in the regulation of mTORC1/S6K signalling.

Initially, detailed bioinformatic analysis of human and mouse databases in combination with an alternative splicing potential of S6K2 gene revealed three novel splicing isoforms. S6K2-S1 splicing isoform is the product of exon 9 alternative splicing, which results in the formation of a truncated splice variant, lacking the kinase domain. We found that S6K2-S1 has the potential to integrate into the mTORC1 signalling complex via specific interaction with the substrate-presenting protein Raptor. Functional analysis of S6K2-S1 revealed that it could inhibit some of mTOR functions in starved conditions and mediate pro-apoptotic signalling. Furthermore, stable overexpression of S6K2-S1

protein in different cell lines inhibited cell migration and dramatically reduced anchorage-independent colony growth in soft agar. Importantly, S6K2-S1 splice variant reduced A549 cell *in vivo* tumour growth in nude mice, while full length S6K2 promoted *in vivo* tumour formation.

Together, the data from this thesis revealed the existence of novel S6K2 splicing isoforms and uncovered a dominant-negative effect of S6K2-S1 on mTORC1 signalling and its tumour suppressive function in cell-based models and xenograft studies.

Dedication

There are a number of people to whom I am deeply grateful for the completion of this thesis.

First of all I would like to thank my supervisor, Professor Ivan Gout, for giving me the opportunity to join his laboratory as a PhD student. During the four years, he has been a dedicated and understanding teacher and has supervised my work with a lot of inspiring enthusiasm.

I am very much grateful to my husband Eugene and my adorable kids Maximilian and Anastasia who spent a lot of time being without me. My family, especially to my Mum who allowed me to finish my experiments and to write this thesis, looking after my kids.

My colleagues, Alex, Yugo, Ahmed, Mahmoud, Pascale, Nadeem, Eddy and many others for the great discussions and new ideas that helped solve problems and progress with my work.

My collaborators at Imperial College London (Prof. M. Seckl and Dr. O. Pardo) and at UCL Cancer Institute (Prof. Barbara Pedley's group), for the work they did. Professors Chris Kay and Kaila Srail, for their useful suggestions during my thesis committee meetings.

I thank you all for these contributions great and small, as without you, this thesis would not have been written.

Table of Contents

| | |
|---|----|
| Declaration..... | 2 |
| Abstract..... | 3 |
| Dedication | 5 |
| Table of Contents | 6 |
| Table of Figures | 12 |
| Publications..... | 16 |
| Abbreviation..... | 17 |
| 1 Introduction | 24 |
| 1.1 The role of signalling pathways in the regulation of cell growth..... | 24 |
| 1.2 Family of ribosomal protein S6 kinases | 25 |
| 1.2.1 AGC family of serine/threonine kinases | 25 |
| 1.3 S6K1 and S6K2 isoforms and their subcellular localisation | 26 |
| 1.4 Structure and domain organisation..... | 27 |
| 1.5 Regulation of S6K activity..... | 29 |
| 1.5.1 The role of PI3K pathway signalling in the activation of S6K..... | 31 |
| 1.5.2 mTOR signalling to S6Ks..... | 34 |
| 1.5.3 Role of the MAPK/ERK pathway in the regulation of S6Ks..... | 36 |
| 1.5.4 Other positive regulators of S6Ks..... | 37 |
| 1.5.5 Negative regulation..... | 38 |

| | | |
|-------|--|----|
| 1.6 | Cellular Functions of ribosomal protein S6 kinases | 39 |
| 1.6.1 | Regulation of translation and ribosomal biogenesis | 40 |
| 1.6.2 | Control of cell cycle progression, cell size and proliferation. | 42 |
| 1.6.3 | Cell survival..... | 44 |
| 1.6.4 | Cytoskeleton rearrangements..... | 46 |
| 1.7 | Other targets for S6K and potential functions..... | 50 |
| 1.8 | Dysregulation of the S6K pathway in human pathologies | 52 |
| 1.8.1 | Malignant transformation..... | 52 |
| 1.8.2 | Metabolic disorders | 55 |
| 1.8.3 | Ageing, learning and memory | 56 |
| 2 | Materials and Methods | 58 |
| 2.1 | General materials..... | 58 |
| 2.1.1 | General laboratory reagents | 58 |
| 2.1.2 | Expression vector and primers..... | 58 |
| 2.1.3 | Antibodies..... | 58 |
| 2.2 | DNA and RNA manipulation | 59 |
| 2.2.1 | Oligonucleotide design | 59 |
| 2.2.2 | DNA amplification by the polymerase chain reaction | 59 |
| 2.2.3 | DNA digestion with restriction endonucleases..... | 59 |
| 2.2.4 | Ethanol precipitation of DNA product | 60 |
| 2.2.5 | Electrophoresis of DNA | 60 |
| 2.2.6 | Purification of DNA fragments from agarose gel | 61 |

| | | |
|--------|---|----|
| 2.2.7 | Dephosphorilation of the vector | 61 |
| 2.2.8 | Ligation of DNA fragments | 61 |
| 2.2.9 | Purification of plasmid DNA | 62 |
| 2.2.10 | Isolation of the Recombinant Bacmid DNA | 63 |
| 2.2.11 | mRNA purification..... | 64 |
| 2.2.12 | RT-PCR analysis | 65 |
| 2.3 | Bacterial methodology | 66 |
| 2.3.1 | Bacterial strains and growth media..... | 66 |
| 2.3.2 | Preparation of competent cells..... | 67 |
| 2.3.3 | Transformation of E.coli..... | 67 |
| 2.3.4 | Transformation of DH10Bac™ E. Coli | 68 |
| 2.4 | Cell culture methodology | 68 |
| 2.4.1 | Cryopreservation of cells | 68 |
| 2.4.2 | Insect Cells culture | 69 |
| 2.4.3 | Mammalian cell culture | 71 |
| 2.4.4 | Characterisation of stable cell lines..... | 74 |
| 2.5 | Production of anti-S6K2-S1 polyclonal antibodies..... | 76 |
| 2.5.1 | Generation of rabbit antisera..... | 76 |
| 2.5.2 | Affinity purification of antibodies | 76 |
| 2.6 | Lentivirus generation | 77 |
| 2.6.1 | Generation of the virus | 77 |
| 2.6.2 | Lentiviral infection | 78 |
| 2.7 | Protein purification and analysis | 78 |

| | | |
|-------|--|-----|
| 2.7.1 | Preparation of mammalian cells extracts | 78 |
| 2.7.2 | Preparation of insect cells extracts | 79 |
| 2.7.3 | Estimating of protein concentration | 79 |
| 2.7.4 | SDS-PAGE electrophoresis | 79 |
| 2.7.5 | Immunoblotting | 80 |
| 2.7.6 | Coomassie Blue staining | 81 |
| 2.7.7 | Immunoprecipitation | 81 |
| 2.7.8 | Affinity purification of S6K2-S1 protein from Sf9 cells..... | 82 |
| 2.8 | Xenograft studies in nude mice | 83 |
| 2.8.1 | Preparation of tumour samples | 83 |
| 3 | Analysis of the existence of potential S6K2 splicing isoforms | 85 |
| 3.1 | Introduction | 85 |
| 3.2 | Results | 88 |
| 3.2.1 | Bioinformatic analysis reveals the existence of potential S6K2 splicing isoforms | 88 |
| 3.2.2 | RT-PCR analysis confirms the existence of S6K2-S1 in HEK293 cells | 99 |
| 3.2.3 | Molecular cloning and mammalian expression of the S6K2-S1 splicing isoform..... | 104 |
| 3.2.4 | Generation and characterisation of specific polyclonal antibodies directed towards S6K2-S1 | 109 |
| 3.3 | Discussion | 115 |
| 4 | S6K2-S1 and S6K2wt form a regulatory complex with Raptor and mTOR | 118 |

| | | |
|-------|--|-----|
| 4.1 | Introduction | 118 |
| 4.2 | Results | 121 |
| 4.2.1 | Generation of baculovirus for Raptor and Rictor | 121 |
| 4.2.2 | Molecular cloning and expression of S6K2-S1 in baculovirus expression system | 128 |
| 4.2.3 | S6K2-S1 specifically interacts with Raptor, but not Rictor in insect cells | 132 |
| 4.2.4 | Lentivirus generation of HEK293 stable cell lines overexpressing full length S6K2 and splicing isoform S6K2-S1.... | 134 |
| 4.2.5 | Raptor and mTOR coimmunoprecipitate with full length S6K2 and splicing isoform S1 <i>in vivo</i> | 140 |
| 4.3 | Discussion | 142 |
| 5 | Functional analysis of the S6K2 S1 splicing isoform | 145 |
| 5.1 | Introduction | 145 |
| 5.2 | Results | 146 |
| 5.2.1 | Overexpression of full length S6K2 and S6K2-S1 splicing isoform affects cell size the opposite way | 146 |
| 5.2.2 | S6K2-S1 isoform does not affect cell proliferation | 156 |
| 5.2.3 | S6K2-S1 can modulate the activity of the mTOR/S6K pathway in starved condition | 158 |
| 5.2.4 | S6K2-S1 is implicated in the regulation of cell migration | 163 |
| 5.2.5 | Cells overexpressing S6K2-S1 show higher sensitivity to drug-induced apoptosis | 169 |

| | | |
|-------|--|-----|
| 5.2.6 | S6K2-S1 is a potential tumour suppressor, whereas full length S6K2 exhibits oncogenic properties | 173 |
| 5.2.7 | Xenograft studies in nude mice..... | 179 |
| 5.3 | Discussion | 183 |
| 6 | General discussion and future studies | 187 |
| 7 | Appendix A | 198 |
| 8 | Appendix B | 202 |
| 9 | Reference list..... | 204 |

Table of Figures

| | |
|---|-----|
| Figure 1.1 Schematic domain organization of S6K1 and S6K2 isoforms. | 28 |
| Figure 1.2 Activation mechanism for S6K. | 31 |
| Figure 1.3 Signalling pathways upstream of ribosomal protein S6 kinases..... | 33 |
| Figure 1.4 Downstream substrates and cellular functions controlled by S6Ks..... | 39 |
| Figure 1.5 S6Ks exist in different complexes..... | 46 |
| Figure 1.6 S6K1 regulates cell migration..... | 48 |
| Figure 3.1 Schematic diagram of alternative splicing of human S6K2 gene and primary structure of potential splicing isoforms. | 91 |
| Figure 3.2 Analysis of S6K2-S1 nucleotide sequence. | 93 |
| Figure 3.3 Analysis of S6K2-S2 nucleotide sequence.. | 94 |
| Figure 3.4 Analysis of S6K2-S3 nucleotide sequence. | 95 |
| Figure 3.5 Protein sequences of S6K2 splicing isoforms. | 100 |
| Figure 3.6 Schematic representation of S6K2 isoforms..... | 101 |
| Figure 3.7 Analysis of S6K2-S1 expression in HEK293 cell lines by RT-PCR. | 103 |
| Figure 3.8 Molecular cloning of S6K2-S1 splicing isoform into pcDNA3.1 expression plasmid..... | 106 |
| Figure 3.9 Generation of stable cell lines overexpressing S6K2-S1. | 107 |
| Figure 3.10 Affinity purification of polyclonal anti-S6K2-S1 antibodies. | 111 |

| | |
|--|-----|
| Figure 3.11 Characterisation of affinity purified polyclonal anti-S6K2-S1 antibodies. | 114 |
| Figure 4.1 A model of regulatory interactions of S6K2wt and S6K2-S1 splicing isoform in TORC1 and downstream signalling..... | 120 |
| Figure 4.2 Generation of recombinant baculovirus and protein expression using Baculovirus Expression System..... | 122 |
| Figure 4.3 Molecular cloning of EE-tagged Raptor into baculovirus expression vector pFastBac1. | 124 |
| Figure 4.4 Molecular cloning of EE-tagged Rictor into baculovirus expression vector pFastBac1. | 126 |
| Figure 4.5 Expression of EE-Raptor and EE-Rictor in insects Sf9 cells.. | 127 |
| Figure 4.6 Molecular cloning and baculovirus expression of N-terminally tagged Strep-S6K2-S1 and His-S6K2-S1..... | 129 |
| Figure 4.7 Molecular cloning, expression and affinity purification of the C-terminally FLAG-tagged S6K2-S1 using baculoviral expression system.. | 131 |
| Figure 4.8 S6K2-S1 specifically interacts with Raptor (mTORC1)..... | 133 |
| Figure 4.9 Overall strategy for Lentivirus generation..... | 135 |
| Figure 4.10 Molecular cloning of S6K2-S1 splicing isoform and S6K2wt into Lentivirus expression vector pLEX. | 136 |
| Figure 4.11 Generation of stable cell lines using Lentivirus constructs for the expression of S6K2wt and S6K2-S1..... | 139 |
| Figure 4.12 Coimmunoprecipitation of overexpressed EE-S6K2wt and EE-S6K2-S1 with endogenous Raptor and mTOR in HEK293 cells. | 141 |
| Figure 5.1 Cell size analysis of HEK293 and NIH3T3RasC40 cells with stable overexpression of S6K2-S1 splicing isoform. | 148 |

| | |
|---|-----|
| Figure 5.2 Generation of MEF TSC2 ^{-/-} p53 ^{-/-} stable cell lines overexpressing full-length S6K2 and splicing variant S6K2-S1. | 151 |
| Figure 5.3 Characterisation of MEF TSC2 ^{-/-} p53 ^{-/-} stable cell lines overexpressing full-length S6K2 and S6K2-S1 splicing isoform.. | 153 |
| Figure 5.4 Overexpression of S6K2-S1 splicing isoform reduces the size of MEF TSC2 ^{-/-} p53 ^{-/-} cells.. | 155 |
| Figure 5.5 Overexpression of S6K2-S1 in HEK293 cells does not affect cell proliferation. | 157 |
| Figure 5.6 Overexpression of S6K2-S1 in HEK293 cells affects the mTOR/S6K pathway in serum-starved cells. | 160 |
| Figure 5.7 Overexpression of S6K2-S1 in MEF TSC2 ^{-/-} p53 ^{-/-} cells affects the mTOR/S6K pathway in serum-starved cells. | 162 |
| Figure 5.8 Generation and characterisation of NIH3T3 RacC40 stable cell lines overexpressing S6K2-S1.. | 165 |
| Figure 5.9 Overexpression of S6K2-S1 in NIH3T3RasC40 cells affects early cell attachment to the plate. | 166 |
| Figure 5.10 Overexpression of S6K2-S1 in NIH3T3RasC40 cells inhibits cell migration measured by wound healing assay. | 168 |
| Figure 5.11 Staurosporin treated A549 cells with stable overexpression of S6K2-S1 shows higher level of cleaved PARP when compared to control cells. | 170 |
| Figure 5.12 Cells overexpressing EE-S6K2-S1 show higher sensitivity to cisplatin-induced apoptosis. | 172 |
| Figure 5.13 Overexpression of S6K2-S1 isoform inhibits anchorage-independent colony formation in soft agar. | 176 |
| Figure 5.14 Overexpression of S6K2-S1 splicing variant in A549 cells supresses colony formation in soft agar.. | 177 |

| | |
|--|-----|
| Figure 5.15 Analysis of tumours growth in a xenograft mouse model.. | 181 |
| | |
| Figure 5.16 Overexpression of S6K2-S1 reduces tumour growth in a xenograft mouse model. | 182 |
| Figure 6.1 Mechanism of alternative splicing of S6K1 gene. | 189 |
| Figure 6.2 Generation of an S6K2-/- allele. | 190 |

Publications

Ismail HM, Myronova O, Tsuchiya Y, Niewiarowski A, Tsaneva I, Gout I. "Identification of the general transcription factor Yin Yang 1 as a novel and specific binding partner for S6 kinase 2". *Cell Signal*. 2013 May; 25(5): 1054-63. doi: 10.1016/j.cellsig.2013.02.002. Epub 2013 Feb 10

Myronova O, Munro C, Pedley B, Pardo O, Seckl J.M, Gout I. "The role of S6K2 splicing isoforms in mTOR signalling and cellular functions", manuscript in preparation, 2015

Ibrahim M, Myronova O, Pardo O, Seckl J.M, Gout I. "Regulation of S6K2 by arginine methylation", manuscript in preparation, 2015

Abbreviation

| | |
|--------|--|
| AMP | Adenosine monophosphate |
| AMPK | AMP-activated protein kinase |
| APC | Anaphase promoting complex |
| ATP | Adenosine triphosphate |
| BAD | Bcl-2-associated death promoter |
| Bcl-2 | B-cell lymphoma 2 |
| Bcl-xL | B-cell lymphoma-extra-large |
| BSA | Bovine serum albumin |
| cAMP | Adenosine 3',5'-cyclic monophosphate |
| CBP | CREB binding protein |
| CBP80 | 80 kDa subunit of RNA cap-binding complex |
| CBC | Cap-binding complex |
| C-CAM1 | Cell-cell adhesion molecule |
| Cdc42 | Cell division control protein 42 homolog |
| cDNA | Complementary DNA |
| CREM | cAMP-responsive activator modulator |
| Deptor | DEP-domain-containing mTOR-interacting protein |

| | |
|-------------|---|
| DMEM | Dulbecco's modified Eagle's medium |
| DMSO | Dimethyl sulphoxide |
| DNA | Deoxyribonucleic acid |
| dNTP | Deoxyribonucleoside triphosphate |
| DTT | Dithiotreitol |
| 4E-BP1 | Eukaryotic initiation factor-4E binding protein 1 |
| ECL | Enhanced chemiluminescence |
| EDTA | Ethylenediaminetetra-acetic acid |
| eIF4A | Eukaryotic initiation factor 4A |
| eIF4B | Eukaryotic initiation factor 4B |
| eEF2K | Eukaryotic elongation factor 2 kinase |
| E2F | Early promoter 2 factor |
| EJC | Exon junction complex |
| EGF | Epidermal growth factor |
| EGTA | Ethyleneglycol-bis(β -aminoethyl)-N,N,N',N'-tetraacetic acid |
| ELISA | Enzyme-linked immunosorbent assay |
| EMT | Epithelial to mesenchymal transition |
| ER α | Estrogen Receptor |

| | |
|------------|---|
| α K | Extracellular signal-regulated kinase |
| EST | Expressed sequence tag |
| FGF | Fibroblast growth factor |
| FBS | Fetal bovine serum |
| FKBP12 | FK506-binding protein 12 |
| FTD | Frontotemporal dementia |
| GAP | GTPase-activating protein |
| GFP | Green Fluorescent Protein |
| GSK | Glycogen synthase kinase |
| HM | Hydrofobic motif |
| hSNF5 | SWI/SNF-related matrix-associated actin-dependent regulator |
| hnRNPs | Heterogeneous nuclear ribonucleoproteins |
| Ig | Immunoglobulin |
| IGF-1 | Insulin-like growth factor 1 |
| IP | Immunoprecipitation |
| IRS-1 | Insulin receptor substrate 1 |
| KLH | Keyhole limpet hemocyanin |
| LAM | Lymphangi leiomyomatosis |

| | |
|----------|--|
| 5`-LTR | Long terminal repeat |
| LY294002 | morpholine-containing chemical compound, inhibitor of phosphoinositide 3-kinases |
| mLST8 | Mammalian lethal with Sec13 protein 8 |
| MAPK | Mitogen-activated protein kinase |
| MEK | MAPK kinase |
| MOPS | 3-(N-morpholino)propanesulfonic acid |
| mRNA | Messenger RNA |
| mRNP | Messenger ribonucleic acid protein |
| mSIN1 | Mammalian stress-activated protein kinase interacting protein |
| mTOR | Mammalian target of rapamycin |
| Ni-NTA | Nickel-nitrilotriacetic acid |
| NLS | Nuclear localisation signal |
| NMD | Nonsense Mediated Decay |
| NSCL | Non-small cell lung cancer |
| OD | Optical density |
| PBS | Phosphate buffered saline |

| | |
|-----------------------------|--|
| PDGF | Platelet-derived growth factor |
| PDK1 | 3`-Phosphoinositide-dependent kinase-1 |
| PDZ | Postsynaptic density-95, discs large, zona occludens-1 |
| PEG | Polyethylene glycol |
| PH | Pleckstrin homology |
| PI(3)K | Phosphatidylinositide-3`-kinase |
| PKA | Protein kinase A |
| PKB/Akt | Protein kinase B |
| PKC | Protein kinase C |
| PCR | Polymerase chain reaction |
| PP2A | Protein-serine/threonine phosphatase 2A |
| p90 ^{RSK} | p90 Ribosomal S6 kinase |
| PtdIns(3)P | Phosphatidylinositol-3-phosphate |
| PtdIns(3,4)P ₂ | Phosphatidylinositol-3,4-bisphosphate |
| PtdIns(3,5)P ₂ | Phosphatidylinositol-3,5-bisphosphate |
| PtdIns(3,4,5)P ₃ | Phosphatidylinositol-3,4,5-trisphosphate |
| Pre-mRNA | Pre-messenger RNA |
| PRAS40 | Prolin-rich Akt substrate 40 kDa |
| Protor-1 | Protein observed with Rictor-1 |

| | |
|----------|---|
| PTC | Premature stop codons |
| PTEN | Phosphatase and tensin homologue, deleted on chromosome 10 |
| PVDF | Polyvinylidene difluoride |
| Rac-1 | Ras-related C3 botulinum toxin substrate 1 |
| Raf | Rapidly Accelerated Fibrosarcoma |
| Raptor | Regulatory-associated protein of mTOR |
| Ras | Rat sarcoma |
| Rictor | Rapamycin-insensitive companion of mTOR |
| RNA | Ribonucleic acid |
| rpS6 | Ribosomal protein S6 |
| rRNA | Ribosomal RNA |
| RSK | Ribosomal proteinS6-related kinases |
| RT-PCR | Real time polymerase chain reaction |
| S6K | Ribosomal protein S6 kinase |
| SDS | Sodium n-dodecyl sulfate |
| SDS-PAGE | SDS-polyacrylamide gel electrophoresis |
| SF2/ASF | Pre-mRNA-splicing factor SF2/ alternative splicing factor 1 |
| SGK1 | Serum- and glucocorticoid-induced protein kinase 1 |

| | |
|-------------|---|
| SH3 | Src homology 3 |
| SKAR | S6K1 Aly/REF-like target |
| snRNA | Small nuclear RNA |
| snRNPs | Small nuclear ribonucleic proteins |
| TOS | TOR signalling motif |
| TGF β | Transforming growth factor β |
| TM | Turn motif |
| TNF | Tumor necrosis factors |
| 5`-TOP | 5`-terminal oligopyrimidine tract |
| TRAIL | TNF-related apoptosis-inducing ligand |
| tRNA | Transfer RNA |
| TSC1 | Tuberous sclerosis 1 protein, hamartin |
| TSC2 | Tuberous sclerosis 2 protein, tuberin |
| Tween 20 | Polyoxyethylenesorbitan monolaurate |
| WW | Tryptophan-tryptophan |
| 5`-UTR | 5`-untranslated region |
| XIAP | X-linked inhibitor of apoptosis protein |

1 Introduction

1.1 The role of signalling pathways in the regulation of cell growth

Mammalian cells sense and promptly respond to changes in their environment through the induction of signalling pathways which are essential for the development, growth and survival of all organisms. Complex signalling mechanisms have developed during evolution of multicellular organisms to control and regulate responses to a great variety of stimuli and stresses. These pathways are activated by growth factors, hormones and nutrients via the interaction with specific cell-surface receptors. Extracellular signals are then transmitted inside cells by multifunctional signalling cascades, which in turn regulate cellular processes, such as cell growth and size, cell cycle progression and proliferation, differentiation etc. (Yang and Xu 2011).

Studies in cell-based and animal models have revealed two major signalling pathways in the regulation of cell growth, proliferation and survival: the MEK/ERK mitogen activated protein (MAP) kinase pathway and the PI3K/mTOR signalling pathway.

In response to mitogenic stimulation, initiation and maintenance of a high level of protein synthesis is one of the major responses, which contribute to the ability of the cell to progress through the cell cycle, leading to cell growth, DNA synthesis, and cell division. This response is associated with the formation of multienzyme regulatory complexes around activated receptors and the increase in covalent post-

translational modification of signalling proteins, such as phosphorylation, ubiquitination, acetylation etc. (Jastrzebski et al. 2007).

The ribosomal protein S6 kinases (S6Ks) are important signalling components of nutrient- and mitogen-stimulated pathways involved in the regulation of cellular biosynthetic processes, cell growth and energy metabolism (Proud 1996).

1.2 Family of ribosomal protein S6 kinases

1.2.1 AGC family of serine/threonine kinases

The ribosomal protein S6 kinase is a member of the AGC superfamily of structurally related Ser/Thr protein kinases, which also include protein kinase C (PKC), protein kinase B (PKB/Akt), phosphoinositide-dependent kinase 1 (PDK1), cyclic-nucleotide-dependent kinases (PKA and PKG), and SGK1 (serum- and glucocorticoid-induced kinase 1). These kinases have a similar mode of activation and preferentially phosphorylate Ser/Thr residues surrounded by basic amino acids, such as lysine and arginine. The main feature of the AGC kinase family members, except PDK1, is the presence of a C-terminal extension (CT) to the catalytic domain that contains a conserved hydrophobic motif (HM) with a phosphorylation site, which in many AGC kinases mediates a docking interaction with PDK1. It has been demonstrated that mTOR phosphorylates the HM site in AGC kinases, which creates a specific binding motif for PDK1. The phosphorylation of the activation loop site by PDK1 culminates the activation process of AGC kinases (Peterson and Schreiber 1999).

1.3 S6K1 and S6K2 isoforms and their subcellular localisation

A family of 70kDa ribosomal S6 kinase include four members (referred to as p70 S6K1 and p85 S6K1, p54 S6K2 and p56 S6K2) which are encoded by two separate genes (S6K1/S6K α and S6K2/S6K β).

Over the last two decades, the majority of published research on ribosomal S6 kinases has been done on p70S6K1. This isoform was cloned from a rat liver cDNA library more than twenty years ago. The p70 S6K1 is ubiquitously expressed and localises predominantly in the cytoplasm. The p85 S6K1 is a product of an alternative start codon, which produces a protein with a 23 amino acids extension at the N-terminus. The presence of a nuclear localisation signal (NLS) in the N-terminal extension targets this isoform to the nucleus (Kozma et al. 1990).

A decade later, a closely related homologue of S6K1 was cloned by several groups and named as S6K2 (Gout et al. 1998;Koh et al. 1999;Shima et al. 1998). The S6K2 gene was also found to generate two isoforms by the use of alternative start codon: the short form (p54S6K2) and the long form (p56S6K2). They differ by the presence of additional 13 amino acids at the N-terminus of p56S6K2, which contain the nuclear localisation signal (Gout et al. 1998). Both S6K2 isoforms contain a second nuclear localisation signal at the C-terminus, which targets them preferentially to the nucleus (Koh et al 1999).

The localisation of the S6K1 and S6K2 to different compartments in the cell suggests that they may have distinct cellular targets and functions.

1.4 Structure and domain organisation

Both S6K2 and S6K1 share domain homology with many serine/threonine kinases. The structure of S6Ks can be divided into several functionally significant regulatory regions and domains: an acidic N-terminus which contains TOS (TOR signalling) motif; catalytic kinase domain that has T-loop; kinase extension domain possessing the TM (turn motif) and HM (hydrofobic motif) sites; the C-terminus, containing a basic autoinhibitory pseudosubstrate region (Figure 1.1). The acidic N-terminus is thought to interact with the basic C-terminal autoinhibitory domain and thus this interaction keeps the kinase in a closed inactive conformation.

The catalytic domains of S6K1 and S6K2 exhibit 83% amino acid identity, with less homology in their N- and C-terminal regions. The pseudosubstrate C-terminal domains and kinase extensions are also analogous and possess a number of conserved serine/threonine phosphorylation sites, important for the activation of these kinases (Gout et al. 1998;Saitoh et al. 1998;Weng et al. 1998).

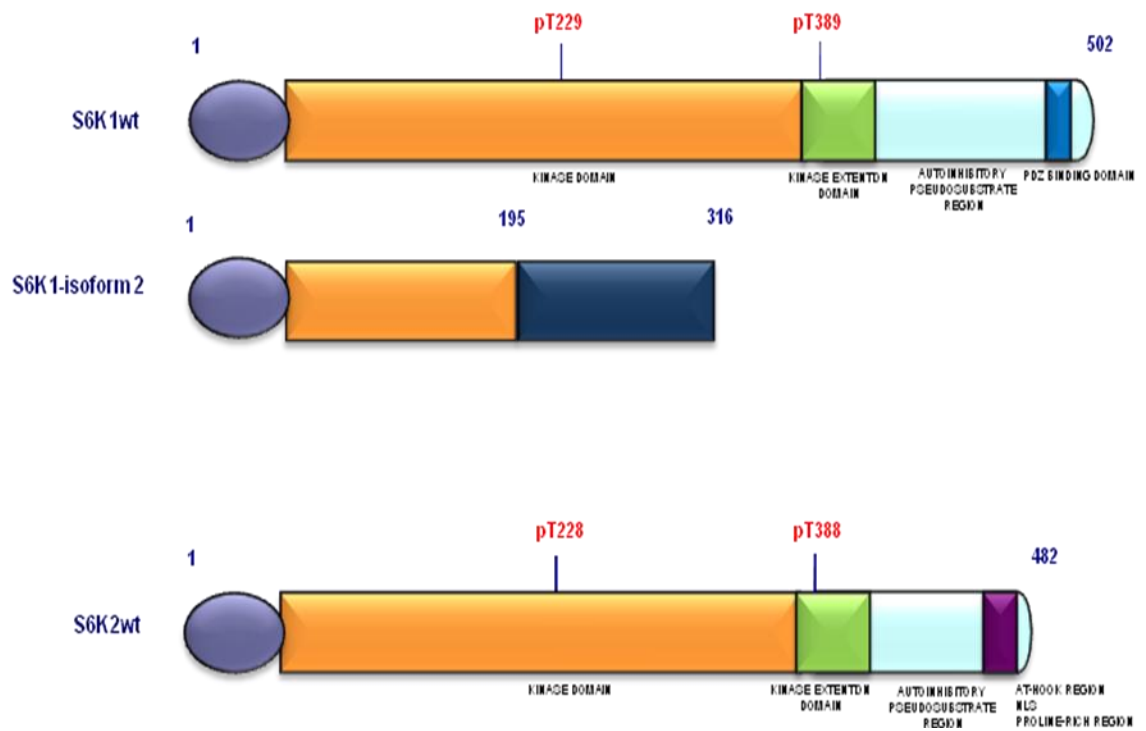


Figure 1.1 Schematic domain organization of S6K1 and S6K2 isoforms. S6K can be divided into several functionally significant regulatory domains: an acidic N-terminus; catalytic kinase domain; kinase extension domain; C-terminus, containing a basic autoinhibitory pseudosubstrate region.

S6K2 and S6K1 differ in their extreme N- and C-terminal domains. At the C-terminus, S6K1 has a PDZ binding motif, which is not present in S6K2. This domain recruits S6K1 to the cytoskeleton via the interaction with neurabin (Burnett et al. 1998). In contrast, S6K2 possesses a unique proline-rich sequence in C-terminus regulatory region which may mediate the interaction with SH3- or WW domain-containing proteins. Moreover, the S6K2 C-terminus contains an amino acid sequence with the high homology to a DNA binding motif, known as the AT hook. This motif is present in a diverse range of cellular proteins and was found to bind to the minor groove of DNA rich in A and T nucleotides, known as 'AT-rich' regions.

Recently, a novel S6K1 splice variant named S6K1-isoform 2, or p31S6K1, was identified (Ben-Hur et al. 2013;Karni et al. 2007). This splicing isoform is a product of a splicing-induced frame shift, which lacks half of the kinase domain, kinase extension and autoinhibitory regions. The shift in the reading frame results in a unique amino acids extension at the C-terminus (Figure 1.1). Interestingly, the p31S6K1 isoform lacks the kinase activity, but possesses an oncogenic potential when tested in cell-based and animal models (Karni et al. 2008). Evidence also exists for yet another S6K1 splice isoform with the molecular weight of approximately 60kDa, which is expressed at detectable level in breast cancer cell lines (Kim et al. 2009). However, this might be the product of proteolytic degradation of the full length S6K1.

Although S6K1 and S6K2 share a high degree of identity in their kinase domains, they have similar as well as distinct functions in the organism (Pende et al. 2000;Pende et al. 2004;Shima, Pende, Chen, Fumagalli, Thomas, & Kozma 1998;Um et al. 2004). Structural differences between S6K2 and S6K1 suggest that: 1) they can have distinct binding partners/substrates; 2) they might be regulated by different mechanisms; 3) they may form different molecular complexes; 4) they might be localized in distinct compartments within the cell.

1.5 Regulation of S6K activity

S6 kinases are activated in response to growth factors, hormones, cellular stresses and nutrients. Availability of nutrients and energy is critical in the induction of cellular biosynthetic processes which provide macromolecules for cell growth and proliferation.

Full activation of S6 kinases requires signals from two major signal transduction pathways: the phosphatidylinositol 3-kinase (PI3K) and the mammalian target of rapamycin (mTOR).

Identification of a number of regulatory phosphorylation sites involved in the activation of S6Ks indicates that the process of activation requires complex stepwise signalling inputs controlled by different Ser/Thr protein kinases.

The first step in the S6K activation in response to different stimuli involves priming phosphorylation of four sites located in the C-terminal autoinhibitory pseudosubstrate region (Ser411, Ser418, Ser421 and Ser424), which were found to be principal sites of mitogen-induced phosphorylation. This step relieves the inhibitory effect, thus inducing protein conformation changes leading to further phosphorylation events at Ser371 and Thr389 residues. The phosphorylation of these sites is blocked in response to rapamycin (specific inhibitor of mTOR) or wortmannin (inhibitor of PI3K) treatment. Finally, maximal S6K activation is achieved when PDK-1 phosphorylates Thr229 site in the T-loop of the catalytic domain (Dennis et al. 1996;Weng et al. 1995). Three of these sites are absolutely critical for the S6K activation: Thr389, Ser371 and Thr229, as mutations of these residues block the kinase activation (Figure 1.2) (Dennis, Pullen, Kozma, & Thomas 1996;Ferrari et al. 1992;Weng et al. 995).

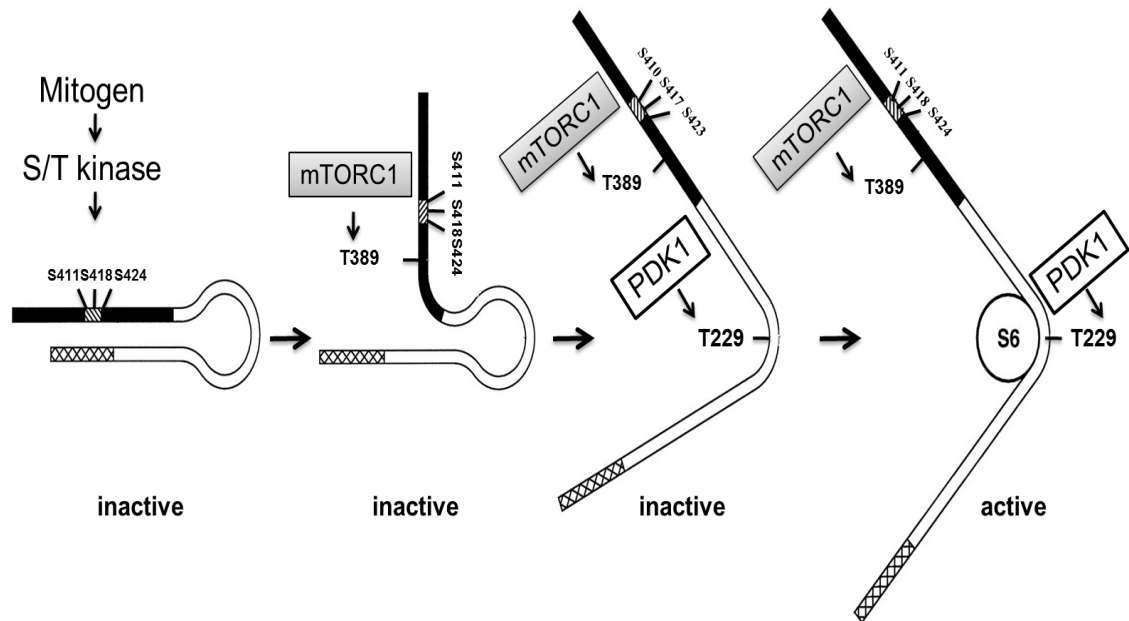


Figure 1.2 Activation mechanism for S6K. The acidic N-terminus interacts with the basic C-terminus autoinhibitory domain and keeps the kinase in a closed inactive conformation. The first step in S6 kinases activation in response to mitogens involves the phosphorylation of four sites located in the C-terminal autoinhibitory pseudosubstrate region. Following these phosphorylation events, mTOR kinase phosphorylates full-length S6K at Thr389 residue located in hydrophobic motif, which in turn allows PDK1 to phosphorylate Thr229 in the kinase domain and fully activate S6 kinase.

It is important to note that these sites, as well as domains where they are located, are conserved in most members of the AGC kinase family. A similar mode of activation has therefore been proposed for the phosphorylation of these sites and subsequent activation of other members of the AGC family.

1.5.1 The role of PI3K pathway signalling in the activation of S6K

The family of phosphoinositide 3-kinases (PI3Ks) consists of four classes of lipid kinases, which are involved in diverse cellular processes, including cell growth and cell survival, angiogenesis and cardiovascular homeostasis, metabolic control and the immune response. Notably, it

is one of the most commonly dysregulated signalling pathways in cancer.

The interaction of different mitogens with their receptors on the cell surface, results in the activation of phosphatidylinositol 3-kinase (PI 3-kinase) and the phosphorylation of phosphatidylinositol 4,5-bisphosphate (PtdIns(4,5)P₂, PIP₂) to generate the phosphatidylinositol 3,4,5-trisphosphate (PtdIns(3,4,5)P₃ or PIP₃). PIP₃ functions as a second messenger and activates various signalling pathways through specific interaction with PH domain-containing proteins, including PKB/Akt and PDK1 (Liu et al. 2009).

PDK1 (3-Phosphoinositide Dependent Protein Kinase 1) functions downstream of PI3K and is the main regulator for the AGC family of kinases. One of the most studied targets of the PI3Ks is serine/threonine protein kinase AKT (also known as protein kinase B (PKB)). It is activated via generated PIP₃, which brings two serine/threonine kinases, PDK1 and AKT into close proximity on the membrane, where AKT is phosphorylated on Thr308 residue by PDK1. Upon activation, AKT phosphorylates and regulates the function of a number of essential proteins, leading to inhibition of apoptosis, stimulation of glucose uptake and storage, promotion of cell division, and others cellular processes. The tumour suppressor PTEN (phosphatase and tensin homologue) is the most significant negative regulator of the PI3K signalling pathway (Figure 1.3) (Mora et al. 2004).

S6K was one of the first AGC kinases identified as downstream effectors of PI3-kinase. Consistently, activation of S6K in response to growth factors is inhibited by specific pharmacological inhibitors of PI3-kinase,

wortmannin and LY294002 (Chung et al. 1994). In addition, overexpression of constitutively active catalytic subunit of PI3-kinase enhances the activity of S6K (Weng et al. 1998).

S6K is one of the main substrates for PDK1, where activated PDK1 phosphorylates Thr229 site in the activation T-loop of S6K kinase domain (Figure 1.3) (Pullen and Thomas 1997).

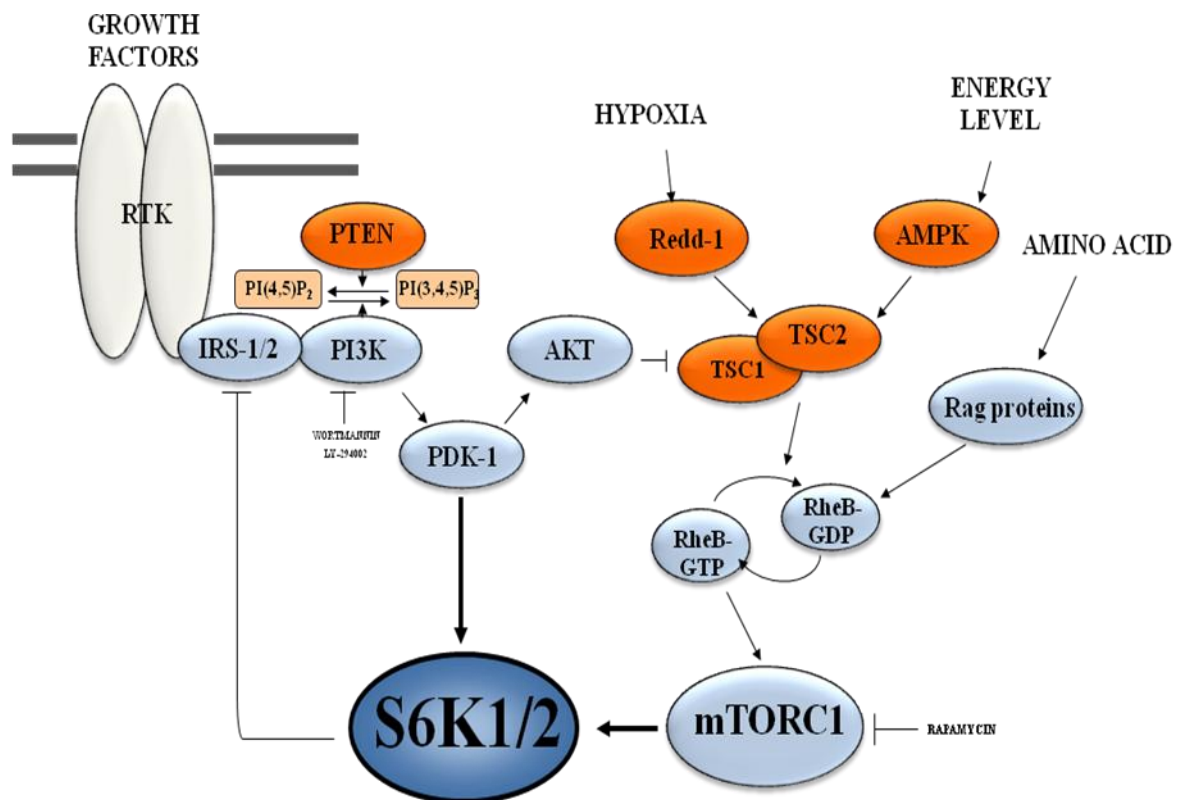


Figure 1.3 Signalling pathways upstream of ribosomal protein S6 kinases. Full activation of S6K requires signals from two pathways which are mediated via the phosphatidylinositol 3-kinase (PI3K) and the mammalian target of rapamycin (mTOR).

1.5.2 mTOR signalling to S6Ks

mTOR is a serine/threonine protein kinase and belongs to the PIKK (PI3K-related kinase family). It responds to diverse cellular signals (e.g. growth factors, mitogens, hormones, nutrients, energy, and stress) and regulates cellular processes such as cell proliferation and growth, apoptosis, cell survival and metabolism (Gentilella et al. 2015;Guertin and Sabatini 2007;Laplante and Sabatini 2012;Zoncu et al. 2011).

mTOR forms two different complexes inside mammalian cells: mTOR complex 1 (mTORC1) and mTOR complex 2 (mTORC2). mTORC1, in addition to mTOR contains four regulatory proteins: proline-rich AKT substrate 40 kDa (PRAS40); mammalian lethal with Sec13 protein 8 (mLST8); regulatory-associated protein of mTOR (Raptor); and DEP-domain-containing mTOR-interacting protein (Deptor). mTORC2 consists of mTOR; rapamycin-insensitive companion of mTOR (Rictor); mLST8; protein observed with Rictor-1 (Protor-1); mammalian stress-activated protein kinase interacting protein (mSIN1) and Deptor (Ma and Blenis 2009).

Growth factors and hormones activate mTOR via the canonical PI3K signalling pathway. Insulin binds to and activates its cell-surface receptors. In an activated state, insulin receptor phosphorylates insulin receptor substrate 1 (IRS-1), which leads to generation of PIP3 through the activation of PI3K. These events promote the recruitment to the membrane and activation of Akt. Akt activates mTORC1 by phosphorylating tuberous sclerosis 2 protein (TSC2; also known as tuberin) to remove its inhibitory effects on mTORC1. In addition, Akt

can also act on mTORC1 via direct phosphorylation of its negative regulator PRAS40 (Guertin & Sabatini 2007).

mTOR senses the level of cellular energy and blocks protein translation when the AMP:ATP ratio is high. The role of an “energy sensor” for mTOR plays AMP-activated protein kinase (AMPK). This kinase is activated when the level of AMP increases. Activated AMPK inhibits mTOR activity via phosphorylation and activation of its negative regulator TSC2.

Low nutrient conditions strongly inhibit mTOR signalling, and the addition of amino acids to starved cells dramatically stimulates the mTOR activity. Recent studies found that Rag proteins, a family of related small GTPases, are responsible for amino acid-mediated activation of mTORC1 (Figure 1.3) (Efeyan et al. 2012;Efeyan and Sabatini 2013;Ma & Blenis 2009).

The most extensively studied downstream targets of mTORC1 are S6Ks and eukaryotic translation initiation factor 4E-binding protein 1 (4E-BP1), both of which are implicated in the regulation of protein biosynthesis.

Following the phosphorylation of the C-terminal autoinhibitory domain of S6K, mTOR kinase phosphorylates the full-length S6K at Thr389 residue located in the hydrophobic motif, which in turn allows PDK1 to phosphorylate Thr229 in the kinase domain and fully activate S6 kinase. It is well established that immunosuppressant drug rapamycin (specific inhibitor of mTOR) blocks S6K activation by all known stimuli, without any effect on PI3K or PDK1 activities (Figure 1.2) (Pullen & Thomas 1997).

1.5.3 Role of the MAPK/ERK pathway in the regulation of S6Ks

Mitogen-activated protein kinase (MAPK) pathways play an important role in the transduction of extracellular signals to cellular compartments. One of four mitogen-activated protein kinase (MAPK) signaling pathways, the MAPK/Ras/Raf/ERK1/2 (extracellular-signal-regulated kinase) is at the centre of signalling networks that induce proliferation, differentiation, cell survival and apoptosis. Dysregulation of the ERK1/2 cascade has been associated with more than half of human cancers.

Activated ERK1/2 can either translocate to the nucleus or stay in the cytoplasm. Nuclear localisation of ERK1/2 is essential for DNA replication and gene expression. ERK1/2 phosphorylates a number of substrates, including transcription factors and a family of 90 kDa ribosomal protein S6-related kinases (RSK) (Dhillon et al. 2007).

MAPK/Ras/Raf/ERK signalling activates the PI3-kinase pathway, where Ras GTPase induces the membrane translocation and activation of the catalytic subunit of class 1A PI3K kinase. This event activates both PI3K and mTOR signalling pathways which leads to the activation of S6Ks. In addition, mTOR can be activated directly by RSK, which is a downstream effector of MAPK/Ras/Raf/ERK signalling. In an activated state, RSK phosphorylates TSC2 and inhibits its negative activity towards mTORC1 (Lawrence et al. 2008).

The MAPK/Ras/Raf/ERK cascade is one of the main pathways implicated in the phosphorylation of the autoinhibitory C-terminal domain of S6Ks, but this process is still not well-understood. It was shown that ERK1/2-dependent kinases are involved in the regulation of S6K2, but not S6K1.

S6K2 responds to the ERK inhibition in a much more sensitive manner than S6K1 (Linjun Wang et al. 2001). That might be explained by the amino acids differences in the C-terminal end of both kinases. It was demonstrated that the deletion of the C-terminal autoinhibitory domain in S6K1 and S6K2 has distinct consequences on the mode of activation. In case of S6K2, the activity is increased and the kinase becomes hypersensitive to PI3K signalling, whereas S6K1 activity is slightly inhibited (Martin et al. 2001b).

1.5.4 Other positive regulators of S6Ks

Protein kinase C (PKC) is a family of Ser/Thr kinases, which are involved in diverse cellular functions and signalling pathways. The members of atypical or novel PKC family were found to interact with mTOR and PDK1, suggesting that they may be involved in the activation of S6Ks. It has been demonstrated that S6Ks interact with the kinase domain of PKC, and this interaction is implicated in the activation of S6Ks (Richardson et al. 2004). Interestingly, it was shown that S6K2 is more sensitive to the activation by PKC than S6K1. This fact provides additional information to the differences in the regulation of S6K1 and S6K2 (Martin et al. 2001a). It was also reported, that S6K2, but not S6K1, is specifically phosphorylated by PKC at Ser486 in the C-terminal regulatory region, which abrogates nucleocytoplasmic shuttling of this isoform (Valovka et al. 2003).

Signalling via small GTPases Rac and Cdc42 has been also implicated in the regulation of S6Ks. Rac1 and Cdc42 are members of the Rho family of small GTPases, which are important for the regulation of actin cytoskeleton. These two proteins were shown to form regulatory

complexes with S6K1, leading to the increase in its kinase activity (Chou and Blenis 1996). At the same time S6K1 can stimulate the activity of Rac1 and Cdc42 and this activation is associated with cytoskeletal reorganisation (Ip et al. 2011).

1.5.5 Negative regulation

Several signalling events have been identified which are implicated in downregulating the S6K activity: a) the action of tumor suppressors PTEN and TSC1/2 and b) dephosphorylation of S6Ks.

Protein phosphatases are responsible for removing the phosphate group from the protein and alter the protein function. Protein phosphatase type 2A (PP2A) is a serine/threonine phosphatase, conserved in all eukaryotes. PP2A regulates DNA replication, transcription, metabolism, cell division, translation, apoptosis and other essential cellular processes.

The protein phosphatase PP2A has been identified as a major phosphatase involved in the inactivation of S6K. Rapamycin treatment, amino acid withdrawal and osmotic stress lead to rapid dephosphorylation and inactivation of S6Ks. Studies have shown that PP2A directly binds and dephosphorylates S6K (Parrott and Templeton 1999; Peterson et al. 1999). mTOR directly regulates PP2A function and inhibits its activity in cells. This process is dependent upon nutrient availability and is sensitive to rapamycin (Peterson, Desai, Hardwick, & Schreiber 1999).

1.6 Cellular Functions of ribosomal protein S6 kinases

Activation of S6Ks leads to phosphorylation of a number of downstream targets, such as ribosomal protein S6, eukaryotic elongation factor 2 kinases (eEF2K), eukaryotic initiation factor 4B (eIF4B), insulin receptor substrate (IRS-1) and many others. They regulate different cellular processes, such as protein synthesis, glucose homeostasis, mRNA processing, cell growth and cell survival (Fenton and Gout 2011; Iadevaia et al. 2014) (Figure 1.4).

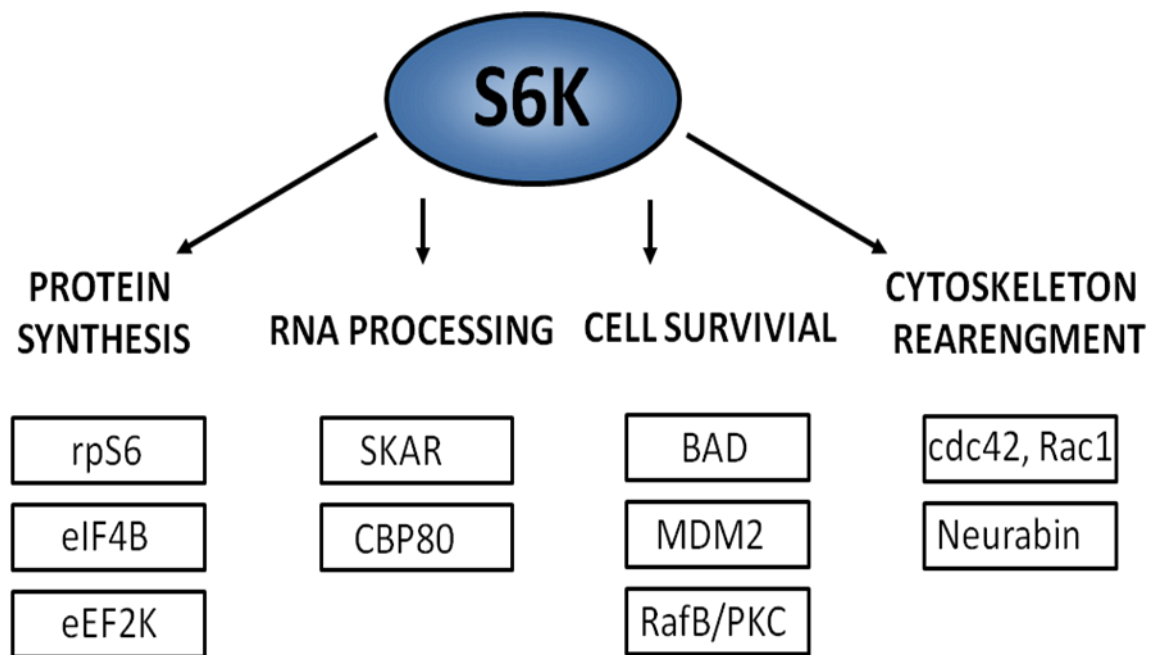


Figure 1.4 Downstream substrates and cellular functions controlled by S6Ks. Activation of S6Ks leads to phosphorylation of a number of downstream targets, which regulate different cellular processes.

Most of the studies have been done for S6K1 and limited information is available about S6K2 specific functions. While both kinases have mostly common substrates, the structural and functional differences between these two enzymes indicate that they might exist in different regulatory complexes and have distinct targets.

1.6.1 Regulation of translation and ribosomal biogenesis

Hormones and growth factors stimulate protein synthesis, but in response to various extracellular stresses this process is inhibited. In mammalian cells the control of mRNA translation involves changes in the phosphorylation and function of multiple components of the translational machinery. These components include ribosomal proteins, initiation and elongation factors (eIFs and eEFs correspondingly) (Iadevaia, Liu, & Proud 2014; Ma & Blenis 2009).

One of the most studied substrates for S6K is ribosomal protein S6 (rpS6), which is implicated in the upregulation of protein biosynthesis needed for cell growth and proliferation. RpS6 is one of the major ribosomal proteins, which is a part of 40S ribosomal subunit. RpS6 directly interacts with mRNA on 40S subunit, and its phosphorylation increases the binding affinity of 40S subunit to mRNA and thus enhances total protein biosynthesis (Jefferies et al. 1997). Phosphorylation of rpS6 in response to mitogens is an extremely conserved process, and several kinases are able to perform this function, such as S6Ks and p90RSK (Pende, Um, Mieulet, Sticker, Goss, Mestan, Mueller, Fumagalli, Kozma, & Thomas 2004).

Phosphorylation sites of rpS6 are represented by serine residues located at the carboxyl-terminus of the protein and the process of

phosphorylation proceeds in the order, Ser236>Ser235≥Ser240>Ser244>Ser247. Interestingly, p90RSK appears to phosphorylate only Ser235 and Ser236, S6K1 and S6K2 are capable to phosphorylate all five C-terminal rpS6 residues (Ferrari, Bannwarth, Morley, Totty, & Thomas 1992).

The phosphorylation of rpS6 is considered to control the translation of the 5'-TOP (tract of pyrimidine) mRNA in a positive manner, this mRNAs tend to encode components of the translation machinery.

In addition to its role in rpS6 phosphorylation, S6K has been implicated in the regulation of other proteins involved in the control of protein translation, such as cap-binding complex component eIF4B (eukaryotic translation initiation factor 4B). This phosphorylation is important for the recruitment of eIF4B to the translational pre-initiation complex. Upon activation S6K phosphorylates eIF4B on Ser422 within the RNA-binding region, and promotes the helicase activity of eIF4A (eukaryotic translation initiation factor 4A). RNA helicase activity of eIF4A is needed to unwind extensive secondary structures in the 5' UTR (untranslated regions) of specific mRNAs, which encode proteins important for cell cycle progression and cell survival.

A role for S6K1 in the regulation of the elongation step of translation is indicated by the demonstration that it phosphorylates eukaryotic elongation factor-2 kinase (eEF2K) at Thr56. This kinase negatively regulates translation elongation and S6K relieves this inhibition by direct phosphorylation. In this study, S6K2 demonstrated lower phosphorylation activity toward eEF2K compared to S6K1. This suggests that eEF2K phosphorylation may be a target for S6K1 in the

regulation of cell growth, a process in which S6K2 plays less important role (Wang et al. 2001).

It was demonstrated that p90RSK can phosphorylate both eIF4B and eEF2K under the same conditions. As a result, the overlapping substrate specificities of S6K and p90RSK allow distinct signalling pathways to regulate process of translation.

It was recently reported that S6K1 and S6K2 deficient mice had a defect in ribosomal biogenesis at a transcriptional level (Chauvin et al. 2014). By performing whole-genome microarray of total and polysomal mouse liver RNA researchers showed that transcription of more than seventy five percent of ribosomal biogenesis factors is controlled by both S6K1 and S6K2.

1.6.2 Control of cell cycle progression, cell size and proliferation

mTOR plays a central role in the coordination of cell growth and division, ensuring that cells reach a certain mass before they proceed into the process of cell division. Well-known downstream effectors of mTOR, S6Ks have been linked to the regulation of cell size in a number of studies.

Much of the information we know about the functions of S6Ks was obtained from genetic studies in mice and *Drosophila*. *Drosophila* has only one S6K gene and its deletion leads to the death of most flies during early development. Survived flies live only for a few weeks and females are sterile. S6K1^{-/-} flies are smaller than wild type and the

decrease in cell size is mostly due to a decrease in individual cell size rather than cell number (Montagne et al. 1999).

Studies in mice showed, that deletion of S6K1 is not fatal, but the mice are around 20% smaller at birth, and rpS6 phosphorylation is not dramatically affected. Expression of S6K2 was significantly increased in all tissues from S6K1-deficient mice. It proved that S6K1 and S6K2 functions are redundant and that a deletion of the S6K1 gene results in a compensatory increase in the S6K2 level. Interestingly, mice deficient for S6K1 exhibit hypoinsulinaemia, resulting in glucose intolerance. This is due to smaller pancreatic beta cells, which consequently produce less insulin (Pende et al. 2000).

S6K2^{-/-} mice grow to normal size, but had significantly decreased levels of S6 phosphorylation. These results suggest that S6K2 and S6K1 might have specific functions through distinct substrates (Pende et al. 2004).

Mice deficient for both genes showed a dramatic decline in viability due to perinatal lethality. Surviving mice exhibit growth reduction but have normal proliferation. Despite the severe suppression of S6 phosphorylation in cells from S6K1^{-/-}/S6K2^{-/-} mice, the translation of 5'-TOP mRNAs and cell cycle progression were not dysregulated. These data show a redundancy between the S6K and the MAPK pathways in regulating protein translation in response to mitogens (Pende et al. 2004).

Data from the S6K1^{-/-} and S6K2^{-/-} deficient mice did not show any dramatic effect on cell cycle progression and cell proliferation. There are some data indicating that the overexpression of S6K1 in NIH-3T3 cells induces the expression of cyclin E required for G1 progression

(Chou et al. 2003). But taken together all available information, one can speculate that although S6K1 has the potential to enhance the entry into S-phase, it is not required for cell cycle progression and may function in this way only in certain cell types or under specific conditions.

1.6.3 Cell survival

A balance between cell death and survival is a main mechanism to prevent the development of tumours. The PI3K/Akt/mTOR pathway is one of the most studied cell survival and cell death signalling pathways in human cancers. It is now well established that both S6Ks are implicated in the regulation of cell survival and apoptosis, involving different mechanisms.

S6K1 has been linked to cell survival and cell death through the regulation of a number of pro- and anti-apoptotic proteins. S6K1 phosphorylates pro-apoptotic protein BAD (Bcl-2-associated death promoter) at Ser136. This phosphorylation prevents BAD from interaction with anti-apoptotic factors Bcl-2 (B-cell lymphoma 2) and Bcl-xL (B-cell lymphoma-extra-large) to promote cell death (Harada et al. 2001). It was shown that reduction in AKT/mTOR/S6K1 signalling leads to the inhibition of Bcl-2. Silencing of S6K1 in human neuroblastoma SK-N-SH cells induced apoptosis accompanied by a decrease in the phosphorylation of BAD (Saito et al. 2012). Moreover, astrocytes deficient for S6K1 and S6K2 had a defect in BAD phosphorylation and in the expression of Bcl-2 and Bcl-xL proteins (Harada et al. 2001; Pastor et al. 2009).

Additionally, S6K1 may also regulate cell survival through phosphorylation of Mdm2 (murine double minute), a negative regulator of the p53 tumor suppressor. Upon genotoxic stress and DNA damage, the mTOR-S6K1 pathway is activated through p38 α MAPK. The activated S6K1 forms a complex with Mdm2 and inhibits Mdm2-mediated p53 degradation, promoting p53 induction. At the same time deactivation of mTOR-S6K1 signalling leads to nuclear localization of Mdm2 and an alteration in p53-dependent cell death. These results reveal the S6K1–Mdm2 complex as a new link between nutrients/energy/ growth factors status and the response to DNA damage (Lai et al. 2010).

In small cell lung cancer, S6K2 has been implicated in FGF-mediated chemoresistance and cell survival. Protein kinase C- ϵ (PKC ϵ) interacts with S6K2 via the Raf/MAPK (mitogen-activated protein kinase) signaling pathway and mediates the pro-survival effects of S6K2 (Figure 1.5A). Complex PKC ϵ /S6K2/BRaf induces the expression of anti-apoptotic proteins XIAP (X-linked inhibitor of apoptosis protein) and Bcl-xL (Pardo et al. 2001).

Recently, S6K2 rather than S6K1 was shown to be required for the survival of breast cancer cells. Silencing of S6K2 resulted in a significant increase in TRAIL (TNF-related apoptosis-inducing ligand) and TNF- α (Tumor necrosis factors) mediated apoptosis. In contrast to S6K1, downregulation of S6K2 inhibits AKT signalling and activate cell death via the regulation of Bid (pro-apoptotic Bcl-2 protein). This finding has a significant implication in the treatment of the breast cancer (Sridharan and Basu 2011).

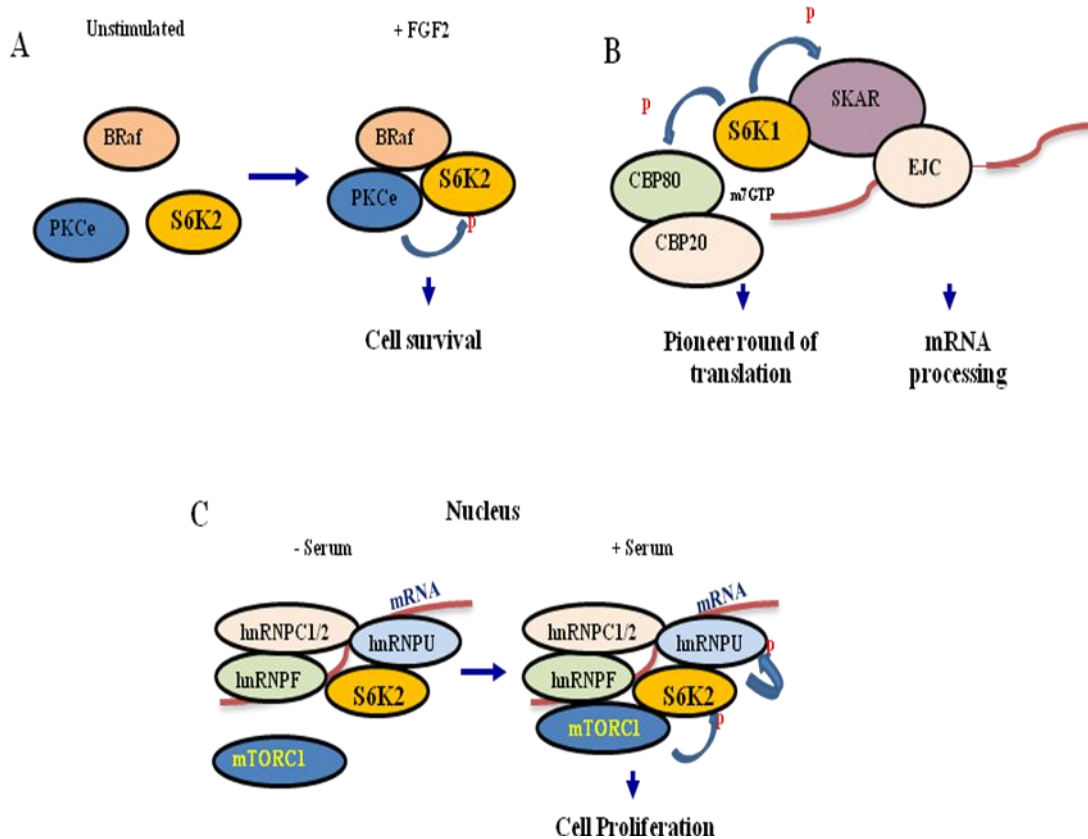


Figure 1.5 S6Ks exist in different complexes. (A) Stimulation cells with FGF2 leads to formation of the complex between S6K2, BRaf and PKC and promote S6K2 activation and cell survival. (B) S6K1 can regulate pioneer round of translation by phosphorylating CBP80 and it is implicated in mRNA processing via interaction with nuclear protein SKAR. (C) S6K2 interacts with hnRNPs, upon stimulation mTORC1 binds to this complex and promotes the activity of S6K2 and cell proliferation.

1.6.4 Cytoskeleton rearrangements

Cytoskeleton is organized to maintain cell shape, polarity and structural integrity. It coordinates important cellular processes such as cell adhesion, motility, migration and cell invasion. Reorganisation of actin cytoskeleton by polymerization and depolymerisation leads to morphological changes in cells, which stimulate migration. Dysregulation of cell migration plays an important role in embryonic development, immune response and wound healing, inflammation and cancer metastasis.

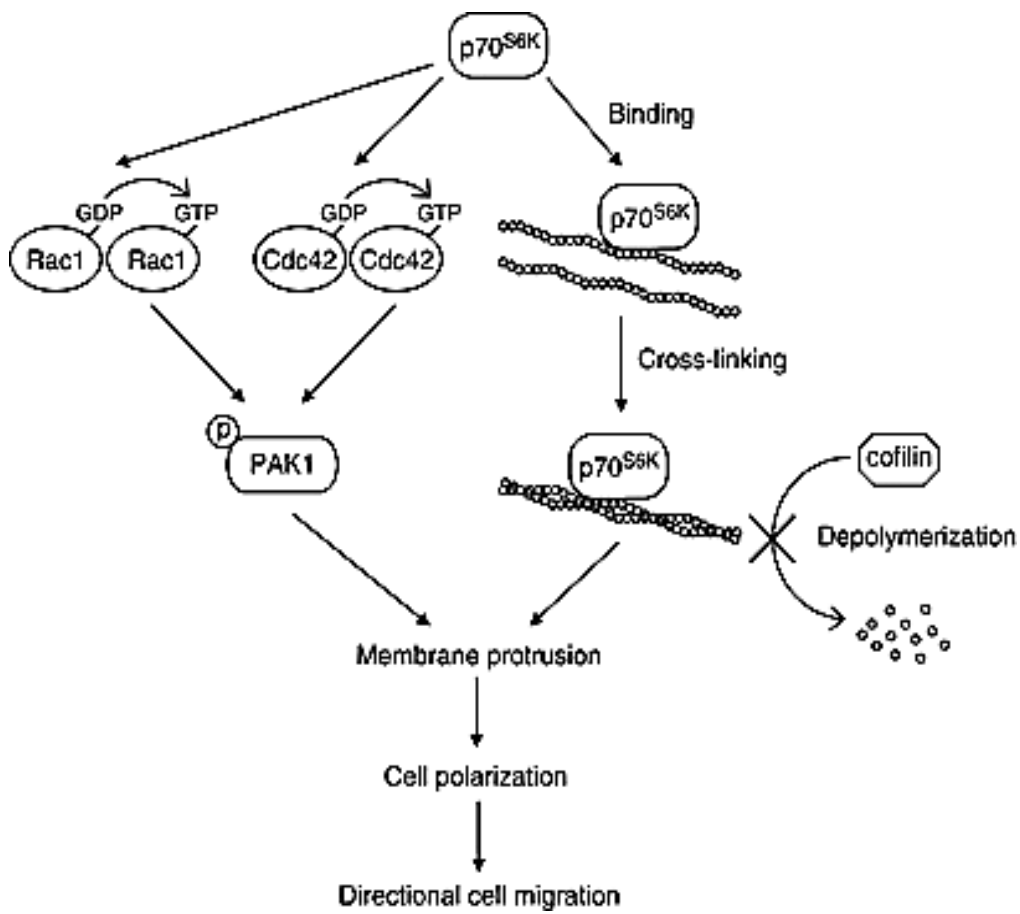
A lot of signalling proteins are implicated in cell migration, from cell receptors to transcription factors. Downstream signalling from activated cell receptors, implicated in migration, is mediated by secondary messengers such as phospholipase C, PKC, Ca^{2+} , Rho and Rac small GTPases, PI3K and MAPK.

Rho GTPases family of proteins is a central point for migration signalling. This family includes 22 different members, and the best-studied members are RhoA, Rac1 and Cdc42 proteins. They regulate cell motility, cell-cell adhesion and the interaction with the extracellular matrix as well as intracellular trafficking of proteins required for cells migration.

Rho GTPases are thought to rearrange the cytoskeleton by regulating the polymerization of actin into filaments that form the base of the cytoskeleton. Rac and Cdc42 stimulate the activation of the proteins to generate cellular extensions at the front of cells, which are required for cell movement (Yang et al. 2006).

Several studies have proposed a role for S6K1 in cytoskeleton reorganisation and, potentially, cell motility. S6K1 was shown to associate with and be activated by the small GTPases Rac1 and Cdc42 (Chou & Blenis 1996). At the same time S6K1 can stimulate the activity of both Rac1 and Cdc42 and their downstream target p21-activated kinase (PAK1), stimulating cell migration. In addition, overexpression of Cdc42 and Rac1 leads to an increase level of S6K1 in cells. Downregulation of S6K1 expression or its activity resulted in dramatic inhibition of actin cytoskeleton reorganization and decreased cell migration, with a related decrease in Cdc42, Rac1 and PAK1 activation

(Figure 1.6) (Ip, Cheung, Ngan, & Wong 2011; Yang, Wang, & Zheng 2006).



Ip, Cheung, Ngan, & Wong, 2011

Figure 1.6 S6K1 regulates cell migration. S6K regulates cell migration through regulation of Rac1 and Cdc42 activity and through binding, cross-linking and stabilizing cofilin filaments.

Additionally, the expression of active p70S6K1 in chicken embryo fibroblasts (CEF) is sufficient to stimulate cell migration and actin filaments re-modelling (Qian et al. 2004). Moreover, in migrating Swiss 3T3 fibroblasts, S6K1 is co-localised with actin-based structures of the leading edge, which is required for cell motility. And treatment of these cells with rapamycin resulted in the disruption of actin stress fibres formation (Berven and Crouch 2000).

S6K1 is highly activated in ovarian cancer and was shown to play a significant role in the metastasis development and progression (Ip, Cheung, Ngan, & Wong 2011; Ip and Wong 2012). Ectopic expression of constitutively active S6K1 in ovarian cancer cells promoted directional cell migration and stimulated reorganization of the actin cytoskeleton (Ip, Cheung, Ngan, & Wong 2011). Interestingly, S6K1 was shown to stimulate the phenotypic changes of cells during the progression of ovarian cancer. Activation of S6K1 results in loosing by cells epithelial and gaining fibroblast-like properties, named epithelial to mesenchymal transition (EMT). EMT is thought to play an important role in invasiveness of the tumour, when cell lose their adhesion and increase migration and invasion abilities. S6K1 are able to downregulate E-cadherin, important for cell adhesion, and to upregulate the expression of N-cadherin and vimetin, which are the markers for mesenchymal phenotype (Pon et al. 2008). Based on these studies, there is a strong link between S6K and cell migration, which is implicated in the progression of the cancer and metastasis.

1.7 Other targets for S6K and potential functions

There are a number of other targets of S6Ks, which are implicated in mRNA splicing and translation. It was shown, that S6K1 can regulate pioneer round of translation by phosphorylating CBP80, component of the cap-binding complex (CBC). S6K1 stimulate the activity of CBC80 to bind to 5' Cap of pre-mRNAs, and subsequently regulates pre-mRNA splicing, translation, nonsense-mediated mRNA decay and mRNA export. This phosphorylation was shown to be sensitive to rapamycin treatment (Figure 1.5B) (Wilson et al. 2000).

Recently a further link between S6K1 and the control of RNA processing was shown. Nuclear protein SKAR (homology to the Aly/REF family of RNA binding proteins) was identified in a yeast two-hybrid screening as a new target specific for S6K1, not S6K2. S6K1 phosphorylates SKAR at Ser383/385 residues *in vitro* and these phosphorylations are mitogen-dependent and sensitive to rapamycin *in vivo*. SKAR is thought to link transcription with pre-mRNA splicing and mRNA export. Decreasing SKAR levels by siRNA makes cells smaller. Taking into account the specific role of S6K1, but not S6K2 in cell growth, SKAR might be one of the effectors for S6K1 important for cell growth signalling (Figure 1.5B) (Ma et al. 2008;Richardson, Broenstrup, Fingar, Julich, Ballif, Gygi, & Blenis 2004).

A regulatory link between S6K2 signalling, cell cycle progression and proliferation has been recently revealed. S6K2 was found to be in a complex with heterogeneous nuclear ribonucleoproteins (hnRNPs), nuclear RNA-binding proteins important for post-transcriptional modification of the newly synthesized pre-mRNA, its splicing and

transport from nucleus. One of the hnRNPs, hnRNP-F is found to be in complex with S6K2. Upon serum stimulation, mTORC1 binds to this complex and promotes the activity of S6K2, and subsequent cell proliferation. Increased cell proliferation by overexpression of hnRNP-F is rapamycin sensitive (Figure 1.5C) (Goh et al. 2010).

A common downstream target for S6K1 and S6K2 kinases is IRS-1 (insulin receptor substrate 1), which is phosphorylated by S6Ks at Ser302 residue. Phosphorylation of IRS-1 at Ser302 is sensitive to rapamycin and downregulation of S6Ks. Moreover, it prevents IRS-1 binding to insulin receptor and plays a crucial role in mediating a negative feedback signalling to PI3K. Additionally, S6K1 and S6K2 decrease protein level of IRS1, by unknown mechanism (Harrington et al. 2004). The downregulation of IRS-1 signalling by S6Ks, named negative feedback loop, explains why S6K1^{-/-} deficient mice are protected against the development of insulin resistance. Analysis of the adipose tissue from these mice, kept on a high fat diet, reveals a dramatic reduction in IRS-1 phosphorylation (Um et al.2004).

Rictor is one of the main components of mTORC2, which plays an important role in the regulation of AKT and PKC. S6K1 was reported to phosphorylate Rictor at Thr1135 residue *in vivo* and *in vitro*, and this process is rapamycin sensitive. Interestingly, this phosphorylation event does not affect the formation of mTORC2, its cellular localisation or kinase activity. Mutation of this site to alanine, results in mTORC2-dependent increase in AKT phosphorylation, indicating that phosphorylation of Rictor by S6K1 inhibits mTORC2 and Akt signalling (Julien et al. 2010).

S6Ks may be directly linked to the regulation of transcription and gene expression by targeting transcription factors. S6K1 in breast cancer cell lines has been shown to increase transcriptional activity of the Estrogen Receptor (ER α) by its direct phosphorylation at Ser167. Phosphorylation at this site is a prognostic marker for breast cancer progression and contributes to the development of drug resistance (Yamnik et al. 2009).

Moreover, S6K1 has been shown to phosphorylate the cAMP response element binding protein (CREB) isoform, CREM τ on a conserved residue required for its transcriptional activity (de Groot et al. 1994). Recently, S6K1 has been implicated in the activation of RNA polymerase I-dependent DNA transcription via signalling to the transcription factor, UBF-1 (Hannan et al. 2003).

1.8 Dysregulation of the S6K pathway in human pathologies

1.8.1 Malignant transformation

Uncontrolled cell division and cell growth are regarded as the consequence of dysregulated signalling pathways inside the cells. Many of the identified proto-oncogenes encode proteins involved in the regulation of growth, differentiation and developmental signals and are often mutated in cancers. Upstream and downstream signalling of mTOR, are frequently dysregulated in tumors. This has increased interest in studying the role of the mTOR/S6K signalling pathway in the development of malignant transformation (Hanahan and Weinberg 2000).

Most of our knowledge about the S6K signalling pathway developed from the study of two tumour suppressor genes upstream of mTOR, TSC1 and TSC2 (hamartin and tuberlin respectively). There is a wide range of common inactivating mutations in *TSC1* and *TSC2* tumour suppressor genes, including nonsense mutations, large genomic deletions, splice site mutations and missense mutations, which results in the development of tuberous sclerosis syndrome (TS). *TSC2* mutations are also implicated in the development of lymphangioleiomyomatosis (LAM), a proliferative disorder that mostly affects women and results in lung cyst formation.

TSC2 forms an active signalling complex with TSC1, which functions as a critical regulator of growth signalling via mTORC1. TSC2, via its GTPase-activating protein (GAP) domain at C-terminus, directly binds to and controls the activity of a small GTPase Rheb. This interaction increases hydrolysis of GTP associated with Rheb, leading to the inhibition of mTORC1 activity. Loss of function of the TSC1-TSC2 complex leads to constitutively activated mTORC1 pathway, resulting in cell size enlargement, ribosome biogenesis and increased protein synthesis. Importantly, activation of S6Ks, downstream targets of mTORC1, results in the inhibition of phosphatidylinositol 3-kinase (PI3K) signalling and AKT activation, via promoting a negative-feedback mechanism affecting IRS proteins (Huang et al. 2008;Huang and Manning 2008;Pollizzi et al. 2009a;Pollizzi et al. 2009b).

Patients with the dominant autosomal disorder, tuberous sclerosis complex (TSC) all have mutations in either TSC1 or TSC2, and it results in the progression of hamartomas (benign tumours) in different tissues,

predominantly in the brain, heart, kidneys, eyes and skin (McManus and Alessi 2002). This disease related to the high occurrence of autism spectrum disorders, epilepsy, and cognitive deficits. Cancer development related to this syndrome is very rare. It has been shown that upregulation of S6K signalling is a main mark of the development of TSC disorder (Goncharova et al. 2002;Kenerson et al. 2002).

The S6K1 gene is located in the chromosome 17q23 region, and genetic analysis revealed that this part of the genome is frequently amplified in breast cancer cell lines. This amplification was accompanied by consequent increases in the expression of S6K1 at mRNA and protein levels (Barlund et al. 1997;Barlund et al. 2000;Courjal and Theillet 1997). In addition, it was showed that the overexpression of S6K1 in primary breast tumours associates with lower survival rates in patients, compared to those without S6K amplification (Barlund, Monni, Kononen, Cornelison, Torhorst, Sauter, Kallioniemi, & Kallioniemi 2000). These results showed evidence that S6K1 itself can demonstrate oncogenic activity in addition to being activated as a result of upstream regulations.

In addition to breast tumours, S6K1 was found to be constitutively activated to different degrees in a panel of human pancreatic and lung cancer cells, while treatment with rapamycin abrogates the transformed phenotype in these cell lines (Grewe et al. 1999). Recently, new S6K1 splice form named S6K1-isoform 2, or p31S6K1, was identified. This splice variant possesses transforming activity in fibroblasts, whereas full length S6K1 does not, and the expression of

S6K1-isoform 2 is essential for cellular transformation mediated via splicing factor SF2/ASF (Karni, Hippo, Lowe, & Krainer 2008).

1.8.2 Metabolic disorders

The role of S6Ks in metabolism was clearly shown in animal models, where the deletion of S6K1 in mice leads to a number of metabolic changes. In this model, an important role for S6K1 signalling in the control of glucose homeostasis has been demonstrated. S6K1 deficient mice display a phenotype that closely parallels to the preclinical type 2 diabetes (Kozma et al. 1990;Pende et al. 2004).

S6K1^{-/-} mice have increased insulin sensitivity and do not develop insulin-resistance on a high-fat diet. These effects are mediated via the S6K negative feedback regulation of insulin receptor signalling. S6K1 deficient mice are lean, have 5 times higher β -oxidation of fatty acids and oxygen consumption. Therefore, the mRNA levels of numerous genes implicated in energy combustion and oxidative phosphorylation are upregulated in white adipose tissue and muscles from these mice. Such mice have normal glucose level during fasting, but are intolerant to glucose because of noticeably decreased level of circulating insulin. Decreased level of insulin is caused by a small size and mass of pancreatic β -cells, which produce less insulin (Um et al. 2004).

The mTOR/S6K1 pathway has been implicated in an early adipocyte differentiation, as S6K1^{-/-} mice had lower number of adipocytes than the wild type (Carnevalli et al. 2010;Castaneda et al. 2012). The

dysfunctions of S6K1 deficient mice clearly demonstrate the critical role of this kinase in the metabolic disease development.

1.8.3 Ageing, learning and memory

It has been known for a long time that caloric restriction and inactivation of components within the insulin signalling pathway extend lifespan and decrease age-dependant diseases in different animal models. Inhibition of the mTOR signalling has a dramatic effect on life expectancy in worms, yeast, flies and mice. Notably, the same effect was observed when animals were treated with rapamycin or it's analogous.

It was demonstrated, that S6K1^{-/-} deficient mice live significantly longer than the wild type, and this effect is contributed to increased energy metabolism and AMPK signalling. Additionally, S6K1^{-/-} deficient mice show decrease aging-related pathologies, including bone, motor and immune pathologies (Pende et al. 2004;Shima et al. 1998;Um et al. 2004). All these results show that the mTOR/S6K pathway plays an important role in aging and life expectancy.

Recent studies also revealed an important role of mTOR/S6K signaling in the regulation of memory and learning. S6K1^{-/-} mice showed behaviour dysfunctions associated with cognitive processing, whereas S6K2 knockout mice displayed memory impairment (Antion et al. 2008a;Antion et al. 2008b). Additionally, reduced S6K2 activity correlated with *GRN* gene mutation (PGRN S116X) in neurons in patient with frontotemporal dementia (FTD) (Almeida et al. 2012).

2 Materials and Methods

2.1 General materials

2.1.1 General laboratory reagents

All general purpose chemicals were purchased from Sigma-Aldrich, ThermoFisher Scientific or Melford Laboratories Ltd unless otherwise stated. General cell culture reagents were purchased from PAA Laboratories. Fetal Bovine Serum (FBS) was purchased from Hyclone (Thermo Fisher Scientific). Prestain molecular weight markers, DNA markers and restriction enzymes were obtained from Thermo Fisher Scientific.

2.1.2 Expression vector and primers

pcDNA3.1 (+) vector, pcDNA4/TO inducible expression plasmid, pFastBac™1 baculovirus expression vector and plasmids for lentivirus generation pLEX-MCS, PLP1, PLP2, PLP-VSVG were purchased from Invitrogen. Designed oligonucleotide primers were ordered from MWG Company.

2.1.3 Antibodies

Anti-phospho S6 Ser240/244, anti-phospho Akt Ser473, anti-phospho 4EBP1 Thr37/46 antibodies were purchased from Cell Signaling Technology; anti-Actin antibodies from Sigma-Aldrich; anti-phospho S6K Thr389, anti-Raptor, anti-Rictor, anti-mTOR antibodies from Millipore.

2.2 DNA and RNA manipulation

2.2.1 Oligonucleotide design

Oligonucleotide primers with specific tags were designed using known DNA sequence of the template and restriction enzyme sites were created to allow subcloning of fragments. Annealing temperatures (T_m) for each primer were calculated using the equation: T_m ($^{\circ}\text{C}$) = $2(A+T) + 4(G+C)$.

2.2.2 DNA amplification by the polymerase chain reaction

The polymerase chain reaction (PCR) was used to amplify required regions of DNA from the templates. PCR was performed in a 25 μl volume containing 2.5 μl 10 mM dNTPs, 2.5 μl 50% DMSO diluted in water, 200 pmoles of each primer and PfuUltraTM II Fusion HS DNA polymerase (Stratagene) in 10X PfuUltraTM II reaction buffer (supplemented with 2 mM MgSO_4) diluted with ddH₂O. Plasmids were used as a template DNA for the PCR reaction with concentration 5-30ng. PCR amplification was performed using a Thermal Cycler (Peltier, MJ Research). Samples were denatured at 98 $^{\circ}\text{C}$ for 30 sec, annealed at a temperature appropriate for the length and sequence of the oligonucleotide primers (54 $^{\circ}\text{C}$) for 30 sec, and extended at 72 $^{\circ}\text{C}$ for 80 sec. 30 cycles were used to amplify DNA fragments. Final extension was applied at 72 $^{\circ}\text{C}$ for 3 min. Quantity and quality of DNA samples were checked by gel electrophoresis (section 2.2.5).

2.2.3 DNA digestion with restriction endonucleases

Restriction enzymes were obtained from standard commercial sources (Thermo Fisher Scientific) and digests were performed in the

appropriate digestion buffer, as recommended. 1µg DNA was digested with 1-3U of restriction enzyme in a volume of 20 µl. Reaction mixtures were incubated at 37°C for 1-2 hours and DNA fragments were analyzed by gel electrophoresis (section 2.2.5). If the restriction fragments were used for purification and ligation 2-5 µg of DNA were used.

2.2.4 Ethanol precipitation of DNA product

After restriction, PCR product and vector were desalted and concentrated by ethanol precipitation. To precipitate the DNA, PCR product was diluted with an equal volume of ddH₂O. 3M sodium acetate pH 4.5 was added in quantity 10% of total mixture volume. 2 volume of 100% ethanol were added to the mixture, mixed gently and placed -20°C for at least 15 min. DNA solution after was centrifuged at 13000 rpm for 10 min. Supernatant was carefully removed not disturbing the DNA pellet. The DNA was washed with 0.5 ml of 70% ethanol, air-dried for 5-10 min and redissolved in an appropriate volume of TE buffer (10 mM Tris-HCl, pH 8.0, 1 mM EDTA).

2.2.5 Electrophoresis of DNA

The electrophoretic mobility of DNA molecules depends on their size. 0.9% (w/v) agarose gels were mostly used. The required amount of agarose was added to TAE buffer (40 mM Tris-Acetate, 1 mM EDTA) and heated to allow the agarose to dissolve. The solution was cooled to approximately 60°C and GelRed™ dye (Biotium) was added with recommended concentration. Melted agarose solution was then poured into a tray and allowed to harden at room temperature. DNA samples were mixed with 6X loading buffer (Thermo Fisher Scientific),

loaded into the gel and fragments were separated by electrophoresis in TAE buffer at 90-100 V. Standard molecular weight markers (1 kb DNA ladder Gene Rule, Thermo Fisher Scientific) were used alongside the samples. DNA was visualized under a long-wave UV light.

2.2.6 Purification of DNA fragments from agarose gel

For purifying DNA from the agarose gel, the DNA fragment of interest was cut out from the gel with a scalpel and purified using the Wizard SV Gel and PCR Clean-Up system (Promega), according to the manufacturer's recommendations.

2.2.7 Dephosphorilation of the vector

To minimize self-ligation of the linearized vector, dephosphorylation of the 5' ends was performed using Alkaline Phosphatase (New England Biolabs), which catalyzes the removal of 5' phosphate groups from DNA. Reaction was performed in total volume of 25 μ l in supplemented buffer, and 2-5U of Alkaline Phosphatase were added following manufacturer's recommendations. The mixture was kept at 37°C for 1 hour. After DNA mixture was loaded onto the agarose gel and DNA was purified using the Wizard SV Gel and PCR Clean-Up system (Promega) (section 2.2.6).

2.2.8 Ligation of DNA fragments

The Rapid DNA Ligation Kit (Thermo Fisher Scientific) was used to clone DNA fragments into plasmids; all procedure was performed following manufacturer's recommendations. To perform ligation reactions and minimize self-ligation of plasmids a 1:3 molar ratio of vector:insert was used, recommended concentration for vector 10-100ng. The reaction

was carried out at room temperature in Rapid ligation buffer in the presence of 5U of T4 DNA ligase in total volume of 20 μ l. After incubation for 5 min, 2 μ l of reaction solution was used to transform competent XL-1 Blue *E. coli* cells.

2.2.9 Purification of plasmid DNA

Plasmid DNA was purified using GeneJet™ Plasmid Purification kit (Thermo Fisher Scientific), following the manufacturer's manual. The plasmid purification protocol is based on a modified alkaline lysis procedure, followed by binding of plasmid DNA to anion-exchange resin under appropriate low salt and pH conditions.

The bacterial pellet from an overnight shaker-culture of XL-1 Blue *E. coli* was resuspended in resuspension buffer (50 mM Tris-HCl, pH 8.0, 10 mM EDTA, 100 μ g/ml RNase A) and an equal amount of Lysis buffer (200 mM NaOH, 1% SDS) was added to the cell suspension. Following 5 min incubation at room temperature, the lysate was neutralized with 0.5 volume of chilled neutralization buffer (3 M potassium acetate, pH 5.5) and incubated for 5 min. Bacterial lysate was centrifuged at 13000 rpm for 5 min. The supernatant was added to a spin-column containing anion-exchange resin and centrifuged at 13000 rpm for 1 min. The resin was washed two times with Wash buffer (50 mM MOPS, pH 7.0, 1 M NaCl, 15% isopropanol) and buffer was removed by centrifugation at 13000 rpm for 1 min. DNA was eluted with an appropriate volume of Elution buffer (50 mM Tris-HCl, pH 8.5, 1.25 M NaCl, 15% isopropanol). Quantity and quality of DNA samples were checked by gel electrophoresis (section 2.2.5).

The plasmids were analyzed by restriction analysis to confirm the presence and correct orientation of the insert (section 2.2.3). Restriction enzyme or combinations of enzymes were used.

2.2.10 Isolation of the Recombinant Bacmid DNA

2 ml of an overnight bacterial culture DH10Bac™ *E. Coli* were centrifugated at 3000 rpm for 5 min. All medium was thoroughly removed. For isolation of bacmid DNA Thermo Fisher Scientific kit was used. 0.4 ml of Cell Resuspension Buffer was added (E1) (15mM Tris-HCl (pH 8.0), 10 mM EDTA, containing RNase A at 0.1 mg/ml), to resuspend the bacterial pellet. Cells were lysed by adding 0.4 ml of Cell Lysis Solution (E2) (200 mM NaOH, 1% SDS) and mixed gently by inverting the capped tube five times (do not vortex) following incubation at room temperature for 5 min. After 0.4 ml of Neutralization Buffer was slowly added (E3) (3 M potassium acetate, pH 5.5) and mixed gently. Samples were put on ice for 5-10 min. The debris was removed by centrifugation at top speed in a microcentrifuge at room temperature for 10 min. Supernatant was gently transferred to the tube with 0.8 ml of absolute 100% isopropanol, mixed carefully and placed on ice for 10 min. After the sample was centrifuged at 13000 rpm for 15 min, supernatant was discarded; DNA pellet was washed with ice-cold 70% ethanol, air-dried for 5-10 min and redissolved in an appropriate volume of TE buffer. DNA was allowed to dissolve for at least 10 min on ice and stored at -20°C. 5 µl of this bacmid preparation can be used for transfection of insect cells.

2.2.11 mRNA purification

RNeasy Mini Kit from Qiagen was used for mRNA purification. 5×10^6 of HEK293 cells were collected and centrifuged for 5 min at 1000rpm in a centrifuge tube. Supernatant was carefully aspirated and pellet was resuspended in 600 μ l of RLT Buffer. Cell lysate was homogenized by passing through a blunt 20-gauge needle (0.9 mm diameter) fitted to an RNase-free syringe at least 5 times. 600 μ l of 70% ethanol was added to the homogenized lysate and mixed well by pipetting. Sample was transferred to an RNeasy spin column placed in a 2 ml collection tube. Sample was centrifuged for 15s at 10,000 rpm, the flow-through was discarded and 350 μ l of RW1 buffer was added to the RNeasy spin column. Sample was centrifuged for 15s 10,000 rpm the flow-through was discarded. 80 μ l of DNase I incubation mix (10 μ l of DNase I stock solution diluted in 70 μ l of RDD buffer) was applied directly into the RNeasy spin column membrane, and incubated for 15 min at room temperature. Next RNeasy spin column was washed by adding 350 μ l of Buffer RW1 and centrifuged for 15 s at 10,000 rpm. Next 500 μ l of RPE buffer was added to the column, column was centrifuge for 15 s at 10,000 rpm. After spin column was put in a new 2 ml collection tube and centrifuged at full speed for 1 min. Next the spin column was placed in a new 1.5 ml collection tube, 30–50 μ l of RNase-free water was added directly to the spin column membrane, RNA was eluted from the membrane centrifuged for 1 min at 10,000 rpm. Concentration of purified RNA was measured by nanodrop.

2.2.12 RT-PCR analysis

For the generation of first-strand cDNA from purified mRNA Thermo Scientific RevertAid Premium Reverse Transcriptase was used. Into a sterile nuclease-free tube 0.5 µg of purified mRNA, 100pm of Oligo(dT)₁₈ primer, 0.5 mM final concentration of dNTP Mix were added on ice in the indicated order and the volume was adjusted to 14.5 µl with DEPC-treated Water. Next the following components were added to the mixture in the indicated order: 4 µl of 5X RT Buffer, 0.5 µl of Thermo Scientific RiboLock RNase Inhibitor and 1 µl of RevertAid Premium Reverse Transcriptase. The mixture was mixed gently and centrifuged briefly. Sample was incubated for 30 min at 50°C, the reaction was terminated by heating at 85°C for 5 minutes. The reverse transcription reaction product can be directly used in PCR or stored at -20°C for up to one week. 1 µl of the reaction mix was used to perform RT-PCR. RT-PCR was performed in a 25 µl volume containing 2.5 µl 10 mM dNTPs, 0.5 µl 50% DMSO diluted in water, 200 pmoles of each primer and 0.5 µl of PfuUltra™ II Fusion HS DNA polymerase (Stratagene) in 10X PfuUltra™ II reaction buffer (supplemented with 2 mM MgSO₄) diluted with ddH₂O. Reaction was performed using a Thermal Cycler (Peltier, MJ Research). First samples were denatured at 98°C for 3 min, than at 97°C for 30 sec, annealed at a temperature appropriate for the length and sequence of the oligonucleotide primers (58°C) for 30 sec, and extended at 72°C for 45 sec. 33 cycles were used to amplify DNA fragments. Final extension was applied at 72°C for 10 min. Quantity and quality of DNA samples were checked by gel electrophoresis (section 2.2.5).

2.3 Bacterial methodology

2.3.1 Bacterial strains and growth media

Escherichia coli XL-1 Blue competent cells (New England Biolabs) Genotype: endA1 gyrA96(nal^R) thi-1 recA1 relA1 lac glnV44 F'[::Tn10 proAB⁺ lacI^q Δ(lacZ)M15] hsdR17(r_K⁻ m_K⁺). Tetracycline resistant (carried on the F plasmid).

MAX Efficiency[®] DH10Bac™ *E. Coli* (Invitrogen) Genotype: F⁻ endA1 recA1 galE15 galK16 nupG rpsL ΔlacX74 Φ80lacZΔM15 araD139 Δ(ara,leu)7697 mcrA Δ(mrr-hsdRMS-mcrBC) λ⁻. Tetracycline and kanamycin resistance encoded by the helper plasmid and bacmid. Resistance to gentamycin would be possible if the cells had been transformed with the pFastBac1 donor vector.

Luria Bertani (LB) medium and Luria Agar were bought from Sigma, and prepared following recommendation then autoclaved at 121°C for 15 min. Ampicillin was prepared as 100 mg/ml stock solutions in ddH₂O, stored at -20°C and used at a final concentration 100 µg/ml. Kanamycin and chloramphenicol were prepared as 50mg/ml stocks in ddH₂O or ethanol and used at concentrations of 50µg/ml respectively. Tetracycline were prepared as 10mg/ml stocks in ethanol and used at final concentrations of 10µg/ml.

Super Optimal broth with Catabolite repression (SOC) medium contains 0.5% Yeast Extract, 2% Tryptone, 10 mM NaCl, 2.5 mM KCl, 10 mM MgCl₂, 10 mM MgSO₄, 20 mM Glucose. Note: Glucose and MgCl₂ were added after autoclaving. Final solution was sterilized by passing it through a 0.2 µm filter.

For Blue/white selection of DH10Bac™ transformants LB agar plates containing 50 µg/ml kanamycin, 7 µg/ml gentamicin, 10 µg/ml tetracycline, 100 µg/ml Bluo-gal, and 40 µg/ml IPTG at their final concentration were used.

2.3.2 Preparation of competent cells

Chemically competent cells were prepared by the following procedure. Single colony of bacterial strain was inoculated in 5 ml of LB medium, then transferred in 250ml LB medium in a flask and incubated with shaking at 37°C, until the OD₆₀₀ reached 0.6. The culture was cooled on ice and the bacteria were then pelleted at 5000 rpm for 5 min and resuspended in 50 ml ice-cold TFB1 buffer (30mM potassium acetate, 50mM MnCl₂, 100 mM RbCl, 10mM CaCl₂, 15% (v/v) glycerol, pH 5.8) by gentle shaking/pipetting. The bacteria were repelleted at 5000 rpm for 5 min and gently resuspended in 5 ml of TFB2 buffer (10 mM NaMOPs, 75 mM CaCl₂, 10 mM RbCl, 15% (v/v) glycerol, pH 6.5). Finally, 0.1 ml aliquots were “snap - frozen” in liquid nitrogen in pre-chilled screw-cap microcentrifuge tubes and stored at -70°C.

2.3.3 Transformation of E.coli

100 µl of competent cells were defrosted on ice and 2µl of DNA ligation mix (or 5-50 ng of plasmid DNA) were added. After 30 min incubation on ice, cells were induced to take up the DNA by heat-shock at 42°C for 45 sec, chilled on ice for 2 min and let to recover in 1 ml of LB medium for 1 hour at 37°C in shaking incubator (225 rpm). The cells were pelleted by centrifugation at 3,000 rpm for 5 min and pellet was resuspended in 100 µl of LB medium. Cell suspension was spread onto pre-warmed LB agar plate containing the appropriate selective

antibiotic and incubated overnight at 37°C. Next day, 5-10 transformed colonies from agar plate were picked and cultured overnight at 37°C in shaking incubator (225 rpm) in LB medium containing appropriate selective antibiotics.

2.3.4 Transformation of DH10Bac™ E. Coli

100 µl of competent cells were defrosted on ice and 1ng of plasmid DNA was added. After 30 min incubation on ice, cells were induced to take up the DNA by heat-shock at 42°C for 45 sec, chilled on ice for 2 min and let to recover in 1 ml of SOC medium for 4 h at 37°C in shaking incubator (225 rpm).

The cells were pelleted by centrifugation at 3,000 rpm for 5 min and pellet was resuspended in 100 µl of SOC medium. Cell suspension was spread onto pre-warmed selective agar plate for Blue/white selection containing the appropriate selective antibiotic (section 2.3.1) and incubated at 37°C for 24-72 hours. Blue/white selection was used to identify colonies containing the recombinant bacmid. Once white colonies were identified, they were grown in 3 ml of LB medium, containing 50 µg/ml kanamycin, 7 µg/ml gentamicin and 10 µg/ml tetracycline overnight. Isolation of recombinant bacmid was performed as described in section 2.2.10.

2.4 Cell culture methodology

2.4.1 Cryopreservation of cells

Cells for freezing should be healthy and in logarithmic phase of growth. Cells on the 100 mm tissue culture plate were washed twice with 2 ml of Dulbecco's phosphate buffered saline (PBS) and detached by adding

1 ml trypsin-EDTA as gently as possible to minimize damage to the cells. Cells were incubated at room temperature (or at 37°C if required) until cells detached from the plastic. Cells were gently resuspended in trypsin and 10 ml of fresh medium was added to neutralize the trypsin. Then, cells were centrifuged at 500 rpm for 5 min and medium was aspirated to the smallest volume without disturbing the cells. Cell pellet was resuspended gently in 3 ml of freezing medium (growth medium with 20% FBS and 10% DMSO) aliquoted into 3 cryogenic storage vials. Vials were placed on ice and the freezing procedure was started within 5 min. Vials were put in an insulated box placed in a -70°C freezer, then transferred into liquid nitrogen storage. Cells growing in suspension were diluted in freezing medium to a concentration of $1-5 \times 10^7$ /ml.

2.4.2 Insect Cells culture

2.4.2.1 Maintenance of insects cells

Spodoptera frugiperda Sf9 insect cells were diluted every 2-3 days to a density of 1×10^6 cells/ml and incubated at 28°C. They should be healthy with greater than 95% viability and should be in the logarithmic phase of growth. Insect-XPRESS™ Medium (Lonza) supplemented with 5% FBS and antibiotics (Penicillin and Streptomycin at a final concentration 100 U/ml and 100 µg/ml), were used for growing cells.

2.4.2.2 Transfection of insects cells

Sf9 insect cells were healthy, growing in the logarithmic phase with a density of $1-2 \times 10^6$ cells/ml before proceeding to transfection. Cells were seeded in a 6-well tissue culture plate at density 1×10^6 cells/ml per well in 2 ml of Insect-XPRESS™ Medium (with antibiotics and FBS). Plate was left at 28°C for at least 1 h to allow cells to attach. In two

sterile tubes, two following solutions were prepared. Solution A: For each transfection, 5 μ l of purified baculovirus DNA (section 2.2.10) diluted into 100 μ l Insect-XPRESS™ Medium without FBS and antibiotics. Solution B: For each transfection, 7 μ l ESCORT™ IV (Sigma) transfection Reagent diluted into 100 μ l Insect-XPRESS™ Medium without FBS and antibiotics. Solution B was added to the tube containing Solution A, mixed gently, and incubated at room temperature for 15-30 min. After 0.8 ml of Insect-XPRESS™ Medium without FBS and antibiotics were added to each tube containing lipid/DNA complexes and mixed gently. While lipid/DNA complexes were forming, Sf9 cells in a 6-well tissue culture plate were washed once with 2 ml per well of Insect-XPRESS™ Medium without FBS and antibiotics. Medium was aspirated, and 1ml of diluted lipid/DNA complexes was overlaid onto the washed cells. Plates were incubated for 5 h in a 28°C incubator. After the transfection mixture was removed and replaced with 2ml per well of Insect-XPRESS™ Medium (supplemented with antibiotics and FBS) and incubate at 28°C for 72 h. The medium containing virus was harvested at 72 h post-transfection, filtered through sterile 0.45 μ m low-protein binding filter and stored at +4°C or at -80°C.

2.4.2.3 Amplification of the Baculoviral stock

10 ml of Sf9 insect cells in a flask with cell density $1-2 \times 10^6$ /ml, growing exponentially in Insect-XPRESS™ Medium supplemented with 5% of Fetal Bovine Serum and antibiotics, were infected with 0.5 ml of the virus stock. Flask was incubated at 27°C for 72 h.

Cells and growth medium containing virus were collected from flask and put into centrifuge tubes, centrifuged at 2000 rpm for 5 min at +4°C. Supernatant containing virus was collected and filtered through sterile 0.45µm low-protein binding filter. The virus stocks can be stored at 4°C for up to 1 year, protected from light, or at -80°C for longer. Cell pellet was used for analysis of protein expression, might be frozen at -20°C.

2.4.2.4 Infection of insects cells

500ml of Sf9 cells in the logarithmic growth phase with a density of 1–2×10⁶ cells/ml were infected with 1ml of the virus stock. After infection cells were monitored every day in the microscope to see the efficiency of infection. After 48-72h cells were collected by centrifugation at 2000 rpm for 5 min and analyzed immediately or frozen at -80°C.

2.4.3 Mammalian cell culture

2.4.3.1 Tissue culture medium

HEK 293T, NIH3T3RasC40, A549, TSC2-/- p53-/- MEF cells were maintained in Dulbecco's Modified Eagle's Medium (DMEM). All complete media were supplemented with heat-inactivated sterile 10% FBS, supplemented with L-glutamine and penicillin/ streptomycin at a final concentration 100 U/ml and 100 µg/ml. All cells were grown in humidified 37°C incubators at 10 % CO₂.

2.4.3.2 Maintenance of cell lines

Cells were passaged every two to four days, or as required. Cell were examined under the microscope before each splitting, they should look healthy with no more than 90% confluency. The medium was aspirated, cells were washed once in PBS and trypsin-EDTA was added. Cells were incubated at room temperature (or at 37°C if required) until they

detached from the plastic. Cells were gently resuspended in trypsin and fresh medium was added to neutralize the trypsin. Cell suspension was gently pipetted up and down repeatedly in order to break up any clumps of cells before dilution into new plates with fresh medium at desired ratio (usually 1:5).

2.4.3.3 Transient transfection

HEK 293 (NIH-3T3 cells) cells were transfected using ExGen 500 reagent (MBI Thermo Fisher Scientific) following manual. This protocol allows transfection of the cells in normal medium (in the presence of serum and antibiotics). The day before transfection, cells were plated at 5×10^5 cells per 60 mm dish to give 50-80% confluency at the time of transfection. When different dish sizes were used the number of seeded cells was scaled up or down according to the manufacturers' instructions. DNA-ExGen complexes were prepared for transfection by diluting 5 μg of plasmid DNA and 17 μl of ExGen 500 (per construct per 60 mm dish) in 200 μl of sterile filtered 150 mM NaCl and vortexed for 10 seconds. The mixture was incubated at room temperature for 10 minutes to allow formation of the DNA-ExGen 500 complexes. During this incubation, the medium from cells was removed and replaced with 2 ml of fresh complete DMEM. The transfection mixture was added to the cells drop-wise and the medium was replaced the following day. Cells were typically harvested 48 hours after transfection.

2.4.3.4 Generation of stable cell lines

The pcDNA3.1(+) vector contain the neomycin resistance gene for selection of stable cell lines using neomycin (Geneticin_R 418). Minimum concentration for Geneticin_R 418, required to kill untransfected host

cells, was determined as 800 µg/ml. Cells were transiently transfected with pcDNA^{3.1} constructs using standard protocol for ExGen 500. Untransfected cells were used as a negative control and the pcDNA^{3.1} empty plasmid as a positive control for selection. After 48 hours post transfection, cells were split into fresh medium, containing 800 µg/ml Geneticin_R 418. Under this concentration of antibiotic, only cells with integrated plasmid will survive. Cells were fed with selective medium every 3-4 days. Complete selection can take from 2 to 3 weeks, until Geneticin_R-resistant cells give separate colonies. For monoclonal selection these colonies were picked up separately using special cloning disk and grown separately till they reach confluency. For polyclonal selection all cells from the plate were pooled together. After cells were harvested and checked for the expression of the protein.

In case where pcDNA^{4TO} constructs were used for generating stable cell lines, selective antibiotic Zeocin was used with working concentration 100 µg/ml. Whole selection procedure is the same as described for pcDNA^{3.1(+)} vector.

2.4.3.5 Starvation and stimulation of cells

HEK 293 cells were plated the day before starvation, so at the time of starvation they were about 50% of confluency. Media from the plates were aspirated carefully and new media without FBS (supplemented with penicillin/ streptomycin) was added to the plate. After 30 hours of starvation, cell were stimulated by adding 10% FBS to the media for 1 hour following by collection and lysis of the cells (2.7.1). 50 000 cells of MEF TSC2^{-/-} p53^{-/-} stable cell lines overexpressing S6K2-S1 (clone 8), S6K2wt (clone 3) and an empty vector were seeded into a 6cm plate.

Next day media was changed for the starvation media without FBS and left for 48h. Then, cells were stimulated with media containing 10% FBS for 2hr. Cells were harvested, lysed and analysed in Western blotting with corresponding antibodies.

2.4.4 Characterisation of stable cell lines

2.4.4.1 Analysis of cell growth and cell size

Total and viable cell number, cell size, cell aggregation factor and percentage of viability were measured by using CASY Model TT cell counter (Innovatis), which uses electronic pulse area analysis for measurements. Corresponding stable cell lines cells were plated in medium containing appropriate selective antibiotic and growth under standard condition. Cell numbers were calculated every day over the next four days. First, the medium was collected, followed by a single wash with PBS. Cells were trypsinized by addition of trypsin for 2 min at 37⁰C, cells were resuspended and this suspension was mixed with previously collected growth medium. 10 µl or 100 µl of resuspended cells were added to 10 ml of CASYTON solution (Innovatis) and samples were analysed using CASY machine.

2.4.4.2 Colony formation assay in soft agar

This assay was used to measure the ability of cells to grow in an anchorage-independent manner. In a 6-well tissue culture plate, 1 ml base layer of 0.8% (w/v) agarose was prepared by adding 200 µl of autoclaved 4% (w/v) agarose solution to 800 µl of DMEM medium supplemented with 10% FCS. Plates were left in the hood for 30 min for agarose to solidify and to dry out from condensate. HEK 293 (or A549) of approximately 80% confluency were carefully washed in pre-warmed

PBS and incubated with trypsin/EDTA for 2 min at 37°C. The cells were resuspended in pre-warmed cell culture medium and the number of cells determined by counting using a CASY machine (section 2.4.4.1). 1 ml of DMEM media containing 2000 HEK 293 cells (or 10000 of A549 cells) was mixed with 100µl of autoclaved 4% (w/v) agarose solution to get top layer of 0.4% agarose. The cell suspension was plated over the base layer 0.8% agarose and allowed to solidify. Plates were incubated at 37°C for 2 weeks. Then, plates were stained with 0.005% crystal violet for 3h at 37°C and photographed. Colonies from soft agar plates were counted using ImageJ software.

2.4.4.3 Drugs treatment

3×10^5 A549 stable cell lines overexpressing EE-S6K2-S1, EE-S6K2wt and empty vector were seeded into 6cm plate. Next day 1µM of staurosporine (or 50 µM cisplatin) diluted in DMSO was added to the plates, DMSO alone was added to the control plates. Cells treated with staurosporine were collected after 3, 5 hours of incubation (for cisplatin treatment cells were collected after 24, 48 hours) and analysed in Western blotting with corresponding antibodies.

2.4.4.4 Wound healing assay

NIH 3T3 RacC40 stable cell lines overexpressing S6K2-S1 splicing isoform and an empty vector were plated at 1×10^6 cells in 6cm tissue culture plate in complete DMEM media. Wound was made to the 90% confluent monolayer of cells with a yellow plastic pipette tip to create a cleared line. The medium was removed and replaced with DMEM media containing 1% FBS and antibiotic. The cells were incubated at 37°C, and cell movement were photographed at different time points.

2.5 Production of anti-S6K2-S1 polyclonal antibodies

2.5.1 Generation of rabbit antisera

The synthetic peptide used for immunization was synthesized and coupled to activated keyhole limpet hemocyanin (KHL). Polyclonal specific antibodies to S6K2-S1 isoform were raised by immunizing two rabbits with KHL-coupled synthetic peptide. Following a standard immunization protocol, sera were collected at various times and analysed using an ELISA with a control or S6K2-S1 peptide. The above procedures were carried out by Eurogentec Ltd (Belgium). Generated antibodies were affinity-purified using S6K2-S1 peptide coupled to cyanogen bromide activated Sepharose beads (Sigma) through sulfo-SMCC (Sigma) linker.

2.5.2 Affinity purification of antibodies

2.5.2.1 Preparation of Sepharose

1 ml of 50% cyanogen bromide activated Sepharose beads, pre-washed once with 1 ml of 1 mM HCl and 2 times with 1 ml of ddH₂O, were mixed with 1 ml 100mM ethylenediamine (pH 10.0 adjusted with HCl) and incubated at +4°C overnight, after beads were washed 3 times with 1 ml of ddH₂O.

5 mg of sulfo-SMCC (Sigma) linker was dissolved in 1 ml of ddH₂O and added to Sepharose beads and incubated at 4°C for 1 hour. Then beads were washed 3 times with 1 ml of PBS (phosphate buffer pH 7.4). 3.5 mg of the synthetic peptide were dissolved in 1 ml of PBS and added to the washed beads. Mixture was incubated at room temperature for 2 h or overnight at +4°C. Then beads were washed 3 times with 1 ml of PBS.

Supernatant was removed and 1 ml of 10 mM cysteine dissolved in PBS was added to the beads and incubated for 2 h. Then beads were washed 3 times with 1 ml of PBS and stored at +4°C in PBS with 0.002% of NaAz to prevent contamination.

2.5.2.2 Affinity purification

15 ml of generated anti-S6K2-S1 polyclonal antiserum was centrifuged at 5000 rpm at +4°C for 10 min. Clarified serum was then mixed with 15 ml of PBS and loaded into a column prepared with peptide coupled to Sepharose beads). The column was allowed to empty by gravity flow and then washed extensively with PBS and last time with PBS containing 500 mM NaCl. Bound antibody was eluted with 0.1 M glycine, pH 3.0 and collected as 1ml fractions into tubes containing 100 µl of 1 M Tris-HCl, pH 8.0. Protein concentration was measured as described in section 2.7.3. Peak protein fractions were combined and dialysed twice against PBS and once against 50% glycerol/PBS and stored at -20°C. Affinity purified antibodies were screened for antigen reactivity by immunoblot analysis.

2.6 Lentivirus generation

2.6.1 Generation of the virus

The gene of interest was cloned into the cloning vector pLEX. HEK 293 cells were seeded one day before co-transfection in 10cm plate. Next day 70% confluent HEK 293 cells were transiently co-transfected with 5.4 µg pLEX/constructs, 3.5 µg pPLP1 and 1.3 µg pLP2 (packaging vectors), 1.8 µg pLP/VSVG (envelope coding vector) using standard protocol for ExGen 500 transfection. As a positive control Lentivirus expression vector (pLEX) containing Green Fluorescent Protein (GFP)

was used for fluorescent detection. The cells produce the viral structural proteins that self-assemble into pseudovirus particles, each containing a cloned gene of your interest. The cells replicate pseudoviruses containing expression constructs and release them into the growth medium. After 24h post-transfection medium was removed and cells were supplemented with fresh medium. After 48h of incubation, the medium with the recombinant lentiviruses was filtered through sterile 0.45 µm low-protein binding filter and kept at -80°C.

2.6.2 Lentiviral infection

One day before infection, HEK 293 cells were seeded in a 6-well plate $5-10 \times 10^4$ cells per well in 2 ml of complete medium. Prior infection old medium was removed and appropriate amount of lentivirus mixed with fresh medium up to 2 ml of total volume were added to cells. 2 µg/ml of polybrene was used to increase the efficiency of infection. After overnight incubation medium was replaced with fresh medium. Cells were grown and split when required. For selection of stable cell lines, 2 µg/ml of puromycin was added to the medium every 3 days. After antibiotic selection cells were tested for recombinant protein expression.

2.7 Protein purification and analysis

2.7.1 Preparation of mammalian cells extracts

Plates were removed from the incubator and cells were washed with ice cold PBS twice. After lysis buffer was added (10 mM Tris HCl (pH 7.5), 150 mM NaCl, 5 mM EDTA, 50 mM NaF, 1 % Triton X-100, 1mM DTT, complete EDTA-free protease inhibitor cocktail (Roche)). Cells

were scraped from the dishes and put into cooled microcentrifuge eppendorfs. Tubes were kept on ice for 30 minutes prior to centrifugation at 13,000 g +4°C for 20 minutes. Supernatants were decanted into new tubes and the protein concentration in each sample was measured by Bradford assay (section 2.7.3).

2.7.2 Preparation of insect cells extracts

Pellets of Sf9 cells were lysed in lysis buffer (PBS, pH 7.4, 0.5% Triton X-100, and 1mM PMSF). Lysates were incubated on ice for 30 minutes and centrifuged at 13,000g +4°C for 20 minutes to pellet the insoluble cell debris. Supernatant was collected into fresh tubes and the protein concentration was measured by Bradford assay (section 2.7.3).

2.7.3 Estimating of protein concentration

To estimate protein concentration in cell lysates the colorimetric method with Coomassie Protein Reagent (Pierce) was used. The method is based on the absorbance shift from 465 to 595 nm which occurs when Coomassie brilliant blue G-250 binds to proteins in an acidic solution. 0.5 ml of Coomassie Protein Reagent was diluted in 0.5 ml of ddH₂O and 1 µl of cell lysate was added to the mixture and mixed. After 5 min of incubation at room temperature the absorbance was measured at OD₅₉₅ and compared with a blank. The protein concentration was then determined by comparison of absorbance values with a bovine serum albumin (BSA) standard curve.

2.7.4 SDS-PAGE electrophoresis

For the SDS-polyacrylamide gel electrophoresis (SDS-PAGE) Mini-PROTEAN TGX™ (BioRad™) precast Tris-glycine 10% and 4-20% gradient

gels were used. Gels were taken from the packaging; the well comb and insulating strip covering the electrode were removed. The gel was inserted into the Mini-PROTEAN Tetra cell™ (BioRad™) according to the manufacturer's instructions. The buffer chambers were filled with premade running buffer (BioRad™) and samples were loaded into the wells. Gels were run at constant potential of 200 V until the dye front reached the end. Gels were used for immunoblotting (section 2.7.5) or for Coomassie Blue staining (section 2.7.6).

2.7.5 Immunoblotting

After electrophoresis tris-glycine gels were removed from precast frame and placed onto premade polyvinylidene difluoride (PVDF) membrane between two layers of filter paper soaked in transfer buffer (BioRad™). Trans-Blot Turbo™ blotting system (BioRad™) were used for semi-dry transfer.

After transfer PVDF membrane was blocked for 1 hour with 5% skim dry milk in TBST buffer (10 mM Tris-HCl (pH 7.5), 150 mM NaCl, 0.1 % Tween 20). For phospho-specific antibodies 1% BSA in TBST was used for blocking the membrane. After blocking, membranes were washed in TBST 3 times for 10 minutes. Primary antibodies were diluted as recommended in TBST containing 2% BSA and 0.02 % sodium azide (to allow storage of diluted antibodies at +4°C). Membranes were incubated with primary antibodies overnight at +4°C prior to washing 3 times for 10 minutes each at room temperature. Secondary antibodies (anti-rabbit and anti-mouse conjugated to horseradish peroxidase, Promega) were diluted 1:10,000 in TBST buffer with 5% skim dry milk. Membranes were incubated with secondary antibodies for 1 hour at

room temperature and washed 3 times for 10-15 minutes each before development by enhanced chemiluminescence (ECL). For ECL, equal volumes of ECL solution 1 (50 mM Tris-HCl pH 8.5, luminol, coumaric acid) and solution 2 (50 mM Tris-HCl pH 8.5, 0.02 % H₂O₂) were mixed together and added to the membrane for 1 minute at room temperature. Excess ECL solution was removed by blotting the membrane on a paper towel and the membrane was wrapped in Saran Wrap ready for exposure to X-ray film or scanning using a Fluor-S imager (Biorad™). Where appropriate, bands were quantified using the Quantity One™ image processing software (Biorad™).

2.7.6 Coomassie Blue staining

Following electrophoresis, gels were stained for the presence of protein by soaking in premade Coomassie Blue stain (Generon™) for 20-30 min, followed by washing in ddH₂O with agitation. The gel was then dried under vacuum at 80°C for 1 hour. Coomassie brilliant blue binds to proteins stoichiometrically, so this staining method is preferable when relative amounts of protein are to be determined by densitometry.

2.7.7 Immunoprecipitation

Cell lysates were prepared as described in sections 2.7.1 and 2.7.2. Immunoprecipitations were performed on equal amounts of total protein (as determined by 2.7.3) and the final volume in each tube was made up with lysis buffer to an equal level. 1µg of antibodies and 30µl of 50% protein A or G-Sepharose suspension (prewashed in ice-cold lysis buffer 3 times) were added to each sample and incubated on a rotating wheel for at least 1 hours at +4°C. The immune complexes

were then pelleted by low speed centrifugation at 3000 rpm for 2 minutes and washed 3 times with ice-cold lysis buffer. After last wash lysis buffer was removed as much as possible and 30µl of 2×SDS-PAGE sample buffer were added. The samples were boiled for 5 minutes before separation by SDS-PAGE (2.7.4).

2.7.8 Affinity purification of S6K2-S1 protein from Sf9 cells

Sf9 cells were infected with the S6K2-S1 baculovirus as described in section 2.4.2, lysates were collected and prepared as described in section 2.7.2.

The anti-FLAG M2 affinity resin (Sigma) was used for purification S6K2-S1. Resin was prewashed in lysate buffer and loaded into the clean chromatography column. Empty column was rinsed twice with PBS. Buffer was allowed to drain from the column and residual of the buffer was left in the column to aid in packing the ANTI-FLAG M2 affinity gel. Resin was thoroughly resuspended by gentle inversion and allowed gel bed to drain. Column was activated by washing the gel with three sequential column volumes of 0.1 M glycine HCl, pH 3.5. After, resin was washed with 5 column volumes of PBS for equilibration and a small amount of buffer was left on the top of the column.

Cell lysate was centrifuged and supernatant was filtered through sterile 0.45 µm low-protein binding filter to remove debris. Sample was loaded onto the column under gravity flow two times with the slow flow rate. Column was washed with 10–20 column volumes of PBS and the column was allowed to drain completely. Elution of the bound FLAG fusion protein was performed by competitive elution with five one-column volumes of a solution containing 100 µg/ml FLAG peptide in

PBS. For regeneration, immediately after use, column was washed with three column volumes of 0.1 M glycine HCl, pH 3.5 and re-equilibrated in PBS until the effluent was at neutral pH. Column was stored in PBS buffer containing 0.02% sodium azide. Collected elution protein was dialysed once against PBS and once against 50% glycerol/PBS at +4°C and stored at -20°C.

2.8 Xenograft studies in nude mice

Generated A549 stable cells expressing empty vector, S6K2wt and S6K2-S1 were injected subcutaneously into flank of nude mice (1×10^6 cells/site in 100 μ l mixed with 100 μ l of Matrigel (BD Bioscience)), using a 25-gauge needle. The mice were divided into three groups with 8 mice in each: (a) implanted A549 cells overexpressing an empty vector (group 1), (b) implanted A549 overexpressing full-length S6K2 (group 2), and (c) implanted with A549 cells overexpressing splicing isoform (group 3). Tumor growth was followed for up to two month. Tumour size was measured 2 times weekly and volume was calculated as $\text{volume} = (\text{length} \times \text{width} \times \text{depth}) / \pi$. Mice were euthanized when the tumor diameter reached 1.1-1.2 cm. Subcutaneous tumors were divided into four parts and frozen immediately at -80 °C. One part was used for Western blot analysis.

2.8.1 Preparation of tumour samples

Tumour samples were removed from the freezer and defrosted on ice. After 0.5 ml of lysis buffer was added to each tumour sample (10 mM Tris HCl (pH 7.5), 150 mM NaCl, 5 mM EDTA, 50 mM NaF, 1 % Triton X-100, 1mM DTT, 1mM PMSF, complete EDTA-free protease inhibitor cocktail (Roche)). Samples were disrupted using TissueLyser II Qiagen

machine. After homogenisation samples were incubated on ice for 30 minutes prior to centrifugation at 13,000 g +4°C for 20 minutes to remove insoluble material. Supernatants were decanted into fresh tubes and the protein concentration in each sample was measured by Bradford assay (section 2.7.3).

3 Analysis of the existence of potential S6K2 splicing isoforms

3.1 Introduction

Alternative splicing is an important mechanism implicated in the regulation of protein diversity and gene expression. In higher eukaryotes, splicing of precursor messenger RNA (pre-mRNA) into a mature mRNA transcript occurs by the removal of introns from the transcribed gene, and multiple mRNAs can be produced from a single pre-mRNA, resulting in functionally and structurally distinct proteins. This process is tightly regulated by the spliceosome – a macromolecular complex formed of pre-mRNA, small nuclear ribonucleic proteins (snRNPs), splicing factors and more than a hundred regulatory proteins (Graveley 2009). Seventy-five percent of all alternatively generated spliced transcripts are functional and the remaining twenty-five percent targeted by Nonsense Mediated Decay (NMD) mechanism (Matlin et al. 2005).

Deregulation in the balance between splicing isoforms or generation of the aberrant alternative splicing variants are implicated in the development of different pathological disorders. Studies investigating the role of alternative splicing events in the development of human diseases are just starting to come out (Yamaguchi et al. 2010).

The expression of many tumour-suppressor and oncogene genes is tightly regulated by alternative splicing. Many genes implicated in cell proliferation, cell survival, apoptosis are alternatively spliced, and often spliced products have an opposite effects on these processes. This suggests that the functions of different proteins are controlled by a

crucial balance between their antagonistic alternatively spliced variants (Pedrotti et al. 2010;Valacca et al. 2010).

For about seventy percent of the alternatively spliced genes, splicing variants are produced by full or partial exon exclusion in the coding mRNA sequence. For example, tumour suppressor cell-cell adhesion molecule (C-CAM1), implicated in the regulation of cell adhesion, has a short splicing variant. It does not include exon 7, which encodes its cytoplasmic domain important for insulin receptor signalling. Significant overexpression of this isoform was reported in 51 NSCL (non-small cell lung cancer) samples compared with normal samples (Wang et al. 2000).

Ninety-nine percent of all exons are flanked by the GT and AG intronic dinucleotides at the 5' and 3' splice ends correspondingly. Single point mutation of these sites usually leads to differential inclusion of the bordering exon. For instance, a GT to AT splice site mutation in SWI/SNF-related matrix-associated actin-dependent regulator (hSNF5) gene causes the constitutive loss of exon 7, a frame shift in coding sequence and a production of truncated protein, which is implicated in the development of infant brain tumours (Taylor et al. 2000). Similarly, an AG to AT mutation leads to the removal of exon 4 in the anaphase promoting complex (APC) gene and this correlates with the development of liver cancer metastases (Kurahashi et al. 1995).

Generation of cryptic exon-containing transcripts by intron retention and alternative choice between two splice sites is another splicing mechanism (Venables 2006;Venables and Burn 2006). For example, oligomeric extracellular matrix glycoprotein Tenascin-C has a larger

splicing variant, generated by the inclusion of eight extra exons. Notably, only longer isoform can induce cell migration by the loss of focal adhesion and protect cancer cells from the immune-surveillance (Puente Navazo et al. 2001).

In mammals, ribosomal S6 kinases (S6Ks) represent a family composed of two distinct genes, S6K1 (RPS6KB1) and S6K2 (RPS6KB2). Generation of two isoforms for both S6K1 and S6K2 were reported (Gout et.al. 1998;Jefferies et al. 1997;Reinhard et al. 1994). They are produced through alternative translation start sites in exon 1 and characterised by their localisation either in nucleus or cytoplasm. p85S6K1 and p56S6K2 correspond to long nuclear forms and p70S6K1 and p54S6K2 to short cytoplasmic forms. In this thesis, full length S6K1 and S6K2 are referred as cytoplasmic forms, unless otherwise stated.

The existence of additional S6K1 short splicing isoforms has been recently reported (Karni et al. 2007). In humans, they are produced by the inclusion of one of the alternative exons (a or c) located before exon 7. Both splicing events introduce a frame shift and a premature stop codon. These two kinase inactive isoforms are identical to the full length S6K1 in their N terminus, but have different C-terminal ends. Notably, both splicing isoforms contain only half of their kinase domains and therefore lack the kinase activity. It was shown that the alternative splicing of RPS6KB1 (S6K1) gene and the expression of truncated isoforms are regulated by SF2/ASF splicing factor (Ben-Hur et al. 2013;Karni et al. 2008). High expression level of short splicing variants was reported in breast cancer tumour samples and cell lines.

Additionally, the overexpression of S6K1 short isoforms induced transformation of human breast epithelial cells (Ben-Hur et al. 2013).

To our knowledge, no splicing variants for S6K2 have been reported so far. Molecular cloning of full-length S6K2 in our laboratory revealed cDNA clones with the potential to encode new splicing isoforms. In this chapter, we report for the first time and provide evidence for the existence of S6K2 splice variants.

3.2 Results

3.2.1 Bioinformatic analysis reveals the existence of potential S6K2 splicing isoforms

Full length S6K2 was cloned from a human HEK293 cDNA library in our laboratory (Gout et al. 1998). Additionally, cDNA clones which might correspond to new splicing isoforms were identified and named clone 1, 2 and 3. These splicing isoforms are further referred to as S6K2-S1, S6K2-S2 and S6K2-S3. Sequencing analysis of these clones showed that they were generated during alternative splicing of S6K2 pre-mRNA. Initially, our efforts were focused on confirming the existence of these splicing variants using bioinformatic approach.

3.2.1.1 Alternative splicing of S6K2 gene has the potential to generate new splicing isoforms

Human S6K2 gene is located on chromosome 11 q13.2, (chr11:67,195,935-67,202,878). S6K2 gene is relatively small and contains 6944 nucleotides with an ORF (Open Reading Frame) of 1449 nucleotides. Bioinformatic analysis of the human S6K2 gene and the coding mRNA sequence (Appendix A) shows that it is encoded by 15

exons listed in Table 3.1. Classic intronic GT and AG splice sites exist at each of the intron/exon boundaries, apart from intron flanked with the exon 9 at the 3' splice end. This intron has a non-classic splice site GC. Taking into account that splice site point mutations is one of the most common mechanisms of alternative splicing, we can assume that there is a very high possibility of exon 9 splicing.

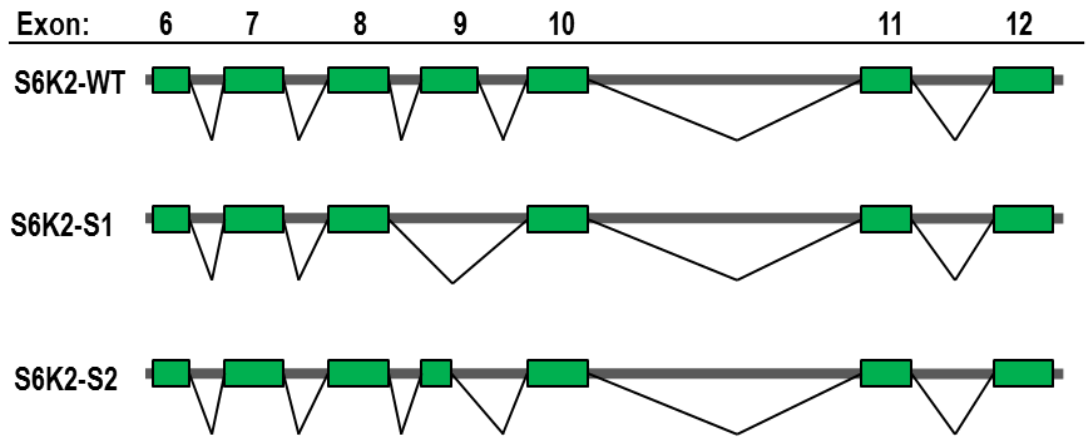
Because of the significant homology between human and mouse S6K2, it was logical to check if mouse S6K2 gene has the same mutated splice site. Analysis of the mouse gene and the coding mRNA sequence revealed the presence of the same evolutionary conserved mutated GC splice site in the region of exon 9 (data not shown).

Sequencing analysis of cDNA clones, isolated from the HEK293 cDNA library, confirms the existence of S6K2-S1 and S6K2-S2 as products of alternative splicing of exon 9. Schematic diagrams of the splicing mechanism for both isoforms are presented in Figure 3.1A.

| EXON | NUCLEOTIDE SEQUENCE |
|------|---|
| 1 | ATG GCGGCCGTGTTTGGATTTGGATTTGGAGACGGAGGAAGGCAGCGAGGGCGAGGGCGAGCC AGAGCTCAGCCCCGCG GT |
| 2 | AGG ACGCATGTCCCCTTGCCGAGTTGAGGGCAGCTGGCCTAGAG GT |
| 3 | AGG CCTGTGGGACACTATGAAGAGGTGGAGCTGACTGAGACCAGCGTGAACGTTGGCCCAGA GCGCATCGGGCCCCACTGCTTTGAGCTGCTGCGTGTGCTGGGCAAGGGGGCTATGGCAAG G T |
| 4 | AGG TGTTCCAGGTGCGAAAGGTGCAAGGCACCAACTTGGGCAAAATATATGCCATGAAAGTC CTAAGGAAG GT |
| 5 | AGG CCAAAATTGTGCGCAATGCCAAGGACACAGCACACACACGGGCTGAGCGGAACATTCTA GAGTCAGTGAAGCACCCCTTTATTGTGGAAGTGGCCTATGCCTTCCAGACTGGTGGCAAAC CTACCTCATCCTTGAGTGCCTCAGT GT |
| 6 | AGG TGGCGAGCTCTTCACGCATCTGGAGCGAGAGGGCATCTTCTGGAAGATACGGCCT GGT |
| 7 | AGC TTCTACCTGGCTGAGATCACGCTGGCCCTGGGCCATCTCCACTCCCAGGGCATCATCTA CCGGGACCTCAAGCCCGAGAACATCATGCTCAGCAGCC GT |
| 8 | AGG CCACATCAAACCTGACCGACTTTGGACTCTGCAAGGAGTCTATCCATGAGGGCGCCGTCA CTCACACCTTCTGCGGCACCATTGAGTACAT GT |
| 9 | AGG GGCCCTGAGATTCTGGTGCAGTGGCCACAACCGGGCTGTGGACTGGTGGAGCCTGGG GGCCCTGATGTACGACATGCTCACTGGATCG GC |
| 10 | AGC CGCCCTTACCCGAGAGAACCGGAAGAAAACCATGGATAAGATCATCAGGGGCAAGCTG GCACTGCCCCCTACCTCACCCAGATGCCCGGGACCTTGTCAAAAAG GT |
| 11 | AGT TTTCTGAAACGGAATCCCAGCCAGCGGATTGGGGGTGGCCAGGGGATGCTGCTGATGTG CAG GT |
| 12 | AGA GACATCCCTTTTTCCGGCACATGAATTGGGACGACCTTCTGGCCTGGCGTGTGGACCCC CCTTTCAGGCCCTGTCT GT |
| 13 | AGC AGTCAGAGGAGGACGTTGAGCCAGTTTGATAACCCGCTTACACGGCAGACGCCGGTGGAC AGTCCTGATGACACAGCCCTCAGCGAGAGTGCCAACCAGGCCCTTCT GT |
| 14 | AGG GGCTTACATACGTGGCGCCGTCTGTCTGGACAGCATCAAGGAGGGCTTCTCCTTCCAG CCCAAGCTGCGCTCACCCAGGCGCTCAACAGTAGCCCCGGGCCCC GT |
| 15 | AGC CCCCCTCAAGTTCTCCCCTTTTGGAGGGTTTCGGCCCAGCCCCAGCCTGCCGGAGCCCCAC GGAGCTACCTCTACCTCCACTCCTGCCACCGCCGCGCCCTCGACCACCGCCCCCTCCCCA TCCGTCCCCCTCAGGGACCAAGAAGTCCAAGAGGGGCGTGGGCGTCCAGGGCGC TAG |

Table 3.1 Intron/exon ends of human S6K2 gene. The human S6K2 gene has 15 exons that encodes full length S6K2 polypeptide. NNNNN – exons, **NN** – classic intron ends, **NN** – non-classic intron ends, **NNN** – standard start/stop codon.

A



B

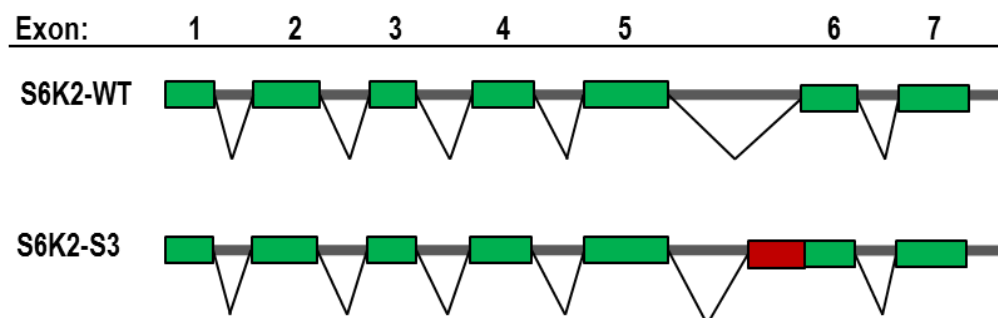


Figure 3.1 Schematic diagram of alternative splicing of human S6K2 gene and primary structure of potential splicing isoforms. Human S6K2 gene (S6K2wt) is alternatively spliced to generate three isoforms. (A) S6K2-S1 is generated through alternate splicing of full exon 9; S6K2-S2 incorporates only a part of exon 9. (B) S6K2-S3 splicing variant is produced by the intron inclusion in front of exon 6. Constitutive exons are shown as green boxes, and exon extension is shown in red box. Introns are shown as horizontal lines, and splicing events are indicated by angled lines.

S6K2-S1 splicing isoform is generated by skipping of the full exon 9 (91 nucleotides) which results in a coding sequence shown in Figure 3.2A. On the other hand, S6K2-S2 splicing variant includes a fragment of exon 9 (69 nucleotides). The splicing machine recognises the classical GT splice site inside the coding sequence of exon 9 and removes 22 nucleotides at the end of this exon. Generated nucleotide sequence is presented in Figure 3.3A. In both cases the splicing events introduce a frame shift in coding sequence and premature stop codons.

Analysis of cDNA nucleotide sequence corresponding to S6K2-S3 shows that it is generated by aberrant splicing of intron 5, resulting in the inclusion of a cryptic exon in the transcript. The splicing machine recognises the classical acceptor AG splice site in the intron 5 sequence and includes it in the coding region. This cryptic exon contains a premature termination codon Figure 3.4A. Schematic representation of the S6K2-S3 splicing mechanism is shown in Figure 3.1B.

In order to identify potential S6K2 splicing isoforms, the GenBank Human expressed sequence tag (EST) database was searched for the presence of the unique exon/exon junction sequences. A BLAST search for the S6K2-S1 splicing isoform demonstrated the presence of two homologous clones: BE879750.1 and BI907520.1 (Figure 3.2B). Moreover, comparison analysis of the S6K2-S2 splicing variant against the EST database yielded homology with 3 clones: AV705502.1, AV705144.1 and BX337503.2 (Figure 3.3B).

A

ATGGCGGCCGTGTTTGATTGGATTTGGAGACGGAGGAAGGCAGCGAGGGCGAGGGCGAGCCAGAGCTCAGCCCCGCGGA
CGCATGTCCCCTTGCCGAGTTGAGGGCAGCTGGCCTAGAGCCTGTGGGACACTATGAAGAGGTGGAGCTGACTGAGACCAGC
GTGAACGTTGGCCAGAGCGCATCGGGCCCCACTGCTTTGAGCTGCTGCGTGTGCTGGGCAAGGGGGGCTATGGCAAGGTGT
TCCAGGTGCGAAAGGTGCAAGGCACCAACTTGGGCAAAATATATGCCATGAAAGTCCTAAGGAAGGCCAAAATTGTGCGCAA
TGCCAAGGACACAGCACACACACGGGCTGAGCGGAACATTCTAGAGTCAGTGAAGCACCCCTTTATTGTGGAAGTGGCCTATG
CCTTCAGACTGGTGGCAAACCTCTACCTCATCCTTGAGTGCCTCAGTGGTGGCGAGCTCTTACGCATCTGGAGCGAGAGGGC
ATCTTCCTGGAAGATACGGCCTGCTTCTACCTGGCTGAGATCACGCTGGCCCTGGGCCATCTCCACTCCCAGGGCATCATCTAC
CGGGACCTCAAGCCCGAGAACATCATGCTCAGCAGCCAGGGCCACATCAAACCTGACCGACTTTGGACTCTGCAAGGAGTCTA
TCCATGAGGGCGCCGTCACCTCACACCTTCTGCGGCACCATTGAGTACAT**CCGCCCTTACC**CGCAGAGAA**CCGGAAGAAA**ACCT
GGATAAGATCATCAGGGGCAAGCTGGCACTGCCCCCTACCTCACCCAGATGCCCGGGACCTTGTCAAAAAGTTT**TGA**

B

| | | |
|---------------------------|---|---|
| | ↓ | |
| S6K2-S1 | | ACCATTGAGTACAT CCGCCCTTACC CGCAGAGAA CCGGAAGAAA ACCATG |
| gi 10328526 gb BE879750.1 | | ACCATTGAGTACAT CCGCCCTTACC CGCAGAGAA_____ |
| gi 16170354 gb BI907520.1 | | ACCATTGAGTACAT CCGCCCTTACC CGCAGAGAA CCGGAAGAAA CAC-ATG |

Figure 3.2 Analysis of S6K2-S1 nucleotide sequence. (A) Coding nucleotide sequence of S6K2-S1. Underlined sequence was used for screening human EST database. (B) ClustalW2 alignment of S6K2-S1 nucleotide sequence with EST clones. The arrows indicate the position of the splicing fusion junction between exons 8 and 10.

A

ATGGCGGCCGTGTTTGATTGGATTGGAGACGGAGGAAGGCAGCGAGGGCGAGGGCGAGCCAGAGCTCAGCCCCG
CGGACGCATGTCCCCTTGCCGAGTTGAGGGCAGCTGGCCTAGAGCCTGTGGGACACTATGAAGAGGTGGAGCTGACT
GAGACCAGCGTGAACGTTGGCCAGAGCGCATCGGGCCCCACTGCTTTGAGCTGTGCGTGTGCTGGCAAGGGGGG
CTATGGCAAGGTGTTCCAGGTGCGAAAGGTGCAAGGCACCAACTGGGCAAATATATGCCATGAAAGTCTTAAGGAA

← Exon 5 →
GGCCAAAATTGTGCGCAATGCCAAGGACACAGCACACACGGGCTGAGCGGAACATTCTAGAGTCAGTGAAGCACC

← Exon 5 →
CCTTTATTGTGGAAGTGGCCTATGCCTCCAGACTGGTGCAAACCTTACCTCATCCTTGAGTGCCTCAGTG

← Intron included in the coding sequence →
TAGACTGAGCGTCCTGAGGGCAGTGGCTGGGTCTCTTCATCCTGTCCCAGCTTACCCAGCACAGGGCCAGGCACCG

← Intron included in the coding sequence →
AGTAGGCGTCGGTAGATGTTTGTGAATTGAATTGAATCCCACGGCAGCTCTGTGAGGCAG

← Exon 6 →
GTGGCGAGCTCTTACGCATCTGGAGCGAGAGGGCATCTTCTGGAAGATACGGCCTG

B

↓

| | |
|----------------------------|---|
| S6K2wt | TGAGTGCCTCAGTG----- |
| gi 8278085 gb BE018075.1 | TGAGTGCCTCAGTG-----ACTGAGCGTCCTGAGGGCAGTGGCTGGGTCT-- |
| gi 14059479 gb BG748826.1 | TGAGTGCCTCAGTG-----ACTGAGCGTCCTGAGGGCAGTGGCTGGGTCTCT |
| gi 146025479 gb DC394569.1 | TGAGTGCCTCAGTG TAGACTGAG CGTCCTGAGGGCAGTGGCTGGGTCTCT |
| gi 78270669 gb DA091729.1 | TGAGTGCCTCAGTG TAGACTGAG CGTCCTGAGGGCAGTGGCTGGGTCTCT |
| gi 146098945 gb DC352664.1 | TGAGTGCCTCAGTG TAGACTGAG CGTCCTGAGGGCAGTGGCTGGGTCTCT |
| gi 66261146 gb DR001273.1 | TGAGTGCCTCAGTG TAGACTGAG CGTCCTGAGGGCAGTGGCTGGGTCTCT |
| gi 61644424 gb DN601754.1 | TGAGTGCCTCAGTG-----ACTGAGCGTCCTGAGGGCAGTGGCTGGGTCTCT |
| gi 16179463 gb BI915444.1 | TGAGTGCCTCAGTG-----ACTGAGCGTCCTGAGGGCAGTGGCTGGGTCTCT |
| gi 19121736 gb BM804913.1 | TGAGTGCCTCAGTG-----ACTGAGCGTCCTGAGGGCAGTGGCTGGGTCTCT |
| gi 15758743 gb BI767165.1 | TGAGTGCCTCAGTG-----ACTGAGCGTCCTGAGGGCAGTGGCTGGGTCTCT |
| gi 90648366 gb BY797633.2 | TGAGTGCCTCAGTG TAGACTGAG CGTCCTGAGGGCAGTGGCTGGGTCTCT |
| gi 15758752 gb BI767174.1 | TGAGTGCCTCAGTG-----ACTGAGCGTCCTGAGGGCAGTGGCTGGGTCTCT |
| gi 22339986 gb BQ924955.1 | TGAGTGCCTCAGTG TAGACTGAG CGTCCTGAGGGCAGTGGCTGGGTCTCT |
| gi 46569685 gb BX377754.2 | TGAGTGCCTCAGTG TAGACTGAG CGTCCTGAGGGCAGTGGCTGGGTCTCT |
| gi 15948145 gb BI836595.1 | TGAGTGCCTCAGTG-----ACTGAGCGTCCTGAGGGCAGTGGCTGGGTCTCT |
| gi 58050365 gb CX753710.1 | TGAGTGCCTCAGTG-----ACTGAGCGTCCTGAGGGCAGTGGCTGGGTCTCT |
| gi 19365855 gb BM915476.1 | TGAGTGCCTCAGTG TAGACTGAG CGTCCTGAGGGCAGTGGCTGGGTCTCT |

Figure 3.4 Analysis of S6K2-S3 nucleotide sequence. (A) Coding nucleotide sequence of S6K2-S3. Underlined sequence was used for screening human EST database. (B) ClustalW2 alignment of S6K2-S3 nucleotide sequence with EST clones. The arrows indicate the position of the splicing fusion junction between exon 5 and intron sequence included in the coding region.

Unexpectedly, as seen from Figure 3.4B, more than fifteen EST-clones homologous to human S6K2-S3 were obtained. Furthermore, screening of the GenBank Mouse EST database showed the existence of 3 EST-clones with the potential to encode mouse S6K2-S3 splicing isoform (data not shown).

The list of all identified human EST-clones, corresponding to S6K2-S1, S6K2-S2 and S6K2-S1, is summarized in Table 3.2. These results demonstrate that S6K2 splicing variants may be expressed in a variety of normal tissues and organs, including testis, cerebellum, foetal brain, placenta, adrenal gland, leucocytes and epithelial cells. Notably, S6K2 splice variants are also found in a range of human malignancies, such as epidermoid carcinoma, amelanotic melanoma, large cell lung carcinoma, cervical and rectum cancer. Furthermore, we believe that additional S6K2 splicing isoforms remained to be identified.

| | Reference: | Tissue type: | Organ: |
|---|--|---|----------------------------|
| S6K2-S1 | http://www.ncbi.nlm.nih.gov/nucest/BE879750.1 | large cell carcinoma, undifferentiated | lung |
| | http://www.ncbi.nlm.nih.gov/nucest/BI907520.1 | leukocyte | |
| S6K2-S2 | http://www.ncbi.nlm.nih.gov/nucest/BX337503.2 | placenta cot 25-normalized | |
| | http://www.ncbi.nlm.nih.gov/nucest/AV705502.1 http://www.ncbi.nlm.nih.gov/nucest/AV705144.1 | Adrenal gland | |
| | http://www.ncbi.nlm.nih.gov/nucest/BX538119 | human rectum tumor | |
| S6K2-S3 | http://www.ncbi.nlm.nih.gov/nucest/BE018075.1 | cervical carcinoma cell line | cervix |
| | http://www.ncbi.nlm.nih.gov/nucest/BG748826.1 | normal pigmented retinal epithelium | eye |
| | http://www.ncbi.nlm.nih.gov/nucest/DC394569.1 | testis | |
| | http://www.ncbi.nlm.nih.gov/nucest/DA091729.1 | cerebellum | |
| | http://www.ncbi.nlm.nih.gov/nucest/DC352664.1 | fetal brain | |
| | http://www.ncbi.nlm.nih.gov/nucest/DR001273.1 | fetal brain | fetal brain |
| | http://www.ncbi.nlm.nih.gov/nucest/DN601754.1 | human embryonic stem cells | |
| | http://www.ncbi.nlm.nih.gov/nucest/BI915444.1 | | brain |
| | http://www.ncbi.nlm.nih.gov/nucest/BM804913.1 | | ovary (pool of 3) |
| | http://www.ncbi.nlm.nih.gov/nucest/BI767165.1 | | pooled lung and spleen |
| | http://www.ncbi.nlm.nih.gov/nucest/BY797633.2 | eye | |
| | http://www.ncbi.nlm.nih.gov/nucest/BI767174.1 | | pooled lung and spleen |
| | http://www.ncbi.nlm.nih.gov/nucest/BQ924955.1 | epidermoid carcinoma, cell line | lung |
| | http://www.ncbi.nlm.nih.gov/nucest/BX377754.2 | placenta cot 25 normalized | |
| | http://www.ncbi.nlm.nih.gov/nucest/BI836595.1 | | pooled spleen and pancreas |
| | http://www.ncbi.nlm.nih.gov/nucest/CX753710.1 | pluripotent cell line derived from blastocyst inner cell mass | blastocyst |
| http://www.ncbi.nlm.nih.gov/nucest/BM915476.1 | amelanotic melanoma, cell line | skin | |

Table 3.2 Analysis of human EST-clones corresponding to S6K2-S1, S6K2-S2 and S6K2-S3 splicing variants.

3.2.1.2 Analysis of amino acid sequences corresponding to new splicing variants

Full length S6K2 protein is 482 amino acids in length and its predicted molecular weight is approximately 55kDa. Generated S6K2-S1 and S6K2-S2 transcripts have the potential to encode proteins of 273 and 296 amino acids in length correspondingly. Predicted molecular weight of S6K2-S1 is approximately 32 kDa, whereas S6K2-S2 is about 34 kDa. S6K2-S3 splice variant is much shorter, 153 amino acids in length, and has a predicted molecular weight of 16kDa (Figure 3.5). As presented in Figure 3.5, all three splicing variants are identical to full length S6K2 at their N-terminus. S6K2-S1 and S6K2-S2 proteins have identical and unique 38 amino acids extension at the C-terminus (highlighted in red in Figure 3.5), as in both cases splicing transcripts have the same frame shift in their coding sequences. Potentially, this specific sequence can function in determining subcellular localization, interaction with binding partners, formation of regulatory complex and downstream signalling for both splicing isoforms. Amino acid analysis of this unique 38 amino acids C-terminal sequence reveals that it is enriched in positively charged arginine and lysine residues. To access whether this sequence is present in any other identified proteins we searched various protein databases. A BLAST screening for the presence of this unique sequence does not reveal any significant homology with known proteins. The presence of unique 38 amino acids extension in S6K2-S1 and S6K2-S2 variants offers the opportunity for generation specific antibodies against these isoforms, as described in chapter 2.5. Interestingly, the

protein sequence of the S6K2-S3 splicing isoform is identical to the N-terminal end of full length S6K2.

Notably, all three splice isoforms lack at least half of the kinase domain, kinase extension and autoinhibitory regions. S6K2-S1 and S6K2-S2 have only one key activation site, pT228, which is phosphorylated by PDK1 (Figure 3.6). S6K2 full length and all identified splicing isoforms possess at their N-terminus the TOR signalling (TOS) motif, important for targeting S6K2 to the mTORC1 signalling cascade.

In this thesis most of the work is focused on studying the role and functions of S6K1-S1.

3.2.2 RT-PCR analysis confirms the existence of S6K2-S1 in HEK293 cells

To confirm the existence of endogenous S6K2-S1 splicing isoform we examined the presence of the corresponding mRNA transcript using RT-PCR analysis.

As described above, S6K2-S1 and S6K2-S2 splicing isoforms are generated by the alternative splicing of exon 9. To begin with, we specifically designed a set of primers (Appendix B), which amplified the cDNA corresponding to exons 8-12 of the human S6K2 gene, as shown in Figure 3.7A. In this experiment, we expected 3 different PCR products corresponding to full length S6K2, S6K2-S1 and S6K2-S2, with different molecular weights depending on the splicing of exon 9. To start with, high quality total mRNA from HEK293 cells was isolated and first strand cDNA was generated (data not shown). This preparation was used as a template for the RT-PCR amplification.

S6K2wt 482aa

MAAVFDLDLETEEGSEGEPELSPADACPLAELRAAGLEPVGHYEEVELTETSVNVGPERIGPHCFELLRLV
GKGGYGKVFQVRKVQGTNLGKIYAMKVLRKAKIVRNAKDTAHTRAERNILESVKHPFIVELAYAFQTGGKLYL
ILECLSGGELFTHLEREGIFLEDTACFYLAETTLALGHLHSQGIIYRDLKPENIMLS SQGHIKLTDGFLCKES
IHEGAVTHTFCGTIEYMAPEILVRS GHNRAVDWWSLGALMYDMLTGSPPFTAENRKKTMDKIIIRGKLALPPYL
TPDARDLVKKFLKRNPSQRIGGGPGDAADVQRHPFFRHMNWDDLAWRVDPFRPCLQSEEDVSQFDTRFTRQ
TPVDS PDDTALSE SANQAF LGFTYVAPSVLDSIKEGFSFQPKLRS PRRLNS SPRAPVSPLKFS PFEGFRPSPS
LPEPTELPLPPLLPPPPPSTTAPLPIRPPSGTKKSKRGRGRPGR

S6K2-S1 273aa

MAAVFDLDLETEEGSEGEPELSPADACPLAELRAAGLEPVGHYEEVELTETSVNVGPERIGPHCFELLRLV
GKGGYGKVFQVRKVQGTNLGKIYAMKVLRKAKIVRNAKDTAHTRAERNILESVKHPFIVELAYAFQTGGKLYL
ILECLSGGELFTHLEREGIFLEDTACFYLAETTLALGHLHSQGIIYRDLKPENIMLS SQGHIKLTDGFLCKES
IHEGAVTHTFCGTIEY *IRPLPQRTGRKPWIRSSGASWHCPPTSPQMPGTL SKSF*

S6K2-S2 296aa

MAAVFDLDLETEEGSEGEPELSPADACPLAELRAAGLEPVGHYEEVELTETSVNVGPERIGPHCFELLRLV
GKGGYGKVFQVRKVQGTNLGKIYAMKVLRKAKIVRNAKDTAHTRAERNILESVKHPFIVELAYAFQTGGKLYL
ILECLSGGELFTHLEREGIFLEDTACFYLAETTLALGHLHSQGIIYRDLKPENIMLS SQGHIKLTDGFLCKES
IHEGAVTHTFCGTIEYMAPEILVRS GHNRAVDWWSLGALL *RPLPQRTGRKPWIRSSGASWHCPPTSPQMPGTL
SKSF*

S6K2-S2 153aa

MAAVFDLDLETEEGSEGEPELSPADACPLAELRAAGLEPVGHYEEVELTETSVNVGPERIGPHCFELLRLV
GKGGYGKVFQVRKVQGTNLGKIYAMKVLRKAKIVRNAKDTAHTRAERNILESVKHPFIVELAYAFQTGGKLYL
ILECLSGGELFTHLEREGIFL

Figure 3.5 Protein sequences of S6K2 splicing isoforms. Unique sequences corresponding to S6K2-S1 and S6K2-S2 isoforms C-terminal amino acid sequences are highlighted in italic red.

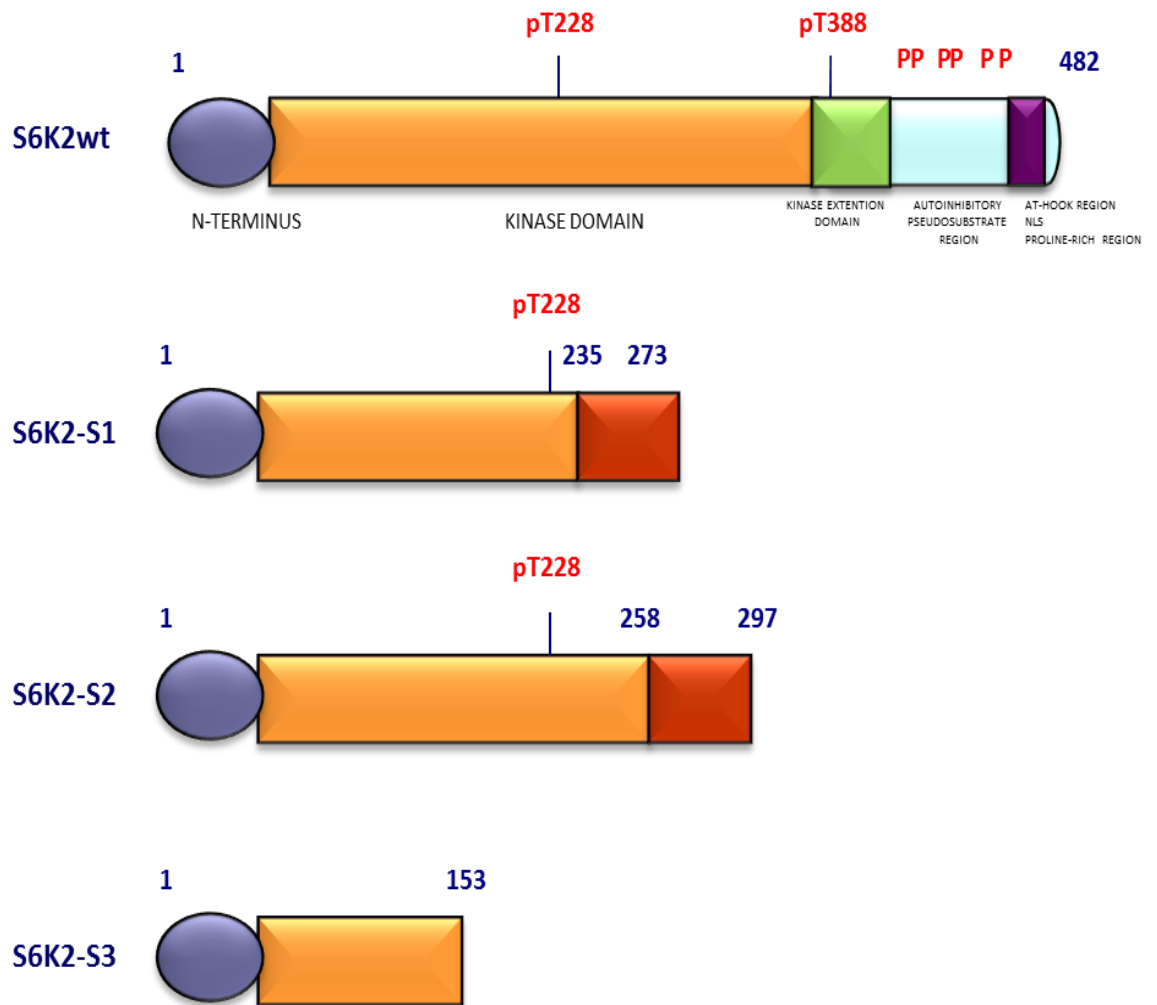


Figure 3.6 Schematic representation of S6K2 isoforms. The full length S6K2 is 482 amino acids in length with the predicated molecular weight of 55kDa. The S6K2-S1 splicing isoform is 273 amino acids in length and has predicted molecular weight of approximately 32 kDa. The S6K2-S2 splicing isoform encodes a protein of 296 amino acids in length and has predicted molecular weight of approximately 34 kDa. Both isoforms lack half of the kinase domain and the C-terminal regulatory region. The shift in the reading frame results in a unique C-terminal 38 amino acid sequence presented by red boxes. The S6K2-S3 splicing variant is 153 amino acids in length and is completely identical to the N-terminus of full length S6K2.

As shown in Figure 3.7B, RT-PCR analysis of mRNA transcripts derived from HEK293 cells revealed the presence of 2 amplified products. The top band of approximately 380bp corresponds to the full length S6K2 splice variant (386bp), and the band below, with the lower molecular weight of approximately 290bp, corresponds to S6K2-S1 splicing isoform (295bp). Based on the intensity of the signals we can conclude that mRNA level of full length S6K2 in HEK293 cells is much higher when compared to that of S6K2-S1. This explains the fact, that due to the overload of the PCR product, in order to detect a weak signal for the splicing isoform, the band corresponding to the full-length S6K2 ran slightly lower than expected.

Theoretically, we expected the appearance of the third band, corresponding to the S6K2-S2 isoform, but unfortunately we did not observe any additional signal in this area. This could be explained by the fact that the amplified products of full length S6K2 and S6K2-S2 differ by just 22 nucleotides and might overlap when separated by gel electrophoresis.

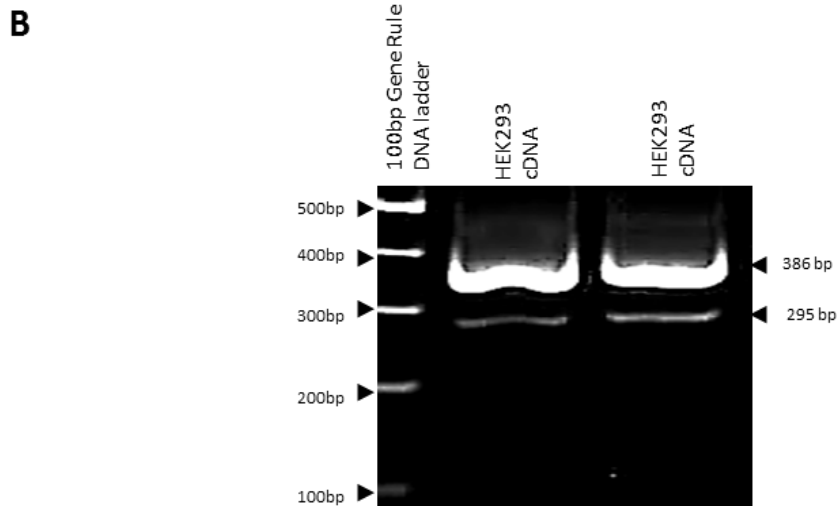
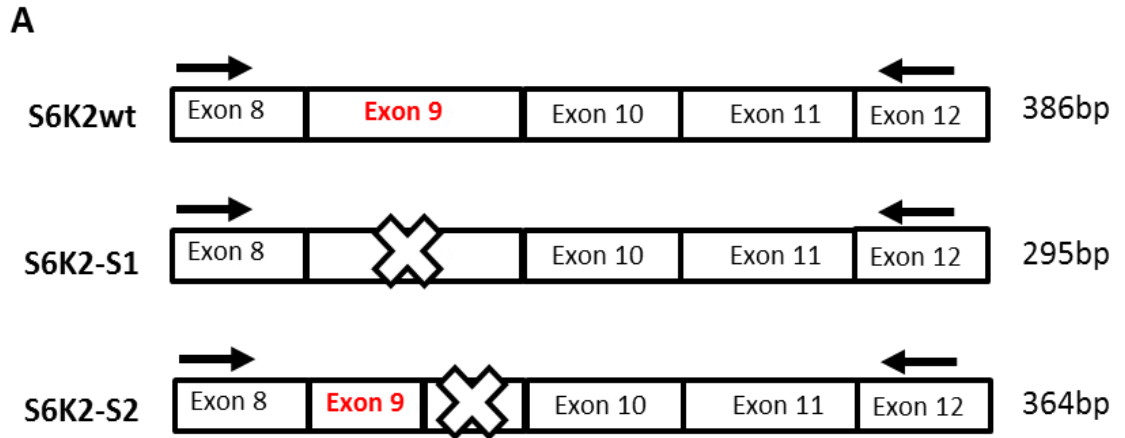


Figure 3.7 Analysis of S6K2-S1 expression in HEK293 cell lines by RT-PCR. (A) Schematic presentation of expected RT-PCR amplified products corresponding to DNA fragments of full length S6K2 and splicing isoforms. (B) Agarose gel electrophoresis of RT-PCR products amplified from cDNA derived from HEK293 cells with a set of specific primers. Total mRNA was extracted from HEK293 cell lines, converted into cDNA and used as a template for RT-PCR amplification with a specific set of primers.

3.2.3 Molecular cloning and mammalian expression of the S6K2-S1 splicing isoform

Molecular cloning of S6K2 from the HEK293 cDNA library in our laboratory resulted in the identification of a large panel of cDNA clones corresponding to the full length S6K2 and several cDNA clones with the potential to encode novel splicing isoforms. One of these clones, BISK/S6K2 clone 1, was used for molecular cloning of S6K2-S1. Sequencing of the full length insert of the BISK/S6K2 clone 1 was completed to verify its mRNA and deduced protein sequences.

In subsequent studies, BISK/S6K2-S1 clone 1 was used as a template for molecular cloning into various expression vectors by PCR amplification with specific sets of primers. To express S6K2-S1 in mammalian cells, the full length coding sequence was cloned into pcDNA3.1 and pcDNA4TO expression vectors. To do so, the forward primer was designed to introduce BamH1 restriction site and the tag sequence at the N-terminus. The initiation start codon was placed in front of the tag and in frame with the S6K2-S1 protein coding sequence. The reverse primer had a stop codon and a restriction site for Not1. All primers used in this work are listed in Appendix B.

As shown in Figure 3.8A, a band of approximately 1500bp was specifically amplified in the PCR set up. The size of the amplified DNA fragment corresponded with that expected from the PCR priming. The band was excised from the gel and amplified DNA was purified by Thermo Fisher Scientific DNA extraction kit. After digestion with BamH1 and Not1 restriction enzymes, amplified DNA was cloned into pre-

digested pcDNA 3.1 (or pcDNA4TO) mammalian expression vectors. Subcloning of S6K2-S1 into pcDNA3.1 was successful, as indicated by the restriction analysis and agarose gel electrophoresis of one of the resulting constructs with BamH1 and Not1 enzymes (Figure 3.8B). Sequence analysis of generated pcDNA3.1/S6K2-S1 clones confirmed the presence of correct sequence.

To check if generated pcDNA3.1/S6K2-S1 construct had the ability to express the protein of interest, it was transiently transfected into HEK293 cells along with an empty vector. After 48 hours post transfection, cells were analysed for the expression of S6K2-S1 splicing isoform in Western blotting using specific anti-S6K2-S1 antibodies (described in the next chapter). As seen in Figure 3.9A, S6K2-S1 expression was confirmed by the presence of a strong immunospecific band in cells transfected with the pcDNA3.1/S6K2-S1 plasmid compared to the control.

To proceed further with our work and to study the function of the S6K2-S1 in cells, we decided to generate stable cell lines overexpressing the S6K2-S1 splicing isoform. To begin with, HEK293 stable cell lines overexpressing S6K2-S1 were generated using pcDNA3.1/S6K2-S1 construct. However, the expression of the splicing isoform in these cell lines was so low, that in a Western blot using 40µg of total lysate only a very weak immunoreactive signal appeared (data not shown).

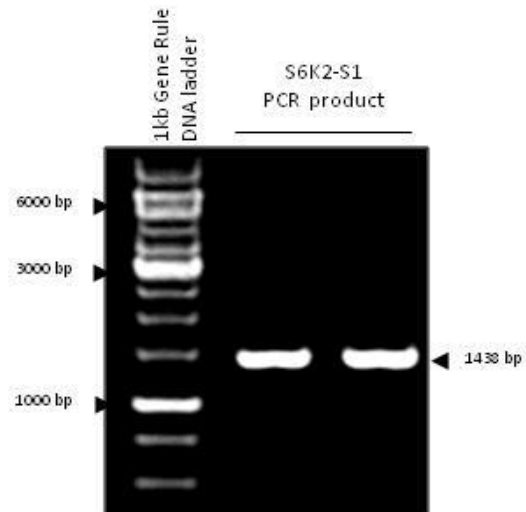
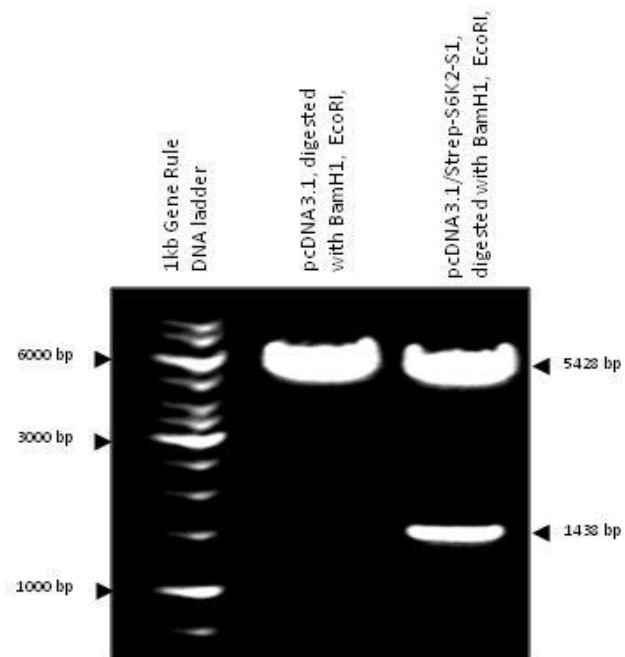
A**B**

Figure 3.8 Molecular cloning of S6K2-S1 splicing isoform into pcDNA3.1 expression plasmid. (A) 1% Agarose gel electrophoresis of PCR amplified S6K2-S1. cDNA clone from human HEK293 cDNA library was used as a template. (B) Restriction analysis of pcDNA3.1/Strep-S6K2-S1 construct and an empty pcDNA3.1 vector. Purified plasmids were digested with BamH1 and Not1 restriction enzymes and then separated by 1% agarose gel electrophoresis.

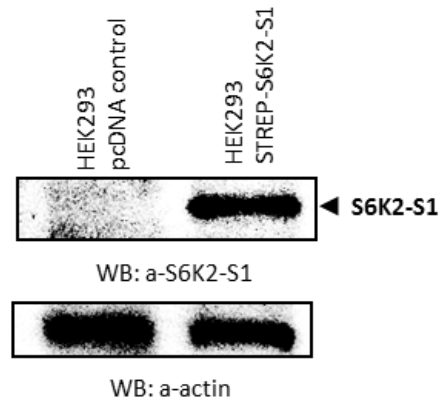
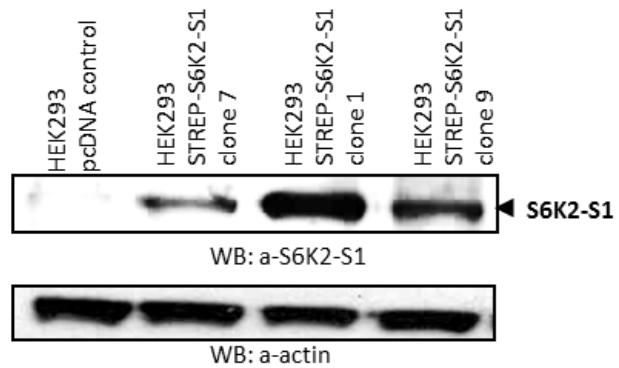
A**B**

Figure 3.9 Generation of stable cell lines overexpressing S6K2-S1. (A) Expression analysis of S6K2-S1 splicing isoform by transient transfection. HEK293 cells were transiently transfected with Strep-tagged S6K2-S1 and empty vector, using a standard protocol for the ExGene 500 transfection reagent. After 48 hours, cells were lysed and analysed by Western blotting with anti-S6K2-S1 affinity purified antibodies. Anti-actin antibodies were used as a control of equivalent protein loading. (B) Generation of monoclonal stable cell lines overexpressing S6K2-S1. 48 hours after transient transfection, HEK293 cells were split into fresh medium with selective antibiotic. Cells were fed with selective medium every 3–4 days, until antibiotic-resistant cells produced separate colonies. These colonies were grown separately till they reached confluency. Next, selected clones were checked for the S6K2-S1 expression in Western blotting using anti-S6K2-S1 antibodies. 30mg of total cell lysate was used for loading. Anti-actin antibodies were used as a control of equivalent protein loading.

Furthermore, the expression of S6K2-S1 in these cells gradually disappeared. This might be explained by the weak Geneticin selection as it took up to 3 weeks to generate cell lines, and as a result cells become resistant to antibiotic. The other possible explanation is that the overexpression of S6K2-S1 affects cell survival/selection; therefore cells do not tolerate high expression level of the splicing isoform.

Based on these observations, first we decided to use pcDNA4TO/S6K2-S1 construct, as it had different antibiotic resistance. Second we performed monoclonal selection of stable cell lines, as it gave us the possibility to generate cell lines with different expression level of the splicing variant. Briefly, HEK293 cells were transfected with pcDNA4TO/S6K2-S1 and an empty vector. Two days after transfection, cells were transferred into the fresh medium with selective antibiotic (Zeocin at 100 µg/ml). Cells were cultured in a selective medium until antibiotic-resistant cells produced separate colonies. The expression of S6K2-S1 was tested in 12 isolated colonies (clones). We observed a diverse range of S6K2-S1 overexpression in tested clones. However, the expression efficiency of S6K2-S1 in generated stable clones was still very low. Expression analysis of selected clones allowed us to isolate only one clone with relatively high level of S6K2-S1 overexpressed, while 9 and 2 clones exhibited low and medium expression respectively (data not shown). Based on these results, we selected 3 clones with different expression levels of S6K2-S1 splicing isoform: clone 1, 7 and 9, to work with (Figure 3.9B). Detailed functional analysis of these stable cell lines is described in chapter 3 of the thesis.

3.2.4 Generation and characterisation of specific polyclonal antibodies directed towards S6K2-S1

Specific antibodies against S6K2-S1 can be directed to a unique 38 amino acid sequence at the C-terminus of splicing isoform. Bioinformatic analysis of this sequence for the best immunogenic region revealed that the best hit corresponding to the extreme C-terminal end of S6K2-S1. Based on this analysis, we synthesised a 16mer peptide, containing unique C-terminal sequence of S6K2-S1 and a cysteine residue at the N-terminus for coupling to activated KHL (see below).

NH₂ – CPPTSPQMPGTLKSKSF – COOH

Anti-S6K2-S1 polyclonal antibodies were raised by immunizing two rabbits with the synthetic peptide, coupled to activated keyhole limpet hemocyanin (KHL). After completing the immunization protocol, serum from both rabbits was collected and tested by ELISA against the antigenic peptide. ELISA results showed a good immune response to injected peptide in both rabbits, so we used the final bleed serum from for affinity purification of S6K2-S1 specific antibodies.

Initially, we tested the immunoreactivity of collected sera in Western blotting. To do so, HEK 293 cells were transiently transfected with empty pcDNA3.1 vector and pcDNA3.1/Strep-S6K2-S1 construct. 48 hours after transfection, cells were lysed and analysed by Western blotting with anti-S6K2-S1 polyclonal serum. As shown in Figure 3.10A, diluted serum specifically recognized an immunoreactive band, corresponding to overexpressed Strep-tagged S6K2-S1, with a predicted molecular weight of 37 kDa. This band was not present in the control sample of cells transfected with pcDNA3.1 empty vector.

Then, we performed affinity purification of anti-S6K2-S1 polyclonal antibodies from the serum collected from both rabbits. Specific antibodies can be purified from the serum of immunized animals by binding to and elution from the immobilized antigen. For generation of affinity matrix, synthetic peptide was coupled to cyanogen bromide activated sepharose through a Sulfo-SMCC linker. Generated affinity matrix was then incubated with the immune serum. Nonspecific binding to the affinity matrix was removed by washing the column with phosphate saline buffer (PBS). Specifically associated IgG antibodies were then eluted from the column with 0.1M glycine and collected as 1 ml fractions. Fractions corresponding to the peak of eluted antibodies were combined and dialysed against 1xPBS. After further dialysis in 50% glycerol/PBS, purified antibodies were stored at -20°C. SDS-PAGE and Coomassie blue staining of eluted fractions clearly shows the presence of both heavy and light chains of purified antibodies corresponding to molecular weight of 55 and 25 kDa (Figure 3.10B).

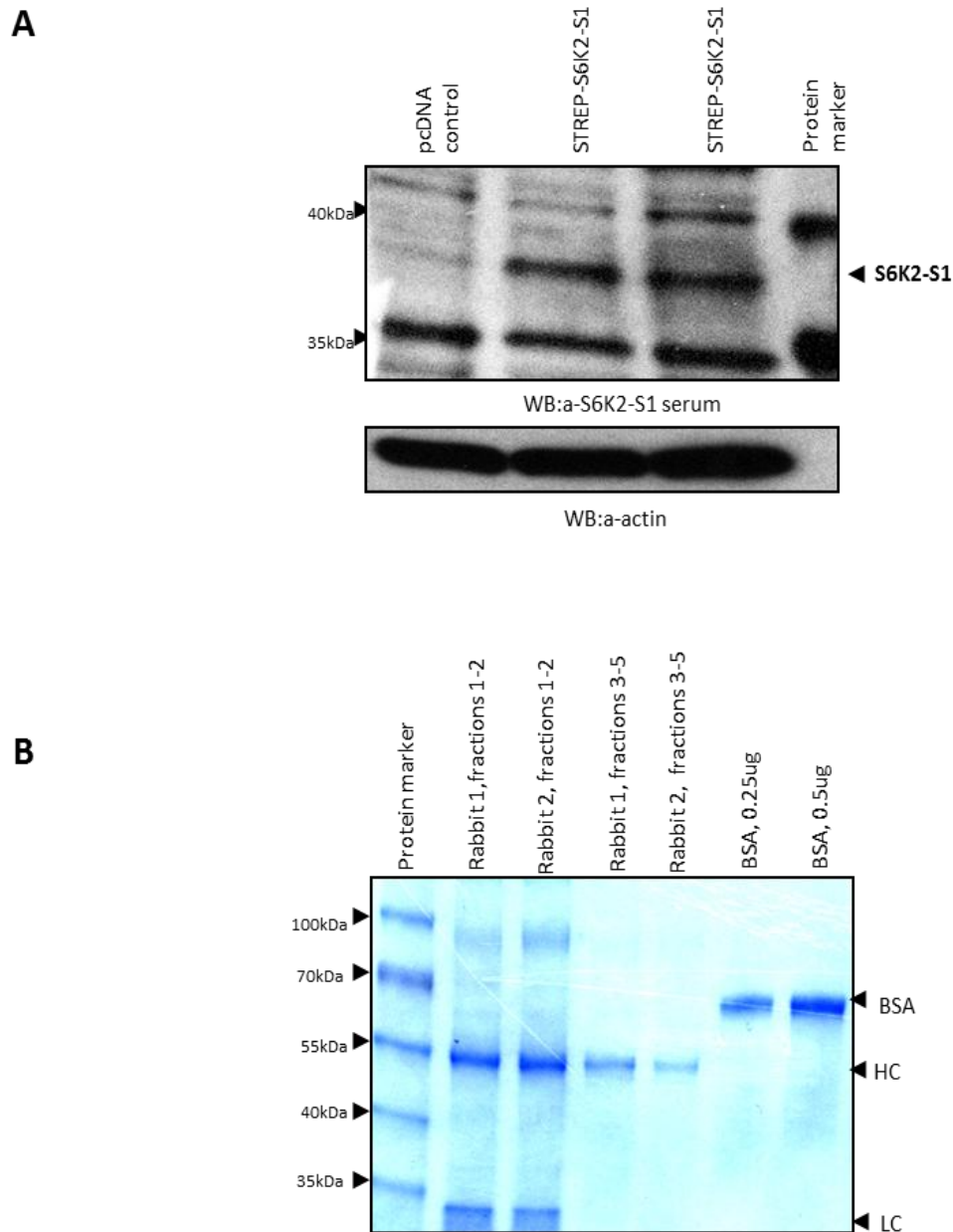


Figure 3.10 Affinity purification of polyclonal anti-S6K2-S1 antibodies. (A) Anti-S6K2-S1 serum specifically recognises overexpressed S6K2-S1. HEK 293 cells were transfected with Strep-tagged S6K2-S1, lysed and analysed in Western blotting with anti-S6K2-S1 serum (1:1000). Anti-actin antibodies were used as a control of equivalent protein loading. (B) SDS-PAGE analysis of affinity purified anti-S6K2-S1 polyclonal antibodies. Polyclonal serum was loaded onto a column prepared with S6K2-S1 C-terminal peptide coupled to Sepharose beads, column was washed with PBS and antibodies were eluted. Antibody containing fractions were combined, dialysed and stored at -20°C . HC-heavy chain of antibodies, LH-light chain of antibodies, BSA – bovine serum albumin standard.

The specificity of affinity purified antibodies was then tested in Western blotting. As shown in Figure 3.11A, affinity purified antibodies specifically recognize in lysates of transfected HEK293 cells Strep-tagged S6K2-S1 protein with a molecular weight of approximately 37 kDa, compared to the control sample. Interestingly, antibodies generated in two rabbits show a different pattern of immunoreactivity in Western blotting. Antibodies produced in rabbit 1 show lower non-specific binding and detect two strong immunoreactive bands with molecular weight of approximately 35-36kDa in control and S6K2-S1 overexpressing cells. Notably, these immunoreactive bands run just below the signal of overexpressed Strep-tagged S6K2-S1. We believe that faster migrating bands correspond to endogenous S6K2 splicing isoforms. On the other hand, antibodies generated in rabbit 2 recognise overexpressed S6K2-S1 protein, but show no additional immunoreactive signals which might correspond to endogenous S6K2-S1 splicing variant. Taking these data into account, we decided to use in further studies antibodies raised in rabbit 1, as they have the potential to recognize both recombinant and endogenous S6K2-S1 splicing isoform. Unfortunately, generated affinity purified polyclonal antibodies were not effective in the immunoprecipitation assay, which significantly restricted their application (data not shown).

Using affinity purified anti-S6K2-S1 antibodies we tested a panel of 6 different cell lines for the presence of endogenous S6K2-S1 protein. As shown in Figure 3.11B, a weak immunoreactive band which runs below the signal corresponding to overexpressed EE tagged S6K2-S1 is detected in tested cell lines. This might indicate the presence of endogenous S6K2-S1 splicing variant. Notably, 5 cell lines have an

additional immunoreactive band just above the signal of overexpressed S6K2-S1 protein. This band might correspond to S6K2-S2 splicing variant, which is bigger than S6K2-S1 by 23 amino acids and possesses the same unique C-terminus.

In summary, bioinformatics of EST clones, sequence analyses of isolated S6K2 specific cDNA clones from HEK293 cDNA library, as well as the expression analysis of transiently expressed and endogenous proteins reveal the existence of novel S6K2 splicing isoforms. Taking into account that identified S6K2 splice isoforms can only encode the N-terminal regions of the kinase domain, the lack of the kinase activity would be the unique features of these splice variants.

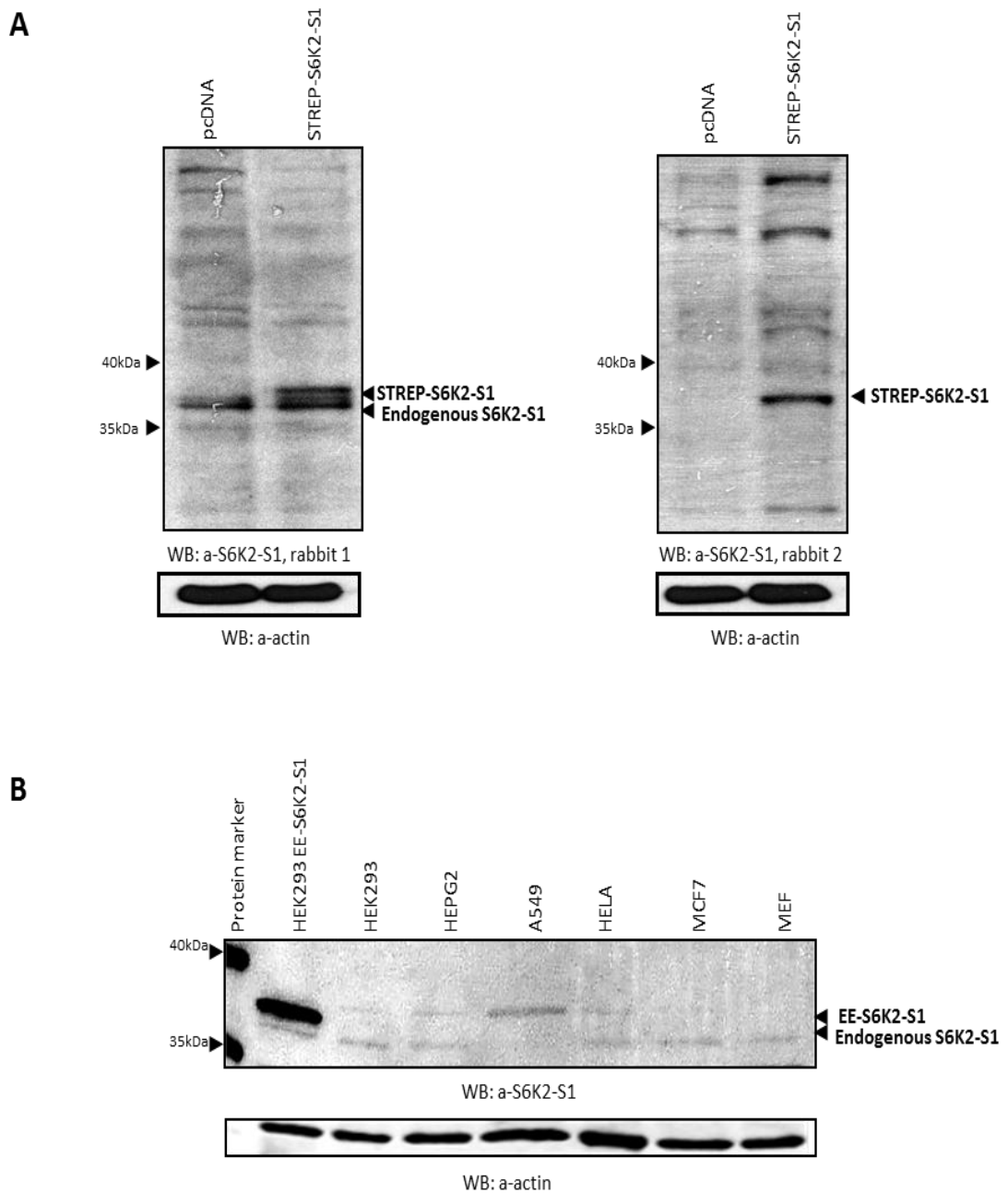


Figure 3.11 Characterisation of affinity purified polyclonal anti-S6K2-S1 antibodies. (A) Testing the specificity of purified antibodies. HEK 293 cells were transiently transfected with pcDNA3.1 empty vector and Strep-tagged S6K2-S1. 48 hours post transfection, cells were lysed and analysed in Western blotting with affinity purified anti-S6K2-S1 polyclonal antibodies (1:500). (B) Protein expression analysis of S6K2-S1 in different cell lines. 60µg of total cell lysate from different cell lines (HEK293 - Human Embryonic Kidney 293 cells, HEPG2 - Hepatocellular carcinoma human, A549 - adenocarcinomic human alveolar basal epithelial cells, HELA - human epithelial cervical cancer, MCF7 - human breast adenocarcinoma cell line, MEF - mouse embryonic fibroblasts) were used for Western blotting. PVDF membrane was blotted with anti-S6K2-S1 antibodies. Anti-actin antibodies were used as a control of equivalent protein loading.

3.3 Discussion

The work presented in this chapter studies S6K2 gene and its potential mechanism of alternative splicing. To date, not much research has been done in this area and we are not aware of any published data on the existence of identified S6K2 splicing isoforms. It has been recently reported that S6K2 gene variations correlate with the greater risk of developing gastric cancer and poor survival (Yoshida S et al., 2013). Additionally, it was shown that variations in intron 2 of S6K2 gene are linked with the higher risks of developing Alzheimer's disease (Vazquez-Higuera et al. 2011). However, the role of S6K2 gene polymorphism and alternative splicing events in the development of human pathologies remain to be investigated.

Regulation of alternative splicing by a large number of splicing factors and other proteins is a multicomplex process. SF2/ASF splicing factor has been shown to play an important role in regulating alternative splicing of RPS6KB1 (S6K1) gene and the expression of different isoforms (Karni et al.2008). The authors reported the identification of a novel S6K1 splice variant, which was found later to possess the oncogenic potential (Ben-Hur et al. 2013). We recognize the importance of studying regulatory mechanism of S6K2 gene alternative splicing, but our efforts have been mainly focused on elucidating their function in the mTOR/S6K signalling pathway and cellular processes.

In this chapter, the evidence is provided for the existence of novel S6K2 splicing isoforms by using three different experimental approaches.

First, detailed bioinformatic analysis of the S6K2 gene revealed high possibilities for alternative splicing especially in exon 9. Sequence

analysis of S6K2-S1 and S6K2-S2 cDNA clones, originated from HEK293 cells, confirmed alternative splicing of exon 9. Additionally, a number of EST-clones in GenBank Human database, corresponding to potential S6K2 splicing isoforms, have been identified. Interestingly, more than fifteen EST clones homologous to human S6K2-S3 splice variant were obtained. These findings prompted us to further investigate the role of identified S6K2 isoforms in health and disease and our work was mainly focused on studying the S6K2-S1 splicing variant.

Secondly, we confirmed the existence of the S6K2-S1 splicing variant at the level of transcription, using RT-PCR analysis. In this study, we used cDNA derived from HEK293 cells, as this was the original source for molecular cloning of full length S6K2 and its splicing isoforms. RT-PCR analysis confirmed that both full length S6K2 and S6K2-S1 transcripts are present in the selected cell line. It is known that many splicing isoforms are expressed in a tissue specific manner, so it would be very interesting to analyse in the future the expression pattern of full length S6K2 and its splicing isoforms in different cell lines and tissues.

Thirdly, the expression of S6K2-S1 at the protein level was confirmed by immunoblotting of cell lysates using isoform specific antibodies. To allow the detection of S6K2-S1 isoform at the protein level, we generated specific polyclonal antibodies directed against the extreme C-terminal end of S6K2-S1. Generated antibodies detected overexpressed S6K2-S1 protein and showed high level of specificity. Screening of a panel of different cell lines in Western blotting revealed the presence of weak but specific immunoreactive bands which might correspond to endogenous S6K2-S1 and S6K2-S2 isoforms.

Amino acid analysis of a unique C-terminal sequence of S6K2-S1 showed that it is enriched with positively charged arginine and lysine amino acids. Post-translational modification of these amino acid residues (acetylation, methylation and ubiquitination) and their contribution in mediating specific protein-protein interactions might be implicated in the regulation of subcellular localization, formation of regulatory complexes, downstream signalling and cellular functions. The N-terminus of all three splicing isoforms are identical to full length S6K2 and possesses the TOS motif. This five-amino acid sequence (FDLDLE) is important for mTORC1/S6K2 signalling. Therefore, our efforts have been focused on investigating the potential role of S6K2-S1 in the regulation of mTORC1 signalling which is described in the next chapter of this thesis.

4 S6K2-S1 and S6K2wt form a regulatory complex with Raptor and mTOR

4.1 Introduction

mTOR forms two functionally different protein complexes inside mammalian cells, named mTORC1 and mTORC2. Both complexes contain a number of common molecules, but differ by the presence of substrate presenting components: Raptor in TORC1 and Rictor in TORC2.

Raptor (regulatory associated protein of mTOR) was identified as a binding partner of mTOR and was shown to be an important regulator of mTORC1 functions (Hara et al. 2002). Key downstream targets for mTORC1 are S6 kinase and translational inhibitor 4EBP1, implicated in the regulation of ribosomal biogenesis and protein synthesis. It was shown that removal of Raptor from mTORC1 dramatically reduced the ability of mTOR to phosphorylate its substrates (S6K and 4EBP1), whereas overexpression of Raptor promoted *in vitro* kinase activity of mTOR (Hara et al.2002). Additionally, siRNA knock down of Raptor in mammalian cells resulted in decreased phosphorylation of S6K and a small cell size (Kim et al. 2002).

It was suggested that Raptor functions as a scaffolding protein to present substrates for the phosphorylation by mTOR, as it was shown that both 4EBP1 and S6K physically associate with Raptor (Hara K., 2002). This hypothesis was confirmed in studies when two mTOR substrates were found to contain a five-amino acid sequence called the TOR signaling motif (TOS motif), responsible for direct interaction with Raptor. Importantly, mutation in TOS motif diminishes S6K and 4EBP1

interaction with Raptor, and these mutants had a very low level of phosphorylation by mTOR (Nojima et al. 2003;Schalm et al. 2003a).

Rictor (Rapamycin-insensitive companion of mTOR) was identified as a binding partner of mTOR in mTORC2, which regulates the phosphorylation of Protein Kinase C α (PKC α) and Protein Kinase B (PKB) (Sarbasov et al. 2004).

Figure 4.1A shows a model of regulatory interaction between the TOS motif (FDLDLE) of S6K2wt and Raptor, which allows mTOR to phosphorylate and subsequently activate S6K2wt. The S6K2-S1 splicing isoform possesses at its N-terminus the TOS sequence, so it has the ability to bind Raptor and form the complex with mTOR (Figure 4.1B). In this complex, S6K2-S1 may function as a dominant negative regulator of mTORC1 signalling, as it does not have the mTOR site for phosphorylation (T388) in the kinase domain.

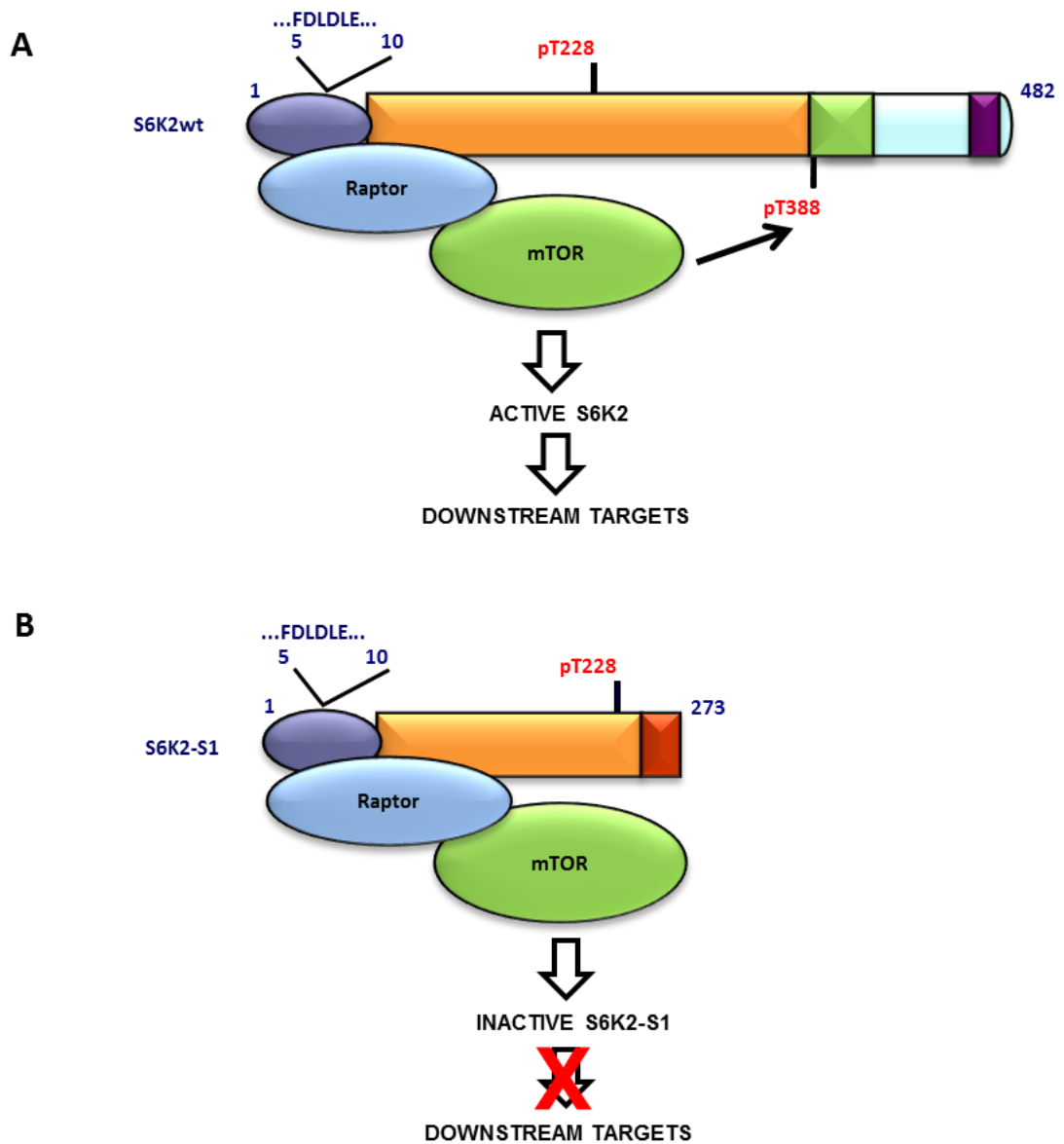


Figure 4.1 A model of regulatory interactions of S6K2wt and S6K2-S1 splicing isoform in TORC1 and downstream signalling. (A) S6K2wt possesses at the N-terminus the TOS motif (TOR Signalling sequence, FDLDE). The TOS motif mediates specific interaction of S6K1/2 with Raptor, which allows mTOR to phosphorylate and activate S6K2wt. (B) S6K2-S1 splicing isoform has the ability to bind Raptor via its TOS sequence and to complex with mTOR. As S6K2-S1 does not possess the site for mTOR phosphorylation (T388) and the kinase domain, it may act as a dominant-negative regulator of mTORC1 signalling.

In this chapter, we present evidence for specific association between S6K2-S1 splicing isoform and Raptor using two approaches. First, we expressed S6K2-S1, Raptor and Rictor using baculovirus expression system. Coinfection of insect cells with corresponding viruses followed by immunoprecipitation and Western blot analysis demonstrated specific interaction of S6K2-S1 with Raptor, but not Rictor. Second, we generated recombinant Lentiviruses for the expression of S6K2wt and splicing isoform and made a HEK293 stable cell lines. Immunoprecipitation of stably expressed S6K2wt and splicing isoform S6K2-S1, showed the formation of the regulatory complex with endogenous Raptor and mTOR.

4.2 Results

4.2.1 Generation of baculovirus for Raptor and Rictor

Baculovirus Expression System provides fast and efficient method for generation of recombinant baculoviruses. This method is based on a site-specific transposition of an expression cassette from pFastBac1 vector into a baculovirus shuttle vector (bacmid) propagated in *E. coli* host strain DH10Bac. Transfection of generated recombinant bacmid into insect cells, allows the production of a recombinant baculovirus, which can be used to infect insect cells and to express protein of interest. Figure 4.2 shows overall strategy for baculovirus generation.

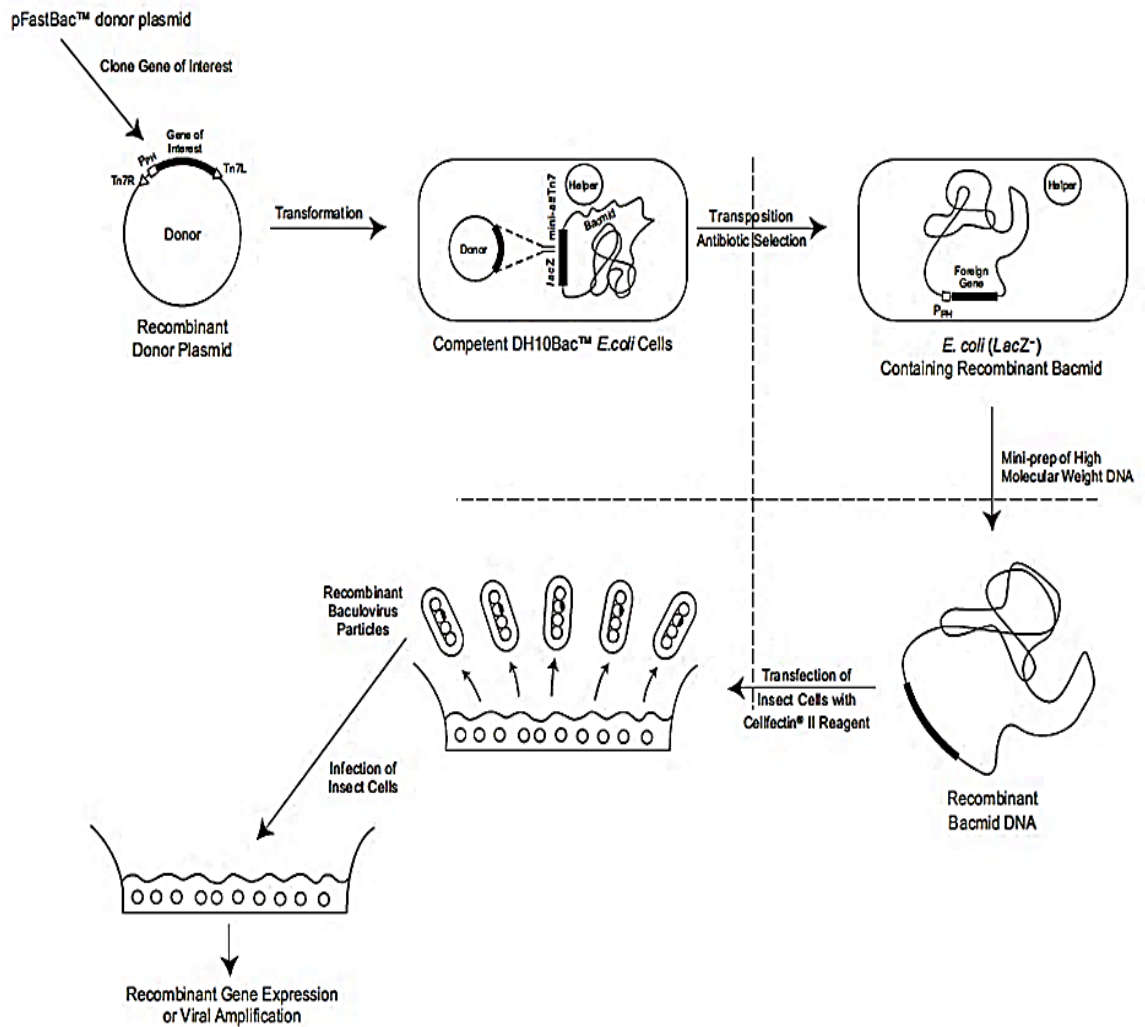


Figure 4.2 Generation of recombinant baculovirus and protein expression using Baculovirus Expression System. The gene of interest is cloned into a pFastBac donor vector; recombinant plasmid is transformed into MAX Efficiency® DH10Bac™ *E. coli* competent cells, which contain bacmid with a mini-attTn7 target site and the helper plasmid. The mini-Tn7 element on pFastBac vector can transpose to the mini-attTn7 target site on the bacmid in the presence of transposition proteins provided by the helper plasmid. Colonies containing recombinant bacmids are identified by the disruption of lacZ α gene and selected via blue/white screening. High molecular weight mini-prep DNA is prepared from selected *E. coli* clones containing the recombinant bacmid; this DNA is then used to transfect insect cells for production of the virus.

Full length coding sequences of Raptor and Rictor were PCR amplified, using specific sets of primers. The EE-tag sequence (MEFMPME) was introduced at the N-terminus to allow the immunodetection of expressed recombinant proteins using specific monoclonal anti-EE antibodies. As a template for PCR reaction we used constructs from Addgene database (8513:HA-Raptor, 11367:myc-Rictor, David Sabatini). Primers for amplification listed in the Appendix B.

The product of PCR amplification (~4000 bp) corresponded to calculated molecular weight of EE-tagged Raptor and was cloned into pFastBac1 expression vector using BamHI/EcoRI restriction sites (Figure 4.3A). After ligation six clones were selected and digested with BglII restriction enzyme to identify Raptor insertion. Restriction analysis of clone 2 and 3 confirmed the presence of EE-Raptor, when compared to an empty pFastBac1 vector (Figure 4.3B). These constructs were used for bacmid preparation and baculovirus generation. Restriction analysis of clone 6 showed different digestion pattern from expected and was not used for further studies.

As shown in Figure 4.4A, the size of PCR amplified EE-tagged Rictor was around 4700 bp, which corresponds to the calculated 4776 bp value. The product of PCR amplification was digested with XhoI/KpnI endonucleases and cloned into pFastBac1 expression vector.

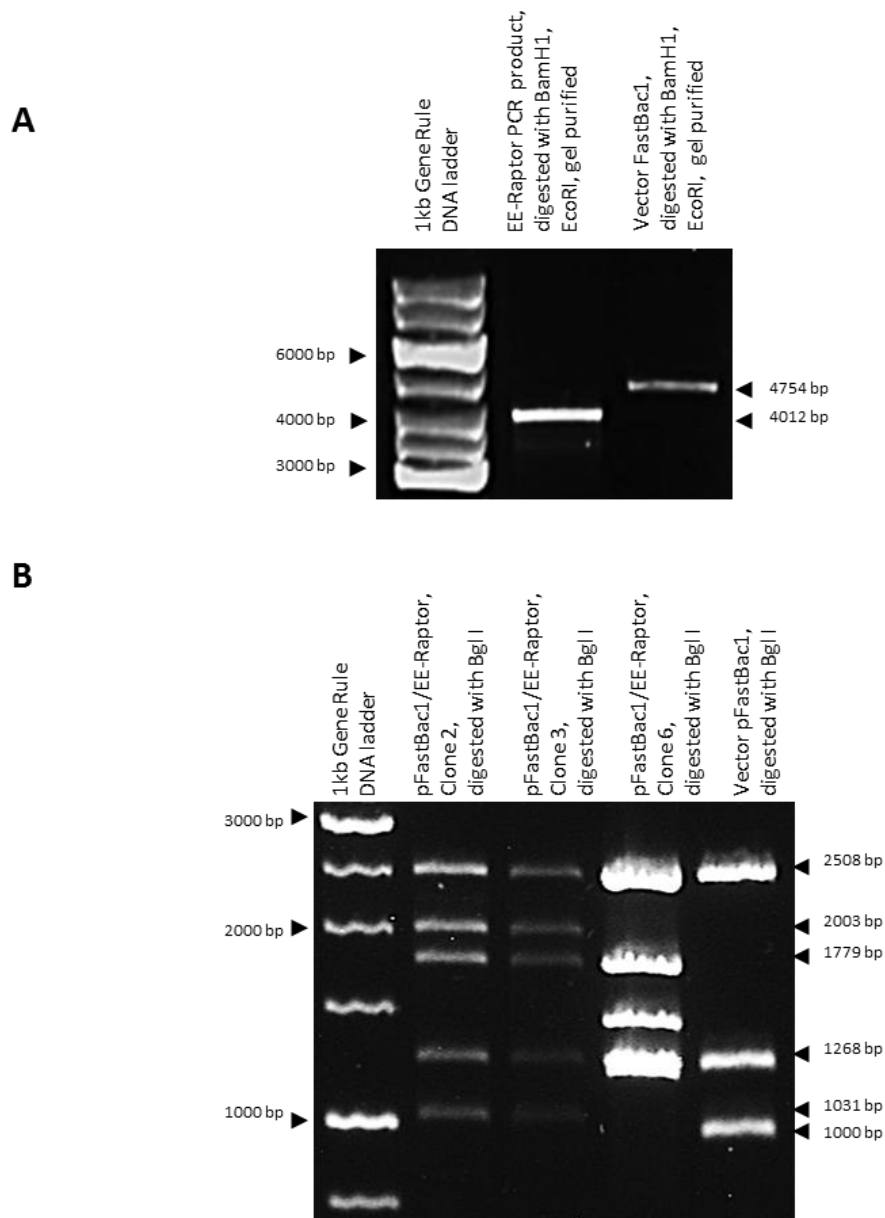


Figure 4.3 Molecular cloning of EE-tagged Raptor into baculovirus expression vector pFastBac1. (A) Agarose gel electrophoresis of PCR amplified full length coding sequence of Raptor with the EE-tag epitope and empty pFastBac1 cloning vector, digested with BamHI and EcoRI restriction enzymes. (B) Restriction analysis of selected clones 2, 3 and 6 for pFastBac1/EE-Raptor and an empty pFastBac1 vector. Purified plasmids were digested with BglI restriction enzyme for 1h and then separated by 1% Agarose gel electrophoresis

Figure 4.4B shows digestion analysis of created constructs (clones 3, 5 and 6) using EcoRV restriction enzyme. The results of restriction clearly indicate on the presence of EE-Rictor insert in all selected clones, compared to an empty pFastBac1 vector. These clones were used for the production of recombinant baculoviruses.

MAX Efficiency[®] DH10Bac™ *E. Coli* cells were transformed with selected pFastBac1/EE-Raptor (clone 2 and 3) and pFastBac1/EE-Rictor (clone 3, 5, 6 and 7) constructs for bacmid preparation. Baculoviruses were generated as described in Materials and Methods. Sf9 insect cells were infected with corresponding baculoviruses and the expression of EE-Raptor and EE-Rictor was analysed by immunoprecipitation using mouse monoclonal anti-EE-tag antibodies.

Raptor is a protein with the molecular weight of 150kDa, and contains a conserved N-terminal domain (the RNC domain), three HEAT domains, and seven WD40 motifs located near the C-terminus. Rictor is a 192 kDa protein, and it contains conserved domains that are important for the substrate recruitment and for the formation of TORC2. As seen from Figure 4.5, all selected clones corresponding to EE-tagged Raptor and Rictor, show high level of protein expression with expected molecular weights, when compared to the control sample. Generated viruses were used for coimmunoprecipitation studies as described further.

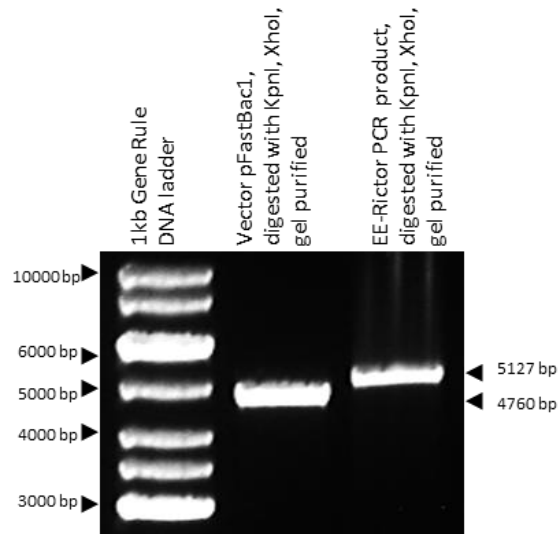
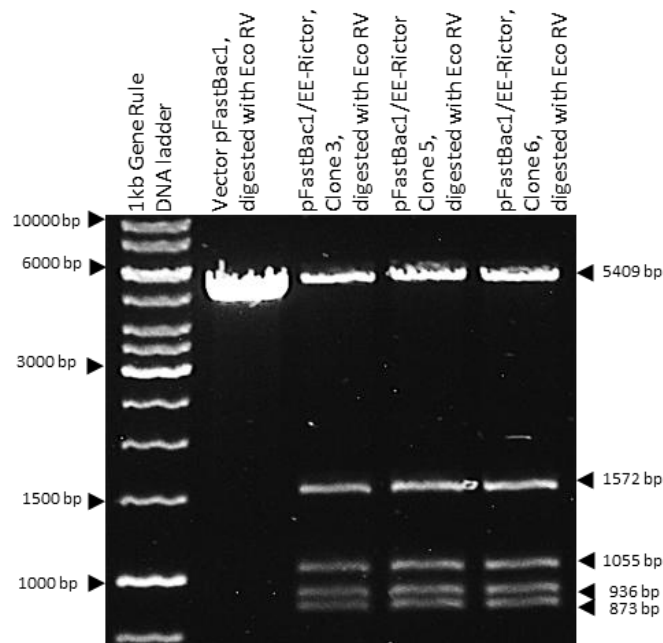
A**B**

Figure 4.4 Molecular cloning of EE-tagged Rictor into baculovirus expression vector pFastBac1. (A) Agarose gel electrophoresis of PCR amplified full length coding sequence of Rictor with the EE-tag epitope and an empty pFastBac1 vector, digested with KpnI and XhoI restriction enzymes. (B) Restriction analysis of selected clones 3, 5 and 6 for pFastBac1/EE-Rictor and an empty pFastBac1 vector. Purified plasmids were digested with EcoRV restriction enzymes and then separated by 1% Agarose gel electrophoresis.

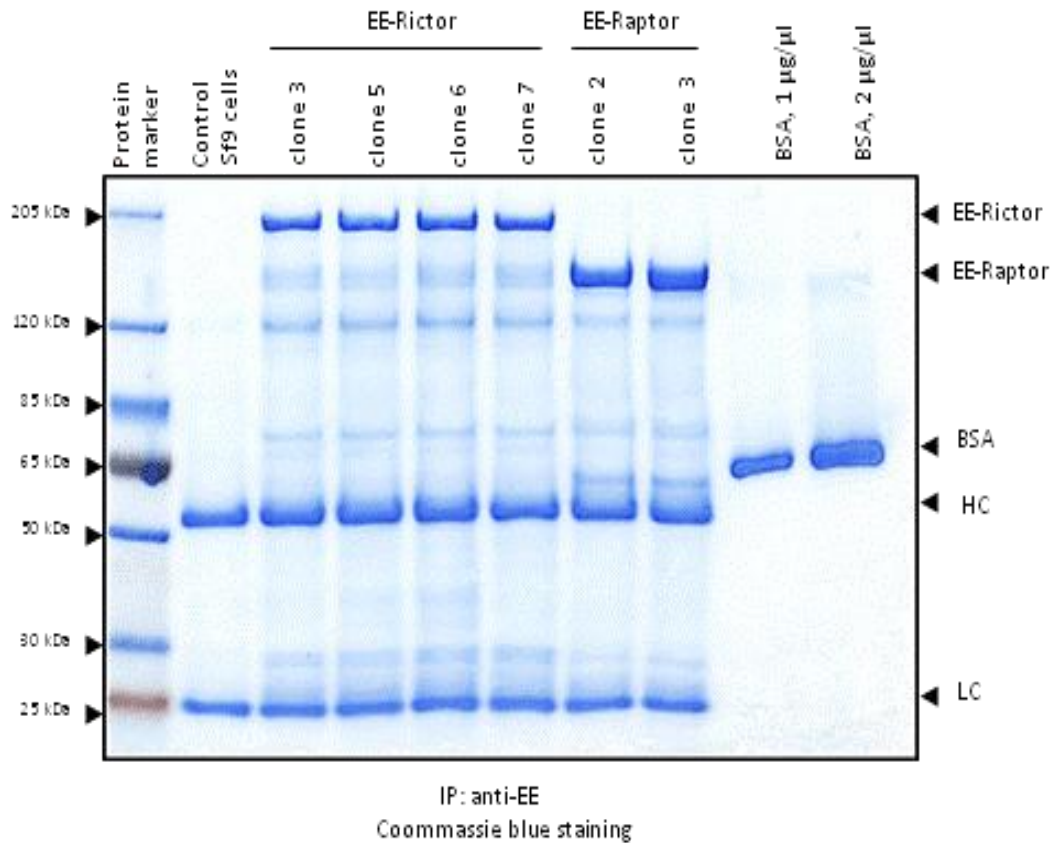


Figure 4.5 Expression of EE-Raptor and EE-Rictor in insects Sf9 cells. Exponentially growing Sf9 insects cells ($1-2 \times 10^6$ cells/ml) were infected with 0.2ml of corresponding baculoviruses (EE-Raptor and EE-Rictor). After 3 days of infection, cells were collected by centrifugation and lysed. Recombinant EE-Raptor and EE-Rictor were immunoprecipitated from the cell extract using protein G-Sepharose loaded with mouse monoclonal anti-EE-tag antibodies (equal amounts of total cell extracts were incubated with beads). After incubation for 1h, beads were washed 3 times in lysis buffer and $20 \mu\text{l}$ of protein loading dye was added. Samples were boiled for 5min, separated by SDS-PAGE and stained with Coomassie blue. HC - heavy chain of antibodies, LH - light chain of antibodies, BSA – bovine serum albumin standard.

4.2.2 Molecular cloning and expression of S6K2-S1 in baculovirus expression system

To clone S6K2-S1 into baculovirus expression system previously generated pcDNA4TO/Strep-S6K2-S1 construct for expression in mammalian cells was used. The Strep-tagged S6K2-S1 sequence was re-cloned into pFastBac1 baculovirus expression vector using BamHI/NotI restriction sites and 3 clones were selected for analysis. Figure 4.6A shows restriction analysis of clone 2 using BamHI/NotI endonucleases. The results of restriction clearly indicate the presence of the expected insert, in comparison to an empty pFastBac1 vector. Selected clones were used for baculovirus generation and infection of Sf21 insect cells. As shown in Figure 4.6B, all selected clones drive a good expression of Strep-S6K2-S1 protein in transiently transfected Sf9 cells when tested by Western blotting of total cell lysates. The highest expression was detected for clone 2, so it was used for further infections. Unfortunately, immunoprecipitation (IP) and affinity purification of Strep-S6K2-S1 from Sf9 cell infected with amplified baculovirus using *Strep*-Tactin was not successful.

Therefore, we decided to generate recombinant baculoviruses with the N-terminal HIS tagged S6K2-S1. The product of PCR amplification, corresponding to HIS-S6K2-S1 (Figure 4.6C,) was cloned into pFastBac1 expression vector using BamHI/NotI restriction sites. Positive clones were identified and used for baculovirus generation. Infection of Sf9 cells with amplified stock of generated baculoviruses resulted in a high level of HIS-S6K2-S1 expression, as detected by Western blotting with anti-S6K1-S1 antibody (Figure 4.6D). Unfortunately, in line with

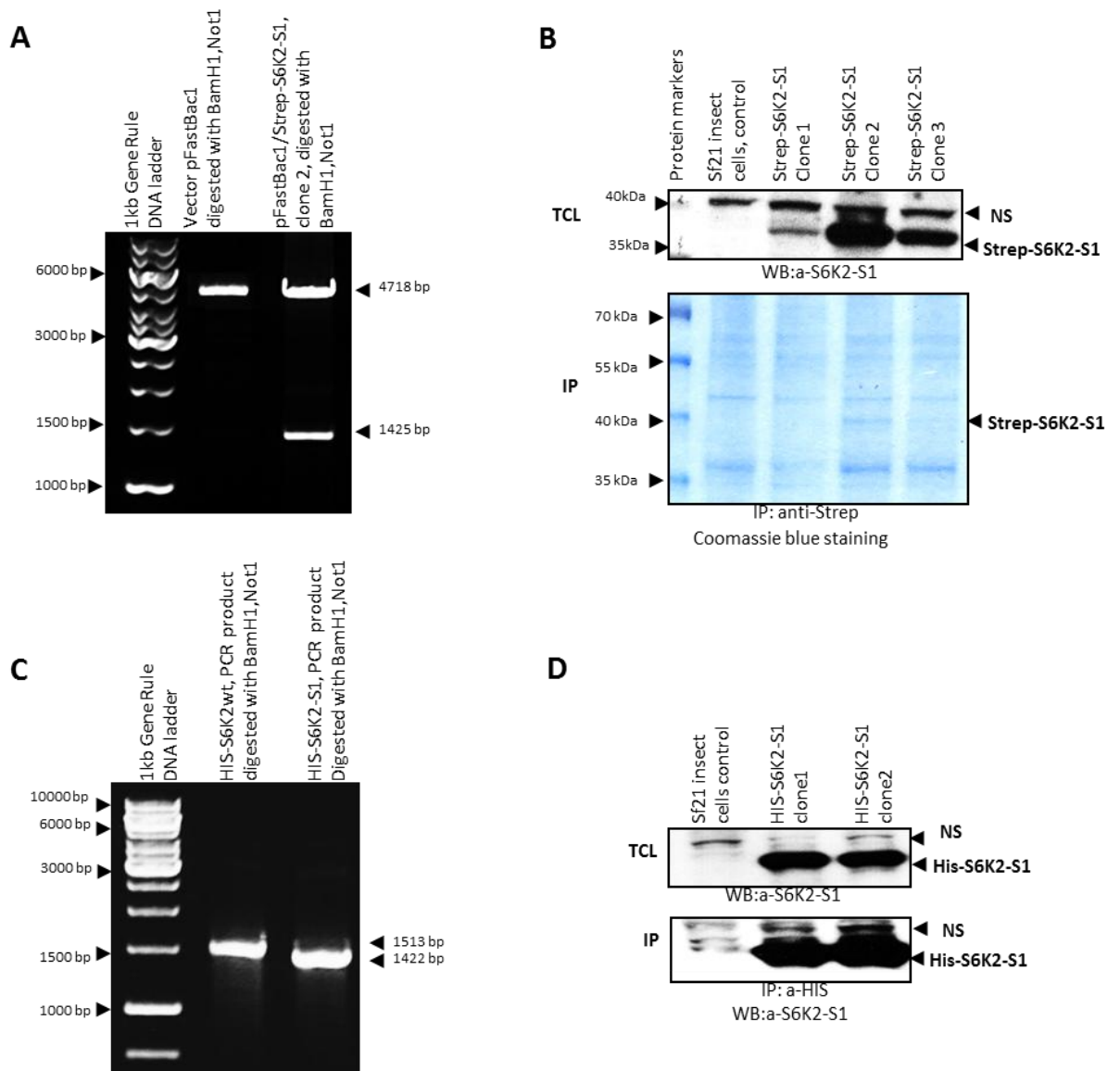


Figure 4.6 Molecular cloning and baculovirus expression of N-terminally tagged Strep-S6K2-S1 and His-S6K2-S1. (A) 1% Agarose gel electrophoresis shows the digestion of pFastBac1/Strep-S6K2-S1 (clone 2) and pFastBac1 vector with BamH1 and Not1 restriction enzymes, to illustrate the presence of S6K2-S1 insert comparing to an empty vector. (B) Expression of Strep-S6K2-S1 isoform in Sf21 insect cell line. Sf21 cells were transfected with a bacmid, corresponding to Strep-S6K2-S1 (clone 1-3), after 48 hours media was collected for the preparation and amplification of the virus stock, cells were lysed and analysed in Western blotting. Immunoprecipitation of Strep-S6K2-S1 expressed in Sf21 cells. 5ml of cells were infected with the Strep-S6K2-S1 baculovirus, after 3 days post-infection cells were collected and lysed. Strep-S6K2-S1 was immunoprecipitated using Strep-beads, separated by SDS-PAGE and stained with Coomassie blue. (C) 1% Agarose gel electrophoresis of PCR amplified His-S6K2wt and His-S6K2-S1. (D) Expression of His-S6K2-S1 in Sf21 insect cell lines. Sf21 cells were transfected with His-S6K2-S1 (clone 1-2) bacmid, after 48 hours media was collected for preparation of the virus stock. Cells were lysed, His-S6K2-S1 were immunoprecipitated (IP) using Ni-NTA-beads, TCL (total cell lysate) and IP were separated using SDS-PAGE and analysed in Western blotting. NS - non-specific signal.

previous results, affinity purification of His-S6K2-S1 using Ni-NTA-resin was not successful.

Taken together these results indicated that in baculovirus expression system both Strep and His tags at the N-terminus of S6K2-S1 are not accessible for affinity purification on Strep-Tactin or Ni-NTA-resin respectively.

To overcome this problem, we decided to generate C-terminal FLAG-tagged S6K2-S1. Specifically, designed primers listed in Appendix B were used for the PCR reaction. Figure 4.7A shows that molecular weight of PCR amplified C-terminal FLAG-tagged S6K2-S1 corresponds to calculated 855 bp. This amplified fragment was digested with BamHI/NotI restriction enzymes and cloned into pFastBac1 vector. Sf9 cells were infected with generated baculoviruses for selected clones and the expression of S6K2-S1-FLAG was monitored by Western blotting and immunoprecipitation. This analysis revealed high level of S6K2-S1-FLAG expression in total cell lysates by Western blotting (Figure 4.7B) and in the immune complexes (Figure 4.7C). Recombinant S6K2-S1-FLAG was expressed in Sf21 insect cells and affinity purified using anti-FLAG M2 affinity resin (Sigma) as described in Materials and Methods section. As shown in Figure 4.7D, elution fractions from the affinity column contain a major band of approximately 35kDa, which correlated with the calculated molecular mass of S6K2-S1-FLAG. Combined fractions were combined and stored for further studies in the storage buffer with 50% glycerol.

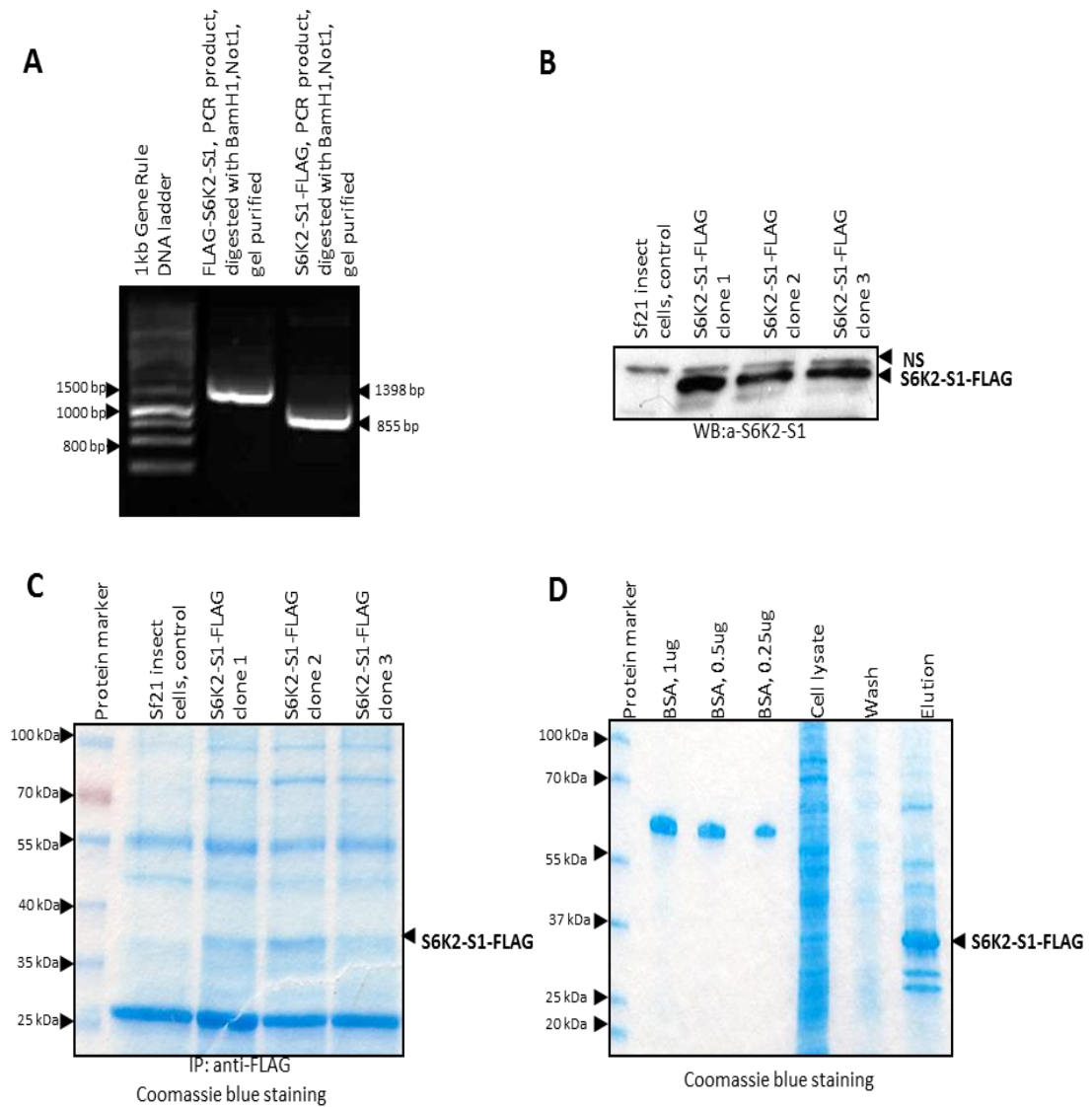


Figure 4.7 Molecular cloning, expression and affinity purification of the C-terminally FLAG-tagged S6K2-S1 using baculoviral expression system. (A) Agarose gel electrophoresis of PCR amplified C- and N-terminal FLAG-tagged S6K2-S1, digested with BamHI and NotI restriction enzymes and gel purified. (B) Western blot analysis of S6K2-S1-FLAG expression in Sf21 cells. Sf21 cells were transfected with bacmid containing S6K2-S1 with the C-terminal FLAG tag (clone 1-3). After 48 hours, virus was collected for amplification, cells were lysed and analysed in Western blotting. NS - non-specific signal. (C) Immunoprecipitation of S6K2-S1-FLAG from Sf21 cells infected with corresponding recombinant baculovirus. 5ml of cells were infected with the S6K2-S1-FLAG baculovirus (clone 1-3). 3 days post-infection cells were collected and lysed. FLAG tagged S6K2-S1 was immunoprecipitated using anti-FLAG M2 affinity resin (Sigma), the immune complexes separated by SDS-PAGE and the gel stained with Coomassie blue. (D) Affinity purification of S6K2-S1-FLAG. For large-scale protein purification, 300ml of Sf21 cells were infected with generated baculovirus. 72 hours later, cells were harvested and lysed. Cell lysate was filtered, centrifuged and loaded onto the prepared anti-FLAG M2 affinity column. Specifically associated protein was then eluted with FLAG-peptide solution. 5ul of eluted fractions were analysed by SDS-PAGE and Coomassie staining. BSA – bovine serum albumin standard.

4.2.3 S6K2-S1 specifically interacts with Raptor, but not Rictor in insect cells

Taking into account that S6K2-S1 splicing isoform possesses the TOS motif at its N-terminus, we speculated that it can interact with Raptor and form the regulatory complex with mTOR. To test this hypothesis, I tested the ability of S6K2-S1 to associate with Raptor and Rictor, and to form mTORC1 and mTORC2. In this study, Rictor was used as a negative control, as it does not recognise the TOS motif and functions as a substrate-presenting protein of mTORC2, but not TORC1. In this study, we used a panel of baculoviruses, which drive the expression of S6K2-S1-FLAG, EE-Raptor and EE-Rictor. To test the interaction between S6K2-S1 and Raptor or Rictor, Sf21 insect cells were infected with corresponding baculoviruses in various combinations. The expression of recombinant EE-Raptor, EE-Rictor and S6K2-S1-FLAG in total cell lysates was verified by Western blotting with anti-EE and anti-S6K2-S1 antibodies (Figure 4.8 top panel). EE-Raptor and EE-Rictor were immunoprecipitated with protein G-Sepharose carrying anti-EE antibodies from Sf9 cells co-infected with recombinant baculoviruses which drive the expression of S6K2-S1-FLAG, EE-Raptor and EE-Rictor. The immunoprecipitates (IP) were analysed in Western blotting using anti-EE and anti-S6K2-S1 antibodies. As shown in Figure 4.8(bottom panel), S6K2-S1-FLAG is specifically detected in immune complexes with EE-Raptor, but not with EE-Rictor, when compared to control samples. The membrane was blotted with anti-EE antibodies to test the efficiency of immunoprecipitation of EE-Raptor and EE-Rictor. Although the expression of EE-Rictor was not high and significant degradation of the recombinant protein was clearly observed in the immune blot of

total cell lysates, the anti-EE immune complexes contained large amount of EE-Rictor. These results demonstrate that S6K2-S1 splicing isoform binds to Raptor specifically and has the potential to form a signalling complex with mTOR.

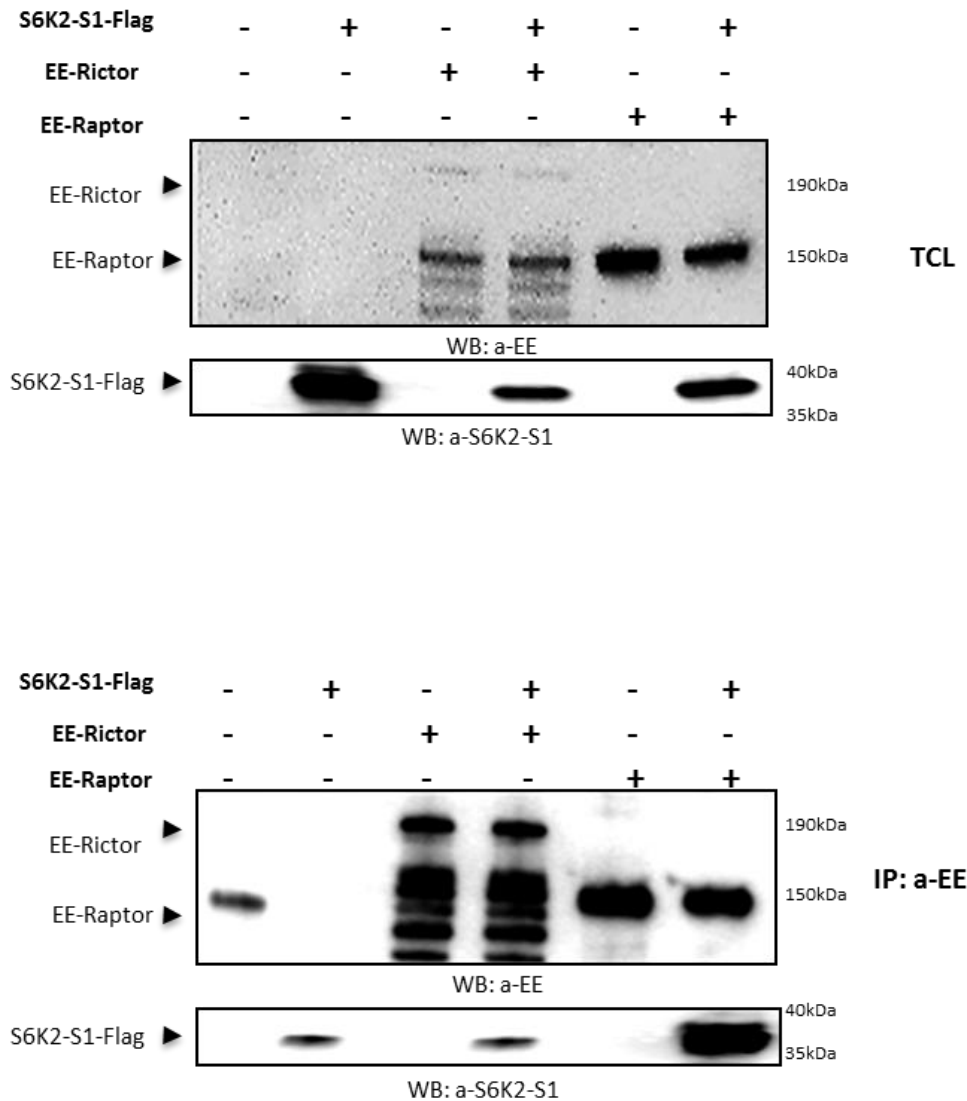


Figure 4.8 S6K2-S1 specifically interacts with Raptor (mTORC1). SF21 insects cells were infected with corresponding baculoviruses (EE-Raptor, EE-Rictor and S6K2-S1-Flag), after 3 days of infection cells were collected and lysed in lysis buffer. Equal amounts of total cell lysate were loaded onto beads, EE-Raptor and EE-Rictor were immunoprecipitated with protein G-Sepharose carrying anti-EE antibodies. Cell lysates (TCL) and anti-EE immunoprecipitates (IP) were analysed in Western blotting using anti-EE and anti-S6K2-S1 antibodies. These results were obtained in at least three individual experiments.

4.2.4 Lentivirus generation of HEK293 stable cell lines overexpressing full length S6K2 and splicing isoform S6K2-S1

To further validate the above findings, we decided to generate HEK293 stable cell lines overexpressing full length S6K2 and S6K2-S1 splicing isoform.

For the generation of stable cell lines we used recombinant lentiviruses. In our laboratory, a 3rd generation HIV-1-based Lentivirus expression system has been established. It allows the production of a replication incompetent lentivirus and facilitates the delivery and expression of the gene of interest. It offers maximal biosafety, when compared to previous generations of lentiviral systems. It contains 4 different plasmids for transfection into HEK293T producer cells (2 packaging plasmids - pLP1, pLP2; an envelope plasmid pLP/VSVG; and a transfer plasmid pLEX). The main differences in the 3rd generation Lentiviral system are as follows: a) the Tat protein has been deleted from the packaging completely; b) the Rev protein is expressed on an independent plasmid; c) the 5'LTR of the transfer plasmid has been modified to include a conventional promoter and delete a portion of the LTR. Once the lentivirus stock is produced, it can be used to infect different types of dividing or non-dividing mammalian cells and provides stable, long-term expression of a target gene. Figure 4.9 represents a schematic strategy for lentivirus generation.

In brief, S6K2-S1 and S6K2wt were recloned from previously generated constructs into pLEX transfer plasmid, using BamHI/NotI and BamHI/EcoRI restriction sites respectively (Figure 4.10A).

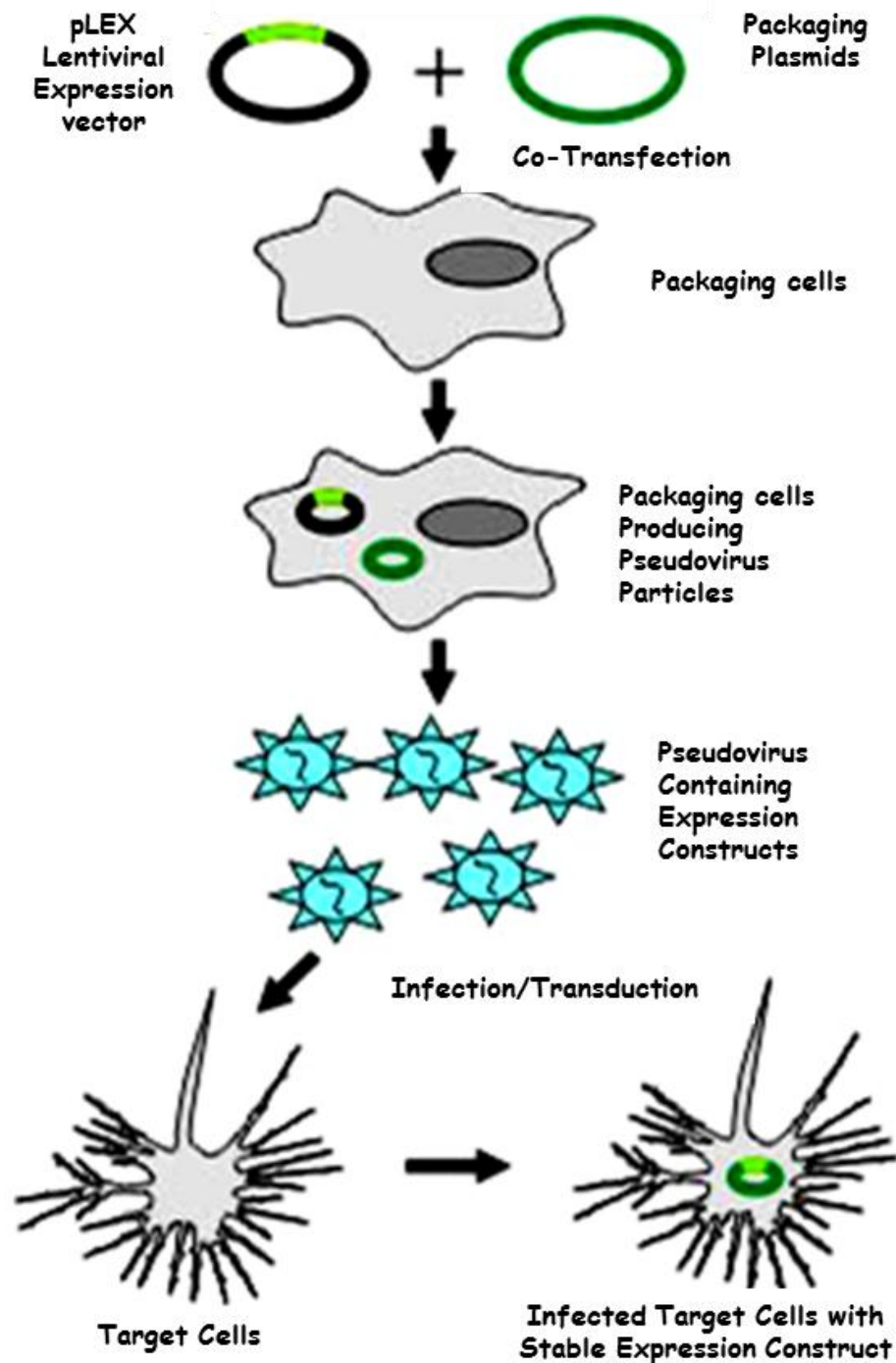


Figure 4.9 Overall strategy for Lentivirus generation. Gene of your interest cloned into Lentivirus expression vector (pLEX) co-transfected into HEK293T cell lines together with three packaging plasmids (pLP1, pLP2 and pLP/VSVG) using transient transfection standard protocol for TurboFect (ThermoFisher). As a positive control Lentivirus expression vector (pLEX) containing Green Fluorescent Protein (GFP) was used for fluorescent detection. The cells produce the viral structural proteins that self-assemble into pseudovirus particles, each containing a cloned gene of your interest. The cells replicate pseudoviruses containing expression constructs and release them into the growth medium. Virus harvested 48-72h posttransfection and filtered using sterile low protein binding 0.45µm PVDF filter. Virus can be aliquoted and stored at -80°C

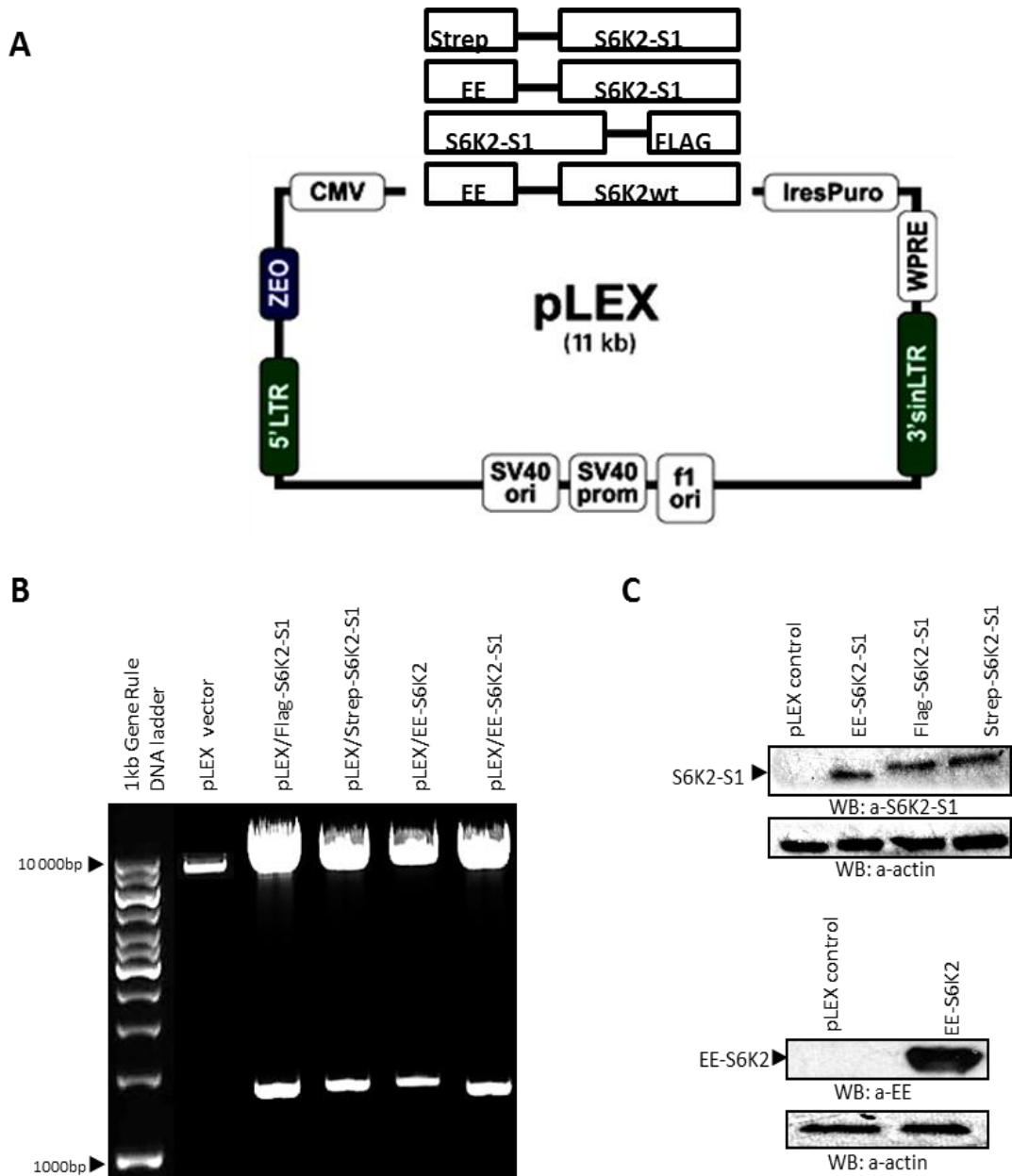


Figure 4.10 Molecular cloning of S6K2-S1 splicing isoform and S6K2wt into Lentivirus expression vector pLEX. (A) Schematic representation of the pLEX cloning vector. Puro-Mammalian selectable marker for selection after viral transduction, Zeo-Bacterial selection marker, 5'LTR-5' long terminal repeat, CMV-RNA Polymerase II promoter, WPRE-Woodchuck hepatitis post-transcriptional regulatory element, IRES-Internal ribosome entry site, 3'sin-LTR 3' Self inactivating long terminal repeat, Zeo-Bacterial selection marker, SV40 ori and SV40 prom-origin of replication Simian vacuolating virus 40 promoter, f1ori-origin of replication from a f1 phage. (B) Agarose gel restriction analysis of pLEX/S6K2wt and pLEX/S6K2-S1 selected constructs and an empty pLEX vector. Purified plasmids were digested with BamHI and Not1 (EcoRI for S6K2wt construct) restriction enzymes for 1h and then separated by 1% Agarose gel electrophoresis. (C) Expression analysis of selected pLEX/S6K2wt and pLEX/S6K2-S1 constructs in HEK293 cells. HEK293 cells were transiently transfected with corresponding plasmids using standard protocol for Exgene transfection. After 48h of transfection cells were collected and analysed in Western blotting with corresponding antibodies.

Figure 4.10B shows restriction analysis of selected pLEX constructs for EE-S6K2wt, FLAG-S6K2-S1, EE-S6K2-S1 and Strep-S6K2-S1 using corresponding endonucleases. The results of restriction analysis clearly show the presence of inserts with predicted molecular weight in all selected clones, when compared to empty pLEX vector. The expression of recombinant proteins from generated pLEX constructs was then tested by transient transfection of HEK293 cells using Exgene 500. As shown in Figure 4.10C, all selected clones mediate good level of expression for EE-S6K2wt, FLAG-S6K2-S1, EE-S6K2-S1 and Strep-S6K2-S1 when total lysates were tested by Western blotting with corresponding antibodies.

Then, lentiviruses for all selected constructs were generated as described in Material and Methods chapter. HEK293 cells were infected with lentiviruses which drive the expression of EE-tagged S6K2wt and S6K2-S1, and GFP protein as a positive control of infection. As seen from Figure 4.11A (left panel) GFP expression in infected HEK293 cells was detected under the microscope 72h post-infection. The efficiency of infection was about 20%, which was lower from expected but still sufficient to initiate the production of stable cell lines. For the generation of stable clones, transfected cells were grown for 48 h in selection media containing puromycin. Analysing cells infected with GFP-expressing Lentivirus under the microscope, we observed that only GFP-positive cells remained attached to the plate, while most of GFP-negative cells were floating in the medium (Figure 4.11A, right panel).

Cells infected with generated Lentiviruses for EE-tagged S6K2wt and S6K2-S1 after applying antibiotic selection displayed the same pattern

as GFP-expressing cells, most of the cells were detached from the plate and puromycin resistant cells grew well and formed small colonies. Western blot analysis of protein expression in generated HEK293 stable cell lines showed good level of expression for EE-S6K2wt and EE-S6K2-S1 (Figure 4.11B).

Finally, generated HEK293 stable cell lines were tested for the presence of mycoplasma contamination, using Mycoplasma PCR Detection Kit. Mycoplasma is the simplest and smallest of bacteria, which parasites in host cells for their energy and biosynthesis requirements. It is known, that cell culture mycoplasma contamination can significantly affect the interpretation of biological results, as it affects DNA, RNA and protein synthesis, reduces amino acid and ATP levels and can affect the expression of many genes such as those encoding for receptors, ion channels, growth factors, and oncogenes (Miller CJ. et al., 2003). For the Mycoplasma detection, we used a test based on PCR amplification of Mycoplasma DNA with a specific set of PCR primers. As seen from Figure 4.11C (before mycoplasma treatment) generated stable cell lines were infected with Mycoplasma, confirmed by the presence of 2 PCR products with the molecular weight of 500 and 700 bp, comparing to a positive control. Cells were treated with anti-mycoplasma reagent for 2 weeks, and then grown in antibiotic free medium for 1 week prior repeating Mycoplasma PCR test. Figure 4.11C (after mycoplasma treatment) shows a complete elimination of Mycoplasma, as only one PCR band with the molecular weight of 700 bp was detected in tested samples and negative control. These cells were used in further experiments.

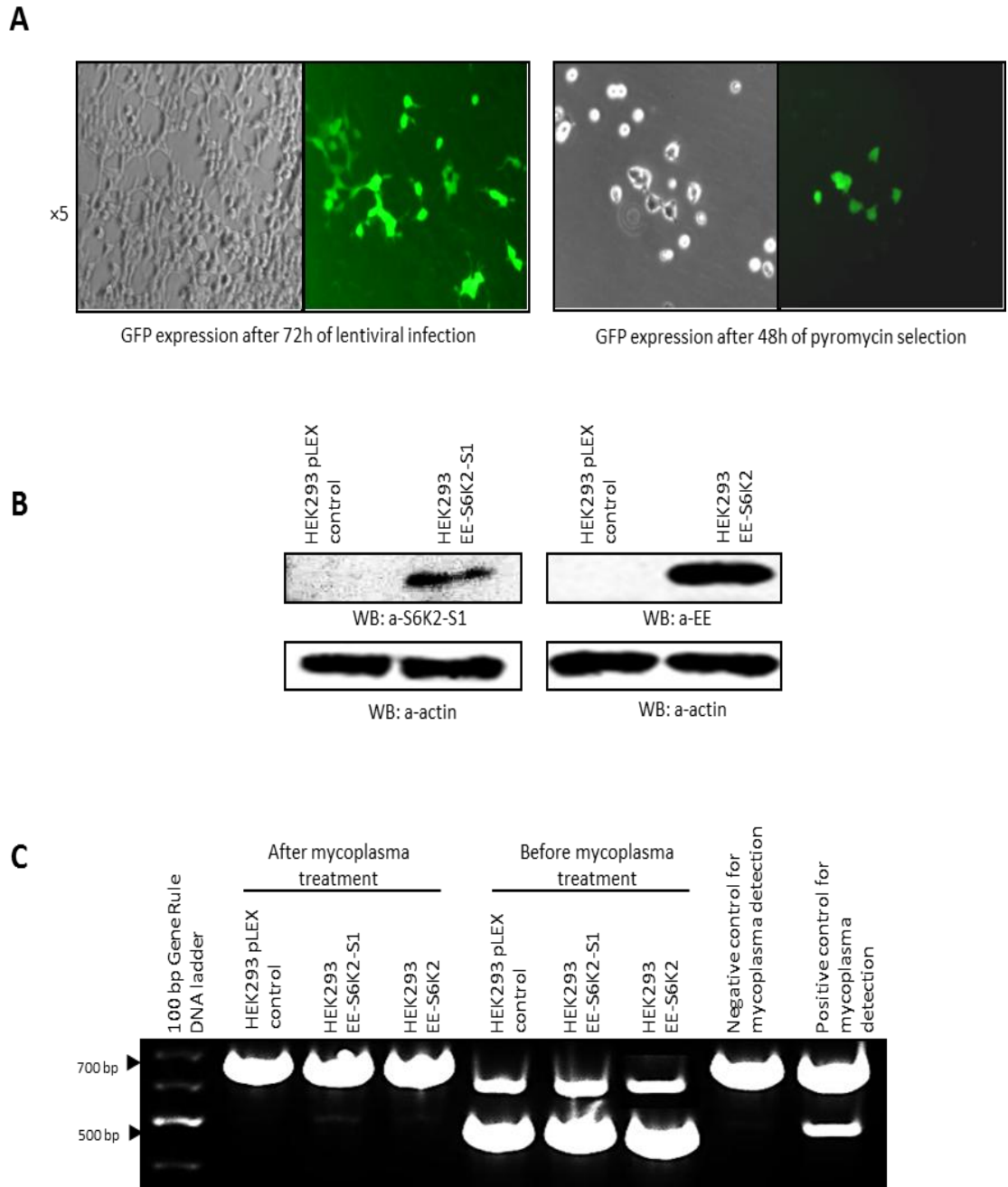


Figure 4.11 Generation of stable cell lines using Lentivirus constructs for the expression of S6K2wt and S6K2-S1. (A) HEK293 cells were infected with Lentiviruses corresponding to the expression of EE-tagged S6K2wt and S6K2-S1, and GFP protein as a positive control of infection. GFP expression in HEK293 cells was observed under the microscope 72h post-infection (left panel). After 48h of antibiotic selection only GFP –expressing cells were growing on the plate (right panel). (B) Generated HEK293 stable cell lines were checked for the expression of EE-S6K2wt EE-S6K2-S1, cells were collected and analysed in Western blotting. (C) Mycoplasma testing of generated HEK293 stable cell lines. The electrophoretic analysis of PCR amplified Mycoplasma DNA in a 2% agarose gel. Briefly, media from growing stable cell lines was collected and analysed for the presence of Mycoplasma using Mycoplasma PCR Detection Kit (PAA). Mycoplasma-infected cells were treated with anti-mycoplasma reagent for 2 weeks, following growing for 1 week in antibiotic free media, and checked for the presence of Mycoplasma.

4.2.5 Raptor and mTOR coimmunoprecipitate with full length S6K2 and splicing isoform S1 *in vivo*

Having established that S6K2-S1 specifically interacts with Raptor in baculovirus expression system, it was necessary to confirm its interaction with Raptor and the formation of a regulatory complex with mTOR in mammalian cells.

In this study we used generated HEK293 stable cells overexpressing EE-S6K2wt and EE-S6K2-S1. EE-S6K2 and EE-S6K2-S1 from total cell lysate were immunoprecipitated with mouse monoclonal anti-EE antibodies and the presence of endogenous Raptor in immune complexes was determined by Western blotting with anti-Raptor antibodies. As shown on Figure 4.12 (top panel), Raptor specifically coimmunoprecipitates with both full length and splicing variant of S6K2, when compared to control beads. Notably, the level of Raptor in EE-S6K2 and EE-S6K2-S1 immunoprecipitates was comparable, indicating similar efficiency of interaction with Raptor for both S6K2 isoforms. Efficient immunoprecipitation of EE-S6K2-S1 and EE-S6K2 was confirmed by immunoblotting with specific antibodies (Figure 4.12 top panel). Re-blotting the same membrane with anti-mTOR antibodies revealed that mTOR is also present in the complex with both EE-S6K2-S1 and EE-S6K2. The expression level of Raptor, mTOR, S6K2, S6K2-S1 and actin in total cell lysates (TCL) was examined with corresponding antibodies (Figure 4.12, bottom panel).

Therefore, we can conclude that both S6K2wt and S6K2-S1 specifically associate with Raptor and mTOR and integrate into mTORC1. These results suggest that S6K2-S1 has the potential to interfere with S6K1/2

association with Raptor and therefore may act as a dominant negative regulator of the mTORC1 signalling complex.

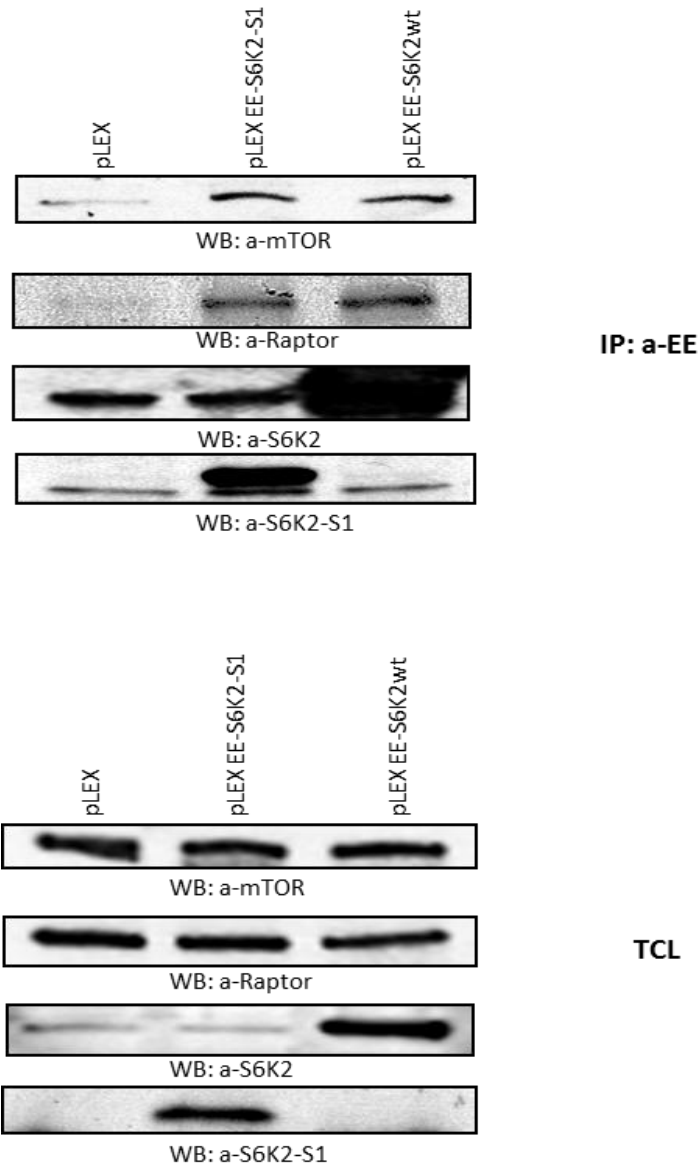


Figure 4.12 Coimmunoprecipitation of overexpressed EE-S6K2wt and EE-S6K2-S1 with endogenous Raptor and mTOR in HEK293 cells. HEK293 stable cell lines overexpressing EE-S6K2wt, EE-S6K2-S1 and empty vector were grown and collected at the confluency 80%. After cells were lysed and equal amount of each total cell lysate were loaded onto protein G sepharose beads prewashed in cold lysis buffer, 2 μ g of a-EE antibodies were added to each precipitation sample. Cell lysates (TCL) and anti-EE immunoprecipitates (IP) were subjected to SDS-polyacrylamide gel electrophoresis and analysed by Western blotting using anti-mTOR, anti-Raptor, anti-S6K2 (C-terminal) and anti-S6K2-S1 antibodies. The results shown are a representative experiment out of three individual experiments.

4.3 Discussion

As described in the introduction for this chapter, both S6K2wt and splicing isoform S6K2-S1 possess the N-terminal TOS motif, which is required for their integration into the mTORC1 and downstream signalling.

The work presented in this chapter investigates the potential of S6K2-S1 to associate with Raptor via its N-terminal TOS motif and to form a complex with mTORC1. First, using the Baculovirus expression system we generated recombinant viruses which drive the expression of FLAG-tagged S6K2-S1, EE-tagged Raptor and Rictor. Co-infection of Sf21 insect cells with generated viruses in various combinations demonstrated that S6K2-S1 specifically binds with Raptor (mTORC1), but not Rictor (mTORC2). To validate these findings further, we used Lentiviral expression system to generate HEK293 stable cell lines expressing EE-S6K2-S1 and EE-S6K2wt. Immunoprecipitation of overexpressed proteins from established cell lines showed that both EE-S6K2-S1 and EE-S6K2 have the ability to form an *in vivo* complex with Raptor and mTOR. These findings suggest that under physiological conditions splicing isoform S6K2-S1 might compete with S6K2 full-length for the binding to Raptor. Importantly, as S6K2-S1 does not possess the mTOR site for phosphorylation and the kinase activity it may act as a dominant negative regulator of mTORC1 signalling. The outcome of this investigation will be presented in the next chapter.

It is known that the mTORC1 assembly is affected by nutrients, growth factors and rapamycin. Rapamycin is an allosteric inhibitor of mTORC1. It binds to ubiquitous protein FKBP12 (FK506-binding protein), and this

complex specifically interacts with mTOR and inhibits its downstream signalling (Sancak et al. 2010;Yip et al. 2010). Therefore, it would be interesting to investigate whether specific interaction of S6K2-S1 with Raptor and complex formation with mTOR can be affected by nutrients and growth factors deprivation or by rapamycin treatment.

It is well established that in inactive state acidic N-terminus of S6K2wt interacts with the basic C-terminus autoinhibitory domain and thus this interaction keeps the kinase in a closed conformation. In response to extracellular stimuli and stresses, the S/T phosphorylation events in the C-terminal autoinhibitory domain and the kinase-extension domain induce conformational changes leading to further phosphorylations by mTOR and PDK1, and full activation of S6K2 (Gout, Minami, Hara, Tsujishita, Filonenko, Waterfield, & Yonezawa 1998;Saitoh, ten, Miyazono, & Ichijo 1998;Weng, Kozlowski, Belham, Zhang, Comb, & Avruch 1998). Acidic N-terminal end of S6K2wt and splicing isoform possess more than ten negatively charged glutamic acid residues. It is interesting to note that a unique C-terminal sequence of S6K2-S1 is enriched with positively charged arginine and lysine residues, resembling basic C-terminus of S6K2 full length. It is plausible to suggest that the basic C-terminal end of S6K2-S1 can be also implicated in mediating the interaction with Raptor and mTOR.

Results presented in this chapter, reviewed the potential of S6K2-S1 to integrate into the mTORC1 signalling complex via specific interaction with substrate-presenting protein Raptor. The next chapter describes our attempts to investigate the cellular functions of S6K2-S1 splicing

isoform and its role in the regulation of mTOR signalling pathway, using different approaches and models.

5 Functional analysis of the S6K2 S1 splicing isoform

5.1 Introduction

Having identified that S6K2-S1 forms a complex with mTOR and Raptor, it remains unclear how splicing variant may participate in the mTORC1 signalling pathway. The possibility of splicing isoforms modulating mTORC1 functions is high. S6K2-S1 directly interacts with Raptor via the TOS motif and forms mTORC1 established in previous chapter. The TOS motif is found in three downstream targets of mTORC1: S6K1, S6K2 and 4EBP1. Taking this into account, we hypothesised that S6K2-S1 splicing variant might affect some of mTORC1 multiple functions. In this chapter, a functional role of S6K2-S1 splicing isoform in mTOR signalling is uncovered.

First, different cell models overexpressing full length S6K2 and S6K2-S1 splicing isoform were generated and characterised. Second, the state of the mTOR/S6K signalling pathway in cells stably expressing S6K2-S1 splicing isoform was assessed under different conditions. Next, considering a diverse range of cellular processes regulated via the mTORC1 pathway, we focused mostly on well-known functions of S6Ks in the regulation of cell size, cell migration and cell survival. Different cellular models were used and described for each experimental method to address these objectives.

Finally, oncogenic potential of full length S6K2 and a splicing isoform was analysed using two approaches: anchorage independent colony formation in soft agar and xenograft studies in nude mice.

The data presented in this chapter shows that S6K2-S1 splicing isoform has the potential to interfere and to downregulate different cellular functions controlled via mTORC1/S6K signalling.

5.2 Results

5.2.1 Overexpression of full length S6K2 and S6K2-S1 splicing isoform affects cell size the opposite way

As described in detail in the Introduction chapter, the mTOR/S6K signalling pathway is a major regulator of cell growth. Genetic studies clearly indicate that S6K1^{-/-} deficient flies and mice are smaller than the wild type. It was shown that this effect is caused by a decrease in an individual cell size, without changing cell proliferation rate (Montagne et al. 1999).

Taking into account the possible role of the spliced isoform as a negative regulator of mTOR/S6K signalling, it was interesting to check whether S6K2-S1 might affect cell size.

The most commonly used technique for measuring cell size is a flow cytometry, where cells flow in a narrow stream and light from the laser beam is reflected from the cell surface. In addition, it can be used for counting cells and analyzing their shape and structures. A CASY counter is also designed to measure cell size. In this technique, an electrical pulse is applied through a narrow pore to measure single cell parameters. However, a number of technical factors need to be considered. Firstly, it is essential that the cells are passing through the measuring pore individually. Secondly, it is important to have a homogenous cell population to get accurate values for average cell size,

allowing meaningful comparisons between populations. This is particularly significant if the changes are expected to be fairly small.

Cell size changes dramatically during the cell cycle. During G1/S/G2 phases the size of a cell is gradually increasing due to DNA replication and protein synthesis and finally in the M phase a cell is divided. In contrast, apoptotic cells usually shrink and lose up to thirty percent of their initial volume. In a population of cells, where one cell might be in the process of cell division whereas another cell undergoes apoptosis, cell size varies considerably. In addition, physical and environmental conditions, such as starvation, stimulation with different growth factors or drug-treatment, cell density and others, affect cell size. In order to reduce the effect of these factors on cell size, in our experiment the same number of cells was plated for each cell line and cell size was measured on the second day after seeding.

Using the CASY machine, we found that generated HEK293 stable cell lines overexpressing S6K2-S1 (described in chapter 3.2.3) did not show significant differences in cell size when compared to control HEK293 cells (Figure 5.1). Interestingly, as seen from Figure 5.1 NIH3T3RasC40 cells overexpressing S6K2-S1 (described in chapter 5.2.4) have a tendency to be smaller than the control cells. These conflicting results from two cell lines motivated us to search for another cell model, which might better reflect the role of the S6K2-S1 spliced variant in the regulation of cell size. Additionally, as a positive control cells overexpressing S6K2wt were used, as it is known to play an important role in the regulation of cell size.

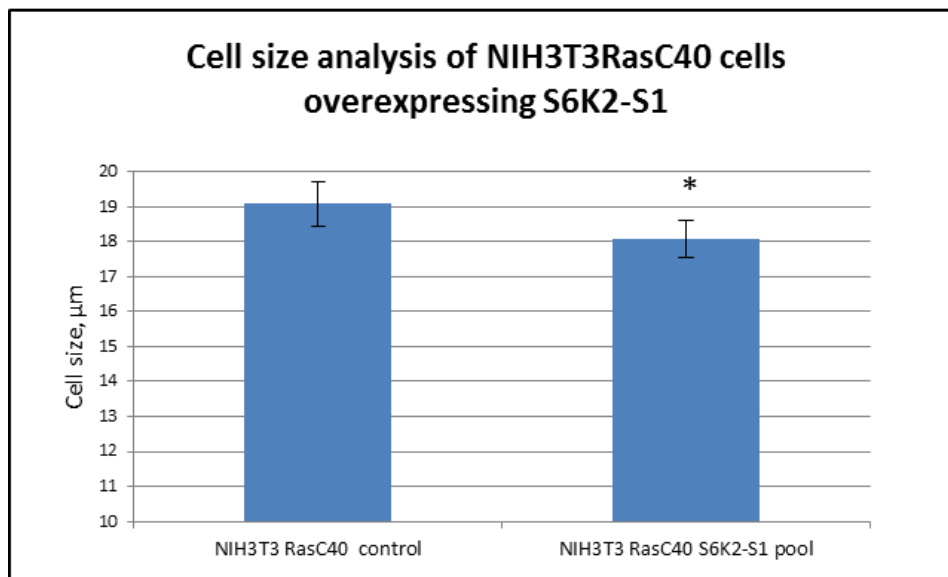
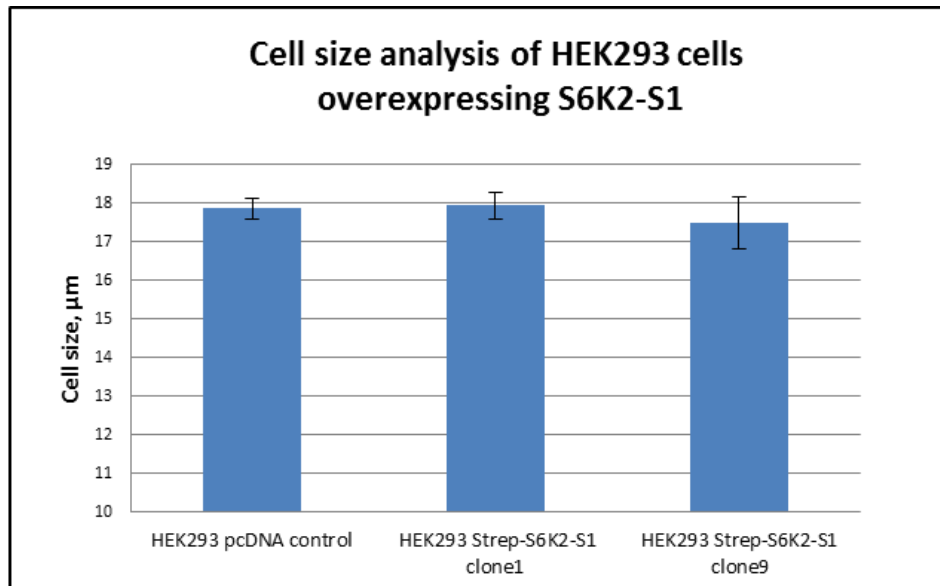


Figure 5.1 Cell size analysis of HEK293 and NIH3T3RasC40 cells with stable overexpression of S6K2-S1 splicing isoform. Cell size was measured by using CASY Model TT cell counter (Innovatis). 50 000 cells of each cell line were plated in 6-well plates in normal medium and growth under standard condition. Seeded cells were collected after 48h of growth. First, the medium was aspirated and cells were washed with PBS. After cells were trypsinized by the addition of 500 μl of trypsin for 2 min at 37^oC, cells were resuspended and this suspension was mixed with 500 μl of PBS. 100 μl of resuspended cells were added to 10 ml of CASYTON isotonic solution (Innovatis) and samples were analysed using CASY machine. Each point represents mean \pm SD from three independent experiments (* $p < 0.05$).

As presented in the introduction chapter, the upstream regulation of the mTOR/S6K pathway involves tumour suppressors TSC1 and TSC2. Loss of function of the TSC1-TSC2 complex leads to constitutively activated mTORC1 pathway. MEF (mouse embryonic fibroblasts) cells, derived from *TSC1* or *TSC2* knockout mouse embryos, show constitutive activation of mTORC1 signalling and subsequent increased phosphorylation of S6K, S6 and 4E-BP1 proteins. Interestingly, *TSC2*^{-/-} as well as *TSC1*^{-/-} mouse fibroblasts display early senescence, which can be rescued by p53 loss. *TSC2*^{-/-} p53^{-/-} MEF cells display mTORC1-dependent feedback inhibition of PI3K signalling and dramatic decrease in AKT phosphorylation; additionally they show loss of mTORC2 activity (Jing Xiang Huang and Brendan D. Manning 2008; David J. Kwiatkowski 2009, 2003). Notably, *TSC2*^{-/-} p53^{-/-} MEF cells are highly dependent on the constitutively activated mTORC1 pathway, and its downregulation has a dramatic effect on them. Based on this, *TSC2*^{-/-} p53^{-/-} MEF cells were selected as a good model to study the role of S6K2 splicing isoform in the regulation of mTORC1 signalling.

TSC2^{-/-} p53^{-/-} MEF stable cell lines overexpressing S6K2-S1 splicing isoform were produced using Lentiviruses generated previously (described in chapter 4.2.4). Briefly *TSC2*^{-/-} p53^{-/-} MEF cells were infected with Lentiviruses corresponding to EE-S6K2 full length, EE-S6K2-S1 splicing isoform and an empty vector. After 24 hours post infection, cells were seeded into the fresh medium, containing selective antibiotic (puromycin at 2µg/ml) and cultured until antibiotic-resistant cells produced separate colonies. Notably, *TSC2*^{-/-} p53^{-/-} MEF cells responded to antibiotic selection very quickly. After two days of

selection control uninfected cells died, whereas cells infected with Lentiviruses started to form separate colonies. As a positive control of infection, cells were infected with GFP-expressing Lentivirus, selection of GFP-infected cells was observed under the microscope. After antibiotic selection, cells were amplified and analysed in Western blotting for the expression of EE-tagged S6K2 full length and the spliced isoform. Unfortunately, cells infected with EE-S6K2-S1 Lentivirus did not show the expression of the spliced isoform. This may be explained by the fact that the overexpression of EE-S6K2-S1 affects the selection process, thus cells with high expression level were eliminated from cell population during selection. On the other hand, cells which show antibiotic resistance but do not show detectable EE-S6K2-S1 expression might express splicing isoform at a very low level. In contrast, overexpression of full length EE-S6K2 in TSC2^{-/-} p53^{-/-} MEF cells was easy to detect (Figure 5.2A).

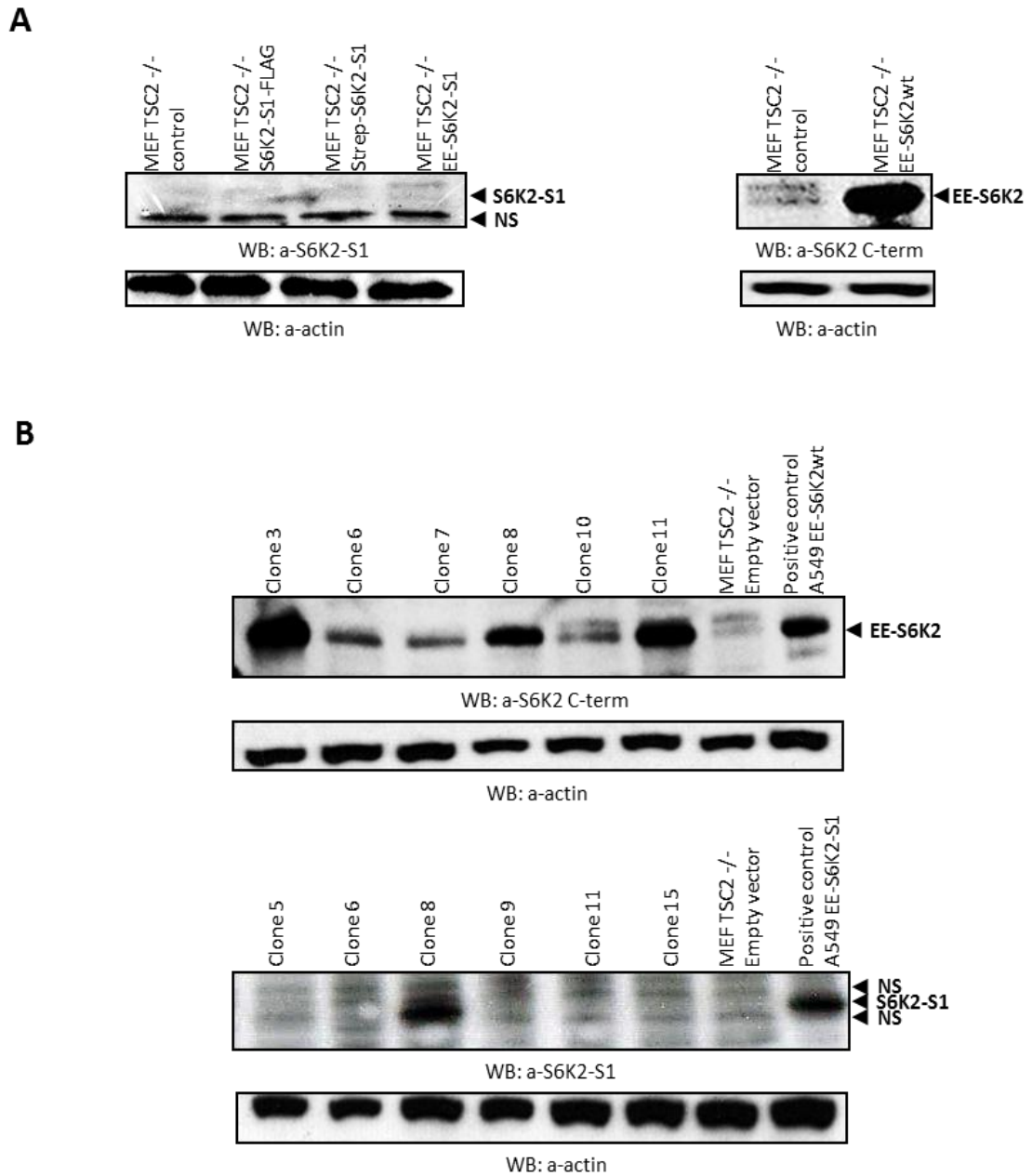
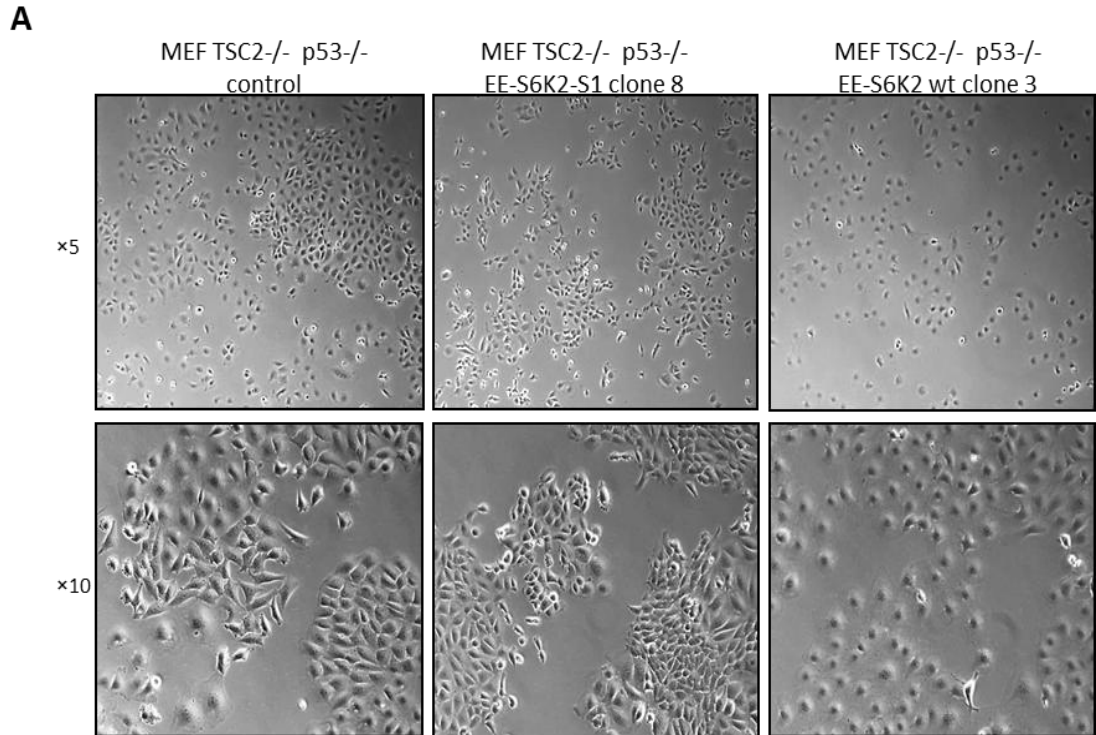


Figure 5.2 Generation of MEF TSC2^{-/-} p53^{-/-} stable cell lines overexpressing full-length S6K2 and splicing variant S6K2-S1. (A) Analysis of EE-S6K2 and EE-S6K2-S1 expression in generated MEF TSC2^{-/-} p53^{-/-} polyclonal stable cell lines in Western blotting, using corresponding antibodies. (B) Generation of monoclonal stable cell lines expressing full length S6K2 and splicing isoform. Analysis of EE-S6K2 and EE-S6K2-S1 expression in selected clones. 50µg of total cell lysate were used for Western blotting. Anti-actin antibodies were used as a control of equivalent protein loading. NS-non-specific signal.

In order to generate TSC2^{-/-} p53^{-/-} MEF stable cell lines overexpressing S6K2-S1, a technique of monoclonal selection was used. After infection, single cell infected with one of the Lentiviruses (EE-S6K2-S1, EE-S6K2, empty vector) formed a small colony of identical cells; these colonies were picked up and grown separately. 18 clones for each construct were analysed for the expression of EE-tagged S6K2 and S6K2-S1 in Western blotting. Among 18 selected clones checked for the expression of S6K2-S1, just one clone 8 expressed splicing isoform to a good detectable level; two clones had a very low expression whereas in all remaining 15 clones the expression of splicing isoform was below the detection limit. In contrast, the overexpression of full length EE-S6K2 in TSC2^{-/-} p53^{-/-} MEF cells was detected in all selected clones, with the highest expression found in clone 3 (Figure 5.2B). Therefore, clone 8 expressing EE-S6K2-S1 and clone 3 expressing EE-S6K2 were used for further analysis.

Simple observation of growing stable cell lines under the microscope revealed different phenotypes of cells overexpressing full length S6K2 and splicing isoform. As seen from Figure 5.3A, cells expressing full length S6K2 appeared to be bigger and more round, whereas S6K2-S1 expressing cells are visibly smaller and have a tendency to grow in groups, when compared to control cells. The overexpression of splicing isoform in TSC2^{-/-} p53^{-/-} MEF cells does not affect their proliferation rate, as shown on Figure 5.3B.



B

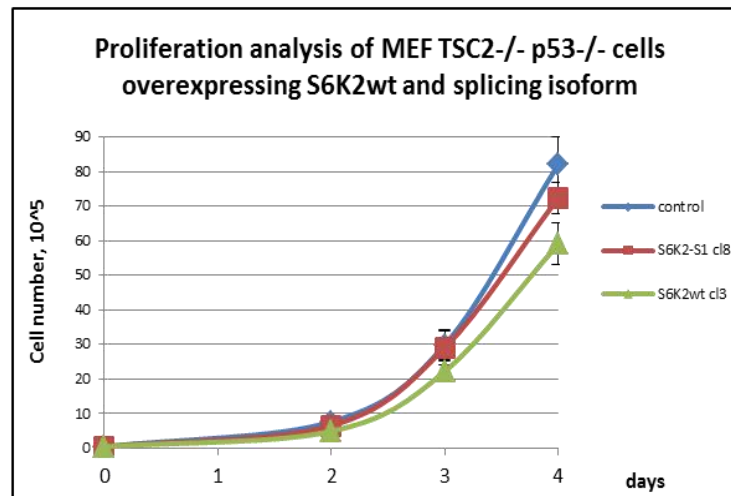


Figure 5.3 Characterisation of MEF TSC2^{-/-} p53^{-/-} stable cell lines overexpressing full-length S6K2 and S6K2-S1 splicing isoform. (A) Representative pictures of MEF TSC2^{-/-} p53^{-/-} stable cell lines overexpressing S6K2 wild type (clone 3) and S6K2-S1 splicing variant (clone 8). (B) Overexpression of S6K2-S1 in MEF TSC2^{-/-} p53^{-/-} cells does not affect cell proliferation. 4 000 cells were plated in 6-well plate in normal medium and grown under standard condition. Seeded cells were collected every following day for a period of 4 days. First, the medium was aspirated and cells were washed with PBS. After cells were trypsinized by the addition of 500 μ l of trypsin for 2 min at 37C, cells were resuspended and this suspension was mixed with 500 μ l of PBS. 100 μ l of resuspended cells were added to 10 ml of CASYTON isotonic solution (Innovatis) and samples were analysed using CASY Model TT cell counter (Innovatis). Each point represents mean \pm SD from three independent experiments.

Next, to verify our previous findings, cell size measurement of TSC2^{-/-} p53^{-/-} MEF cells clone 8 and clone 3, expressing EE-S6K2-S1 and EE-S6K2 correspondingly (Figure 5.4A), was performed using CASY machine. Comparative analysis of cell size distribution of these cell lines presented on Figure 5.4B shows that overexpression of splicing isoform significantly reduced cell size in contrast to full length S6K2 compared to control cells. To verify these findings four subsequent experiments were performed. Generated results confirm our previous observations obtained in NIH3T3RasC40 cells. Taken together, this study indicates that S6K2-S1 splicing variant has the potential to modulate the cell size and this effect is possibly mediated via downregulation of the mTORC1/S6K signalling pathway. On the other hand, we have shown that the overexpression of S6K2wt in TSC2^{-/-} p53^{-/-} MEF cells results in the increase in cell size, compared to control (Figure 5.4B).

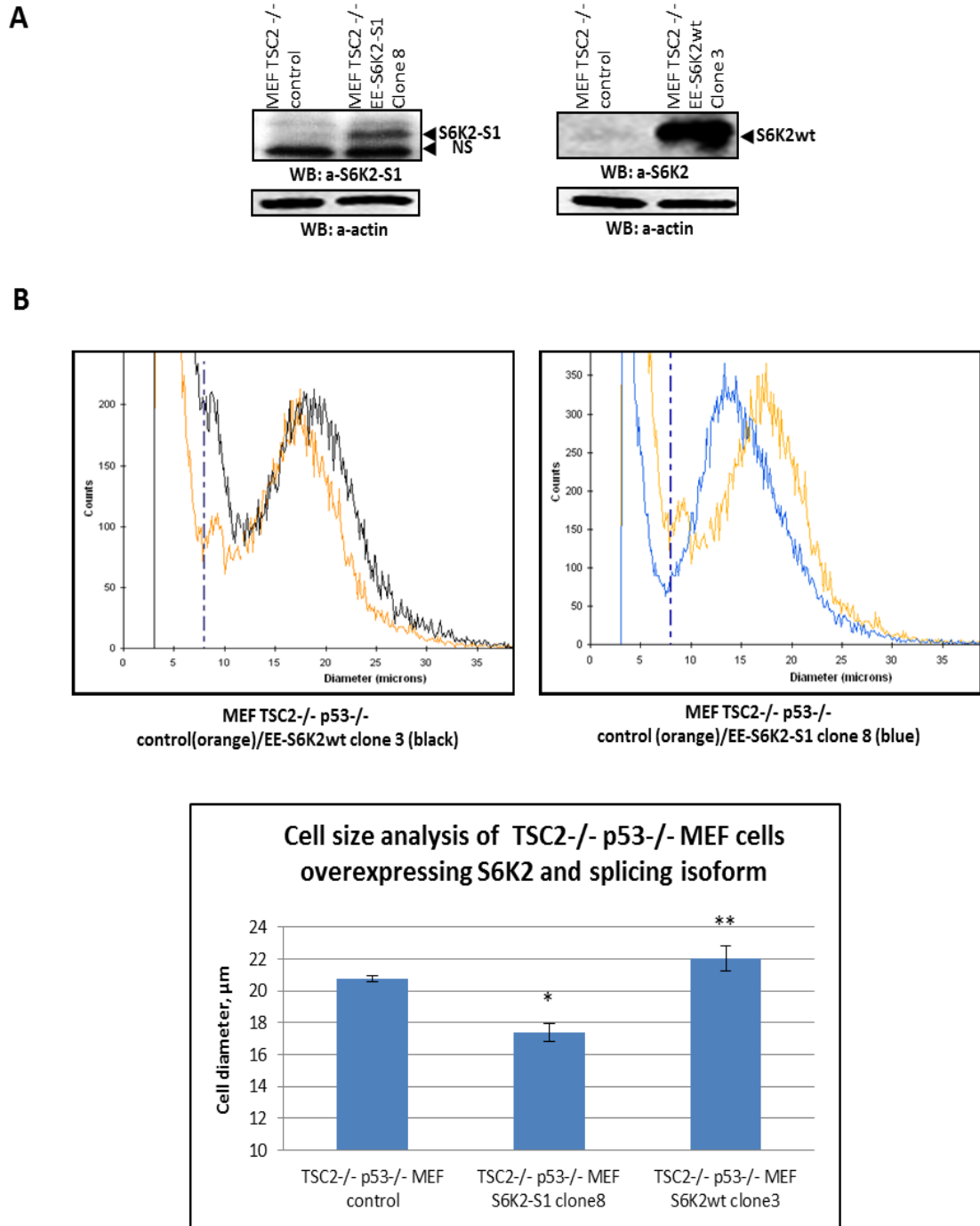


Figure 5.4 Overexpression of S6K2-S1 splicing isoform reduces the size of MEF TSC2^{-/-} p53^{-/-} cells. (A) Analysis of S6K2-S1 (clone 8) and S6K2wt (clone 3) protein expression in MEF TSC2^{-/-} p53^{-/-} monoclonal stable cell lines used for cell size measurement. 30 μg of total cell lysate was used for loading. Anti-actin antibodies were used as a control of equivalent protein loading. NS - non-specific signal. (B) Graphic representation of cell size distribution of MEF TSC2^{-/-} p53^{-/-} cells overexpressing S6K2wt (clone 3) and S6K2-S1 (clone 8), compared to control cells using CASY machine software. The same number of cells for each cell line was seeded and after 48h of growth were trypsinised, diluted in isotonic solution and cell size was measured using CASY counting machine. Each point on the graph represents mean \pm SD from four separate experiments (* $p < 0.001$, ** $p < 0.01$)).

5.2.2 S6K2-S1 isoform does not affect cell proliferation

Data from the S6K1^{-/-} and S6K2^{-/-} deficient animal models did not show any dramatic effect on cell proliferation (Montagne et al. 1999). To investigate whether S6K2-S1 splicing variant may affect cell growth, cell proliferation assays were performed. Previously generated HEK293 stable cell lines overexpressing S6K2-S1 clone 1 and clone 9 and a control cells (Figure 5.5A) were seeded with the same density into 6-well plates and every other day cells were collected and counted. Analysis of results presented in Figure 5.5B clearly indicates that there is no significant difference in the proliferation rate between control cells and cells overexpressing S6K2-S1. These results were subsequently confirmed in all generated stable cell lines used in this work (data not shown).

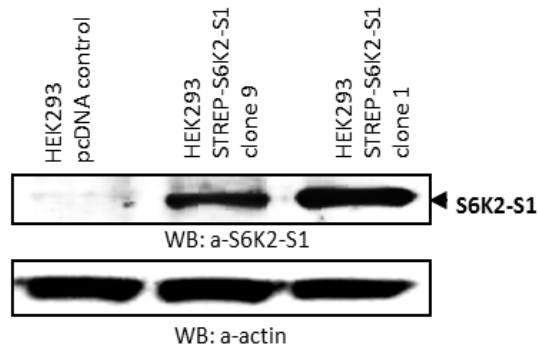
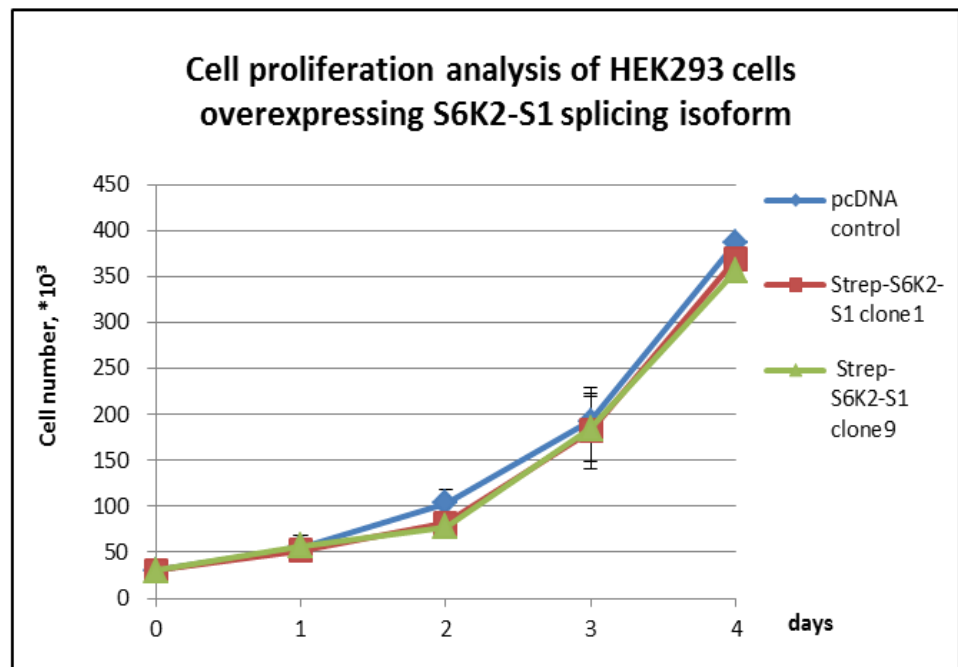
A**B**

Figure 5.5 Overexpression of S6K2-S1 in HEK293 cells does not affect cell proliferation. (A) The expression of S6K2-S1 splicing isoform was monitored in Western blotting. 30 μ g of total cell lysate was used for analysis. Anti-actin antibodies were used as a control of equivalent protein loading. (B) 30 000 cells of corresponding HEK293 stable cell lines were seeded into a 6-well plate in normal medium and grown under standard condition. Seeded cells were collected every following day for a period of 4 days. First, the medium was aspirated and cells were washed with PBS. After cells were trypsinized by the addition of 500 μ l of trypsin for 2 min at 37C, cells were resuspended and this suspension was mixed with 500 μ l of PBS. 100 μ l of resuspended cells were added to 10 ml of CASYTON isotonic solution (Innovatis) and samples were analysed using CASY Model TT cell counter (Innovatis). Each point represents mean \pm SD from three independent experiments.

5.2.3 S6K2-S1 can modulate the activity of the mTOR/S6K pathway in starved condition

Our findings presented in Chapter 4 of this thesis indicated a direct interaction of S6K2-S1 with Raptor and mTOR. These results suggest that under physiological conditions the splicing isoform might compete with the full length S6K2 for the binding to Raptor. Additionally, it may also interfere with S6K1 and 4EBP1 interaction with Raptor and thus affect their functions. Importantly, as S6K2-S1 does not have kinase activity it may act as a dominant negative regulator of mTORC1 signalling.

In order to gain further knowledge about physiological functions of the S6K2-S1 spliced isoform, the state of the mTOR/PI3K pathway in normal conditions was analysed using a panel of phospho-specific antibodies. Phosphorylation level of key downstream effectors of mTORC1: S6K1 at Thr389, 4EBP1 protein at Thr37/46 and S6 protein at Ser240/244 was assessed. In addition, the phosphorylation state of Akt/PKB at Ser473 was also examined, as it is known that S6Ks affect the Akt/PKB activity via the negative feedback loop to IRS-1 (Harrington, L.S., 2004).

As seen from Figure 5.6, HEK293 stable cells overexpressing S6K2-S1 (clone 1 and 9) do not show any significant changes in the phosphorylation level of S6K, S6, 4EBP1 and Akt/PKB in normal condition, when compared to control cells. The same results were obtained in A549, NIH3T3RasC40 and MEFTSC2-/-p53-/- stable cell lines overexpressing the spliced isoform (data not shown). There may be several explanations for this. Firstly, although splicing isoform interacts with Raptor and forms mTORC1, it may not be involved in the

regulation of mTOR and S6K activity and as a result the phosphorylation level of downstream targets remains unchanged. Secondly, cell models used for this experiment might not be appropriate to study this effect. Finally, the most feasible explanation might be that under this experimental condition the role of S6K2-S1 is eliminated due to a strong interaction between mTOR, Raptor, S6Ks and 4EBP1.

It is now well established that the mTORC1 assembly is affected by nutrients and growth factors. Therefore, we sought to determine whether S6K2-S1 can alter the phosphorylation level of S6K at Thr389, 4EBP1 at Thr37/46, S6 protein at Ser240/244 and Akt/PKB at Ser473 under serum-starved conditions. HEK293 cells with stable overexpression of splicing isoform (clone 1 and 9) were used for this analysis, since they express relatively high levels of S6K2-S1. Cells were grown to 50-60% confluence and the medium was replaced with DMEM without serum for a starvation period of 30 hours and then stimulated by the addition of 10% FCS for 1 hour. Cells were collected and analysed in Western blotting. Interestingly, three independent experiments confirmed that HEK293 cells overexpressing S6K2-S1 (clone 1 and 9) showed significant reduction in the phosphorylation of S6 protein and 4EBP1 under starved conditions, when compared to control cells (Figure 5.6). Interestingly, the phosphorylation level of Akt/PKB was reduced as well. This finding agrees with our suggestion that the S6K2-S1 splicing variant can negatively regulate some of mTOR functions and interfere with S6K activity. In addition, it can affect events upstream of mTOR, possible though regulating S6K negative feedback loop affecting the activation of Akt/PKB or through unknown mechanisms.

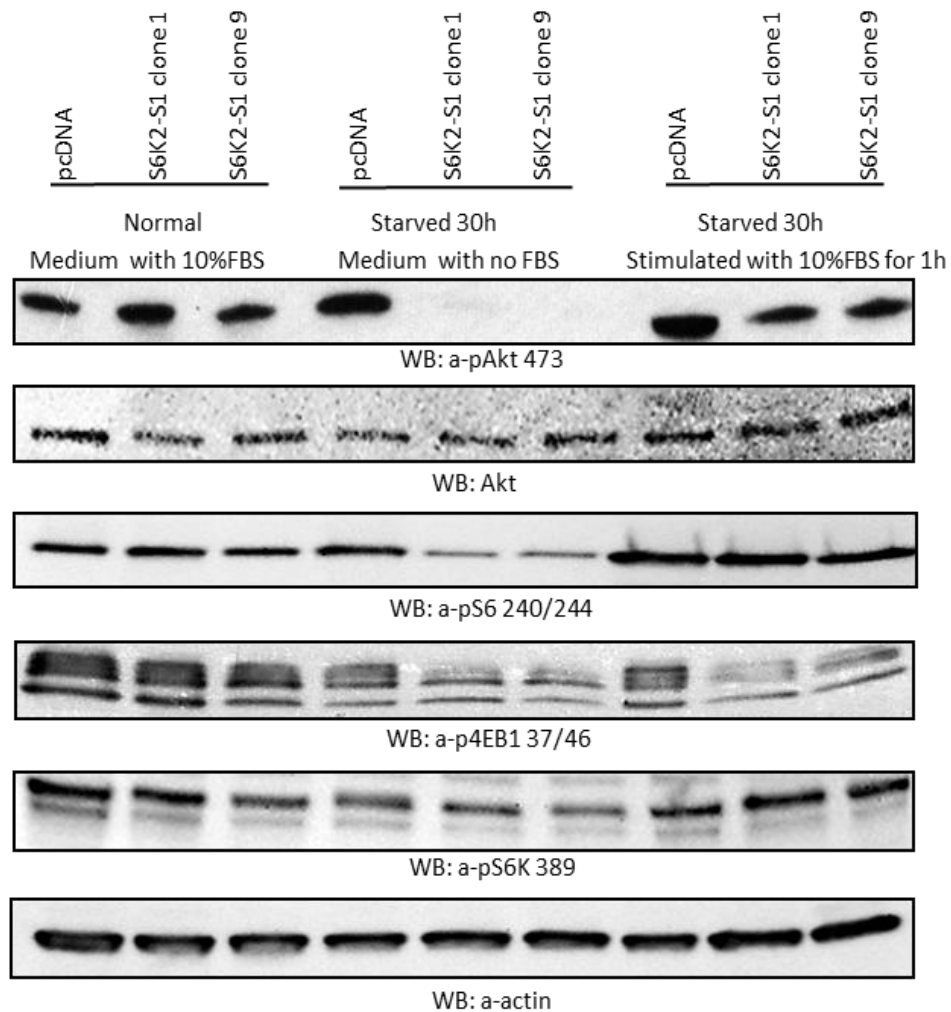


Figure 5.6 Overexpression of S6K2-S1 in HEK293 cells affects the mTOR/S6K pathway in serum-starved cells. HEK293 stable cell lines overexpressing S6K2-S1 (clone 1 and 9) and an empty vector were seeded at the same density to achieve 50% confluency in 24h. Next day media was changed for the starvation media without FBS and left for 30h. Then, cells were stimulated with media containing 10% FBS for 1h. Cells were harvested, lysed and analysed in Western blotting with corresponding antibodies. Anti-actin antibodies were used as a control of equivalent protein loading. The results shown are a representative outcome out of three individual experiments.

To further strengthen these novel findings, we examined the effect of starvation on the phosphorylation status of mTOR signalling molecules in different cell lines. As shown in Figure 5.7, serum deprivation of TSC2^{-/-} p53^{-/-} MEF stable cell lines overexpressing S6K2-S1 resulted in the significant downregulation of S6K1 and S6 protein phosphorylation when compared to control. As a positive control, cells overexpressing wild type S6K2 were used and showed higher level of S6K and S6 protein phosphorylation in normal and starved conditions when compared to control. These results were confirmed in three independent experiments. When A549 stable cell lines overexpressing S6K2-S1 were tested in this experimental set up, no significant changes in the phosphorylation level of selected proteins were observed under serum deprivation (data not shown). This may be due to the quality of cells used, or possibly a longer starvation period should have been chosen. However, from results obtained using HEK293 and TSC2^{-/-} p53^{-/-} MEF stable cell lines, it is obvious that S6K2-S1 splicing variant can negatively regulate some of the mTOR functions in serum-starved cells.

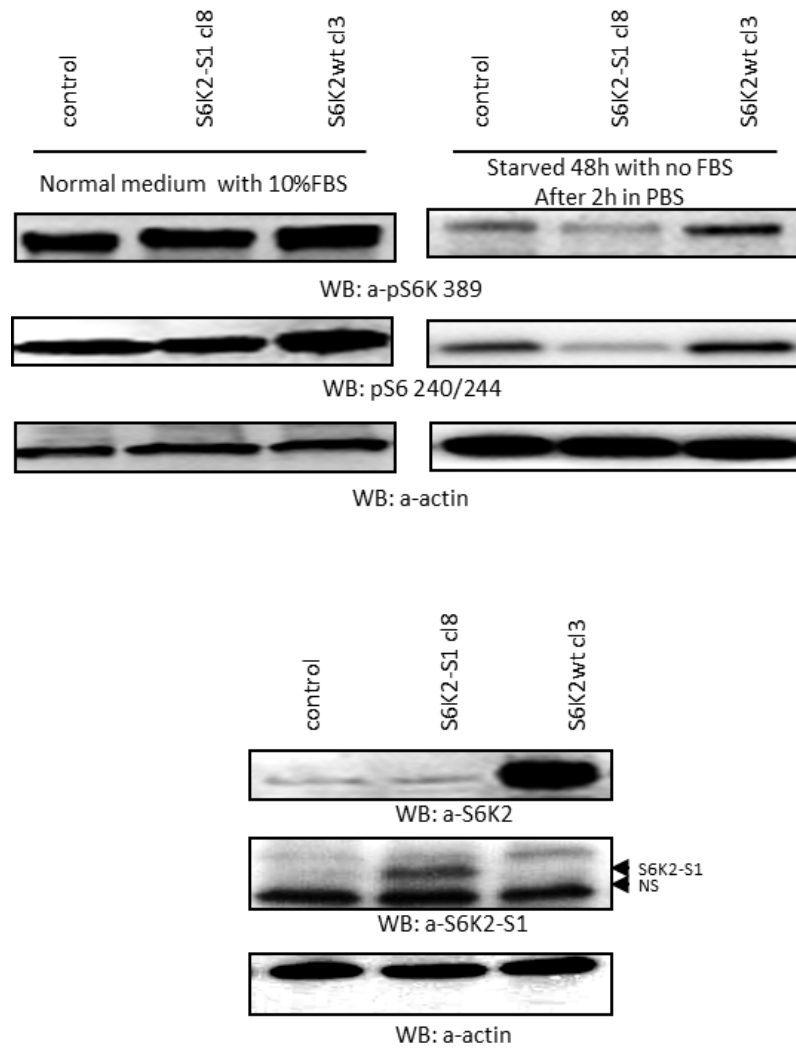


Figure 5.7 Overexpression of S6K2-S1 in MEF TSC2^{-/-} p53^{-/-} cells affects the mTOR/S6K pathway in serum-starved cells. 50 000 cells of MEF TSC2^{-/-} p53^{-/-} stable cell lines overexpressing S6K2-S1 (clone 8), S6K2wt (clone 3) and an empty vector were seeded into a 6cm plate. Next day media was changed for the starvation media without FBS and left for 48h. Then, cells were additionally starved for 2h in PBS. Cells were harvested, lysed and analysed in Western blotting with corresponding antibodies. Anti-actin antibodies were used as a control of equivalent protein loading. The results shown are a representative outcome out of three individual experiments. NS-non-specific signal.

5.2.4 S6K2-S1 is implicated in the regulation of cell migration

The important role of S6K1 in the regulation of cytoskeleton reorganisation is well established and described in detail in the Introduction chapter. Although few researchers have examined the function of S6K2 in this process, we decided to investigate whether the S6K2-S1 splicing variant can affect cytoskeleton reorganisation, focusing on cell migration.

A simple approach to study cell migration is a wound healing assay. Briefly, cells are grown on a plate and then a long scratch is introduced to the cell monolayer disrupting cellular growth. Cells respond to the injury by attempting to fill the gap and close the wound. Not all cell lines are suitable for this experiment. HEK293 cells have a weak cell-ECM and a strong cell-cell attachment; on the other hand A549 cells are very strongly attached to the surface, which makes it difficult to inflict a “good” wound. A literature search pointed us to the good cell model for this assay - mouse embryonic fibroblast (NIH3T3) cell line.

Considering the potential role of S6K2-S1 as a negative regulator of mTORC1 functions in this study we decided to use transformed NIH3T3RasC40 cell line. In comparison to parental NIH3T3, this cell line overexpresses Ras GTPase with two independent mutations: a) RasV12 activating mutation which results in Ras-induced cell transformation; b) Ras C40 mutation retains Ras binding to the p110 catalytic subunit of PI3kinase, but abrogates the activation of the MAPK signalling pathway (Andreas Behren et al., 2005). So, using these cells we can check whether the overexpression of S6K2-S1 might suppress cell transformation mediated through the PI3K pathway.

As shown in Figure 5.8A, we managed to generate polyclonal stable NIH3T3RasC40 cells with a good expression of S6K2-S1 splicing isoform. This cell line does not show any changes in their proliferation rate compared to control (Figure 5.8B). Interestingly, cells overexpressing S6K2-S1 looked morphologically different when compared to control cells. Control NIH3T3RasC40 cells have the spindle/fibroblastic shape that is characteristic of cells transformed with an oncogene such as Ras (Janda E et al., 2003). As seen from Figure 5.8C, cells overexpressing S6K2-S1 appear more round and show less actin-rich projections in the form of lamellipodia and filopodia, in comparison to parental cells. This difference was especially visible just after trypsinization and plating cells in the time-scale from 1 to 6 hours (Figure 5.9), while 24 hours later the difference was less obvious. These observations do not prove anything on their own, but they suggest that S6K2-S1 splicing variant might affect cell adhesion and migration.

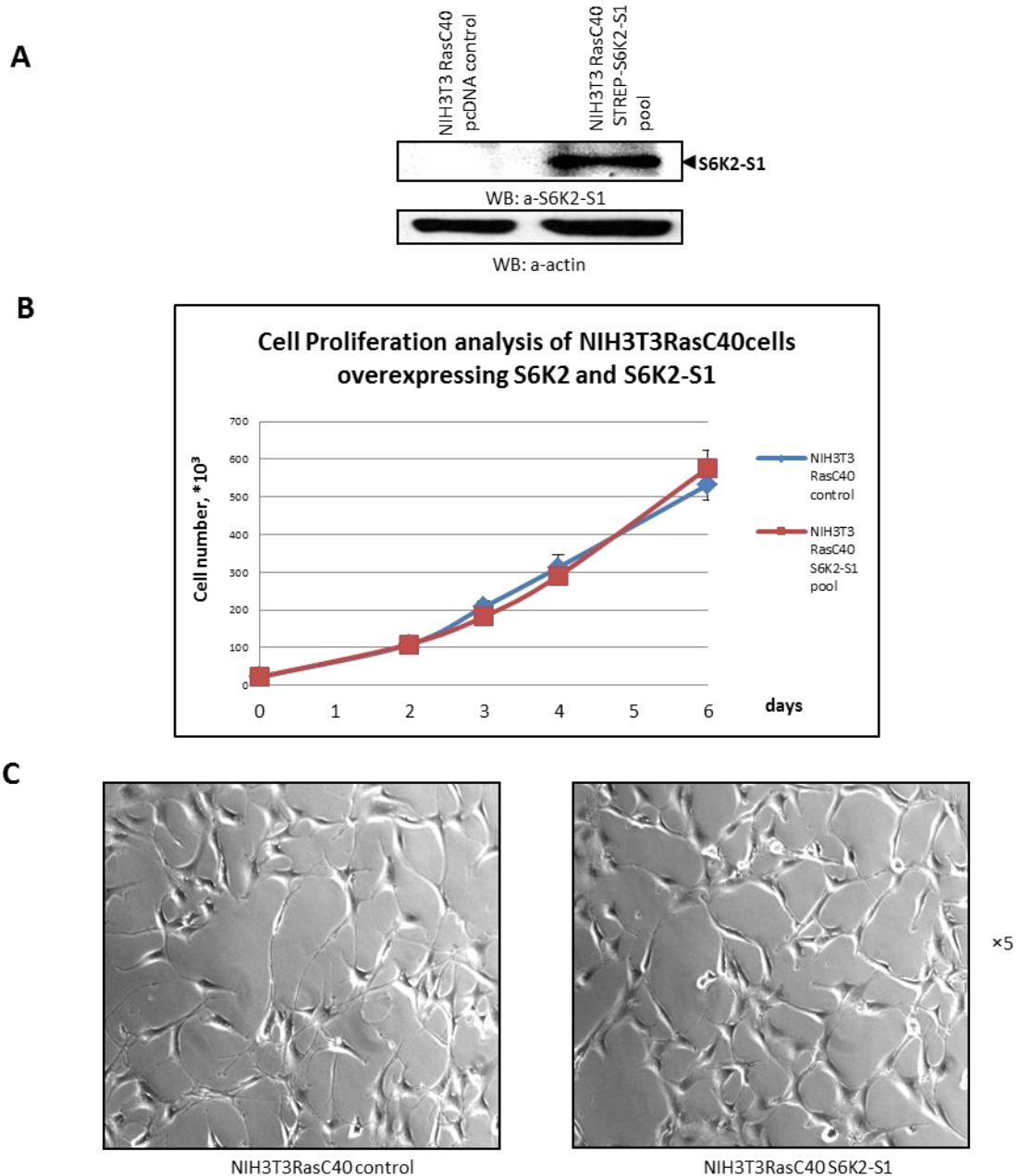


Figure 5.8 Generation and characterisation of NIH3T3 RasC40 stable cell lines overexpressing S6K2-S1. (A) NIH3T3 RasC40 cells were transiently transfected with pcDNA/S6K2-S1 and an empty vector. After 48 hours post transfection, cells were split into fresh medium with selective antibiotic. After selection, cells were harvested and checked for the expression of splicing isoform in Western blotting with specific antibodies. 30mg of total cell lysate was used for loading. Anti-actin antibodies were used as a control of equivalent protein loading. (B) Overexpression of S6K2-S1 in NIH3T3RasC40 cells does not affect cell proliferation. 20 000 cells were seeded into a 6-well plate and cell number was counted using CASY counting machine every following day. Each point represents mean \pm SD from three separate experiments. (C) Representative pictures of NIH3T3RasC40 stable cell lines overexpressing S6K2-S1 splicing variant and an empty vector.

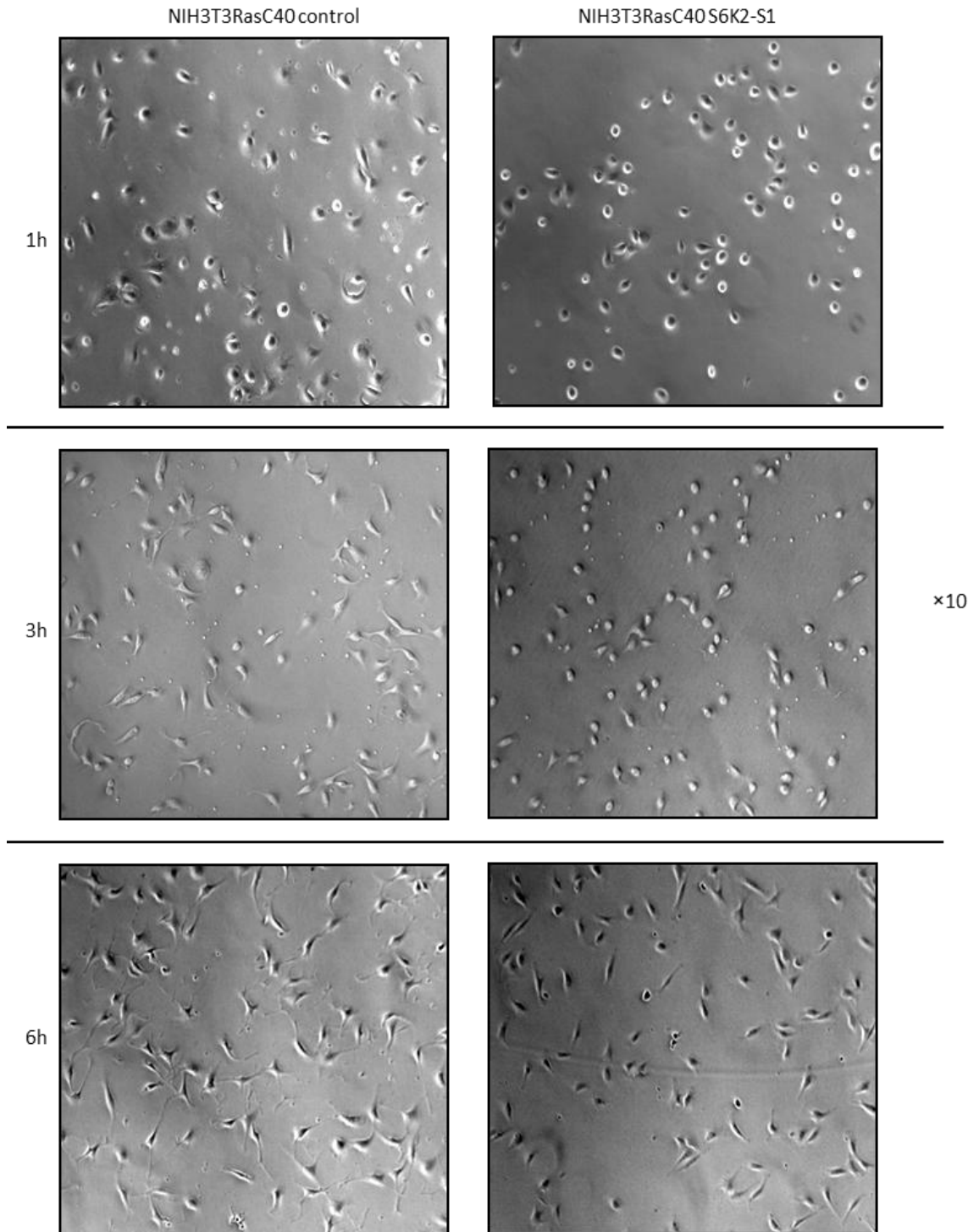


Figure 5.9 Overexpression of S6K2-S1 in NIH3T3RasC40 cells affects early cell attachment to the plate. Growing cells were washed with PBS, trypsinized by the addition of trypsin for 2 min at 37C, after cells were resuspended and this suspension was mixed with normal medium. 100 μ l of resuspended cells were added to 10 ml of CASYTON isotonic solution (Innovatis) and the number of cells was counted using CASY Model TT cell counter (Innovatis). 250 000 cells of each cell line were seeded into 6cm plate. Representative images of the cells were taken after 1, 3 and 6h after seeding.

To investigate if the splicing isoform can regulate cell migration, we performed tissue culture wound healing assay. Cells were plated at the same density and the wound was introduced to 90% confluent monolayer of cells. As seen from Figure 5.10 NIH3T3RacC40 cells expressing S6K2-S1 isoform showed lower (up to forty percent) migration rate compared to control cells. These results were reproduced in four independent experiments. In addition, our collaborators from Imperial College London (Prof. M. Seckl and Dr. O. Pardo) confirmed our findings and showed that overexpression of S6K2-S1 isoform in NIH3T3RacC40 cells significantly reduced their migration and invasion into collagen in response to EGF treatment (data not shown).

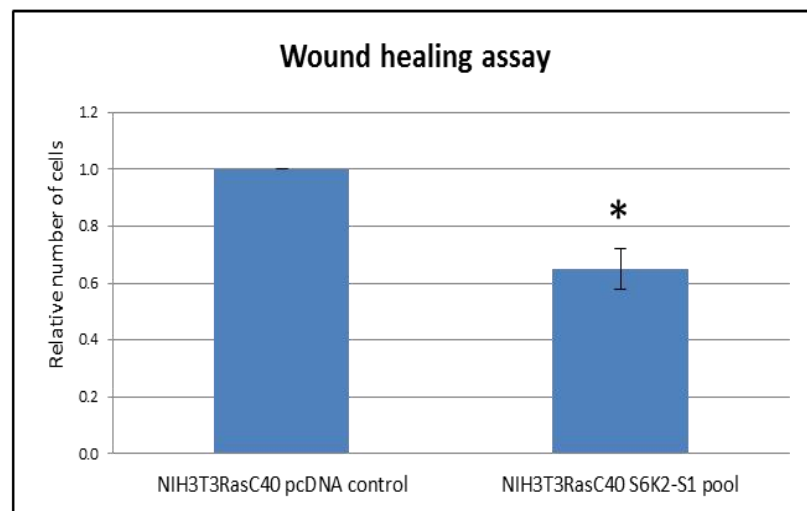
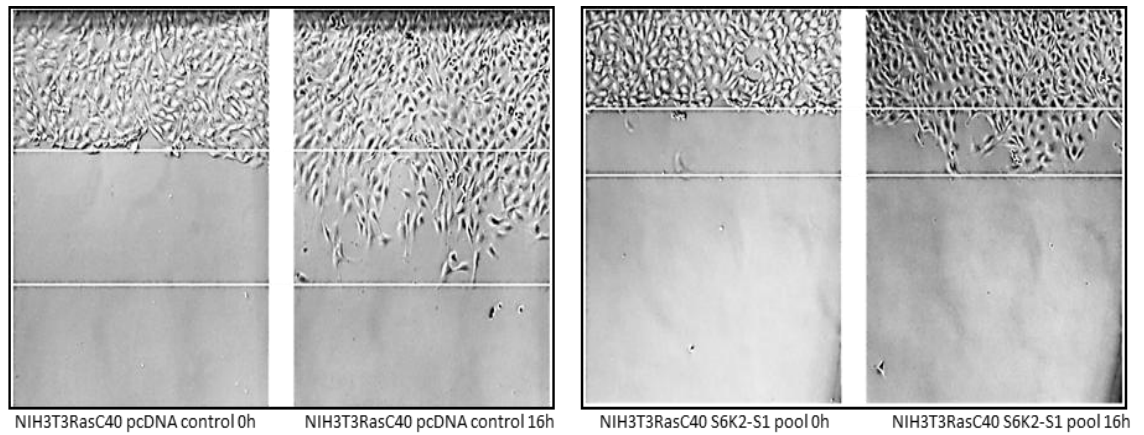


Figure 5.10 Overexpression of S6K2-S1 in NIH3T3RasC40 cells inhibits cell migration measured by wound healing assay. Representative images of the wound were taken immediately after the scratch and 16h later. For the assay, 0.5 million cells were seeded in 6cm plates, when cells reached 90% confluence, a single wound was made in the centre of the cell monolayer; media was carefully changed to remove cell debris. The number of migrated cells from the start point to the point of 16h incubation was counted. Graphs represent mean \pm SD of four independent experiments (* $p < 0.05$).

5.2.5 Cells overexpressing S6K2-S1 show higher sensitivity to drug-induced apoptosis

It is now well-established that S6K signalling is implicated in the regulation of cell survival. Taking into account the important role of S6K2 in mediating pro-survival signalling in chemoresistant NSCLC (non-small cell lung cancer), the decision was made to study the role of S6K2-S1 splicing isoform in cell survival in A549 human lung carcinoma cell line. A549 cells were infected with the Lentiviruses (described in chapter 4.2.4) corresponding to EE-tagged full length S6K2 and S6K2-S1 splicing variant. Generated stable cell lines showed a relatively high level of overexpressed proteins (Figure 5.11A). To assess how the overexpression of splicing isoform may affect cell survival generated stable cell lines were treated with staurosporine and cisplatin, which are commonly used for the induction of apoptosis in various cellular models.

Staurosporine is a general protein kinase inhibitor, which induces apoptosis as determined by cell morphology and the activity of caspases. A549 stable cell lines overexpressing full length S6K2 and splicing isoform were exposed to 1 μ M of staurosporine for 3h and 5h. As seen from Figure 5.11B, at this concentration staurosporine induced a marked cleavage of poly-(ADP-ribose) polymerase (PARP), dramatic downregulation of S6 kinase and S6 protein phosphorylation. PARP (116 kDa) is proteolytically cleaved during caspase- dependent apoptosis resulting in the appearance of the 85 kDa fragment, which is specifically detected only in apoptotic cells.

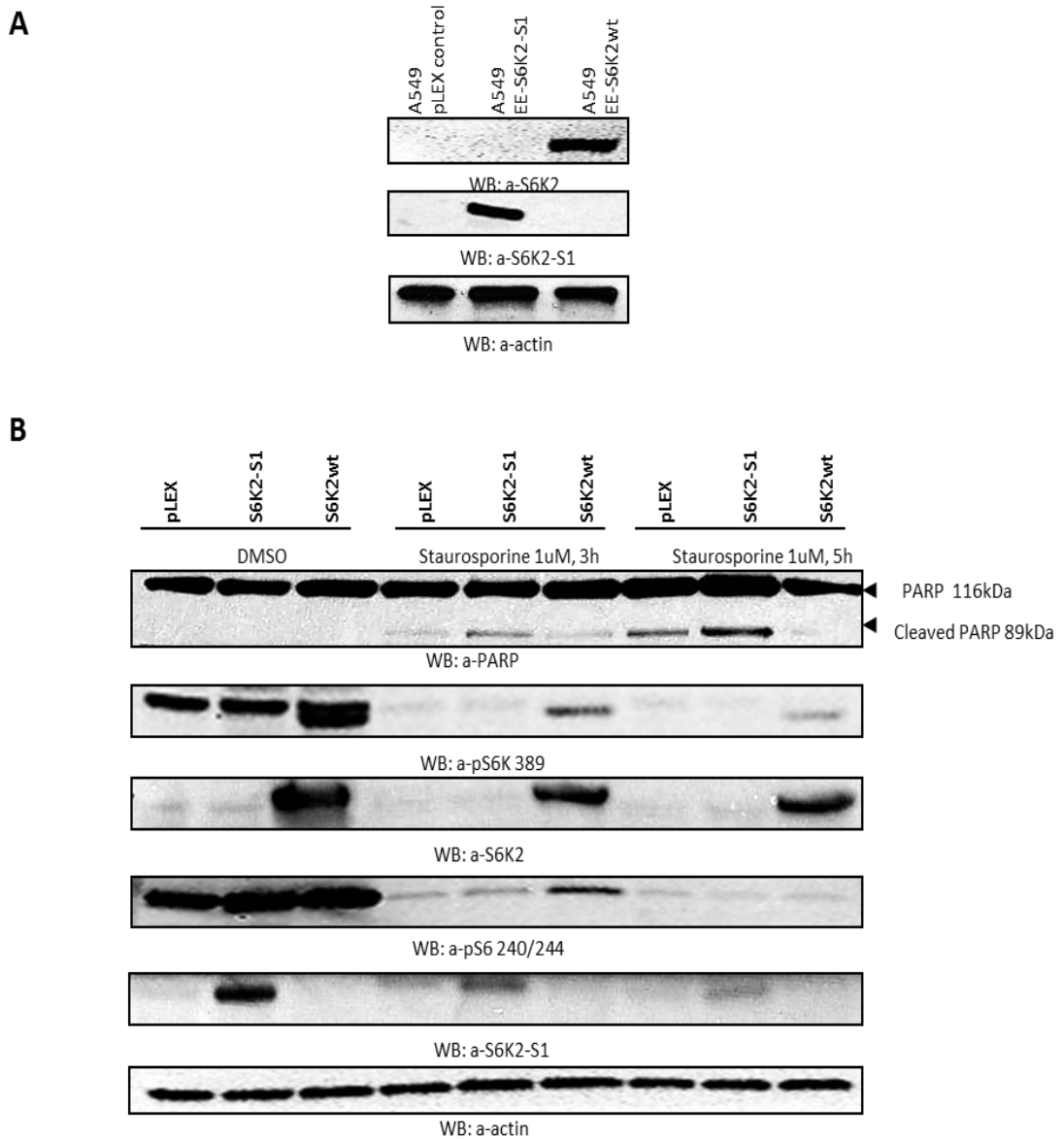


Figure 5.11 Staurosporin treated A549 cells with stable overexpression of S6K2-S1 shows higher level of cleaved PARP when compared to control cells. (A) A549 stable cell lines overexpressing S6K2-S1 isoform, EE-S6K2wt and control cells were analysed in Western blotting. Anti-actin antibodies were used as a control of equivalent protein loading. (B) 300 000 cells of A549 stable cell lines overexpressing pLEX empty vector, EE-S6K2-S1 and EE-S6K2 were seeded into 6cm plate. Next day, 1 μ M of staurosporine diluted in DMSO was added to each plate. DMSO alone was added as a control. After 3 and 5 hours of incubation cells were collected and lysed in cold lysis buffer. 30 μ g of total cell lysate was used for Western blotting. PVDF membranes were blotted with corresponding antibodies. Anti-actin antibodies were used as a control of equivalent protein loading. The results shown are representative outcomes out of three individual experiments.

It is clear that cells overexpressing S6K2-S1 exhibit higher level of cleaved PARP compared to the control, therefore we can conclude that the overexpression of splicing isoform downregulates pro-survival signalling in A549 cells in response to staurosporine. These findings were subsequently confirmed in TSC2^{-/-} p53^{-/-} MEF cell lines stably expressing S6K2 and S6K2-S1 (data not shown).

Next, we investigated how S6K2-S1 splicing isoform would affect DNA damage-induced cell death by treating cells with cisplatin, a chemotherapy drug that targets actively proliferating cells. Treatment of A549 cells with 50 μ M of the drug induced cell death as observed under the microscope. Apoptotic signalling was detected by measuring the level of cleaved PARP by Western blotting.

Figure 5.12 shows that after 24 hours of treatment cells overexpressing S6K2-S1 have slightly higher level of cleaved PARP compared to control, which is in line with previous findings. Following cisplatin treatment, the level of phosphorylation of S6K at Thr389 and S6 protein at Ser240/244 was checked. Importantly, as seen from Figure 5.12, treated A549 stable cells overexpressing S6K2-S1 show reduced phosphorylation of S6 protein at Ser240/244 and S6K at Thr389, when compared to control. This might indicate that under these experimental conditions, S6K2-S1 downregulates the activity of mTOR and S6K measured by the phosphorylation level of S6K and S6 protein.

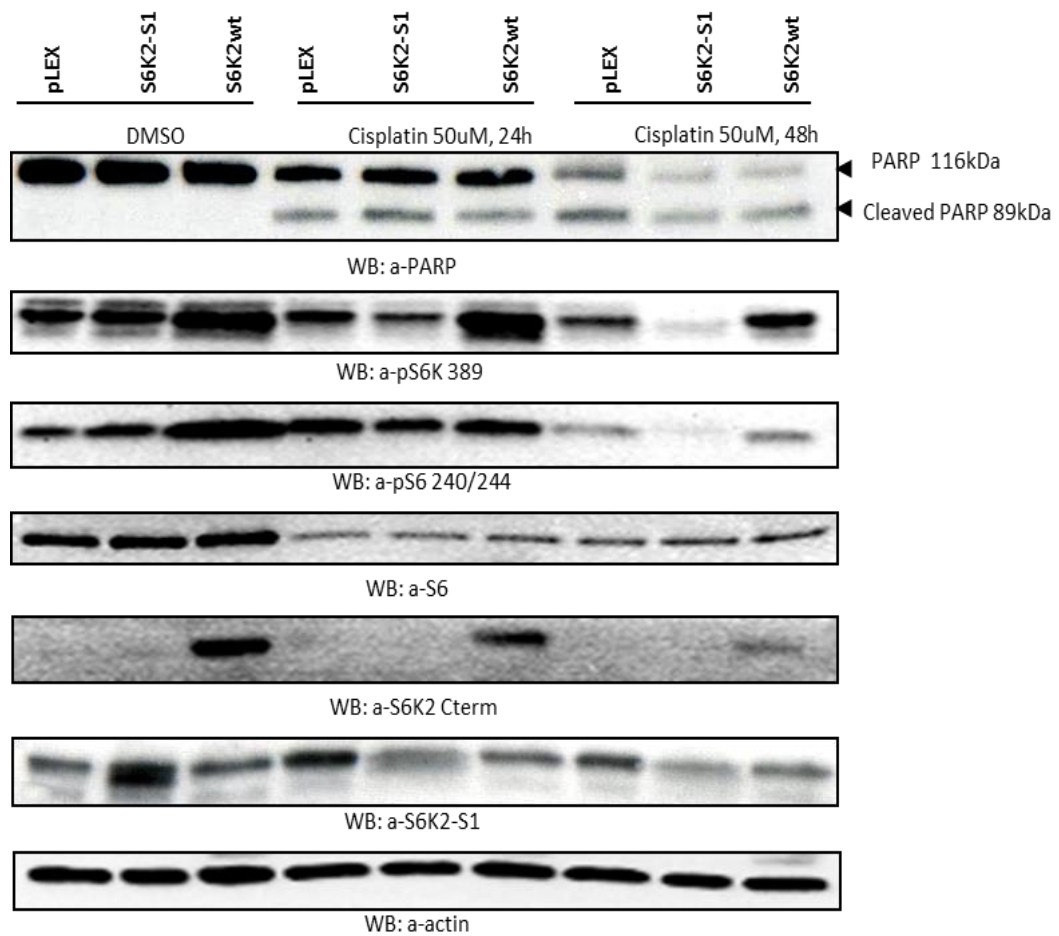


Figure 5.12 Cells overexpressing EE-S6K2-S1 show higher sensitivity to cisplatin-induced apoptosis. 300 000 cells of A549 stable cell lines overexpressing pLEX empty vector, EE-S6K2-S1 and EE-S6K2 were seeded into 6cm plates. Next day, cells were treated with 50 μ M of cisplatin diluted in DMSO. DMSO alone was added to control plates. After 24 and 48 hours of incubation, cells were collected and lysed in cold lysis buffer. 30 μ g of total cell lysate was used for Western blotting. PVDF membrane was blotted with corresponding antibodies. Anti-actin antibodies were used as a control of equivalent protein loading. The results shown are representative outcomes out of three individual experiments.

Taken together, these results reveal the potential of S6K2-S1 to mediate pro-apoptotic signalling and suggest that it may reduce cell resistance to apoptosis, possibly by interfering with the mTOR/S6K pathway or through yet unknown mechanisms.

5.2.6 S6K2-S1 is a potential tumour suppressor, whereas full length S6K2 exhibits oncogenic properties

A recent publication showed that the overexpression of p31S6K1 spliced isoform has the potential to induce transformation of human breast epithelial cells, in contrast to full length S6K1 (Karni R et al., 2012). Taking this into account and the similarity in the splicing mechanism of S6K1 and S6K2 genes, it was logical to investigate whether S6K2wt and S6K2-S1 splicing isoform had a tumorigenic potential. There is no direct evidence that full length S6K2 is an oncogene on its own, but high expression level of S6K2 has been found in a diverse range of tumours and cancer cell lines (Pardo O et al., 2006; Filonenko VV Et al., 2004; Perez-Tenorio G et al., 2011).

Initially, the oncogenic potential of wild type S6K2 and splicing isoform was examined using an anchorage-independent colony formation assay. Anchorage-independent cell growth in soft agar is one of the main characteristics of cellular transformation. Typically, normal cells are not able to grow in a semi-solid medium, as contact between cells and extracellular matrix (ECM) is crucial for cell proliferation and survival. Disruption of this interaction leads to cell apoptosis. Transformed cells are usually resistant to apoptosis and are able to grow in an anchorage-independent manner. Tumour cells tend to form aggregates in a suspension culture which correlates with colony formation in soft agar.

These processes play a very important role in tumour development and metastasis (Grossmann J et al., 2002).

To set up a colony formation assay, generated HEK293 stable cell lines overexpressing S6K2-S1 isoform (clone 1 and clone 9), S6K2wt and an empty vector were used. Briefly, the same number of cells was mixed with the semi-solid medium/agarose mixture and left to grow for two weeks. The resulting number of colonies were visualized and counted. Data presented in Figure 5.13A clearly show that cells overexpressing S6K2-S1 form significantly lower number of colonies in soft agar. Moreover, the colonies are much smaller when compared with control. Notably, the inhibition of colony formation and growth shows a good correlation with the expression level of S6K2-S1 spliced isoform. For example, the expression level of S6K2-S1 in clone 1 is higher than that in clone 9, which correlates with the number of colonies in a soft agar assay. In contrast, overexpression of full length S6K2 increases the number and size of the colonies in soft agar. These results were reproduced in three independent experiments. Analysis of data presented in Figure 5.13B shows that the overexpression of S6K2-S1 in HEK293 cells suppresses anchorage-independent growth up to 50%, while a significant increase up to 30% in the colonies number is observed in cells overexpressing full length S6K2, when compared to control. The expression level of S6K2-S1 and full length S6K2 in selected cell lines were confirmed in Western blotting (Figure 5.13C).

To further verify these findings, A549 cells with stable expression of S6K2-S1 and wild type S6K2 (described previously in this chapter) were also used in the colony formation assay. The results of four independent

experiments clearly demonstrate that full length S6K2 promoted anchorage-independent growth, whereas S6K2-S1 splicing isoform downregulated colony formation (Figure 5.14A). Analysis of data shows that the overexpression of S6K2-S1 suppresses colony formation up to 40%, while overexpression of full length S6K2 leads to 40% increase in the colonies number, when compared to control (Figure 5.14B). In addition, the colonies of cells with overexpressed wild type S6K2 are bigger, when compared to control or S6K2-S1 expressing cells. These results completely reproduce data obtained in HEK293 cells. The expression level of S6K2-S1 and full length S6K2 in selected cell lines were confirmed in Western blotting (Figure 5.14C).

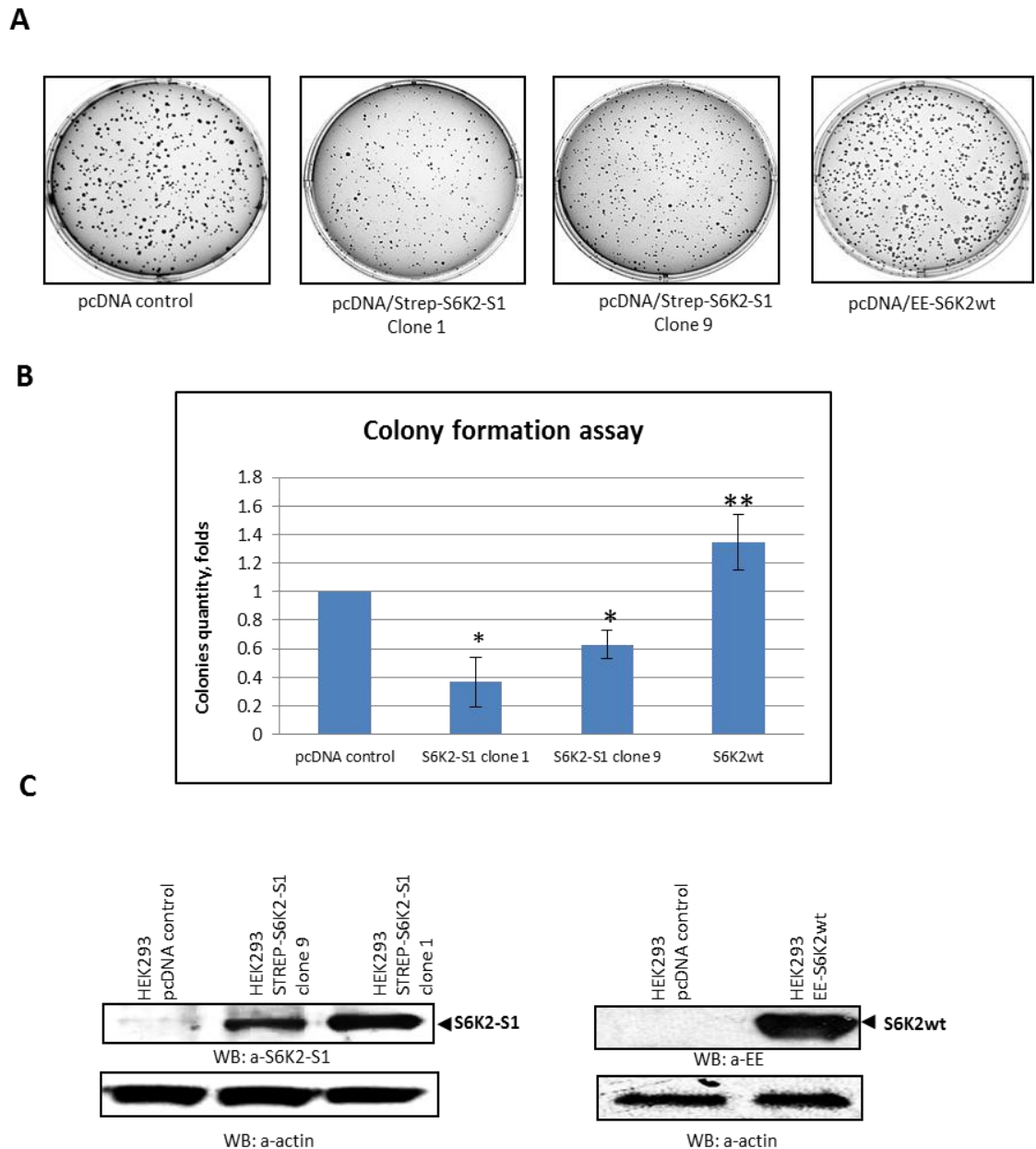


Figure 5.13 Overexpression of S6K2-S1 isoform inhibits anchorage-independent colony formation in soft agar. (A) Representative pictures of soft-agar plates with HEK293 stable cell lines overexpressing S6K2-S1 (clone 1 and clone 9), S6K2wt and an empty vector. 2 000 cells of each cell lines were plated in semi-solid agar, as described in Materials and Methods. Colonies growth was monitored over a period of weeks. (B) Visualized colonies were counted using ImageJ software (Colonies with the area more than 25 pixels were counted). Data are mean \pm SD of three independents experiments (* p <0.005, ** p <0.0005). (C) Analysis of S6K2-S1 and S6K2wt protein expression in stable cell lines. 30 μ g of total cell lysate was used for loading. Anti-actin antibodies were used as a control of equivalent protein loading.

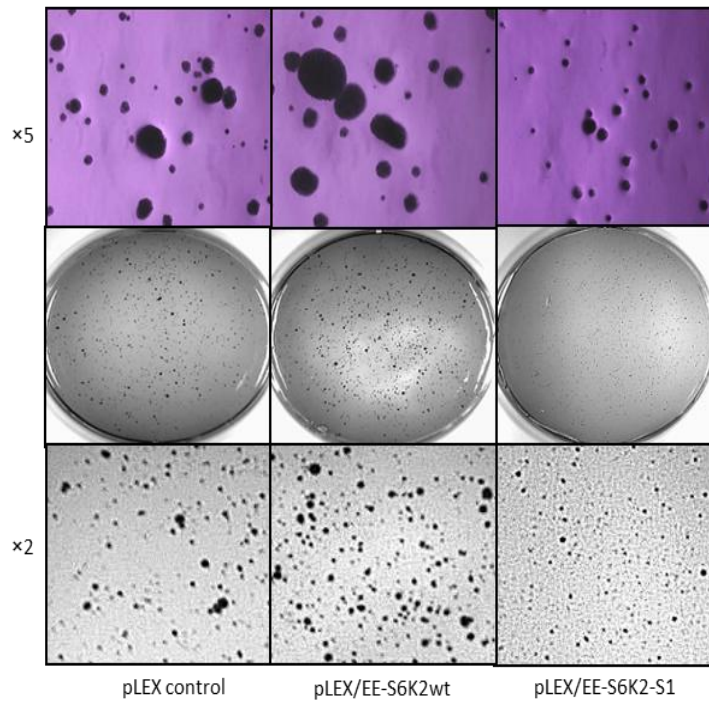
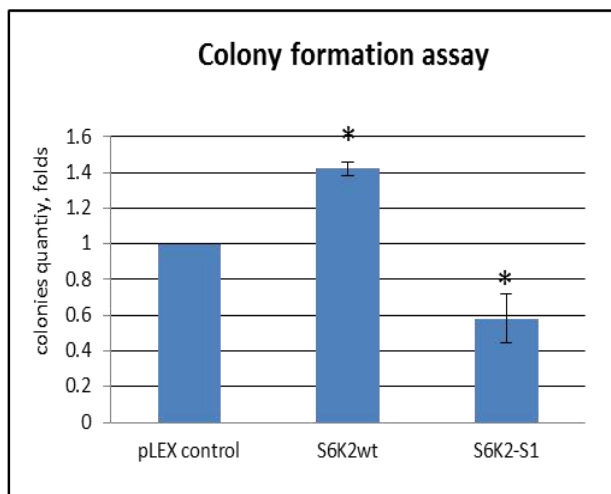
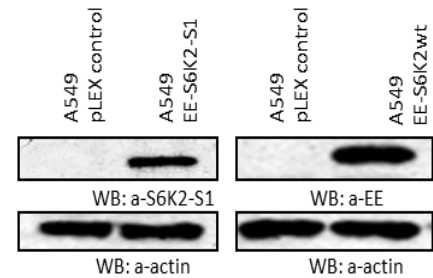
A**B****C**

Figure 5.14 Overexpression of S6K2-S1 splicing variant in A549 cells suppresses colony formation in soft agar. (A) Representative fields from soft-agar plates with A549 stable cell lines overexpressing S6K2wt, splicing isoform and an empty vector. 10 000 cells for each cell line were plated in semi-solid agar as described in Material and Methods. Colonies growth was monitored over a period of weeks. (B) Visualized colonies were counted using ImageJ software (Colonies with the area more than 6 pixels were counted). Data are mean \pm SD of four independent experiments (* $p < 0.005$). (C) Stable cell lines overexpressing S6K2-S1 isoform, EE-S6K2wt and control cells were analysed in Western blotting. Anti-actin antibodies were used as a control of equivalent protein loading.

Taken together, results in colony formation assay obtained in HEK293 and A549 cell lines demonstrate for the first time that overexpression of wild type of S6K2 induces colonies growth, while S6K2-S1 splicing isoform acts as a potential tumour suppressor. As we shown in chapter 5.2.2 that stable overexpression of full length S6K2 and S6K2-S1 in several cell lines did not change their proliferation rate in comparison to control, it is most likely that other cellular processes contribute to the outcome of the colony formation assay.

To further substantiate our results, the colony formation assay was set up with generated TSC2^{-/-} p53^{-/-} MEF stable cells lines everexpressing S6K2 wild type and splicing isoform (described in chapter 5.2.1). Literature searches revealed no studies on the use of MEFs in an anchorage-independent colony formation assay, so soft agar assay for TSC2^{-/-} p53^{-/-} MEF cell lines was carried out as described for HEK293 cells. This study showed that all tested TSC2^{-/-} p53^{-/-} MEF stable cell lines started to form colonies after 5-6 days in the assay. However, the colonies didn't expand with time or started to decline gradually. As the size of colonies was very small, we were not able to quantitate the outcome of this experiment using ImageJ software. Analysis of colonies under the microscope confirmed that overexpression of full length S6K2 leads to the formation of bigger colonies in contrast to S6K2-S1 splicing isoform and control (data not shown). These observations are in line with data presented in Figure 5.13 and Figure 5.14.

Based on the fact that anchorage-independent growth is one of characteristics of transformed cell phenotype, the data presented

above suggest that S6K2 has an oncogenic potential, whereas S6K2-S1 is a potential tumour suppressor.

5.2.7 Xenograft studies in nude mice

To confirm our findings, one of the most commonly used animal models to study human cancer was used. In a xenograft model, human tumour cells are injected into mice either under the skin or into the organ type from which tumour is originated. In these studies, nude athymic (nu/nu) immunocompromised mice deficient for B- and T-cells are used, as they do not reject human cells. Established *in vitro* human cell lines as well as human tumour tissue derived from biopsy or autopsy can be transplanted directly into these mice, allowing subcutaneous growth and reconstitution of solid tumours.

To explore the oncogenic activity of full length S6K2 and S6K2-S1 *in vivo*, A549 stable cell lines, generated in the frame of this project, were injected into the flank of an individual athymic nude mouse. As a control, A549 stable cell line overexpressing an empty vector was used. Tumour growth was monitored every 3-4 days over a period of two months and measurement of the tumour volume began once the subcutaneous tumours became palpable and continued until day 50. Growth of the tumour xenografts in three groups was compared. As seen from the graphs presented in Figure 5.15, mice in group 2, injected with A549 cells overexpressing full length S6K2, developed tumours more rapidly, whereas tumour growth in S6K2-S1 group 3 was much slower, compared to control group 1. On day 50 four mice in S6K2 group 2 developed big tumours with volume range from 0.68 to 1.13 cm³ in comparison to control group 1, where just two mice developed

tumours with size 0.64 and 0.98 cm³ correspondingly. On the other hand, in S6K2-S1 group 3 two mice had small tumours with volume 0.53 and 0.68 cm³. Analysis of results in Figure 5.16A shows that the overexpression of S6K2-S1 splicing variant in A549 cells reduces *in vivo* tumour growth, while full length S6K2 promotes tumour formation in nude mice. The expression of S6K2 and S6K2-S1 in tumour samples was monitored by Western Blotting (Figure 5.16B).

Taking together, these results demonstrate for the first time that full length S6K2 exhibits oncogenic properties, whereas S6K2-S1 splicing variant functions as a tumour suppressor.

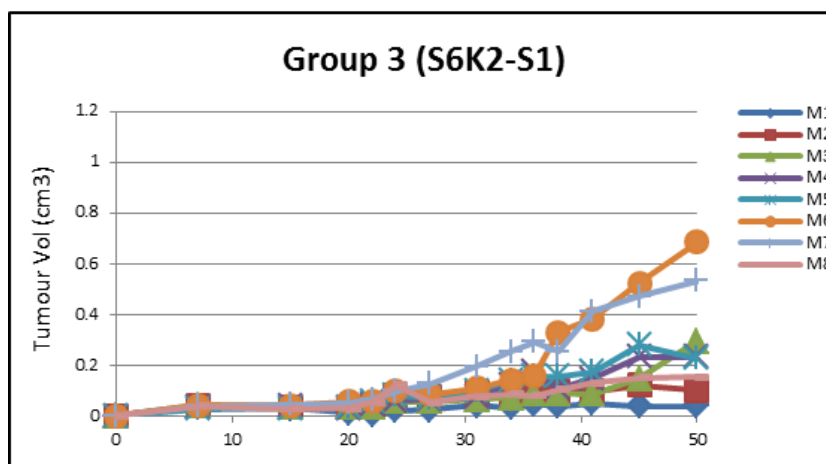
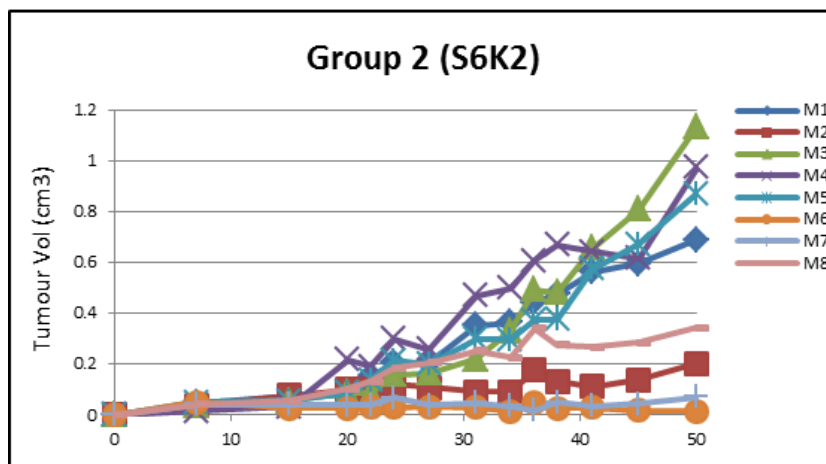
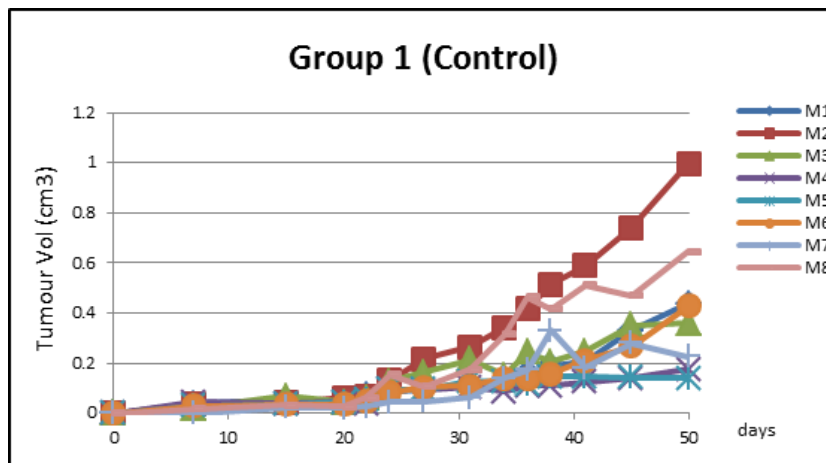
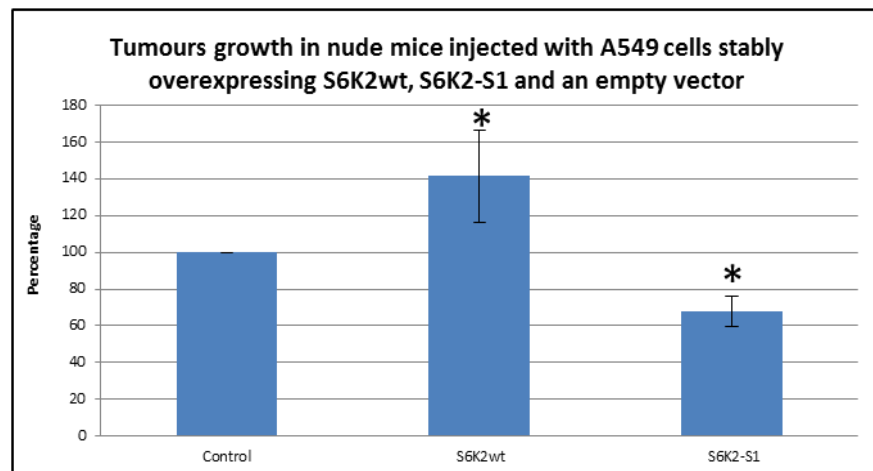
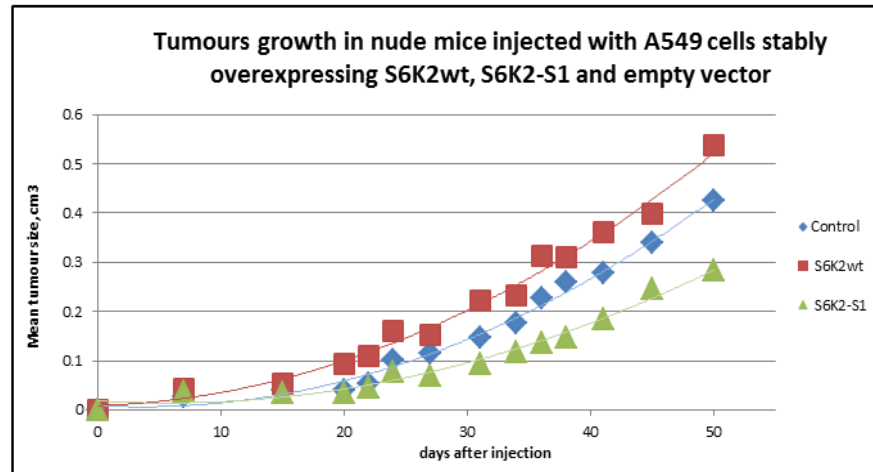


Figure 5.15 Analysis of tumours growth in a xenograft mouse model. 100 μ l of viable A549 cells resuspended in normal medium (1×10^6 cells/site) stably expressing S6K2wt, S6K2-S1 and an empty vector were mixed with 100 μ l of chilled to +4°C Matrigel. This mixture was subcutaneously injected into flanks of nu/nu mice (eight mice per group). Tumours were measured twice weekly over a period of 50 days, and volumes were calculated as volume = (length \times width \times depth)/ π . Tumour volume of each mouse in the group at each time point is shown.

A



B

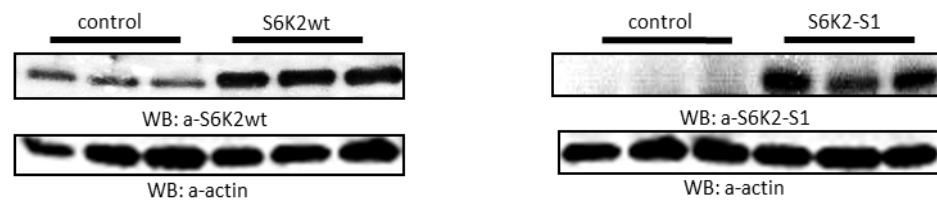


Figure 5.16 Overexpression of S6K2-S1 reduces tumour growth in a xenograft mouse model. (A) Tumours were measured 2 times weekly over a period of 50 days, and volumes were calculated as volume = (length×width×depth)/ π . Mean tumour volumes for each group (n=8/group) of mice at each time point is shown. The line indicates the nonlinear regression using an exponential growth fit. Mean tumour volumes for S6K2-S1 and S6K2wt group (n=8/group) of mice were compared to control group at each time point, starting at day 15, after tumour growth were established (mean \pm SD; *p<0.0005). (B) Expression of S6K2wt and S6K2-S1 in tumour samples were confirmed in Western blotting.

5.3 Discussion

The identification of a direct interaction between S6K2-S1, Raptor and mTOR, described in previous chapter, laid a strong basis for the study of the potential role of the spliced isoform in the regulation of mTORC1 signalling. The N-terminal TOS sequence is fully functional in S6K2-S1 and competes with S6K1, S6K2 and 4EBP1 for binding with Raptor, which is critical for the formation of mTORC1 and downstream signalling. The importance of the TOS motif in mTORC1 downstream targets is now well established (Hara K., 2002; Nojima H., 2003).

To confirm our hypothesis the state of mTORC1 signalling in cells overexpressing S6K2-S1 splicing variant was assessed. Although no significant differences were detected under normal physiological conditions, several interesting results were obtained from the analysis of mTORC1/S6K signalling in HEK293 cells with stable overexpression of S6K2-S1 in response to serum starvation. Firstly, serum starvation results in a greater reduction in S6K activity compared to control, as measured by blotting with phospho-specific antibodies against S6K target sites in S6 protein. Secondly, phosphorylation of 4EBP1 protein by mTORC1 is significantly reduced under starved conditions in HEK293 cells overexpressing S6K2-S1, when compared to control. The same results were reproduced in TSC2^{-/-} p53^{-/-} MEF stable cell lines, indicating that S6K2-S1 splicing isoform has the potential to negatively regulate mTORC1 signalling. Finally, we were surprised to find that HEK293 cells overexpressing S6K2-S1 show dramatic reduction of Akt/PKB phosphorylation in response to serum starvation, when compared to control.

The revealed role of S6K2-S1 in the regulation of mTORC1 signalling is very interesting. Therefore, our efforts were focused on studying the physiological significance of this regulatory event. Based on known functions of S6Ks, we investigated the role of S6K2-S1 in the regulation of cell size, proliferation, survival and migration. Using several cell models, we showed that the overexpression of S6K2-S1 splicing isoform did not show any significant changes in their proliferation rate compared to control. Given the crucial role S6Ks play in the control of cell size, we assessed whether cells expressing splicing isoform differ in their size. In this study, we found that overexpression of S6K2-S1 did not affect the size of HEK293 cells, but the reduction in size was observed in NIH3T3RasC40 cells. To draw a definite conclusion on this issue, we generated TSC2^{-/-} p53^{-/-} MEF cells with stable overexpression of S6K2^{wt} and S6K2-S1 splicing variant. The outcome of the cell size analysis in this cell model revealed that the overexpression of the spliced isoform dramatically decreased the size of TSC2^{-/-} p53^{-/-} MEF cells, whereas full length S6K2 overexpression resulted in the upregulation of the cell size. These findings clearly indicate that full length S6K2 and splicing isoform exhibit opposite effects on signalling pathways which regulate cell size.

Studying the role of splicing isoform in the regulation of cell migration in NIH3T3RasC40 cells, we have shown that S6K2-S1 reduced cell ability to migrate up to forty percents, checked in wound healing assay. Taking these results into account, we can speculate that S6K2-S1 spliced isoform interferes with cell migration signalling coordinated via the mTORC1/S6K pathway. These data were subsequently confirmed by our

collaborators from Imperial College London (Prof. M. Seckl and Dr. O. Pardo).

mTORC1/S6Ks signalling play an important role in the regulation of cell survival. To check whether the splicing isoform may affect cell survival in A549 cells, we treated them with staurosporine and cisplatin. Interestingly, in contrast to full length S6K2, the overexpression of splicing isoform in A549 cells resulted in a higher sensitivity to staurosporine treatment as measured by the level of cleaved PARP. The same results were obtained in TSC2^{-/-} p53^{-/-} MEF cell lines stably expressing S6K2^{wt} and S6K2-S1. Surprisingly, A549 cells overexpressing splicing isoform showed dramatic downregulation of mTORC1/S6K signalling in response to cisplatin treatment, when compared to control cells. These results demonstrate that S6K2-S1 downregulates pro-survival signalling in A549 cells, possibly by interfering with the mTORC1/S6K pathway.

It has been recently demonstrated that a short splicing isoform of S6K1, in contrast to full length protein, possesses an oncogenic potential in human breast epithelial cells (Karni R et al, 2012). Based on this, tumorigenic potential of S6K2 and S6K2-S1 splicing isoform was examined using two different approaches: anchorage-independent colony formation assay and xenograft studies in nude mice. First, in colony formation assay stable expression of full length S6K2 in HEK293 and A549 cells resulted in a significant increase (30%) of the number of colonies, while cells overexpressing S6K2-S1 suppressed anchorage-independent colony growth up to 50%, when compared to parental cells. Second, to confirm our findings tumorigenic potential of S6K2

and splicing isoform was assessed by performing xenograft studies in nude mice using A549 stable cell lines. This study showed that overexpression of the full length S6K2 in A549 cells resulted in the formation of bigger tumours, whereas S6K2-S1 splicing isoform had an opposite effect and suppressed tumour formation in nude mice, compared to control group. These findings are in good agreement with the data obtained in soft agar assay and show for the first time that S6K2wt is a potential oncogene, whereas S6K2-S1 splicing variant acts as a tumor suppressor.

6 General discussion and future studies

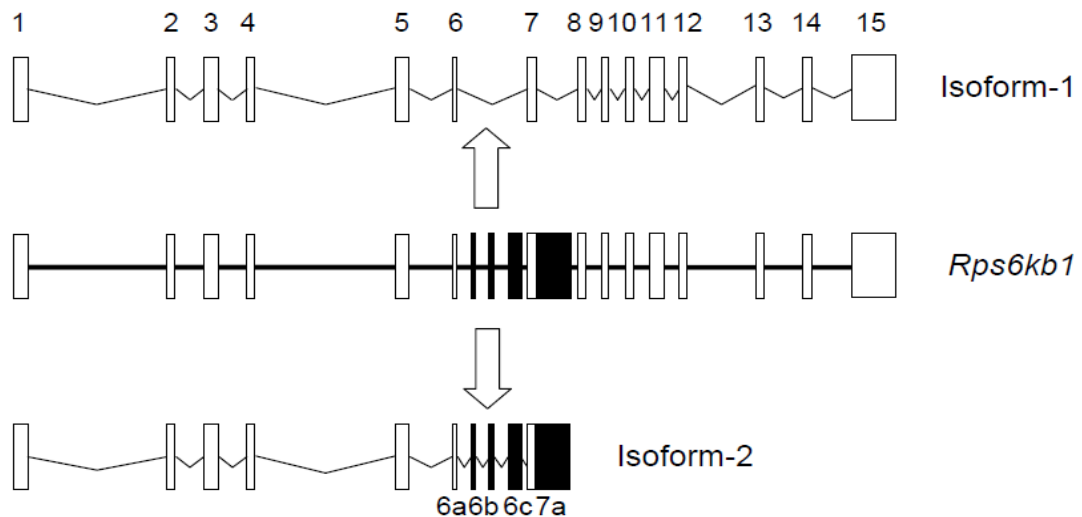
The important role of S6 kinase signalling in health and pathologies, particularly cancer, has been described in detail in chapter one. S6K is an important signalling component of mitogen- and nutrient-stimulated signalling cascades implicated in the regulation of cell growth, biosynthetic processes and energy metabolism (Fenton & Gout 2011;ladevaia et al. 2012;Proud 1996).

A family of 70kDa ribosomal S6 kinases include S6K1 and S6K2 proteins, which are encoded by two different genes. Most of the published research has been done on S6K1, which was discovered more than twenty-five years ago. Ten years later, S6K2 was cloned by several groups (Gout et al. 1998). These two kinases possess highly similar kinase domains; have the same mechanism of activation by common upstream pathways and a number of overlapping substrates.

Much of the information we know about the functions of S6Ks was obtained from genetic studies in mice and flies. *Drosophila* has only one S6K gene and its deletion leads to the death of most flies during early development, whereas survived S6K1^{-/-} flies are smaller than the wild type (Montagne et al. 1999). Studies in mice showed that deletion of S6K1 was not lethal, but the mice were smaller and S6 phosphorylation was not significantly affected (Pende et al. 2000). On the other hand, S6K2^{-/-} mice grew to a normal size, but had a significantly decreased level of S6 phosphorylation (Pende et al. 2004). Therefore, different phenotypes displayed in animal models with the deletion of S6K1 or

S6K2 genes points toward distinct downstream targets and functions. The studies revealing S6K1- or S6K2-specific substrates have started to emerge, which are essential for providing more information on their different cellular functions (Goh et al. 2010;Richardson, Broenstrup, Fingar, Julich, Ballif, Gygi, & Blenis 2004;Sridharan & Basu 2011).

Recent identification of a novel S6K1 splice variant, named S6K1-isoform 2, makes the situation more complex and provides a new insight into the S6K1 genetic studies. As seen from Figure 6.1, S6K1-isoform 2 is generated by the inclusion of three additional exons (a-b-c) located between exon 6 and 7. These exon inclusions generate an early stop codon in exon 6c in mice and in exons 6a or 6c in humans. Generated transcripts contain half of the original S6K1 coding sequence and a significant part of the kinase domain (Karni, Hippo, Lowe, & Krainer 2008).

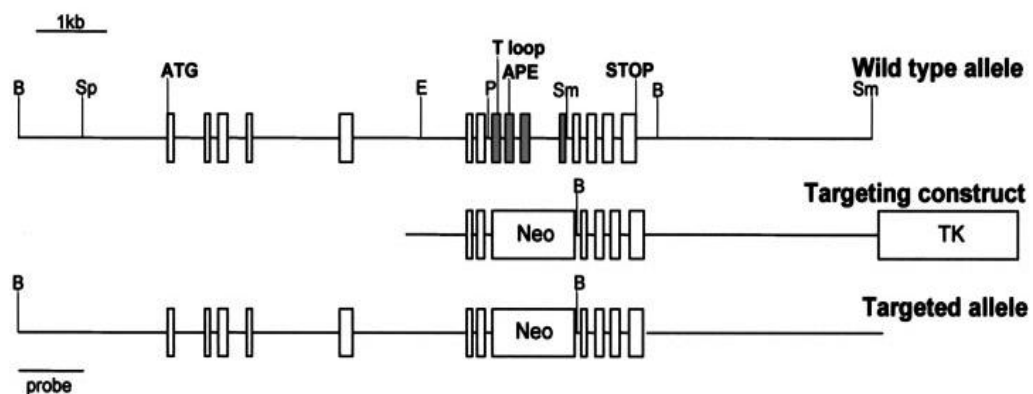


Karni et al. 2008. *Proc Natl Acad Sci U.S.A.*

Figure 6.1 Mechanism of alternative splicing of S6K1 gene. Rectangles represent the coding exons of the S6K1 gene. Black rectangles show the inclusion of three additional exons (a-b-c) located between exon 6 and 7 into coding sequence. These exon inclusions generate an early stop codon in exon 6c in mouse and in exons 6a or 6c in humans.

Interestingly, in animal model S6K1 gene disruption was created by homologous recombination and a targeting construct was produced by replacing 1.2 kb of the genomic sequence in exons 8-10 with a neomycin resistance cassette (Pende et al. 2004; Shima et al. 1998; Um et al. 2004). Thus, half of the gene up to exon 8 is transcribed producing shorter splicing isoform. Taking into account that this splice variant possesses an oncogenic potential, whereas the full length S6K1 does not, it is difficult to assess whether the observed phenotype of S6K1^{-/-} mice is not affected by the expression of S6K1-isoform 2.

As described in chapter 3 of this thesis, three new splicing isoforms of S6K2 were identified in our laboratory. Detailed bioinformatics analysis of isolated cDNA clones and EST sequences from various databases indicates that the S6K2-S1 and S6K2-S2 splicing variants are generated by alternative splicing of exon 9. Analysis of cDNA nucleotide sequence corresponding to S6K2-S3 shows that it is generated by aberrant splicing of intron 5, resulting in the inclusion of a cryptic exon in the transcript. Similarly to the S6K1 strategy, S6K2 gene disruption in S6K2^{-/-} mice was created by replacing genomic sequence corresponding to exons 8-10 with a neomycin resistance cassette (Figure 6.2).



Pende M. et al., 2004. *Mol. Cell Biol.*

Figure 6.2 Generation of an S6K2^{-/-} allele. Murine S6K2 gene map and targeting vector. Rectangles represent the coding exons of the S6K2 gene. The exons containing the T loop and APE sequences and the start and stop codons are indicated. The four exons deleted following the homologous recombination event are shown in grey. Restriction sites: B, BamHI; Sp, SpeI; E, EcoRI; P, PstI; Sm, SmaI.

In this case, S6K2-S1 and S6K2-S2 splicing variants will not be present as they contain exon 8 in their coding sequence. On the other hand, S6K2-S3 will be expressed in S6K2^{-/-} model, as the stop codon is localised in exon 6 of the coding sequence. Taking into account the abundance of this isoform in the EST database, it may play an important role in cellular functions and can dramatically affect the phenotype of S6K2^{-/-} knockout mice generated by M. Pende et al.

With the knock in mice model, all S6K2 splicing variants would be expressed and form specific cellular complexes. In this model S6K2 full-length would lack its kinase activity and the phenotype of S6K2 knock in mice would not be dramatically affected by the other splicing isoforms. More studies have to be performed to address this question.

Both S6K1 and S6K2 were found to contain at their N-termini TOS motifs, responsible for the direct interaction with Raptor, which presents them for the phosphorylation by mTOR (Nojima et al. 2003;Schalm et al. 2003b). As discussed in chapter 3, all three S6K2 splicing variants are identical to the full length S6K2 at their N-termini. Additionally, S6K2-S1 and S6K2-S2 proteins have a unique 38 amino acids extension at their C-termini, which was used for generation of specific polyclonal antibodies. Affinity purified anti-S6K2-S1 antibodies specifically recognized overexpressed protein, as well as an additional immunoreactive band of slightly lower molecular weight, which might represent endogenous splicing variant in HEK293 cells. Unfortunately, generated affinity purified polyclonal antibodies exhibited high non-specific immunoreactivity in Western blotting, which significantly restricted their application. Generation of specific monoclonal

antibodies against splicing S6K2-S1 variant would give us the opportunity to study the functions of splicing isoform using immunoprecipitation and immunohistochemistry.

Significantly, the results presented in chapter 3 suggest a direct physical interaction between S6K2-S1, Raptor and mTOR. Using different experimental approaches, we showed that S6K2-S1 splicing isoform and the full length S6K2 have the ability to interact with Raptor via their N-terminal TOS sequence. This finding provides a valuable clue as to the potential function of S6K2-S1, suggesting that under physiological conditions it may compete not only with S6K2, but also with S6K1 and 4EBP1 for the binding to Raptor. It is now well known that these mTORC1 downstream targets are characterised by the presence of the TOS motif in their sequences (Hara et al. 2002; Nojima et al. 2003). Importantly, as S6K2-S1 does not possess the mTOR site for phosphorylation and lacks half of the kinase domain, it may act as a dominant negative regulator of mTORC1 signalling.

The identification of a direct interaction between S6K2-S1, Raptor and mTOR, laid a strong basis for us to study the potential role of this isoform in the regulation of mTORC1 signalling described in detail in chapter 5.

The mTOR/S6K signalling pathway has been implicated as a main regulator of cell growth and cell size. Genetic studies clearly show that S6K1^{-/-} deficient animals have smaller cell size when compared to the wild type (Montagne et al. 1999). In a view of these findings, the role of S6K2-S1 splicing isoform in the regulation of cell size was investigated. Using TSC2^{-/-} p53^{-/-} MEF cells, we were able to show that

overexpression of the S6K2-S1 splicing isoform results in the decrease of cell size, when compared to control or cells with overexpressed S6K2wt.

With the use of phospho-specific antibodies, we showed that S6K2-S1 did not affect the mTOR/S6K signalling pathway in cells cultured under normal physiological conditions. Interestingly, serum deprivation resulted in a significant reduction in the phosphorylation of rpS6 and 4EBP1 proteins in cell lines overexpressing S6K2-S1 when compared to control. These findings suggest that S6K2-S1 splicing isoform may be a negative regulator of mTORC1 signalling in serum-starved cells. Surprisingly, in starved condition the phosphorylation state of Akt/PKB at Ser473 was also significantly reduced compared to control. It is interesting to note that both S6K1 and S6K2 were shown to play an important role in a feedback loop, implicated in the inactivation of the PI3K/PKB/Akt signalling via IRS1 (Harrington et al. 2004). But on the other hand, it was shown that in MCF-7 cells, S6K1 and S6K2 played an opposite role in Akt/PKB activation and cell survival (Sridharan & Basu 2011). Taking this into account it is difficult to speculate about the role of S6K2-S1 splicing isoform in the Akt/PKB signalling and more work should be done to address this issue.

Another interesting question to answer in future studies would be whether Rapamycin treatment has the same effect on S6K2-S1 expressing cells as serum starvation. It is known that both experimental conditions affect mTORC1 assembly and downregulate its signalling. In our study, we did not investigate the physiological relevance of the inhibition of 4EBP1 phosphorylation by mTORC1 in S6K2-S1 expressing

cells during starvation. Based on known functions of 4EBP1 protein, we can assume that it may affect cap-dependent translation. More experiments have to be conducted to prove our suggestions.

Although the S6K2-S1 splicing isoform does not affect cell proliferation under normal cell culturing conditions, it would be interesting to examine its role in regulating cell proliferative signalling in serum-starved cells.

One of the important cellular processes controlled via the mTOR/S6K pathway is cytoskeletal reorganisation, which coordinates cell migration, invasion and cell adhesion. These cellular processes play a significant role in malignant transformation, invasion and metastasis. The importance of S6K1 in the regulation of cell migration was demonstrated in different cellular models, including Swiss 3T3 fibroblasts, chicken embryo fibroblast (CEF) and in ovarian cancer cells (Berven & Crouch 2000; Ip, Cheung, Ngan, & Wong 2011; Qian, Corum, Meng, Blenis, Zheng, Shi, Flynn, & Jiang 2004). Studying the role of the S6K2 spliced isoform in the regulation of cell migration we were able to show that its overexpression decreased the ability of NIH3T3RasC40 cells to migrate up to forty percent. These data were confirmed by our collaborators from Imperial College London (Prof. M. Seckl and Dr. O. Pardo). As discussed in the Introduction chapter, S6K1 can stimulate actin cytoskeleton reorganization and cell migration by activating Rac1, Cdc42 and p21-activated kinase (PAK1). Rac1, Cdc42 are members of the Rho GTPases family of proteins, which play a central role in cell motility and cell adhesion (Ip, Cheung, Ngan, & Wong 2011; Khotskaya et al. 2014; Yang, Wang, & Zheng 2006). Another question to answer in

future experiments would be whether S6K2-S1 is implicated in the regulation and/or downstream signalling from Rho GTPases. It is important to understand that cell adhesion is a complex process that involves many different molecular interactions and changes in the intracellular signalling pathways. Cell-ECM and cell-cell interactions are important for cell migration and adhesion, mediated by specific molecules, such as cadherins and integrins. It has been shown that S6K1 can modulate the expression level of E-cadherin, N-cadherin and vimentin (Pon et al. 2008). Therefore, it would of interest to investigate whether S6K2-S1 splicing isoform can modulate the level and function of these cell adhesion molecules.

The mTOR/S6K signalling pathway, especially via S6K2, has been shown to play an important role in cell survival in lung and breast cancer (Pardo et al. 2011). To check how S6K2-S1 splicing isoform may affect cell survival, we treated A549 cells overexpressing full length S6K2 and splicing variant with cytotoxic drugs. We were able to show that A549 cells overexpressing S6K2-S1 splicing isoform showed higher sensitivity to staurosporine, in contrast to control or cells with overexpressed wtS6K2. These results were confirmed in TSC2^{-/-} p53^{-/-} MEF cell lines with stable overexpression of S6K2wt and S6K2-S1. Surprisingly, cisplatin treatment of A549 cells overexpressing splicing isoform resulted in a dramatic downregulation of mTOR/S6K signalling, when compared to control cells. These results demonstrate that S6K2-S1 activated pro-apoptotic signalling in A549 cells, possibly by interfering with mTOR/S6K signalling.

There is growing evidence that S6Ks can contribute to the development, growth and spreading of tumours. S6K1 gene amplification has been reported in almost 10 percent of breast carcinomas which correlated with poor prognosis (Couch et al. 1999;van der Hage et al. 2004). Additionally, a recent publication shows that S6K1 increases the invasiveness of breast cancer and specific pharmacological inhibition of S6K1 activity could be used for the prevention of cancer metastasis and improving poor prognosis (Khotskaya et al. 2014). Clinical potential of S6K1 and S6K2 inhibition in breast cancer has been reviewed recently (Perez-Tenorio et al. 2011). It has been also demonstrated that the short isoform of S6K1, in contrast to full length protein, possesses an oncogenic potential in human breast epithelial cells (Karni, Hippo, Lowe, & Krainer 2008). So far, very little is known about the potential oncogenic role of S6K2. The overexpression of S6K2 has been reported in small cell lung cancer cell lines and breast tumors (Pardo et al. 2001;Savinska et al. 2004). To our knowledge, there are no published studies describing oncogenic properties of S6K2. In the frame of this project, we examined oncogenic potential of S6K2 and S6K2-S1 splicing isoform using two different approaches: anchorage-independent colony formation assay and xenograft studies in nude mice. Firstly, expression of full length S6K2 in HEK293 and A549 cells resulted in significant increase in the formation of colonies in soft agar, while S6K2-S1 suppressed anchorage-independent colony growth up to 50 percent in both cell lines. Secondly, in line with previous results, we demonstrated that full length S6K2 promoted tumour formation in nude mice, whereas S6K2-S1 splicing isoform had an opposite effect and inhibited tumour growth.

Another important question to answer in future experiments would be to check the expression level of different splicing isoforms in normal and cancer tissues. Tissue microarray assay with specifically designed primers can be used to show the relative expression of all S6K2 splicing variants in different tissue samples.

In conclusion, this study describes for the first time the existence of 3 novel S6K2 splicing isoforms and reveals the functional role of S6K2-S1 as a negative regulator of mTOR/S6K signalling. Firstly, both full-length S6K2 and S6K2-S1 we found to bind directly to Raptor and to be an integral part of mTORC1. Secondly, S6K2-S1 splicing isoform downregulated mTOR/S6K signalling in serum-starved HEK293 cells and suppressed pro-survival signalling in A549 cells in response to cytotoxic drugs. Importantly, the overexpression of S6K2-S1 splicing variant in MEF TSC2^{-/-} p53^{-/-} cells resulted in smaller cell size, in contrast to S6K2wt. Additionally, S6K2-S1 was able to affect cell migration of NIH3T3RasC40 cells. Finally, we showed for the first time that full length S6K2 can function as a potential oncogene, whereas S6K2-S1 splicing variant exhibits tumour suppressor properties.

7 Appendix A

| | | |
|----------|---|------|
| S6K2gene | GGAGAGATGATGTTTAGGTCCGGGACTGTCAGTCAGTGC GCGGCCAGGTACGGGCCGACG | 60 |
| S6K2mRNA | GGAGAGATGATGTTTAGGTCCGGGACTGTCAGTCAGTGC GCGGCCAGGTACGGGCCGACG | 60 |
| ***** | | |
| S6K2gene | GGCCCGCGGGCCGCGCCGCCATGCGCGCCGTGTTTGATTTGGATTTGGAGACGGAGGA | 120 |
| S6K2mRNA | GGCCCGCGGGCCGCGCCGCCATGCGCGCCGTGTTTGATTTGGATTTGGAGACGGAGGA | 120 |
| ***** | | |
| S6K2gene | AGGCAGCGAGGGCGAGGGCGAGCCAGAGCTCAGCCCCGCGT GAGTGCCTTCCTGGCG | 180 |
| S6K2mRNA | AGGCAGCGAGGGCGAGGGCGAGCCAGAGCTCAGCCCCGCG----- | 160 |
| ***** | | |
| <hr/> | | |
| S6K2gene | GGCACCTTCCTTGCTCTTACCCCTCGGTTTCTCACAGGACGCATGTCCCTTGCCGAGT | 540 |
| S6K2mRNA | -----GACGCATGTCCCTTGCCGAGT | 182 |
| ***** | | |
| S6K2gene | TGAGGGCAGCTGGCCTAGAGTGAGTGAGGGTCGTGTTGGGGAGGGGGAATGGAGTGGG | 600 |
| S6K2mRNA | TGAGGGCAGCTGGCCTAGA----- | 202 |
| ***** | | |
| S6K2gene | GAAGGGAACTGGGGAGCACTGGAGCCTTGTCTCATTAACCTCTTGTGTCCGTAGCCCT | 660 |
| S6K2mRNA | -----GCCT | 205 |
| *** | | |
| S6K2gene | GTGGGACACTATGAAGAGGTGGAGCTGACTGAGACCAGCGTGAACGTTGGCCAGAGCGC | 720 |
| S6K2mRNA | GTGGGACACTATGAAGAGGTGGAGCTGACTGAGACCAGCGTGAACGTTGGCCAGAGCGC | 265 |
| ***** | | |
| S6K2gene | ATCGGGCCCCACTGCTTTGAGCTGCTGCGTGTGCTGGGCAAGGGGGGCTATGGCAAGGTA | 780 |
| S6K2mRNA | ATCGGGCCCCACTGCTTTGAGCTGCTGCGTGTGCTGGGCAAGGGGGGCTATGGCAAG--- | 322 |
| ***** | | |
| S6K2gene | GGGGCGGGCGCACCCCTCCTCCTGGCCTCACAGCCTCCATCTGGAGGCAGCAAAGGGTTCT | 840 |
| S6K2mRNA | ----- | |
| <hr/> | | |
| S6K2gene | GGATGTGGAGAGGGAAGTTGATCCTGTCTCCCCTGCCCTACAGGTGTTCCAGGTGCGAAA | 1080 |
| S6K2mRNA | -----GTGTTCCAGGTGCGAAA | 339 |
| ***** | | |
| S6K2gene | GGTGCAAGGCACCAACTTGGGCAAAATATATGCCATGAAAGTCCTAAGGAAGTGAGTCA | 1140 |
| S6K2mRNA | GGTGCAAGGCACCAACTTGGGCAAAATATATGCCATGAAAGTCCTAAGGAAG----- | 391 |
| ***** | | |
| S6K2gene | CTCGTTCAGCCAACGAATACTGTGTGGCTGCCATTCCCAACATGCTGTACCAGGCTTTGG | 1200 |
| S6K2mRNA | ----- | |
| <hr/> | | |
| S6K2gene | TCTAACCAATTCCTGTATCTCCAGGCCAAAATTGTGCGCAATGCCAAGGACACAGCACAC | 2940 |
| S6K2mRNA | -----GCCAAAATTGTGCGCAATGCCAAGGACACAGCACAC | 427 |
| ***** | | |
| S6K2gene | ACACGGGCTGAGCGGAACATTCTAGAGTCAGTGAAGCACCCCTTTATTGTGGAAGTGGCC | 3000 |
| S6K2mRNA | ACACGGGCTGAGCGGAACATTCTAGAGTCAGTGAAGCACCCCTTTATTGTGGAAGTGGCC | 487 |
| ***** | | |
| S6K2gene | TATGCCTTCCAGACTGGTGGCAAACCTCTACCTCATCCTTGAGTGCCTCAGTGTATGAGT | 3060 |
| S6K2mRNA | TATGCCTTCCAGACTGGTGGCAAACCTCTACCTCATCCTTGAGTGCCTCAGTGTATGAGT | 539 |
| ***** | | |
| S6K2gene | GCGGGCCAGGCAGGGGTGCTGGGGTTCGCGGGGGGCGAGCGAGCCAGCAAAGGAAGCTC | 3120 |

S6K2mRNA -----

S6K2gene ATCTCAGCATCCCCTTAAAGTCCCAGCAAACCGCGCTTCTCTGTTCTGTTCTGTTGGGA 3780
S6K2mRNA -----

S6K2gene TTCACTCTGTCTCCCTGTCTTCTCTGCGAGATCTTTTGGGCTAAGCTCTTGAGCTGTG 3840
S6K2mRNA -----

S6K2gene GCCTGGGCTGGCGTATTAGAGCCGTTGTGTACATGTCTGTCTCCCACTAGACTGAGCG 3900
S6K2mRNA -----

S6K2gene TCCTGAGGGCAGTGGCTGGGTCTTTCATCCTGTCCCCAGCTTACCCAGCACAGGGCCA 3960
S6K2mRNA -----

S6K2gene GGCACCGAGTAGCGTCGGTAGATGTTTGTGTAATTGAATTGAATCCCCACGGCAGCTCT 4020
S6K2mRNA -----

S6K2gene GTGAGGCAGGTAGGGCGGAATTATGAGCCCTCTTCCCAAGAAGAAATAAAGACTCA 4080
S6K2mRNA -----

S6K2gene GAAAGCACAAGGGGCTTGGACCCAGCACGTGGCTGCTGACGTGTTTGTGTGGCAGGTGG 4140
S6K2mRNA -----GTGG 543

S6K2gene CGAGCTCTTCACGCATCTGGAGCGAGAGGGCATCTTCCCTGGAAGATACGGCCTGTGGGT 4200
S6K2mRNA CGAGCTCTTCACGCATCTGGAGCGAGAGGGCATCTTCCCTGGAAGATACGGCCTG----- 597

S6K2gene GTTAATCCTCCGCTTTCCTGAGGCTGCCAGGTCCTCTACTCCCGCCTTCACCCTGT 4260
S6K2mRNA -----

S6K2gene CTTGTTTCTGCACTTCTACCTGGCTGAGATCACGCTGGCCCTGGGCCATCTCCACTCCC 4320
S6K2mRNA -----CTTCTACCTGGCTGAGATCACGCTGGCCCTGGGCCATCTCCACTCCC 644

S6K2gene AGGGCATCATCTACCGGACCTCAAGCCCGAGAACATCATGCTCAGCAGCCAGGTGCGC 4380
S6K2mRNA AGGGCATCATCTACCGGACCTCAAGCCCGAGAACATCATGCTCAGCAGCCAGG----- 698

S6K2gene ATGTGTGTGCGGGCAGCTGCAGGCGGGTCTGCAATCTGTGGGAGGGCTGAGGACCTCT 4440
S6K2mRNA -----

S6K2gene GTGGGTGGGGTGGGGCCCTGGTCACGCCTCTCCAACACCCTTCCTCAGGCCACATCAAAC 4500
S6K2mRNA -----GCCACATCAAAC 710

S6K2gene TGACCGACTTTGGACTCTGCAAGGAGTCTATCCATGAGGGCGCCGTCCTCACACCTTCT 4560
S6K2mRNA TGACCGACTTTGGACTCTGCAAGGAGTCTATCCATGAGGGCGCCGTCCTCACACCTTCT 770

S6K2gene GCGGCACCATTGAGTACATGTAAGTGGACCTGGCTGGCCAGGGGTCGGGAGGACAGCC 4620
S6K2mRNA GCGGCACCATTGAGTACAT----- 790

S6K2gene CGAAGGGGCACGGCCTGACTGACAGTTCACCTGGACCCAGGGCCCTGAGATTCTGGT 4680
S6K2mRNA -----GGCCCTGAGATTCTGGT 807

S6K2gene GCGCAGTGGCCACAACCGGGCTGTGGACTGGTGGAGCCTGGGGGCCCTGATGACGACAT 4740
S6K2mRNA GCGCAGTGGCCACAACCGGGCTGTGGACTGGTGGAGCCTGGGGGCCCTGATGACGACAT 867

S6K2gene GCTCACTGGATCGCAAGTCCAGCCCCGGGAGGAGGGGCAGGGCAGAGGTGGGA 4800
S6K2mRNA GCTCACTGGATCG----- 880

S6K2gene GTAGCCCCCTCCTGGGGCAAGGGCAGGGCCTGGTGGGAGGCCACAAGGCTCCTCTCAC 4860
S6K2mRNA -----

S6K2gene CTTCCTCCTCCTCCAGCCGCCCTTCACCGCAGAGAACCGGAAGAAAACCATGGATAAGAT 4920
S6K2mRNA -----CCGCCCTTCACCGCAGAGAACCGGAAGAAAACCATGGATAAGAT 924

S6K2gene CATCAGGGGCAAGCTGGCACTGCCCCCTACCTCACCCAGATGCCCGGGACCTTGTCAA 4980
S6K2mRNA CATCAGGGGCAAGCTGGCACTGCCCCCTACCTCACCCAGATGCCCGGGACCTTGTCAA 984

S6K2gene AAAGGTGCAGCTCCCTTCTCTCTCTCCGGGGCCTGCCAGCCATTCTGCACGTGTTCT 5040
S6K2mRNA AAAG----- 988

S6K2gene GAGTCTCTCTGGGCTGTGGGGAAGCCAGGGCCACCCCGCCTGTGCAGTTTGCCTCTGGG 5100
S6K2mRNA -----

S6K2gene GCTAGCCCTGGGACCCGGGGACACATGAGCAGTACTTGCCAGGCCCTCACCTCTCTCC 5520
S6K2mRNA -----

S6K2gene TGGTCCCGCAGTTTCTGAACCGAATCCAGCCAGCGGATTGGGGGTGGCCAGGGGATG 5580
S6K2mRNA -----TTTCTGAACCGAATCCAGCCAGCGGATTGGGGGTGGCCAGGGGATG 1037

S6K2gene CTGCTGATGTGCAGGTGGGTTTGGGACCACCACAGGGGTAGGGCTGAGTCTCCAAGGGT 5640
S6K2mRNA CTGCTGATGTGCAG----- 1051

S6K2gene GCCGGAAATGGGGCAGGGCCCCAGGGCAGAGGGAGTGACCGGGGGCAAGCAGGGTGAG 5700
S6K2mRNA -----

S6K2gene CTGTTAGTGGGTTTGGTGCATTCTCTACCTACAGACATCCCTTTTCCGGCACATGAA 5760
S6K2mRNA -----AGACATCCCTTTTCCGGCACATGAA 1077

S6K2gene TTGGGACGACCTTCTGGCCTGGCGTGTGGACCCCCCTTTCAGGCCCTGTCTGTGAGCAG 5820
S6K2mRNA TTGGGACGACCTTCTGGCCTGGCGTGTGGACCCCCCTTTCAGGCCCTGTCTG----- 1129

S6K2gene CAGGGCTGGTGGCCAGTGGCCGGTGGCGGGTGGCAAGTGGAGAACCTGCATCTTGGTGCC 5880
S6K2mRNA -----

S6K2gene CTCTGACCCCTCCCCACTCTGGTCGGCCACAGCAGTCAGAGGAGGACGTGAGCCAGTTT 5940
S6K2mRNA -----CAGTCAGAGGAGGACGTGAGCCAGTTT 1156

S6K2gene GATACCCGCTTCACACGGCAGACGCCGGTGGACAGTCCGTGATGACACAGCCCTCAGCGAG 6000
S6K2mRNA GATACCCGCTTCACACGGCAGACGCCGGTGGACAGTCCGTGATGACACAGCCCTCAGCGAG 1216

S6K2gene AGTGCCAACCAGGCCTTCTGTGAGTGCGGGGCCTGAGGCCTGTGGGACCAGGGCAGC 6060
S6K2mRNA AGTGCCAACCAGGCCTTCTGT----- 1237

S6K2gene GATCGTGACTAAGGATGGCAGGCACTGAGTGTGCGCATGGCCCTGCCTCCGCCCCCAAGG 6120
S6K2mRNA -----GG 1239
**

S6K2gene CTCACATACGTGGCGCCGTCTGTCTGGACAGCATCAAGGAGGGCTTCTCCTTCCAGCC 6180
S6K2mRNA CTCACATACGTGGCGCCGTCTGTCTGGACAGCATCAAGGAGGGCTTCTCCTTCCAGCC 1299

S6K2gene CAAGCTGCGCTCACCCAGGCGCCTCAACAGTAGCCCCGGGCCCCCGTCAGTACTGAGG 6240
S6K2mRNA CAAGCTGCGCTCACCCAGGCGCCTCAACAGTAGCCCCGGGCCCCCGTCAG----- 1350

```

S6K2gene      GACGTGGGGGTGTGTGGCTGGGTTAGGGACGCTGGCAGGCAGGATGCCAGCTCCAGCCTT 6300
S6K2mRNA      -----

S6K2gene      GCCTGTGTGCCTGGGAGGTGGGAAAGGCTGCCTTCCCTGACTGAGTGCTGGGAGCCTCT 6480
S6K2mRNA      -----

S6K2gene      GGAGGGCTAGGAGGCTCTTATTCTGCCTTGGTTCCCTGCAGCCCCCTCAAGTTCTC 6540
S6K2mRNA      -----CCCCCTCAAGTTCTC 1365
                *****

S6K2gene      CCCTTTTGAGGGGTTTCGGCCCAGCCCAGCCTGCCGGAGCCCACGGAGCTACCTCTACC 6600
S6K2mRNA      CCCTTTTGAGGGGTTTCGGCCCAGCCCAGCCTGCCGGAGCCCACGGAGCTACCTCTACC 1425
                *****

S6K2gene      TCCACTCCTGCCACCGCCGCGCCTCGACCACCGCCCCTCTCCCATCCGTCCCCCTC 6660
S6K2mRNA      TCCACTCCTGCCACCGCCGCGCCTCGACCACCGCCCCTCTCCCATCCGTCCCCCTC 1485
                *****

S6K2gene      AGGGACCAAGAAGTCCAAGAGGGCCGTGGGCGTCCAGGGCGCTAGGAAGCCGGTG 6720
S6K2mRNA      AGGGACCAAGAAGTCCAAGAGGGCCGTGGGCGTCCAGGGCGCTAGGAAGCCGGTG 1545
                *****

S6K2gene      GTGAGGGTAGCCCTTGAGCCCTGTCCCTGCGGCTGTGAGAGCAGCAGGACCCTGGGCCAG 6780
S6K2mRNA      GTGAGGGTAGCCCTTGAGCCCTGTCCCTGCGGCTGTGAGAGCAGCAGGACCCTGGGCCAG 1605
                *****

S6K2gene      TTCCAGAGACCTGGGGGTGTGTCTGGGGGTGGGGTGTGAGTGCGTATGAAAGTGTGTGC 6840
S6K2mRNA      TTCCAGAGACCTGGGGGTGTGTCTGGGGGTGGGGTGTGAGTGCGTATGAAAGTGTGTGC 1665
                *****

S6K2gene      TGGTGGGGCAGCTGTGCCCTGAATCATGGGCACGGAGGGCCGCCCGCCACGCCCCGCGC 6900
S6K2mRNA      TGGTGGGGCAGCTGTGCCCTGAATCATGGGCACGGAGGGCCGCCCGCCACGCCCCGCGC 1725
                *****

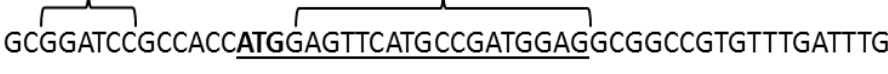
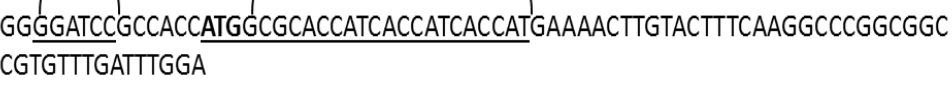
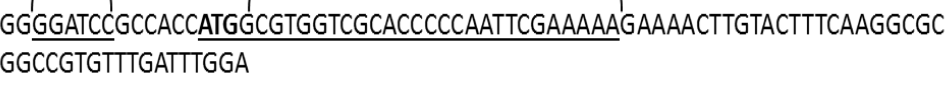
S6K2gene      TCAACTGCTCCCCTGGAAGATTAAGGGCTGAATCATGGTGCTGA----- 6945
S6K2mRNA      TCAACTGCTCCCCTGGAAGATTAAGGGCTGAATCATGGTGCTGAAAAAAAAAAAAA 1782
                *****

```

Appendix A. ClastalW alignment of S6K2 gene and mRNA coding sequence. Human S6K2 gene is located on chromosome 11 q13.2, (chr11:67,195,935-67,202,878). **NN** – classic intron ends, **NN** – non-classic intron ends, **NNN** – standard start/stop codon, **NNN** – alternative stop codon, **NNNNN** – exon skipped during alternative splicing in S6K2-S1, **NN** – alternative intron ends in S6K2-S2 isoform, **NNNNN** – “pseudoexon”, fragment of the intron 4 spliced into mRNA between exon 4 and exon 5 in splicing isoform S6K2-S3, **NN** – classic intron ends used in “pseudoexon” splicing of S6K2-S3 isoform, **NNNNN** – represents polyadenylation signal.

8 Appendix B

List of primers designed for molecular cloning in this study

| |
|---|
| Forward: S6K2 |
| <p style="text-align: center;">BamHI</p> <p style="text-align: center;">  </p> |
| Forward: S6K2 N-terminal EE-tag |
| <p style="text-align: center;">BamHI</p> <p style="text-align: center;">EE-tag</p> <p style="text-align: center;">  </p> |
| Forward: S6K2 N-terminal FLAG-tag |
| <p style="text-align: center;">BamHI</p> <p style="text-align: center;">FLAG-tag</p> <p style="text-align: center;">  </p> |
| Forward: S6K2 N-terminal HIS-tag |
| <p style="text-align: center;">BamHI</p> <p style="text-align: center;">HIS-tag</p> <p style="text-align: center;">  </p> |
| Forward: S6K2 N-terminal Strep-tag |
| <p style="text-align: center;">BamHI</p> <p style="text-align: center;">Strep-tag</p> <p style="text-align: center;">  </p> |
| Reverse: S6K2 |

| |
|---|
| <p>NotI</p> <p>CGTGGGCGTCCAGGGCGCTAGAAAGCTT<u>GCGGCCGC</u>CATGT</p> |
| Reverse: S6K2-S1 C-terminal FLAG-tag |
| <p>FLAG-tag</p> <p>NotI</p> <p>GGGACCTTGTCAAAAAGTTTC<u>GACTACAAGGACGACGATGACAAGTAGCGGCCGCTG</u></p> |
| Forward: Raptor N-terminal EE-tag |
| <p>BamHI</p> <p>EE-tag</p> <p>GCGGATCCGCCACCATG<u>GGAATTCATGCCGATGGAGTCCGAAATGCTGCAATC</u></p> |
| Reverse: Raptor |
| <p>EcoRI</p> <p>GGAGAAGCGTGTTCAGATG<u>GAATTC</u>AG</p> |
| Forward: Rictor, N-terminal EE-tag |
| <p>XhoI</p> <p>EE-tag</p> <p>GCACTCGAGGCCACCATG<u>GGAATTCATGCCGATGGAGGCGGCCGATCGGTCGTG</u></p> |
| Reverse: Rictor |
| <p>KpnI</p> <p>GATACATCTGCTGAATCCTGAG<u>GGTACCGG</u></p> |
| RT-PCR primers: |
| Forward: |
| TCAAAGTACCGACTTTGGA |
| Reverse: |
| AAGGTCGTCCTCAATTCATGT |

9 Reference list

Almeida, S., Zhang, Z., Coppola, G., Mao, W., Futai, K., Karydas, A., Geschwind, M.D., Tartaglia, M.C., Gao, F., Gianni, D., Sena-Esteves, M., Geschwind, D.H., Miller, B.L., Farese, R.V., Jr., & Gao, F.B. 2012. Induced pluripotent stem cell models of progranulin-deficient frontotemporal dementia uncover specific reversible neuronal defects. *Cell Rep.*, 2, (4) 789-798 available from: PM:23063362

Antion, M.D., Hou, L., Wong, H., Hoeffler, C.A., & Klann, E. 2008a. mGluR-dependent long-term depression is associated with increased phosphorylation of S6 and synthesis of elongation factor 1A but remains expressed in S6K-deficient mice. *Mol.Cell Biol.*, 28, (9) 2996-3007 available from: PM:18316404

Antion, M.D., Merhav, M., Hoeffler, C.A., Reis, G., Kozma, S.C., Thomas, G., Schuman, E.M., Rosenblum, K., & Klann, E. 2008b. Removal of S6K1 and S6K2 leads to divergent alterations in learning, memory, and synaptic plasticity. *Learn.Mem.*, 15, (1) 29-38 available from: PM:18174371

Barlund, M., Monni, O., Kononen, J., Cornelison, R., Torhorst, J., Sauter, G., Kallioniemi, O.L.L.I., & Kallioniemi, A. 2000. Multiple genes at 17q23 undergo amplification and overexpression in breast cancer. *Cancer Res.*, 60, (19) 5340-5344 available from: PM:11034067

Barlund, M., Tirkkonen, M., Forozan, F., Tanner, M.M., Kallioniemi, O., & Kallioniemi, A. 1997. Increased copy number at 17q22-q24 by CGH in breast cancer is due to high-level amplification of two separate regions. *Genes Chromosomes.Cancer*, 20, (4) 372-376 available from: PM:9408753

Ben-Hur, V., Denichenko, P., Siegfried, Z., Maimon, A., Krainer, A., Davidson, B., & Karni, R. 2013. S6K1 alternative splicing modulates its oncogenic activity and regulates mTORC1. *Cell Rep.*, 3, (1) 103-115 available from: PM:23273915

Berven, L.A. & Crouch, M.F. 2000. Cellular function of p70S6K: a role in regulating cell motility. *Immunol.Cell Biol.*, 78, (4) 447-451 available from: PM:10947872

Burnett, P.E., Blackshaw, S., Lai, M.M., Qureshi, I.A., Burnett, A.F., Sabatini, D.M., & Snyder, S.H. 1998. Neurabin is a synaptic protein linking p70 S6 kinase and the neuronal cytoskeleton. *Proc.Natl.Acad.Sci.U.S.A*, 95, (14) 8351-8356 available from: PM:9653190

Carnevali, L.S., Masuda, K., Frigerio, F., Le, B.O., Um, S.H., Gandin, V., Topisirovic, I., Sonenberg, N., Thomas, G., & Kozma, S.C. 2010. S6K1 plays a critical role in early adipocyte differentiation. *Dev.Cell*, 18, (5) 763-774 available from: PM:20493810

Castaneda, T.R., Abplanalp, W., Um, S.H., Pfluger, P.T., Schrott, B., Brown, K., Grant, E., Carnevali, L., Benoit, S.C., Morgan, D.A., Gilham, D., Hui, D.Y., Rahmouni, K., Thomas, G., Kozma, S.C., Clegg, D.J., &

Tschop, M.H. 2012. Metabolic control by s6 kinases depends on dietary lipids. *PLoS.One.*, 7, (3) e32631 available from: PM:22412899

Chauvin, C., Koka, V., Nouschi, A., Mieulet, V., Hoareau-Aveilla, C., Dreazen, A., Cagnard, N., Carpentier, W., Kiss, T., Meyuhas, O., & Pende, M. 2014. Ribosomal protein S6 kinase activity controls the ribosome biogenesis transcriptional program. *Oncogene*, 33, (4) 474-483 available from: PM:23318442

Chou, M.M. & Blenis, J. 1996. The 70 kDa S6 kinase complexes with and is activated by the Rho family G proteins Cdc42 and Rac1. *Cell*, 85, (4) 573-583 available from: PM:8653792

Chou, M.M., Masuda-Robens, J.M., & Gupta, M.L. 2003. Cdc42 promotes G1 progression through p70 S6 kinase-mediated induction of cyclin E expression. *J.Biol.Chem.*, 278, (37) 35241-35247 available from: PM:12842876

Chung, J., Grammer, T.C., Lemon, K.P., Kazlauskas, A., & Blenis, J. 1994. PDGF- and insulin-dependent pp70S6k activation mediated by phosphatidylinositol-3-OH kinase. *Nature*, 370, (6484) 71-75 available from: PM:8015612

Couch, F.J., Wang, X.Y., Wu, G.J., Qian, J., Jenkins, R.B., & James, C.D. 1999. Localization of PS6K to chromosomal region 17q23 and determination of its amplification in breast cancer. *Cancer Res.*, 59, (7) 1408-1411 available from: PM:10197603

Courjal, F. & Theillet, C. 1997. Comparative genomic hybridization analysis of breast tumors with predetermined profiles of DNA

amplification. *Cancer Res.*, 57, (19) 4368-4377 available from: PM:9331100

de Groot, R.P., Ballou, L.M., & Sassone-Corsi, P. 1994. Positive regulation of the cAMP-responsive activator CREM by the p70 S6 kinase: an alternative route to mitogen-induced gene expression

1. *Cell*, 79, (1) 81-91 available from: PM:7923380

Dennis, P.B., Pullen, N., Kozma, S.C., & Thomas, G. 1996. The principal rapamycin-sensitive p70(s6k) phosphorylation sites, T-229 and T-389, are differentially regulated by rapamycin-insensitive kinase kinases. *Mol.Cell Biol.*, 16, (11) 6242-6251 available from: PM:8887654

Dhillon, A.S., Hagan, S., Rath, O., & Kolch, W. 2007. MAP kinase signalling pathways in cancer. *Oncogene*, 26, (22) 3279-3290 available from: PM:17496922

Efeyan, A. & Sabatini, D.M. 2013. Nutrients and growth factors in mTORC1 activation. *Biochem.Soc.Trans.*, 41, (4) 902-905 available from: PM:23863153

Efeyan, A., Zoncu, R., & Sabatini, D.M. 2012. Amino acids and mTORC1: from lysosomes to disease. *Trends Mol.Med.*, 18, (9) 524-533 available from: PM:22749019

Fenton, T.R. & Gout, I.T. 2011. Functions and regulation of the 70kDa ribosomal S6 kinases. *Int.J.Biochem Cell Biol.*, 43, (1) 47-59 available from: PM:20932932

Ferrari, S., Bannwarth, W., Morley, S.J., Totty, N.F., & Thomas, G. 1992. Activation of p70s6k is associated with phosphorylation of four

clustered sites displaying Ser/Thr-Pro motifs. *Proc.Natl.Acad.Sci.U.S.A.*, 89, (15) 7282-7286 available from: PM:1496022

Gentilella, A., Kozma, S.C., & Thomas, G. 2015. A liaison between mTOR signaling, ribosome biogenesis and cancer. *Biochim.Biophys.Acta* available from: PM:25735853

Goh, E.T., Pardo, O.E., Michael, N., Niewiarowski, A., Totty, N., Volkova, D., Tsaneva, I.R., Seckl, M.J., & Gout, I. 2010. Involvement of heterogeneous ribonucleoprotein F in the regulation of cell proliferation via the mammalian target of rapamycin/S6 kinase 2 pathway. *J.Biol.Chem.*, 285, (22) 17065-17076 available from: PM:20308064

Goncharova, E.A., Goncharov, D.A., Eszterhas, A., Hunter, D.S., Glassberg, M.K., Yeung, R.S., Walker, C.L., Noonan, D., Kwiatkowski, D.J., Chou, M.M., Panettieri, R.A., Jr., & Krymskaya, V.P. 2002. Tuberin regulates p70 S6 kinase activation and ribosomal protein S6 phosphorylation. A role for the TSC2 tumor suppressor gene in pulmonary lymphangiomyomatosis (LAM). *J.Biol.Chem.*, 277, (34) 30958-30967 available from: PM:12045200

Gout, I., Minami, T., Hara, K., Tsujishita, Y., Filonenko, V., Waterfield, M.D., & Yonezawa, K. 1998. Molecular cloning and characterization of a novel p70 S6 kinase, p70 S6 kinase beta containing a proline-rich region. *J.Biol.Chem.*, 273, (46) 30061-30064 available from: PM:9804755

Graveley, B.R. 2009. Alternative splicing: regulation without regulators. *Nat.Struct.Mol.Biol.*, 16, (1) 13-15 available from: PM:19125169

Grewe, M., Gansauge, F., Schmid, R.M., Adler, G., & Seufferlein, T. 1999. Regulation of cell growth and cyclin D1 expression by the constitutively active FRAP-p70s6K pathway in human pancreatic cancer cells. *Cancer Res.*, 59, (15) 3581-3587 available from: PM:10446965

Guertin, D.A. & Sabatini, D.M. 2007. Defining the role of mTOR in cancer. *Cancer Cell*, 12, (1) 9-22 available from: PM:17613433

Hanahan, D. & Weinberg, R.A. 2000. The hallmarks of cancer. *Cell*, 100, (1) 57-70 available from: PM:10647931

Hannan, K.M., Brandenburger, Y., Jenkins, A., Sharkey, K., Cavanaugh, A., Rothblum, L., Moss, T., Poortinga, G., McArthur, G.A., Pearson, R.B., & Hannan, R.D. 2003. mTOR-dependent regulation of ribosomal gene transcription requires S6K1 and is mediated by phosphorylation of the carboxy-terminal activation domain of the nucleolar transcription factor UBF. *Mol.Cell Biol.*, 23, (23) 8862-8877 available from: PM:14612424

Hara, K., Maruki, Y., Long, X., Yoshino, K., Oshiro, N., Hidayat, S., Tokunaga, C., Avruch, J., & Yonezawa, K. 2002. Raptor, a binding partner of target of rapamycin (TOR), mediates TOR action. *Cell*, 110, (2) 177-189 available from: PM:12150926

Harada, H., Andersen, J.S., Mann, M., Terada, N., & Korsmeyer, S.J. 2001. p70S6 kinase signals cell survival as well as growth, inactivating the pro-apoptotic molecule BAD

1. *Proc.Natl.Acad.Sci.U.S.A*, 98, (17) 9666-9670 available from: PM:11493700

Harrington, L.S., Findlay, G.M., Gray, A., Tolkacheva, T., Wigfield, S., Rebholz, H., Barnett, J., Leslie, N.R., Cheng, S., Shepherd, P.R., Gout, I., Downes, C.P., & Lamb, R.F. 2004. The TSC1-2 tumor suppressor controls insulin-PI3K signaling via regulation of IRS proteins. *J.Cell Biol.*, 166, (2) 213-223 available from: PM:15249583

Huang, J., Dibble, C.C., Matsuzaki, M., & Manning, B.D. 2008. The TSC1-TSC2 complex is required for proper activation of mTOR complex 2. *Mol.Cell Biol.*, 28, (12) 4104-4115 available from: PM:18411301

Huang, J. & Manning, B.D. 2008. The TSC1-TSC2 complex: a molecular switchboard controlling cell growth. *Biochem.J.*, 412, (2) 179-190 available from: PM:18466115

Iadevaia, V., Huo, Y., Zhang, Z., Foster, L.J., & Proud, C.G. 2012. Roles of the mammalian target of rapamycin, mTOR, in controlling ribosome biogenesis and protein synthesis. *Biochem.Soc.Trans.*, 40, (1) 168-172 available from: PM:22260684

Iadevaia, V., Liu, R., & Proud, C.G. 2014. mTORC1 signaling controls multiple steps in ribosome biogenesis. *Semin.Cell Dev.Biol.*, 36, 113-120 available from: PM:25148809

Ip, C.K., Cheung, A.N., Ngan, H.Y., & Wong, A.S. 2011. p70 S6 kinase in the control of actin cytoskeleton dynamics and directed migration of ovarian cancer cells. *Oncogene*, 30, (21) 2420-2432 available from: PM:21258406

Ip, C.K. & Wong, A.S. 2012. Exploiting p70 S6 kinase as a target for ovarian cancer. *Expert.Opin.Ther.Targets.*, 16, (6) 619-630 available from: PM:22564017

Jastrzebski, K., Hannan, K.M., Tchoubrieva, E.B., Hannan, R.D., & Pearson, R.B. 2007. Coordinate regulation of ribosome biogenesis and function by the ribosomal protein S6 kinase, a key mediator of mTOR function. *Growth Factors*, 25, (4) 209-226 available from: PM:18092230

Jefferies, H.B., Fumagalli, S., Dennis, P.B., Reinhard, C., Pearson, R.B., & Thomas, G. 1997. Rapamycin suppresses 5'TOP mRNA translation through inhibition of p70s6k. *EMBO J.*, 16, (12) 3693-3704 available from: PM:9218810

Julien, L.A., Carriere, A., Moreau, J., & Roux, P.P. 2010. mTORC1-activated S6K1 phosphorylates Rictor on threonine 1135 and regulates mTORC2 signaling. *Mol.Cell Biol.*, 30, (4) 908-921 available from: PM:19995915

Karni, R., de, S.E., Lowe, S.W., Sinha, R., Mu, D., & Krainer, A.R. 2007. The gene encoding the splicing factor SF2/ASF is a proto-oncogene. *Nat.Struct.Mol.Biol.*, 14, (3) 185-193 available from: PM:17310252

Karni, R., Hippo, Y., Lowe, S.W., & Krainer, A.R. 2008. The splicing-factor oncoprotein SF2/ASF activates mTORC1. *Proc.Natl.Acad.Sci.U.S.A*, 105, (40) 15323-15327 available from: PM:18832178

Kenerson, H.L., Aicher, L.D., True, L.D., & Yeung, R.S. 2002. Activated mammalian target of rapamycin pathway in the pathogenesis of tuberous sclerosis complex renal tumors. *Cancer Res.*, 62, (20) 5645-5650 available from: PM:12384518

Khotskaya, Y.B., Goverdhan, A., Shen, J., Ponz-Sarvise, M., Chang, S.S., Hsu, M.C., Wei, Y., Xia, W., Yu, D., & Hung, M.C. 2014. S6K1 promotes invasiveness of breast cancer cells in a model of metastasis of triple-

negative breast cancer. *Am.J.Transl.Res.*, 6, (4) 361-376 available from: PM:25075253

Kim, D., Akcakanat, A., Singh, G., Sharma, C., & Meric-Bernstam, F. 2009. Regulation and localization of ribosomal protein S6 kinase 1 isoforms. *Growth Factors*, 27, (1) 12-21 available from: PM:19085255

Kim, D.H., Sarbassov, D.D., Ali, S.M., King, J.E., Latek, R.R., Erdjument-Bromage, H., Tempst, P., & Sabatini, D.M. 2002. mTOR interacts with raptor to form a nutrient-sensitive complex that signals to the cell growth machinery. *Cell*, 110, (2) 163-175 available from: PM:12150925

Koh, H., Jee, K., Lee, B., Kim, J., Kim, D., Yun, Y.H., Kim, J.W., Choi, H.S., & Chung, J. 1999. Cloning and characterization of a nuclear S6 kinase, S6 kinase-related kinase (SRK); a novel nuclear target of Akt. *Oncogene*, 18, (36) 5115-5119 available from: PM:10490848

Kozma, S.C., Ferrari, S., Bassand, P., Siegmann, M., Totty, N., & Thomas, G. 1990. Cloning of the mitogen-activated S6 kinase from rat liver reveals an enzyme of the second messenger subfamily. *Proc.Natl.Acad.Sci.U.S.A*, 87, (19) 7365-7369 available from: PM:1699226

Kurahashi, H., Takami, K., Oue, T., Kusafuka, T., Okada, A., Tawa, A., Okada, S., & Nishisho, I. 1995. Biallelic inactivation of the APC gene in hepatoblastoma. *Cancer Res.*, 55, (21) 5007-5011 available from: PM:7585543

Lai, K.P., Leong, W.F., Chau, J.F., Jia, D., Zeng, L., Liu, H., He, L., Hao, A., Zhang, H., Meek, D., Velagapudi, C., Habib, S.L., & Li, B. 2010. S6K1 is a multifaceted regulator of Mdm2 that connects nutrient status and DNA

damage response. *EMBO J.*, 29, (17) 2994-3006 available from: PM:20657550

Laplante, M. & Sabatini, D.M. 2012. mTOR signaling in growth control and disease. *Cell*, 149, (2) 274-293 available from: PM:22500797

Lawrence, M.C., Jivan, A., Shao, C., Duan, L., Goad, D., Zaganjor, E., Osborne, J., McGlynn, K., Stippec, S., Earnest, S., Chen, W., & Cobb, M.H. 2008. The roles of MAPKs in disease. *Cell Res.*, 18, (4) 436-442 available from: PM:18347614

Liu, P., Cheng, H., Roberts, T.M., & Zhao, J.J. 2009. Targeting the phosphoinositide 3-kinase pathway in cancer. *Nat.Rev.Drug Discov.*, 8, (8) 627-644 available from: PM:19644473

Ma, X.M. & Blenis, J. 2009. Molecular mechanisms of mTOR-mediated translational control. *Nat.Rev.Mol.Cell Biol.*, 10, (5) 307-318 available from: PM:19339977

Ma, X.M., Yoon, S.O., Richardson, C.J., Julich, K., & Blenis, J. 2008. SKAR links pre-mRNA splicing to mTOR/S6K1-mediated enhanced translation efficiency of spliced mRNAs. *Cell*, 133, (2) 303-313 available from: PM:18423201

Martin, K.A., Schalm, S.S., Richardson, C., Romanelli, A., Keon, K.L., & Blenis, J. 2001a. Regulation of ribosomal S6 kinase 2 by effectors of the phosphoinositide 3-kinase pathway. *J.Biol.Chem.*, 276, (11) 7884-7891 available from: PM:11108711

Martin, K.A., Schalm, S.S., Romanelli, A., Keon, K.L., & Blenis, J. 2001b. Ribosomal S6 kinase 2 inhibition by a potent C-terminal repressor

domain is relieved by mitogen-activated protein-extracellular signal-regulated kinase kinase-regulated phosphorylation. *J.Biol.Chem.*, 276, (11) 7892-7898 available from: PM:11108720

Matlin, A.J., Clark, F., & Smith, C.W. 2005. Understanding alternative splicing: towards a cellular code. *Nat.Rev.Mol.Cell Biol.*, 6, (5) 386-398 available from: PM:15956978

McManus, E.J. & Alessi, D.R. 2002. TSC1-TSC2: a complex tale of PKB-mediated S6K regulation. *Nat.Cell Biol.*, 4, (9) E214-E216 available from: PM:12205484

Montagne, J., Stewart, M.J., Stocker, H., Hafen, E., Kozma, S.C., & Thomas, G. 1999. Drosophila S6 kinase: a regulator of cell size. *Science*, 285, (5436) 2126-2129 available from: PM:10497130

Mora, A., Komander, D., van Aalten, D.M., & Alessi, D.R. 2004. PDK1, the master regulator of AGC kinase signal transduction. *Semin.Cell Dev.Biol.*, 15, (2) 161-170 available from: PM:15209375

Nojima, H., Tokunaga, C., Eguchi, S., Oshiro, N., Hidayat, S., Yoshino, K., Hara, K., Tanaka, N., Avruch, J., & Yonezawa, K. 2003. The mammalian target of rapamycin (mTOR) partner, raptor, binds the mTOR substrates p70 S6 kinase and 4E-BP1 through their TOR signaling (TOS) motif. *J.Biol.Chem.*, 278, (18) 15461-15464 available from: PM:12604610

Pardo, O.E., Arcaro, A., Salerno, G., Tetley, T.D., Valovka, T., Gout, I., & Seckl, M.J. 2001. Novel cross talk between MEK and S6K2 in FGF-2 induced proliferation of SCLC cells. *Oncogene*, 20, (52) 7658-7667 available from: PM:11753643

Parrott, L.A. & Templeton, D.J. 1999. Osmotic stress inhibits p70/85 S6 kinase through activation of a protein phosphatase. *J.Biol.Chem.*, 274, (35) 24731-24736 available from: PM:10455142

Pastor, M.D., Garcia-Yebenes, I., Fradejas, N., Perez-Ortiz, J.M., Mora-Lee, S., Tranque, P., Moro, M.A., Pende, M., & Calvo, S. 2009. mTOR/S6 kinase pathway contributes to astrocyte survival during ischemia. *J.Biol.Chem.*, 284, (33) 22067-22078 available from: PM:19535330

Pedrotti, S., Bielli, P., Paronetto, M.P., Ciccocanti, F., Fimia, G.M., Stamm, S., Manley, J.L., & Sette, C. 2010. The splicing regulator Sam68 binds to a novel exonic splicing silencer and functions in SMN2 alternative splicing in spinal muscular atrophy. *EMBO J.*, 29, (7) 1235-1247 available from: PM:20186123

Pende, M., Kozma, S.C., Jaquet, M., Oorschot, V., Burcelin, R., Le Marchand-Brustel, Y., Klumperman, J., Thorens, B., & Thomas, G. 2000. Hypoinsulinaemia, glucose intolerance and diminished beta-cell size in S6K1-deficient mice. *Nature*, 408, (6815) 994-997 available from: PM:11140689

Pende, M., Um, S.H., Mieulet, V., Sticker, M., Goss, V.L., Mestan, J., Mueller, M., Fumagalli, S., Kozma, S.C., & Thomas, G. 2004. S6K1(-/-)/S6K2(-/-) mice exhibit perinatal lethality and rapamycin-sensitive 5'-terminal oligopyrimidine mRNA translation and reveal a mitogen-activated protein kinase-dependent S6 kinase pathway. *Mol.Cell Biol.*, 24, (8) 3112-3124 available from: PM:15060135

Perez-Tenorio, G., Karlsson, E., Waltersson, M.A., Olsson, B., Holmlund, B., Nordenskjold, B., Fornander, T., Skoog, L., & Stal, O. 2011. Clinical

potential of the mTOR targets S6K1 and S6K2 in breast cancer. *Breast Cancer Res.Treat.*, 128, (3) 713-723 available from: PM:20953835

Peterson, R.T., Desai, B.N., Hardwick, J.S., & Schreiber, S.L. 1999. Protein phosphatase 2A interacts with the 70-kDa S6 kinase and is activated by inhibition of FKBP12-rapamycinassociated protein. *Proc.Natl.Acad.Sci.U.S.A.*, 96, (8) 4438-4442 available from: PM:10200280

Peterson, R.T. & Schreiber, S.L. 1999. Kinase phosphorylation: Keeping it all in the family. *Curr.Biol.*, 9, (14) R521-R524 available from: PM:10421571

Pollizzi, K., Malinowska-Kolodziej, I., Doughty, C., Betz, C., Ma, J., Goto, J., & Kwiatkowski, D.J. 2009a. A hypomorphic allele of Tsc2 highlights the role of TSC1/TSC2 in signaling to AKT and models mild human TSC2 alleles. *Hum.Mol.Genet.*, 18, (13) 2378-2387 available from: PM:19357198

Pollizzi, K., Malinowska-Kolodziej, I., Stumm, M., Lane, H., & Kwiatkowski, D. 2009b. Equivalent benefit of mTORC1 blockade and combined PI3K-mTOR blockade in a mouse model of tuberous sclerosis. *Mol.Cancer*, 8, 38 available from: PM:19527517

Pon, Y.L., Zhou, H.Y., Cheung, A.N., Ngan, H.Y., & Wong, A.S. 2008. p70 S6 kinase promotes epithelial to mesenchymal transition through snail induction in ovarian cancer cells. *Cancer Res.*, 68, (16) 6524-6532 available from: PM:18701475

Proud, C.G. 1996. p70 S6 kinase: an enigma with variations. *Trends Biochem Sci.*, 21, (5) 181-185 available from: PM:8871403

Puente Navazo, M.D., Valmori, D., & Ruegg, C. 2001. The alternatively spliced domain TnFnIII A1A2 of the extracellular matrix protein tenascin-C suppresses activation-induced T lymphocyte proliferation and cytokine production. *J.Immunol.*, 167, (11) 6431-6440 available from: PM:11714809

Pullen, N. & Thomas, G. 1997. The modular phosphorylation and activation of p70s6k. *FEBS Lett.*, 410, (1) 78-82 available from: PM:9247127

Qian, Y., Corum, L., Meng, Q., Blenis, J., Zheng, J.Z., Shi, X., Flynn, D.C., & Jiang, B.H. 2004. PI3K induced actin filament remodeling through Akt and p70S6K1: implication of essential role in cell migration. *Am.J.Physiol Cell Physiol*, 286, (1) C153-C163 available from: PM:12967912

Reinhard, C., Fernandez, A., Lamb, N.J., & Thomas, G. 1994. Nuclear localization of p85s6k: functional requirement for entry into S phase. *EMBO J.*, 13, (7) 1557-1565 available from: PM:8156994

Richardson, C.J., Broenstrup, M., Fingar, D.C., Julich, K., Ballif, B.A., Gygi, S., & Blenis, J. 2004. SKAR is a specific target of S6 kinase 1 in cell growth control. *Curr.Biol.*, 14, (17) 1540-1549 available from: PM:15341740

Saito, Y., Tanaka, Y., Aita, Y., Ishii, K.A., Ikeda, T., Isobe, K., Kawakami, Y., Shimano, H., Hara, H., & Takekoshi, K. 2012. Sunitinib induces apoptosis in pheochromocytoma tumor cells by inhibiting VEGFR2/Akt/mTOR/S6K1 pathways through modulation of Bcl-2 and BAD. *Am.J.Physiol Endocrinol.Metab*, 302, (6) E615-E625 available from: PM:21878661

Saitoh, M., ten, D.P., Miyazono, K., & Ichijo, H. 1998. Cloning and characterization of p70(S6K beta) defines a novel family of p70 S6 kinases. *Biochem Biophys.Res.Commun.*, 253, (2) 470-476 available from: PM:9878560

Sancak, Y., Bar-Peled, L., Zoncu, R., Markhard, A.L., Nada, S., & Sabatini, D.M. 2010. Ragulator-Rag complex targets mTORC1 to the lysosomal surface and is necessary for its activation by amino acids. *Cell*, 141, (2) 290-303 available from: PM:20381137

Sarbassov, D.D., Ali, S.M., Kim, D.H., Guertin, D.A., Latek, R.R., Erdjument-Bromage, H., Tempst, P., & Sabatini, D.M. 2004. Rictor, a novel binding partner of mTOR, defines a rapamycin-insensitive and raptor-independent pathway that regulates the cytoskeleton. *Curr.Biol.*, 14, (14) 1296-1302 available from: PM:15268862

Savinska, L.O., Lyzogubov, V.V., Usenko, V.S., Ovcharenko, G.V., Gorbenko, O.N., Rodnin, M.V., Vudmaska, M.I., Pogribniy, P.V., Kyyamova, R.G., Panasyuk, G.G., Nemazanyy, I.O., Malets, M.S., Palchevskyy, S.S., Gout, I.T., & Filonenko, V.V. 2004. Immunohistochemical analysis of S6K1 and S6K2 expression in human breast tumors. *Eksp.Onkol.*, 26, (1) 24-30 available from: PM:15112576

Schalm, S.S., Fingar, D.C., Sabatini, D.M., & Blenis, J. 2003a. TOS motif-mediated raptor binding regulates 4E-BP1 multisite phosphorylation and function. *Curr.Biol.*, 13, (10) 797-806 available from: PM:12747827

Schalm, S.S., Fingar, D.C., Sabatini, D.M., & Blenis, J. 2003b. TOS motif-mediated raptor binding regulates 4E-BP1 multisite phosphorylation and function. *Curr.Biol.*, 13, (10) 797-806 available from: PM:12747827

Schoenberg, D.R. & Maquat, L.E. 2012. Regulation of cytoplasmic mRNA decay. *Nat.Rev.Genet.*, 13, (4) 246-259 available from: PM:22392217

Shima, H., Pende, M., Chen, Y., Fumagalli, S., Thomas, G., & Kozma, S.C. 1998. Disruption of the p70(s6k)/p85(s6k) gene reveals a small mouse phenotype and a new functional S6 kinase. *EMBO J.*, 17, (22) 6649-6659 available from: PM:9822608

Sridharan, S. & Basu, A. 2011. S6 kinase 2 promotes breast cancer cell survival via Akt. *Cancer Res.*, 71, (7) 2590-2599 available from: PM:21427355

Taylor, M.D., Gokgoz, N., Andrulis, I.L., Mainprize, T.G., Drake, J.M., & Rutka, J.T. 2000. Familial posterior fossa brain tumors of infancy secondary to germline mutation of the hSNF5 gene. *Am.J.Hum.Genet.*, 66, (4) 1403-1406 available from: PM:10739763

Um, S.H., Frigerio, F., Watanabe, M., Picard, F., Joaquin, M., Sticker, M., Fumagalli, S., Allegrini, P.R., Kozma, S.C., Auwerx, J., & Thomas, G. 2004. Absence of S6K1 protects against age- and diet-induced obesity while enhancing insulin sensitivity. *Nature*, 431, (7005) 200-205 available from: PM:15306821

Valacca, C., Bonomi, S., Buratti, E., Pedrotti, S., Baralle, F.E., Sette, C., Ghigna, C., & Biamonti, G. 2010. Sam68 regulates EMT through alternative splicing-activated nonsense-mediated mRNA decay of the SF2/ASF proto-oncogene. *J.Cell Biol.*, 191, (1) 87-99 available from: PM:20876280

Valovka, T., Verdier, F., Cramer, R., Zhyvoloup, A., Fenton, T., Rebholz, H., Wang, M.L., Gzhegotsky, M., Lutsyk, A., Matsuka, G., Filonenko, V.,

Wang, L., Proud, C.G., Parker, P.J., & Gout, I.T. 2003. Protein kinase C phosphorylates ribosomal protein S6 kinase beta1 and regulates its subcellular localization. *Mol.Cell Biol.*, 23, (3) 852-863 available from: PM:12529391

van der Hage, J.A., van den Broek, L.J., Legrand, C., Clahsen, P.C., Bosch, C.J., Robanus-Maandag, E.C., van de Velde, C.J., & van de Vijver, M.J. 2004. Overexpression of P70 S6 kinase protein is associated with increased risk of locoregional recurrence in node-negative premenopausal early breast cancer patients. *Br.J.Cancer*, 90, (8) 1543-1550 available from: PM:15083183

Vazquez-Higuera, J.L., Mateo, I., Sanchez-Juan, P., Rodriguez-Rodriguez, E., Pozueta, A., Calero, M., Dobato, J.L., Frank-Garcia, A., Valdivieso, F., Berciano, J., Bullido, M.J., & Combarros, O. 2011. Genetic variation in the tau kinases pathway may modify the risk and age at onset of Alzheimer's disease. *J.Alzheimers.Dis.*, 27, (2) 291-297 available from: PM:21811019

Venables, J.P. 2006. Unbalanced alternative splicing and its significance in cancer. *Bioessays*, 28, (4) 378-386 available from: PM:16547952

Venables, J.P. & Burn, J. 2006. EASI--enrichment of alternatively spliced isoforms. *Nucleic Acids Res.*, 34, (15) e103 available from: PM:16951290

Wang, L., Lin, S.H., Wu, W.G., Kemp, B.L., Walsh, G.L., Hong, W.K., & Mao, L. 2000. C-CAM1, a candidate tumor suppressor gene, is abnormally expressed in primary lung cancers. *Clin.Cancer Res.*, 6, (8) 2988-2993 available from: PM:10955775

Wang, X., Li, W., Williams, M., Terada, N., Alessi, D.R., & Proud, C.G. 2001. Regulation of elongation factor 2 kinase by p90(RSK1) and p70 S6 kinase. *EMBO J.*, 20, (16) 4370-4379 available from: PM:11500364

Weng, Q.P., Andrabi, K., Kozlowski, M.T., Grove, J.R., & Avruch, J. 1995. Multiple independent inputs are required for activation of the p70 S6 kinase. *Mol.Cell Biol.*, 15, (5) 2333-2340 available from: PM:7739516

Weng, Q.P., Kozlowski, M., Belham, C., Zhang, A., Comb, M.J., & Avruch, J. 1998. Regulation of the p70 S6 kinase by phosphorylation in vivo. Analysis using site-specific anti-phosphopeptide antibodies. *J.Biol.Chem.*, 273, (26) 16621-16629 available from: PM:9632736

Wilson, K.F., Wu, W.J., & Cerione, R.A. 2000. Cdc42 stimulates RNA splicing via the S6 kinase and a novel S6 kinase target, the nuclear cap-binding complex. *J.Biol.Chem.*, 275, (48) 37307-37310 available from: PM:10973943

Yamaguchi, H., Fujimoto, T., Nakamura, S., Ohmura, K., Mimori, T., Matsuda, F., & Nagata, S. 2010. Aberrant splicing of the milk fat globule-EGF factor 8 (MFG-E8) gene in human systemic lupus erythematosus. *Eur.J.Immunol.*, 40, (6) 1778-1785 available from: PM:20213738

Yamnik, R.L., Digilova, A., Davis, D.C., Brodt, Z.N., Murphy, C.J., & Holz, M.K. 2009. S6 kinase 1 regulates estrogen receptor alpha in control of breast cancer cell proliferation. *J.Biol.Chem.*, 284, (10) 6361-6369 available from: PM:19112174

Yang, L., Wang, L., & Zheng, Y. 2006. Gene targeting of Cdc42 and Cdc42GAP affirms the critical involvement of Cdc42 in filopodia induction, directed migration, and proliferation in primary mouse

embryonic fibroblasts. *Mol.Biol.Cell*, 17, (11) 4675-4685 available from:
PM:16914516

Yang, X. & Xu, T. 2011. Molecular mechanism of size control in development and human diseases. *Cell Res.*, 21, (5) 715-729 available from: PM:21483452

Yip, C.K., Murata, K., Walz, T., Sabatini, D.M., & Kang, S.A. 2010. Structure of the human mTOR complex I and its implications for rapamycin inhibition. *Mol.Cell*, 38, (5) 768-774 available from: PM:20542007

Zoncu, R., Efeyan, A., & Sabatini, D.M. 2011. mTOR: from growth signal integration to cancer, diabetes and ageing. *Nat.Rev.Mol.Cell Biol.*, 12, (1) 21-35 available from: PM:21157483